University of Salamanca

Institute of Neuroscience of Castilla y León

STIMULUS-SPECIFIC ADAPTATION IN THE AUDITORY BRAIN: STRUCTURE AND FUNCTION CORRELATE

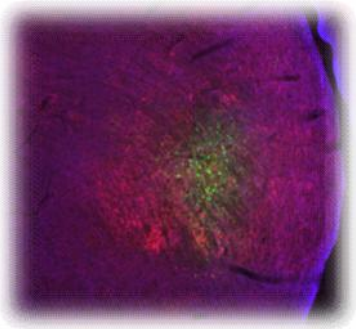

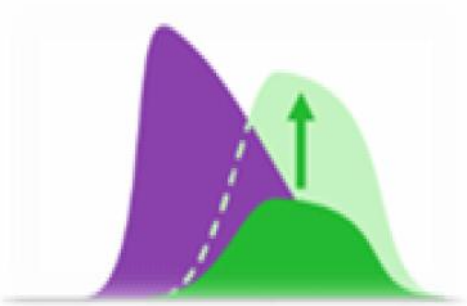

Yaneri Aguilar Ayala

Doctoral Thesis

June, 2015.

INSTITUTO DE NEUROCIENCIAS CASTILLA Y LEÓN

VNIVERSIDAD D SALAMANCA

Doctoral thesis supervised by

Dr. Manuel Sánchez Malmierca

Laboratory of Auditory Neurophysiology,
Institute of Neuroscience of Castilla y León.
University of Salamanca.

Acknowledgements

I heartily thank to my thesis director Manuel S. Malmierca for letting me be part of his crew and for his everlasting enthusiasm and support. For show me that patience and constancy are key stones for running a lab. Also, to my labmates for sharing good times along these years, David, Flora, Dani, Xin, Blanca, Javier, Rui, Catalina, Gloria, Guillermo. Special thanks to David for accompanying me during my first surgeries and recordings, and to Rui for sharing his passion on science though endless discussions.

To Prof. Douglas L. Oliver for receiving me in his lab and for teaching me that one thing at once works. Thank you for letting me be part of your science.

To Prof. Nell B. Cant for sharing with me her knowledge and for her constant and kind support to my work. Thank you for improving my scientific writing.

To my friends Roger, Kathy, Tao, Xin, Enzo, Azu, Mercedes, Bego, Flora, Vero, Dani for all the blessed and unforgettable moments we shared at the INCyL and for supporting me despite oceans and continents. Mercedes, Begoña, thanks for your words and sageness which drive me to move along with stride. I will be right behind all of you.

Also, sincere thanks to Cata, Gloria, Marta, Miriam, Lymma, Mamen, Clara, Maryani for their joyfulness during the overwhelming days. To the coffee-time team for the good times. Special thanks to Nacho for being an example of hard-work and for his kind help to resolve my lab troubles.

To Ethel and Janosch for staying by my side despite the distance, for taking care of my happiness. Der Aufwand wird sich lohnen.

To my mom Sara and my sister Yareni for inspiring me. To my family; Tunyun, Bertha, Linda, Piño, David, Justo, Prado, Meme, my endless gratitude. Nacanu' tobisi' na' ne lii.

This study was funded by the European Union (EUI2009-04083), the Spanish MINECO (BFU2009-07286, BFU2013- 43608-P), the JCyL (GR221, SA343U14) and USAL grant (Program 1, 2014: KAQJ) to Manuel Sánchez Malmierca.

Yaneri Aguilar Ayala held fellowships for Postgraduate Studies from the Mexican Council for Science and Technology (CONACyT, 216106) and from the Mexican Ministry for Public Education (SEP).

Este trabajo ha sido financiado por los proyectos otorgados por la Unión Europea (EUI2009-04083), el Ministerio Español de Ciencia e Innovación (BFU2009-07286, BFU2013- 43608-P), la Junta de Castilla y León (SA343U14) y la Universidad de Salamanca (Programa 1, 2014: KAQJ) a Manuel Sánchez Malmierca.

Yaneri Aguilar Ayala contó con becas para Estudios de Postgrado del Consejo Nacional de Ciencia y Tecnología (CONACyT, 216106) y de la Secretaria de Educación Pública del Gobierno Mexicano.

La tesis titulada **'Adaptación a estímulos específicos en el cerebro auditivo: correlato funcional y estructural'** que presenta Yaneri Aguilar Ayala para obtener el título de Doctorado en Neurociencias corresponde a un **compendio de trabajos científicos** previamente publicados o aceptados para publicación. Los artículos se citan a continuación.

The thesis entitled **'Stimulus-specific adaptation in the auditory brain: structure and function correlate'** presented by Yaneri Aguilar Ayala to obtain the degree of PhD in Neuroscience corresponds to **a compendium of scientific articles** already published or accepted for publication. The articles are listed below.

Study I

Frequency discrimination and stimulus deviance in the inferior colliculus and cochlear nucleus.

Authors: Yaneri Aguilar Ayala[1], David Pérez-González[1], Daniel Duque Doncos[1], Israel Nelken[2], Manuel Sánchez Malmierca[1,3].
Affilation: [1]Auditory Neurophysiology Laboratory, Institute of Neuroscience of Castilla y León, University of Salamanca Salamanca, Spain. [2]Department of Neurobiology, Institute of Life Sciences, The Interdisciplinary Center for Neural Computation and the Edmond and Lily Safra Center for Brain Sciences, The Hebrew University of Jerusalem, Jerusalem, Israel. [3]Department of Cell Biology and Pathology, Faculty of Medicine, University of Salamanca, Salamanca, Spain.
Journal: Frontiers in Neural Circuits. 2013 Jan 14;6:119.
DOI: 10.3389/fncir.2012.00119. eCollection 2012.

Study II

Stimulus-specific adaptation and deviance detection in the inferior colliculus.

Authors: Yaneri Aguilar Ayala[1], Manuel Sánchez Malmierca[1,2].
Affilation: [1]Laboratory for the Neurobiology of Hearing, Auditory Neurophysiology Unit, Institute of Neuroscience of Castilla y León, University of Salamanca Salamanca, Spain. [2]Department of Cell Biology and Pathology, Faculty of Medicine, University of Salamanca, Salamanca, Spain.
Journal: Frontiers in Neural Circuits. 2013 Jan 17;6:89.
DOI: 10.3389/fncir.2012.00089. eCollection 2012.

Study III

Differences in the strength of cortical and brainstem inputs to SSA and non-SSA neurons in the inferior colliculus.

Authors: Yaneri Aguilar Ayala[1], Adanna Udeh[2], Kelsey Dutta[2], Deborah Bishop[2], Manuel Sánchez Malmierca[1,2], Douglas L. Oliver[2].
Affilation: [1]Auditory Neurophysiology Laboratory. Institute of Neuroscience of Castilla Y León, University of Salamanca, C/Pintor Fernando Gallego, 1, 37007 Salamanca, Spain.
[2]Department of Neuroscience, University of Connecticut Health Center, Farmington, CT, USA 06030-3401
[3]Department of Cell Biology and Pathology, Faculty of Medicine, University of Salamanca, Campus Miguel de Unamuno, 37007 Salamanca, Spain.
Journal: Scientific Reports. 5:10383
DOI: 10.1038/srep10383

Study IV

Cholinergic modulation of stimulus-specific adaptation in the inferior colliculus.

Authors: Yaneri Aguilar Ayala[1], Manuel S. Malmierca[1,2].
Affilation: [1]Auditory Neurophysiology Laboratory. Institute of Neuroscience of Castilla Y León, University of Salamanca, C/Pintor Fernando Gallego, 1, 37007 Salamanca, Spain.
[2]Department of Cell Biology and Pathology, Faculty of Medicine, University of Salamanca, Campus Miguel de Unamuno, 37007 Salamanca, Spain.
Journal: J Neurosci Submitted

Study V

Deviance detection in auditory subcortical structures: what can we learn from neurochemistry and neural connectivity?

Authors: Daniel Duque Doncos[1*], Yaneri Aguilar Ayala[1*], Manuel Sánchez Malmierca[1,2].
Affilation: [1]Auditory Neuroscience Laboratory, Institute of Neuroscience of Castilla y León (INCyL), University of Salamanca, C/ Pintor Fernando Gallego, 1, Salamanca, 37007, Spain.
[2]Department of Cell Biology and Pathology, Faculty of Medicine, University of Salamanca, Salamanca, Spain.
*Equal contribution
Journal: Cell and Tissue Research. 2015 Mar 8. [Epub ahead of print]
DOI: 10.1007/s00441-015-2134-7

Study VI

Stimulus-specific adaptation in the inferior colliculus: The role of excitatory, inhibitory and modulatory inputs.

Authors: Yaneri Aguilar Ayala[1], David Pérez-González[1], Manuel S. Malmierca[1,2].
Affilation: [1]Auditory Neurophysiology Laboratory. Institute of Neuroscience of Castilla Y León, University of Salamanca, C/Pintor Fernando Gallego, 1, 37007 Salamanca, Spain.
[2]Department of Cell Biology and Pathology, Faculty of Medicine, University of Salamanca, Campus Miguel de Unamuno, 37007 Salamanca, Spain.
Journal: Biological Psychology Submitted

MANUEL SÁNCHEZ MALMIERCA, PROFESOR TITULAR DE UNIVERSIDAD DEL DEPARTAMENTO DE BIOLOGÍA CELULAR Y PATOLOGÍA DE LA UNIVERSIDAD DE SALAMANCA E INVESTIGADOR DEL INSTITUTO DE NEUROCIENCIAS DE CASTILLA Y LEÓN

CERTIFICA

Que la tesis doctoral titulada:

STIMULUS-SPECIFIC ADAPTATION IN THE AUDITORY BRAIN: STRUCTURE AND FUNCTION CORRELATE

ha sido redactada en inglés, contiene un resumen en español, y describe el trabajo de investigación realizado por ***Dña. Yaneri Aguilar Ayala*** bajo mi dirección durante los últimos 5 años.

La memoria de este estudio recoge un análisis detallado y exhaustivo de los mecanismos de adaptación específicos a estímulos en el colículo inferior y su susbtrato anatómico. Los datos presentados en esta memoria constituyen una aportación original y puedo afirmar que ponen de manifiesto un gran avance y progreso en el área de las Neurociencias.

Por todo ello, considero que esta tesis reúne la calidad y rigor científicos necesarios para que sea defendida en la Universidad de Salamanca como requisito para que ***Dña. Yaneri Aguilar Ayala*** opte a los grados de '*Doctor*' y '*Mención Doctor Internacional*' por la Universidad de Salamanca.

Y para que así conste, firmo el presente certificado en Salamanca a 8 de Junio Mayo de 2015.

Prof. Manuel Sánchez Malmierca

Content

1. Abbreviations …….....…… **1**
2. Introduction …….....……. **2**
3. Hypothesis ……..……. **6**
4. Objectives ……..……. **8**
5. Summary of Results ……...……. **9**
6. General Discussion and Final Remarks …….……... **12**
7. Conclusions ……..……. **15**
8. References ……...……..….. **17**
9. Appendices in Spanish …….…..……..….. **23**
10. Publications …….……..... **39**

1. Abbreviations

A1: primary auditory cortex

ACh: acetylcholine

CN: cochlear nucleus

GABA: gamma-Aminobutyric acid

IC: inferior colliculus

ICC: central nucleus of the inferior colliculus

ICCx: cortices of the inferior colliculus

ISIs: interstimulus intervals

MGB: medial geniculate body

NMDA: N-methyl-D-aspartate

SSA: stimulus-specific adaptation

2. Introduction

Representation of an ever-changing sensory environment with many simultaneously occurring streams of information requires neural codes that account for its complex statistical and dynamical structure. Pioneering work by E.D. Adrian demonstrated that the spiking activity of sensory nerve fibers varies as a function of stimulus intensity and that this spiking rate decreases under sustained static stimulation (Adrian and Zotterman, 1926a, b). These results led to a fundamental principle of neural encoding, namely, sensory neurons represent external information in sequences of action potentials (rate code, Shadlen and Newsome, 1994). Since then, a key, and not yet completely resolved, question in neurophysiology is how much information about ongoing stimulation is carried by the spiking activity of a single neuron (Bialek et al., 1991).

Natural stimuli are not static but rather vary in space and time, and sensory neurons adapt their sensitivity to the statistical distribution of inputs. Thus, their responses are not linear but depend on the context in which the stimuli are embedded (Muller et al., 1999; Brenner et al., 2000; Fairhall et al., 2001; Dean et al., 2005). For example, auditory processing requires neural mechanisms suited for representing sequential incoming sounds in the context of preceding events (Shamma, 2001; Bendixen et al., 2012; May et al., 2015). From an information processing perspective, response adaptation is a neural strategy that accounts for non-linear sensory encoding (Carandini, 2007; Maravall, 2013). Neural adaptation serves to reduce the redundancy of sensory information (Chechik et al., 2006) and to adjust the operating point of neurons to maximize the efficiency of sensory coding (Muller et al., 1999; Dean et al., 2005). Thus, an unvarying stimulus or its repetitive presentation evokes a suppression or decrease in the neural responses.

Neural adaptation to the repetitive presentation of a stimulus has been found to occur in many brain areas and across different sensory modalities (Grill-Spector et al., 2006; Todorovic and de Lange, 2012; Summerfield and de Lange, 2014). For example, neurons of the inferior temporal cortex (Baylis and Rolls, 1987; Desimone, 1996; Kaliukhovich and Vogels, 2014), medial temporal cortex (Brown et al., 1987; Ringo,

1996), striate cortex (Muller et al., 1999), and superior colliculus (Boehnke et al., 2011) adapt to repetitive visual stimulation. Similarly, specialized neurons in the auditory brain signal the occurrence of sounds based on their probability of occurrence rather than on their simple physical identity. This effect, i.e., a reduced response to a repetitive sound that is restored by presenting a different sound, was first described in the auditory thalamus (cat: Calford, 1983; guinea-pig: Kraus et al., 1994) and in the torus semicircularis (a nucleus analogous to the mammalian inferior colliculus) in the frog (Bibikov, 1977).

More recently, Ulanovsky and colleagues (2003) demonstrated that single neurons in the primary auditory cortex (A1) discriminate between sounds presented with different probabilities of occurrence. These A1 neurons exhibit stimulus-specific adaptation [SSA, a term first used by Movshon and Lennie (1979)], defined as a reduction in their response to a repetitive sound that does not generalize, or only partially generalizes, to other, infrequently occurring sounds. In their study, the sequential presentation of a pure tone with high-probability of occurrence (standard) was occasionally replaced by a different, low-probability tone (deviant). Using the same stimulation protocol as in the A1 study, Malmierca and colleagues (2009), found that neurons of the inferior colliculus (IC) also exhibit SSA responses. This study confirmed the rapid and pronounced adaptation that a subclass of IC neurons exhibits to the repetitive presentation of pure tones and amplitude-modulated sounds (Bibikov, 1977; Pérez-González et al., 2005). Subsequent studies demonstrated that SSA is also found in the medial geniculate body (MGB) (Anderson et al., 2009; Antunes et al., 2010), suggesting that SSA is a ubiquitous phenomenon along the auditory pathway rather than a unique property of higher-order cortical processing as originally suggested (Ulanovsky et al., 2003). Neurons exhibiting SSA are ideally suited to detect changes or deviations in the ongoing flow of sensory, auditory information (Grill-Spector et al., 2006; Winkler et al., 2009). SSA neurons are likely to integrate sensory information over time by changing the efficacy of their synaptic connections depending on recent activity e.g. (Friauf et al., 2015). Moreover, SSA has been considered a form of neural habituation that contributes to a more general brain process known as saliency mapping (Gutfreund, 2012).

A hallmark of SSA is its sensitivity to a variety of stimulus parameters such as the stimulus probability, the frequency contrast and the time interval between stimuli (Ulanovsky et al., 2003; Malmierca et al., 2009; von der Behrens et al., 2009; Yu et al., 2009; Antunes et al., 2010; Zhao et al., 2011). A1 neurons exhibit reliable SSA with only small changes in stimulus parameters, i.e., they strongly adapt to repetitive sounds regardless of small frequency contrast (hyperacuity), and even more interestingly, regardless of low presentation rates. For example, SSA occurs even at long interstimulus intervals (ISIs) of up to 2 s. Because of the long duration of the 'memory trace' or 'adaptation' exhibited by A1 neurons (Ulanovsky et al., 2003), it was assumed that cortical SSA could be a neural correlate of deviance detection reflected in event-related evoked responses. Deviance detection requires information storage and comparison over time (Naatanen et al., 2001), and the temporal scale of seconds is consistent with the duration of sensory (echoic) memory in monkeys and humans, which is estimated to be on the order of magnitude of a few seconds (Javitt et al., 1994; Naatanen and Escera, 2000). In the IC, the strongest SSA responses are elicited by ISIs of 250 ms, although IC neurons also show SSA to stimuli presented at longer ISIs, i.e. 500 ms (Malmierca et al., 2009). MGB neurons exhibit SSA at the same time intervals as A1 neurons (Antunes et al., 2010).

Extreme SSA levels in subcortical nuclei are limited to their non-lemniscal divisions. In the IC, these are the cortical regions (ICCx; Malone et al., 2002; Pérez-González et al., 2005; Malmierca et al., 2009; Lumani and Zhang, 2010), and in the MGB, the medial and dorsal divisions (Antunes et al., 2010). In both structures, these regions are strongly innervated by descending projections from the A1, higher order auditory cortex divisions and even non-auditory nuclei (Loftus et al., 2008; Lee and Sherman, 2011; Malmierca and Ryugo, 2011; Malmierca et al., 2015). Cortical neurons in the IC usually exhibit a predominance of onset response patterns and longer response latencies than the neurons of the central nucleus (ICC). Also, the morphology of ICCx and ICC neurons differs. Neurons in the dorsal and rostral IC regions possess large, non-oriented and widespread dendritic arbors, whereas in the ICC, the neurons are highly oriented with restricted dendritic arbors (Malmierca et al., 1993; Malmierca et al., 1995b; Malmierca et al., 2011). The different SSA sensitivities between non-lemniscal and lemniscal neurons of

the IC suggests that the intrinsic properties of the neuron and/or its local and afferent connectivity contributes to the emergence of SSA. Likewise, those neural properties or connections are likely to be common to clusters of IC neurons exhibiting SSA since the amplitude of local field potentials in the IC is larger for those sounds elicited by frequency deviants than by repetitive ones (Patel et al., 2012).

Several studies have suggested that synaptic inputs may play a role in generating and/or shaping SSA responses (Eytan et al., 2003; Duque et al., 2012; Thomas et al., 2012). For example, SSA is not a property homogeneously distributed throughout the neuron's frequency response area, and therefore is not likely to reflect a characteristic property of the neuron (Duque et al., 2012). More importantly, microiontophoretic studies in the IC (Pérez-González et al., 2012) and MGB (Duque et al., 2014) revealed that inhibitory inputs modulate SSA by exerting a gain control on the neural excitability. More specifically, blockade of the $GABA_A$-mediated inhibition on IC neurons exerts an overall increase in the neural excitability affecting the response to both low- and high probability tones. It is likely that additional synaptic inputs participate in the generation of the specific adaptation evoked by the repetitive sounds. Neuromodulatory systems provide contextual or feedback signals (Ranganath and Rainer, 2003; Thiele, 2013; Froemke, 2015). In this regard, a study of event-related responses in humans (Moran et al., 2013) demonstrated that the systemic application of galantamine, an acetylcholinesterase inhibitor, attenuated the adaptation in the response to consecutive presentation of the same tone (i.e., repetition suppression). Also, nicotine enhances or diminishes change detection according to the baseline sensitivity of each subject (Knott et al., 2014). Therefore, it is plausible to propose that the neuronal adaptation in the IC reflects high level network computations involving specific synaptic inputs converging on SSA neurons.

3. Hypothesis

Currently, exact and detailed mechanisms underlying the generation of SSA remain unknown. A feature of SSA at the level of the A1 (Ulanovsky et al., 2003; Ulanovsky et al., 2004) and the auditory thalamus (Antunes et al., 2010) that distinguishes it from other forms of adaptation is that SSA responses occur at long interstimulus intervals (on the order of seconds). Whether SSA at the temporal scale of seconds also occurs in the IC has not been explored so far. The presence of SSA at low stimulation rates indicates that mechanisms such as neural fatigue or neural refractoriness elicited by high stimulation rates (Maravall, 2013) do not, or at least do not totally, generate SSA responses. Thus, it is more likely that short-term plasticity mechanisms such as synaptic depression (Friauf et al., 2015) occurring at the inputs converging on SSA neurons might contribute to the specific adaptation of the repetitively stimulated inputs (Eytan et al., 2003; Grill-Spector et al., 2006; Nelken, 2014). Likewise, the distribution of extreme SSA levels in the non-lemniscal divisions of subcortical nuclei (Malmierca et al., 2009; Antunes et al., 2010; Duque et al., 2012) suggests the existence of unique local circuits in those subdivisions that may exert a key role in the generation of SSA. Since lemniscal and non-lemniscal auditory pathways emerge in the IC (Lee and Sherman, 2011) it is likely that SSA also emerges for first time in these subdivisions. However, the presence of SSA has not been explored in auditory nuclei below the IC.

SSA neurons may receive a specific set of synaptic inputs that shape response adaptation. In this regard, previous studies suggest that inhibition modulates but does not generate SSA in the IC (Pérez-González et al., 2012) and MGB (Duque et al., 2014). Hence, other neuroactive substances may participate in the generation of SSA. One probable candidate is acetylcholine (ACh) because it is well known that ACh mediates short-term plasticity in the spectral sensitivity of auditory neurons without major changes in overall excitability or broadband gain (Metherate and Weinberger, 1989; Froemke et al., 2007; Froemke et al., 2013; Froemke, 2015). It is also known to affect deviance detection reflected in event-related potentials in humans (Moran et al., 2013).

Considering the findings discussed above, I hypothesized that:

I. IC neurons are able to detect deviant frequencies at temporal scales on the order of seconds, and frequency resolution of those neurons correlates with their degree of SSA.

II. Neurons with strong SSA responses are confined to the cortices of the IC and receive a different set of inputs than those neurons lacking SSA. Thus, SSA would be a local feature of specific neural circuits that is not ubiquitous in the auditory brain, but mostly confined to non-lemniscal structures.

III. Modulatory cholinergic synaptic inputs affect the SSA responses of IC neurons.

4. Objectives

Based on my hypotheses, my objectives were the following:

I. Determine whether or not IC neurons exhibit SSA responses and frequency hyperacuity at long inter-stimulus intervals (on the order of seconds).

II. Describe to what extent frequency discriminability reflects the expression of SSA and how it is modified by the stimulation parameters.

III. Determine whether SSA is a ubiquitous feature of auditory processing by examining auditory nuclei below the IC.

IV. Determine the sources of inputs that converge on SSA neurons in the IC.

V. Probe whether cholinergic inputs affect SSA responses of IC neurons.

5. Summary of Results

Study I

We recorded single-unit responses from the IC where SSA is known to occur and we explored for the first time SSA in the cochlear nucleus (CN) of rats. We analyzed an important functional outcome of SSA, the extent to which frequency discriminability depends on sensory context. We reproduced the finding that many neurons in the IC exhibit SSA, but we did not observe significant SSA in our CN sample. We concluded that strong SSA is not a common phenomenon in the CN (if it occurs at all). As predicted, frequency discriminability was enhanced in IC when stimuli were presented in an oddball context, and this enhancement was correlated with the degree of SSA shown by the neurons. In contrast, frequency discrimination by CN neurons was independent of stimulus context. Our results demonstrated that SSA does not occur along the entire auditory pathway, and also suggest that SSA increases frequency discriminability of single neurons beyond that expected from their tuning curves.

Study II

We found that single neurons in the IC of the anesthetized rat exhibit SSA to pure tones presented at ISIs of 0.5, 1 and 2 seconds. Under these low stimulation rates, the first spike latency evoked by the deviant tone were earlier than those evoked by the same tone when it was used as the standard, suggesting that the cellular mechanisms that discriminate between deviant and standard responses are functional at the temporal scale of seconds. The degree of SSA at those ISIs was sensitive to the frequency separation of the tones.

Study III

We tested whether neurons exhibiting SSA and those without are part of the same networks in the IC. We recorded the responses to frequent and rare sounds and then marked the sites of these neurons with a retrograde tracer to correlate the source of projections with the

physiological response. SSA neurons were confined to the non-lemniscal subdivisions and exhibited broad receptive fields, while the non-SSA neurons were confined to the central nucleus and displayed narrow receptive fields. SSA neurons receive strong inputs from auditory cortical areas and very poor or even absent projections from the brainstem nuclei. In contrast, the major sources of inputs to the neurons that lacked SSA were from the brainstem nuclei.

Study IV

We addressed how microiontophoretic application of ACh modulates SSA in the IC. We found that ACh decreased SSA in IC neurons by increasing the response to the repetitive tone. This effect was mediated mainly by muscarinic receptors. The strength of the cholinergic modulation depended on the baseline SSA level, exerting its greatest effect on neurons with intermediate SSA responses across cortical IC subdivisions. Our data demonstrate that ACh alters the sensitivity of partially-adapting IC neurons by switching neural discriminability to a more linear transmission of sounds. This change serves to increase ascending sensory-evoked afferent activity propagated through the thalamus *en route* to the cortex. Our results provide empirical support for the notion that high ACh levels may enhance attention to the environment, making neural circuits more responsive to external sensory stimuli.

Study V

We present a review of the state of the art of SSA in auditory subcortical nuclei, i.e., the inferior colliculus and medial geniculate body of the thalamus, and discuss the differential receptor distribution and neural connectivity of those regions in which extreme SSA has been found. Further, we review both SSA and mismatch negativity-like responses in auditory and non-auditory areas that exhibit multimodal sensitivities that we suggest conform to a distributed network that encodes for deviance detection. Understanding the

neurochemistry and response similarities across these different regions will contribute to a better understanding of the neural mechanisms underlying deviance detection.

Study VI

We review current knowledge on the effect of $GABA_A$-mediated inhibition and the modulation of acetylcholine on SSA in the inferior colliculus, and we add unpublished original data about the role of glutamate receptors. We found that the blockade of $GABA_A$ and glutamate receptors mediates an overall increase or decrease of the neural response, respectively, while acetylcholine affects only the response to the repetitive sounds. These results demonstrate that GABAergic, glutamatergic and cholinergic receptors play different and complementary roles in shaping SSA.

6. General Discussion and Final Remarks

My results support the conclusion that SSA is not a ubiquitous property found throughout the auditory brain but rather is a property that appears in the IC and forebrain. CN neurons failed to adapt to high-probability sounds even when they were presented at high repetition rates (up to 20 Hz). On the other hand, IC neurons exhibit strong SSA responses even on the temporal scale of seconds, *i.e.*, low repetition rates. Likewise, frequency discriminability of IC neurons reflects the extent of SSA they exhibit. SSA enhances deviant frequency saliency in the firing output of IC neurons by diminishing the response to repetitive sounds in a context-dependent manner (Figure 1).

SSA was strongest in the non-lemniscal regions of the IC and was low or virtually absent in the lemniscal subdivision. The extent of SSA correlates with the broadness of the frequency response area in the IC neurons. Highly-adapting neurons exhibit wider spectral tuning (values as high as 30 – 40 kHz) suggesting those neurons integrate across many more frequency inputs than those neurons with low or absent SSA. The spectral tuning and loci of SSA neurons is consistent with the denser dendritic arborization described for neurons of the cortices of the IC (Malmierca et al., 2011). The extensive dendritic arborization would allow more synaptic contacts to converge on SSA neurons allowing the integration of spectral information. In agreement with this, my retrograde tracer data demonstrated that SSA neurons are confined to IC regions that integrate dense cortical inputs from multiple auditory cortical areas, whereas sites of non-SSA neurons are strongly innervated by brainstem projections. Also, SSA recording sites receive inputs from the ICC, which are likely to convey ascending spectral information from brainstem nuclei. Collateral axons from ICC neurons may terminate on the SSA neurons *en route* to the brachium of the IC and medial geniculate body (Kudo and Niimi, 1980; Oliver et al., 1991; Saldana and Merchan, 1992; Malmierca et al., 1995a). Thus, the A1 and ICC projections as well as the broad response areas of SSA neurons support the suggestion that adapting neurons integrate feedforward inputs with different frequency selectivity and feedback inputs that modulate the extent of SSA. In this regard, previous work in our lab (Anderson et al., 2009) showed that the corticofugal projection exerts mainly a gain control over the

SSA response, eliciting changes in SSA in either direction, increasing or decreasing it. However, very few SSA responses are generated *de novo* or abolished completely by inactivation of the cortical inputs. The diverse effects of cortical manipulation on SSA responses might be explained by direct A1 inputs to synaptic domains in IC that contain neurons with different SSA sensitivities. Likewise, changes in A1 excitability may affect SSA in the IC by triggering the release of ACh through the disynaptic A1 → pontomesencephalic tegmentum → IC projection previously described (Motts and Schofield, 2009; Schofield, 2010).

In agreement with the above discussion, my iontophoresis experiments demonstrated that ACh exerts a baseline-dependent effect on SSA responses, exerting its greatest effect on IC neurons with intermediate SSA responses. ACh decreases the amount of SSA by increasing the response to the standard tone mainly through the activation of muscarinic receptors. A common mechanism by which ACh modulates neural activity is by transiently disrupting the excitatory-inhibitory balance of neural circuits (Froemke, 2015). This unbalance can be achieved by modulating the release of neurotransmitters (Metherate, 2011), for example, by decreasing the release of GABA from interneurons (Salgado et al., 2007) or by eliciting the activation of NMDA receptor-mediated glutamatergic neurotransmission (Metherate and Hsieh, 2003; Metherate, 2004; Liang et al., 2008). Thus, local augmentation of ACh contributes to the maintenance of the encoding of repetitive acoustical input by decreasing adaptation. Adjustment in the neural sensitivity in the IC to frequently occurring frequencies would contribute to boosting the bottom-up sensory information *en route* to the auditory cortex and agrees with the evidence that neuromodulators lead to enduring modifications of neural circuits via transient disinhibition (Froemke, 2015).

Overall, the data from my doctoral thesis show that SSA neurons are in a position to integrate higher-level signals with incoming sensory information and that the filtering of sensory feedforward information is under a fast, top-down adjustment of IC neural sensitivity likely via a direct feedback loop from auditory cortical areas and by the indirect activation of cholinergic synaptic inputs.

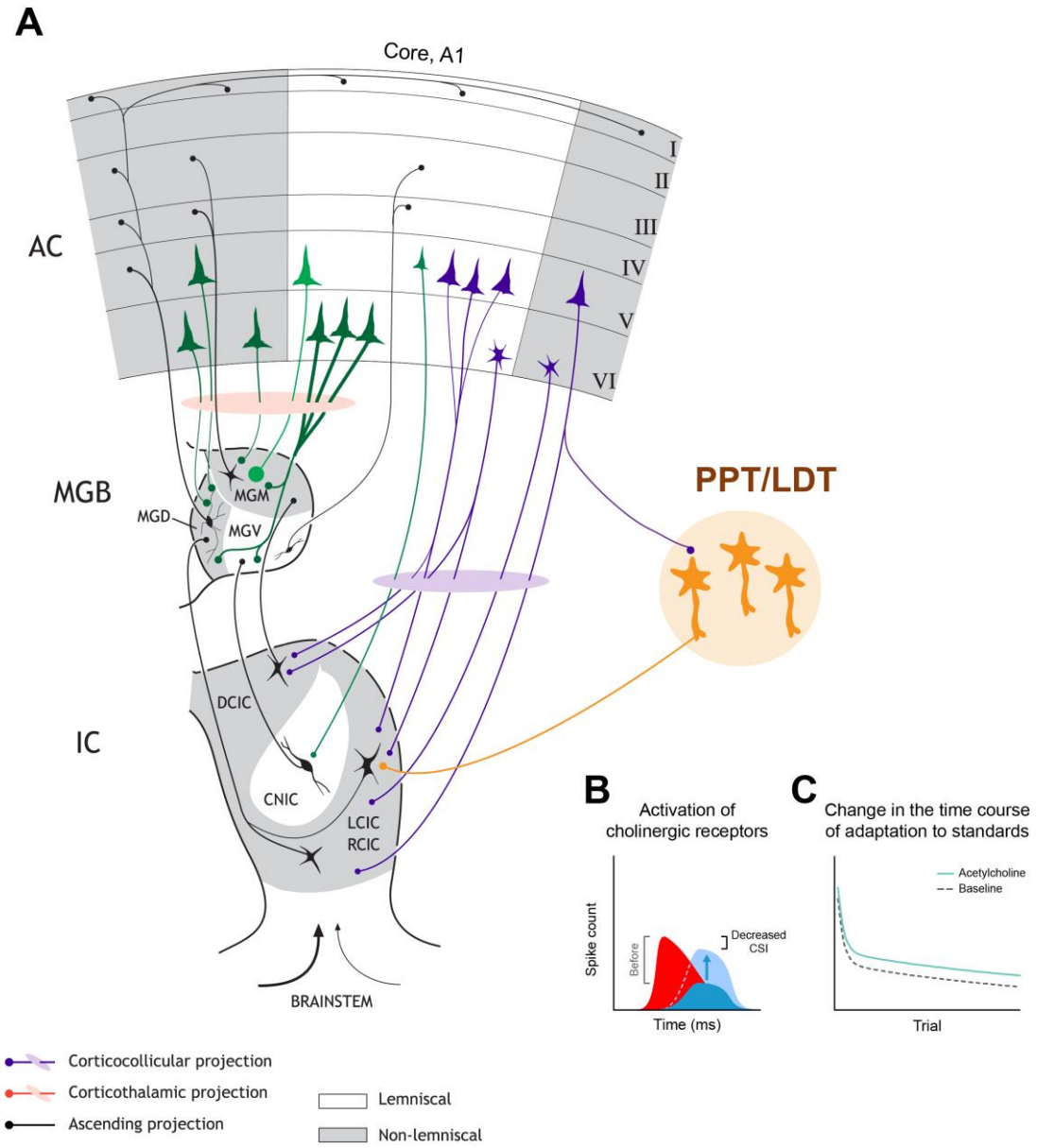

Figure 1. Schema of the connectivity between the auditory cortex and the inferior colliculus. SSA neurons are located in the non-lemniscal subdivisions of the inferior colliculus (IC) and they receive dense inputs from areas of the auditory cortex (AC) including the primary auditory field (A1). AC neurons innervate cholinergic neurons of the tegmental nuclei (PPT: pedunculopontine, LDT: laterodorsal tegmental nucleus) which project to the IC. The cholinergic inputs diminish the SSA of IC neurons by increasing only the responses to the standard tone (B). Likewise, acetylcholine increases the sustained component of the adaptation while the initial component of fast and slow decay remains unaffected (C). MGB: Medial geniculate body; MGM, MGD, MGV: medial, dorsal and ventral divisions of the MGB, respectively; DCIC, LCIC, RCIC; dorsal, lateral and rostral cortices of the IC, respectively; CNIC; central nucleus of the IC. CSI: SSA-Common Index. *Figure modified from Malmierca et al., 2015.*

7. Conclusions

I. SSA responses occur in the inferior colliculus at low stimulation rates on a time scale on the order of magnitude of seconds, whereas cochlear nucleus neurons fail to show SSA responses even at fast repetition rates. Thus, SSA is not a ubiquitous property of auditory neurons.

II. The persistence of SSA at long inter-stimulus intervals, similar to the time scale of cognition (Ulanovsky et al., 2003; Ulanovsky et al., 2004; Nelken and Ulanovsky, 2007), suggests that SSA is not merely a result of mechanisms such as synaptic fatigue and that subcortical SSA may contribute to the perceptual organization of the components of complex auditory stimuli (Winkler et al., 2009).

III. Neurons with extreme SSA levels are confined to the non-lemniscal divisions of the IC. Those neurons are likely to participate in synaptic domains formed by broadly tuned neurons characterized by non-oriented and widespread dendritic arbors.

IV. There is a segregation of cortical and brainstem inputs to the sites where SSA and non-SSA neurons are located within the IC, suggesting that there are unique microcircuits that generate SSA.

V. SSA neurons show a consistent pattern of afferent projections such that they receive strong inputs from auditory cortical areas and very few or even absent projections from the brainstem nuclei.

VI. SSA is modulated by cholinergic inputs such that acetylcholine affects SSA in a baseline-dependent manner, exerting its greatest effect on partially-adapting IC neurons.

VII. Acetylcholine decreases SSA in the IC by increasing the response to the standard tone mainly through the activation of the muscarinic receptors. The resulting adjustment in the IC neural sensitivity boosts the ascending auditory information converging in the auditory thalamus *en route* to the auditory cortex.

8. References

Adrian ED, Zotterman Y (1926a) The impulses produced by sensory nerve-endings: Part II. The response of a Single End-Organ. J Physiol 61:151-171.

Adrian ED, Zotterman Y (1926b) The impulses produced by sensory nerve endings: Part 3. Impulses set up by Touch and Pressure. J Physiol 61:465-483.

Anderson LA, Christianson GB, Linden JF (2009) Stimulus-specific adaptation occurs in the auditory thalamus. J Neurosci 29:7359-7363.

Antunes FM, Nelken I, Covey E, Malmierca MS (2010) Stimulus-specific adaptation in the auditory thalamus of the anesthetized rat. PLoS One 5:e14071.

Baylis GC, Rolls ET (1987) Responses of neurons in the inferior temporal cortex in short term and serial recognition memory tasks. Exp Brain Res 65:614-622.

Bendixen A, SanMiguel I, Schroger E (2012) Early electrophysiological indicators for predictive processing in audition: a review. Int J Psychophysiol 83:120-131.

Bialek W, Rieke F, de Ruyter van Steveninck RR, Warland D (1991) Reading a neural code. Science 252:1854-1857.

Bibikov NG (1977) ["Novelty" neurons in the frog auditory system]. Zh Vyssh Nerv Deiat Im I P Pavlova 27:1075-1082.

Boehnke SE, Berg DJ, Marino RA, Baldi PF, Itti L, Munoz DP (2011) Visual adaptation and novelty responses in the superior colliculus. Eur J Neurosci 34:766-779.

Brenner N, Bialek W, de Ruyter van Steveninck R (2000) Adaptive rescaling maximizes information transmission. Neuron 26:695-702.

Brown MW, Wilson FA, Riches IP (1987) Neuronal evidence that inferomedial temporal cortex is more important than hippocampus in certain processes underlying recognition memory. Brain Res 409:158-162.

Calford MB (1983) The parcellation of the medial geniculate body of the cat defined by the auditory response properties of single units. J Neurosci 3:2350-2364.

Carandini M (2007) Melting the iceberg: contrast invariance in visual cortex. Neuron 54:11-13.

Chechik G, Anderson MJ, Bar-Yosef O, Young ED, Tishby N, Nelken I (2006) Reduction of information redundancy in the ascending auditory pathway. Neuron 51:359-368.

Dean I, Harper NS, McAlpine D (2005) Neural population coding of sound level adapts to stimulus statistics. Nat Neurosci 8:1684-1689.

Desimone R (1996) Neural mechanisms for visual memory and their role in attention. Proc Natl Acad Sci U S A 93:13494-13499.

Duque D, Malmierca MS, Caspary DM (2014) Modulation of stimulus-specific adaptation by GABA(A) receptor activation or blockade in the medial geniculate body of the anaesthetized rat. J Physiol 592:729-743.

Duque D, Perez-Gonzalez D, Ayala YA, Palmer AR, Malmierca MS (2012) Topographic distribution, frequency, and intensity dependence of stimulus-specific adaptation in the inferior colliculus of the rat. J Neurosci 32:17762-17774.

Eytan D, Brenner N, Marom S (2003) Selective adaptation in networks of cortical neurons. J Neurosci 23:9349-9356.

Fairhall AL, Lewen GD, Bialek W, de Ruyter Van Steveninck RR (2001) Efficiency and ambiguity in an adaptive neural code. Nature 412:787-792.

Friauf E, Fischer AU, Fuhr MF (2015) Synaptic plasticity in the auditory system: a review. Cell Tissue Res.

Froemke RC (2015) Plasticity of Cortical Excitatory-Inhibitory Balance. Annu Rev Neurosci.

Froemke RC, Merzenich MM, Schreiner CE (2007) A synaptic memory trace for cortical receptive field plasticity. Nature 450:425-429.

Froemke RC, Carcea I, Barker AJ, Yuan K, Seybold BA, Martins AR, Zaika N, Bernstein H, Wachs M, Levis PA, Polley DB, Merzenich MM, Schreiner CE (2013) Long-term modification of cortical synapses improves sensory perception. Nat Neurosci 16:79-88.

Grill-Spector K, Henson R, Martin A (2006) Repetition and the brain: neural models of stimulus-specific effects. Trends Cogn Sci 10:14-23.

Gutfreund Y (2012) Stimulus-specific adaptation, habituation and change detection in the gaze control system. Biol Cybern 106:657-668.

Javitt DC, Steinschneider M, Schroeder CE, Vaughan HG, Jr., Arezzo JC (1994) Detection of stimulus deviance within primate primary auditory cortex: intracortical mechanisms of mismatch negativity (MMN) generation. Brain Res 667:192-200.

Kaliukhovich DA, Vogels R (2014) Neurons in macaque inferior temporal cortex show no surprise response to deviants in visual oddball sequences. J Neurosci 34:12801-12815.

Knott V, Impey D, Philippe T, Smith D, Choueiry J, de la Salle S, Dort H (2014) Modulation of auditory deviance detection by acute nicotine is baseline and deviant dependent in healthy nonsmokers: a mismatch negativity study. Hum Psychopharmacol 29:446-458.

Kraus N, McGee T, Littman T, Nicol T, King C (1994) Nonprimary auditory thalamic representation of acoustic change. J Neurophysiol 72:1270-1277.

Kudo M, Niimi K (1980) Ascending projections of the inferior colliculus in the cat: an autoradiographic study. J Comp Neurol 191:545-556.

Lee CC, Sherman SM (2011) On the classification of pathways in the auditory midbrain, thalamus, and cortex. Hear Res 276:79-87.

Liang K, Poytress BS, Weinberger NM, Metherate R (2008) Nicotinic modulation of tone-evoked responses in auditory cortex reflects the strength of prior auditory learning. Neurobiol Learn Mem 90:138-146.

Loftus WC, Malmierca MS, Bishop DC, Oliver DL (2008) The cytoarchitecture of the inferior colliculus revisited: a common organization of the lateral cortex in rat and cat. Neuroscience 154:196-205.

Lumani A, Zhang H (2010) Responses of neurons in the rat's dorsal cortex of the inferior colliculus to monaural tone bursts. Brain Res 1351:115-129.

Malmierca MS, Ryugo DK (2011) Descending connections of auditory cortex to the midbrain and brainstem. In: The Auditory Cortex. (Winer JA, Schreiner CE, eds), pp 189-208. New York: Springer.

Malmierca MS, Seip KL, Osen KK (1995a) Morphological classification and identification of neurons in the inferior colliculus: a multivariate analysis. Anat Embryol (Berl) 191:343-350.

Malmierca MS, Blackstad TW, Osen KK (2011) Computer-assisted 3-D reconstructions of Golgi-impregnated neurons in the cortical regions of the inferior colliculus of rat. Hear Res.

Malmierca MS, Anderson LA, Antunes FM (2015) The cortical modulation of stimulus-specific adaptation in the auditory midbrain and thalamus: a potential neuronal correlate for predictive coding. Front Syst Neurosci 9:19.

Malmierca MS, Rees A, Le Beau FE, Bjaalie JG (1995b) Laminar organization of frequency-defined local axons within and between the inferior colliculi of the guinea pig. J Comp Neurol 357:124-144.

Malmierca MS, Cristaudo S, Perez-Gonzalez D, Covey E (2009) Stimulus-specific adaptation in the inferior colliculus of the anesthetized rat. J Neurosci 29:5483-5493.

Malmierca MS, Blackstad TW, Osen KK, Karagulle T, Molowny RL (1993) The central nucleus of the inferior colliculus in rat: a Golgi and computer reconstruction study of neuronal and laminar structure. J Comp Neurol 333:1-27.

Malone BJ, Scott BH, Semple MN (2002) Context-dependent adaptive coding of interaural phase disparity in the auditory cortex of awake macaques. J Neurosci 22:4625-4638.

Maravall M (2013) Adaptation and sensory coding. In: Principles of neural coding (Quiroga RQ, Panzeri S, eds), pp 357-377. Boca Raton, FL: CRC Press.

May PJ, Westo J, Tiitinen H (2015) Computational modelling suggests that temporal integration results from synaptic adaptation in auditory cortex. Eur J Neurosci 41:615-630.

Metherate R (2004) Nicotinic acetylcholine receptors in sensory cortex. Learn Mem 11:50-59.

Metherate R (2011) Functional connectivity and cholinergic modulation in auditory cortex. Neurosci Biobehav Rev 35:2058-2063.

Metherate R, Weinberger NM (1989) Acetylcholine produces stimulus-specific receptive field alterations in cat auditory cortex. Brain Res 480:372-377.

Metherate R, Hsieh CY (2003) Regulation of glutamate synapses by nicotinic acetylcholine receptors in auditory cortex. Neurobiol Learn Mem 80:285-290.

Moran RJ, Campo P, Symmonds M, Stephan KE, Dolan RJ, Friston KJ (2013) Free energy, precision and learning: the role of cholinergic neuromodulation. J Neurosci 33:8227-8236.

Motts SD, Schofield BR (2009) Sources of cholinergic input to the inferior colliculus. Neuroscience 160:103-114.

Muller JR, Metha AB, Krauskopf J, Lennie P (1999) Rapid adaptation in visual cortex to the structure of images. Science 285:1405-1408.

Naatanen R, Escera C (2000) Mismatch negativity: clinical and other applications. Audiol Neurootol 5:105-110.

Naatanen R, Tervaniemi M, Sussman E, Paavilainen P, Winkler I (2001) "Primitive intelligence" in the auditory cortex. Trends Neurosci 24:283-288.

Nelken I (2014) Stimulus-specific adaptation and deviance detection in the auditory system: experiments and models. Biol Cybern 108:655-663.

Nelken I, Ulanovsky N (2007) Mismatch negativity and simulus-specific adaptation in animal models. J Psychophysiol 21:214 –223.

Oliver DL, Kuwada S, Yin TC, Haberly LB, Henkel CK (1991) Dendritic and axonal morphology of HRP-injected neurons in the inferior colliculus of the cat. J Comp Neurol 303:75-100.

Patel CR, Redhead C, Cervi AL, Zhang H (2012) Neural sensitivity to novel sounds in the rat's dorsal cortex of the inferior colliculus as revealed by evoked local field potentials. Hear Res 286:41-54.

Pérez-González D, Malmierca MS, Covey E (2005) Novelty detector neurons in the mammalian auditory midbrain. Eur J Neurosci 22:2879-2885.

Pérez-González D, Hernandez O, Covey E, Malmierca MS (2012) GABA(A)-Mediated Inhibition Modulates Stimulus-Specific Adaptation in the Inferior Colliculus. PLoS One 7:e34297.

Ranganath C, Rainer G (2003) Neural mechanisms for detecting and remembering novel events. Nat Rev Neurosci 4:193-202.

Ringo JL (1996) Stimulus specific adaptation in inferior temporal and medial temporal cortex of the monkey. Behav Brain Res 76:191-197.

Saldana E, Merchan MA (1992) Intrinsic and commissural connections of the rat inferior colliculus. J Comp Neurol 319:417-437.

Salgado H, Bellay T, Nichols JA, Bose M, Martinolich L, Perrotti L, Atzori M (2007) Muscarinic M2 and M1 receptors reduce GABA release by Ca2+ channel

modulation through activation of PI3K/Ca2+ -independent and PLC/Ca2+ -dependent PKC. J Neurophysiol 98:952-965.

Schofield BR (2010) Projections from auditory cortex to midbrain cholinergic neurons that project to the inferior colliculus. Neuroscience 166:231-240.

Shadlen MN, Newsome WT (1994) Noise, neural codes and cortical organization. Curr Opin Neurobiol 4:569-579.

Shamma S (2001) On the role of space and time in auditory processing. Trends Cogn Sci 5:340-348.

Summerfield C, de Lange FP (2014) Expectation in perceptual decision making: neural and computational mechanisms. Nat Rev Neurosci 15:745-756.

Thiele A (2013) Muscarinic signaling in the brain. Annu Rev Neurosci 36:271-294.

Thomas JM, Morse C, Kishline L, O'Brien-Lambert A, Simonton A, Miller KE, Covey E (2012) Stimulus-specific adaptation in specialized neurons in the inferior colliculus of the big brown bat, Eptesicus fuscus. Hear Res.

Todorovic A, de Lange FP (2012) Repetition suppression and expectation suppression are dissociable in time in early auditory evoked fields. J Neurosci 32:13389-13395.

Ulanovsky N, Las L, Nelken I (2003) Processing of low-probability sounds by cortical neurons. Nat Neurosci 6:391-398.

Ulanovsky N, Las L, Farkas D, Nelken I (2004) Multiple time scales of adaptation in auditory cortex neurons. J Neurosci 24:10440-10453.

von der Behrens W, Bauerle P, Kossl M, Gaese BH (2009) Correlating stimulus-specific adaptation of cortical neurons and local field potentials in the awake rat. J Neurosci 29:13837-13849.

Winkler I, Denham SL, Nelken I (2009) Modeling the auditory scene: predictive regularity representations and perceptual objects. Trends Cogn Sci 13:532-540.

Yu XJ, Xu XX, He S, He J (2009) Change detection by thalamic reticular neurons. Nat Neurosci 12:1165-1170.

Zhao L, Liu Y, Shen L, Feng L, Hong B (2011) Stimulus-specific adaptation and its dynamics in the inferior colliculus of rat. Neuroscience 181:163-174.

9. Apartado en Español

Correlación Morfofuncional de la Adaptación a Estímulos Específicos en el Cerebro Auditivo

Tesis Doctoral elaborada por:

Yaneri Aguilar Ayala

Índice

1. Introducción…….…….…….x
2. Hipótesis…….…….……...x
3. Objetivos……x
4. Resumen de Resultados……...…….x
5. Conclusiones…….……x

1. Introducción

La representación neural de un ambiente sensorial altamente cambiante requiere de mecanismos especializados que codifiquen su estructura dinámica. Los trabajos clásicos de E.D. Adrian demostraron que el disparo de potenciales de acción de las fibras aferentes primarias varía en función de la intensidad del estímulo y, más aún, que la actividad de disparo decrece ante una estimulación mantenida a lo largo del tiempo (Adrian y Zotterman, 1926a,b). Estos resultados dieron lugar a un principio fundamental en el estudio de la codificación neuronal que indica que las neuronas sensoriales representan la ocurrencia y propiedades de los estímulos mediante un código de frecuencia de disparo (Shadlen y Newsome, 1994). A partir de ese momento, surgió un área de investigación en neurociencias que busca averiguar cuánta información sobre el mundo externo se puede representar en el disparo de una sola neurona (Bialek et al., 1991).

Dado que los estímulos naturales no son estáticos sino que varían a lo largo del tiempo y espacio, las neuronas sensoriales adaptan su excitabilidad a la distribución estadística de los mismos. Dicho de otro modo, las respuestas neuronales no son lineales sino que dependen del contexto de estimulación (Muller et al., 1999; Brenner et al., 2000; Fairhall et al., 2001; Dean et al., 2005). Por ejemplo, la representación de señales acústicas requiere de mecanismos neuronales sensibles al contexto de estimulación previa (Shamma, 2001; Bendixen et al., 2012; May et al., 2015). Uno de estos mecanismo es la adaptación en la respuesta neural ante un estímulo repetitivo ya que de esta manera las neuronas auditivas disminuyen la transmisión de información redundante (Chechik et al., 2006) y ajustan su rango dinámico de sensibilidad para seguir codificando nuevos estímulos (Muller et al., 1999; Dean et al., 2005). Podemos afirmar, que existen distintos procesos de adaptación ante estímulos repetitivos de diferentes modalidades sensoriales en muchas áreas cerebrales (Grill-Spector et al., 2006; Todorovic and de Lange, 2012; Summerfield and de Lange, 2014). Por ejemplo, neuronas de la corteza temporal inferior (Baylis y Rolls, 1987; Desimone, 1996; Kaliukhovich y Vogels, 2014), la corteza medial temporal (Brown et al., 1987; Ringo, 1996), la corteza estriada (Muller et al., 1999), y el colículo superior (Boehnke et al., 2011) disminuyen o suprimen su disparo ante estímulos visuales invariantes. De manera similar, neuronas especializadas en el cerebro auditivo codifican la

ocurrencia de sonidos en función de su probabilidad de aparición independientemente de la identidad física del estímulo. La existencia de neuronas auditivas que adaptan su respuesta ante un estímulo repetitivo pero que restablecen su disparo ante la presentación de un sonido diferente, se describieron por primera vez en el tálamo auditivo (gato: Calford, 1983; cobaya: Kraus et al., 1994) y en el *torus semicirulares*, un núcleo análogo al colículo inferior de los mamíferos (sapo; Bibikov, 1977).

Más recientemente, Ulanovsky y colaboradores (2003) demostraron que neuronas de la corteza auditiva primaria (A1) son capaces de representar la ocurrencia de sonidos discrepantes y repetitivos variando su tasa de disparo. Estas neuronas exhiben una propiedad de respuesta llamada adaptación a estímulos específicos (SSA; por sus siglas en ingles de stimulus-specific adaptation). La SSA se define como una reducción en la respuesta neural a estímulos repetitivos que no se generaliza, o solo parcialmente, a otros, sonidos infrecuentes. En el estudio original de Ulanovsky y colaboradores, se realizó una estimulación empleando el paradigma discrepante compuesto por una secuencia de sonidos formada por un tono puro presentado con alta probabilidad de ocurrencia (estímulo estándar) que era remplazado aleatoriamente por otro sonido de baja probabilidad de ocurrencia (estímulo desviado). Malmierca y colaboradores (2009) usando el mismo protocolo de estimulación, demostraron que algunas neuronas del colículo inferior (CI) de la rata también exhibían SSA en su respuesta. Este estudio confirmó observaciones previas que indicaban la existencia de una clase de neuronas del CI que muestra una adaptación rápida y pronunciada ante la presentación repetitiva de sonidos (Bibikov, 1977; Pérez-González et al., 2005). Estudios subsecuentes demostraron que neuronas del cuerpo geniculado medial (CGM) (Anderson et al., 2009; Antunes et al., 2010) también presentaban SSA, indicando que, más que una propiedad específica de áreas superiores de procesamiento auditivo (Ulanovsky et al., 2003), la SSA era un fenómeno común a lo largo de la vía auditiva. Es muy probable que las neuronas que presentan SSA integren información espectral a lo largo del tiempo a través de cambios plásticos en sus conexiones sinápticas (Friauf et al., 2015). Por ello, se ha considerado que la SSA podría ser una forma de habituación neuronal que contribuye a procesos observados a escalas temporales y

espaciales mayores y que involucran múltiples circuitos en diversas áreas cerebrales. Estos procesos en su conjunto se conocen como *'saliency mapping'* (Gutfreund, 2012).

La SSA se caracteriza por una sensibilidad muy exquisita y delicada a los parámetros de estimulación, tales como, la probabilidad de ocurrencia, el contraste entre las frecuencias de los sonidos estándar y repetitivo, así como el intervalo de tiempo entre estímulos (Ulanovsky et al., 2003; Malmierca et al., 2009; von der Behrens et al., 2009; Yu et al., 2009; Antunes et al., 2010; Zhao et al., 2011). Por otro lado, la SSA de las neuronas de A1 es muy sensible a cambios muy pequeños en los parámetros de estimulación. Así por ejemplo, estas neuronas discriminan sonidos de frecuencias muy cercanas entre sí (de tan solo 0.15 octavas de diferencia) sólo si son presentados con diferente probabilidad de ocurrencia. La SSA en A1 se mantiene a frecuencias de estimulación con intervalos entre estímulos muy largos de hasta 2 segundos (Ulanovsky et al., 2003). Dado que la duración de la adaptación en las neuronas de A1 puede ser muy larga, se sugirió que la SSA podría ser el correlato neuronal de señales de detección de estímulos novedosos reflejadas en estudios de potenciales evocados en humanos. La detección de novedad sensorial requiere de mecanismos de acumulación y comparación de información a lo largo del tiempo (Naatanen et al., 2001) y, la escala temporal de segundos en la que ocurre la SSA cortical es compatible con la duración de la memoria sensorial (ecoica) en monos y humanos (Javitt et al., 1994; Naatanen y Escera, 20009). En el CI, se observa SSA a intervalos entre estímulos de 500 ms sin embargo las respuestas de SSA más fuertes son evocadas por estímulos presentados a intervalos entre estímulos de 250 ms (Malmierca et al., 2009). De manera similar, las neuronas del CGM también exhiben SSA a intervalos de tiempo en la escala de los segundos como las neuronas de A1 (Antunes et al., 2010).

Neuronas con niveles altos de SSA se encuentran localizadas en las divisiones no-lemniscales de núcleos subcorticales. Estas áreas corresponden a las cortezas del CI (CxIC; Malone et al., 2002; Pérez-González et al., 2005; Malmierca et al., 2009; Lumani and Zhang, 2010), así como la división medial y dorsal del CGM (Antunes et al., 2010). Tanto en el CI como en el CGM, las subdivisiones no-lemniscales están inervadas fuertemente por proyecciones provenientes de A1 y de áreas no auditivos (Loftus et al., 2008; Lee y Sherman, 2011; Malmierca and Ryugo, 2011; Malmierca et al., 2015). Las propiedades de

respuesta y morfología de las neuronas de las CxIC difieren del núcleo central (NCCI) que es la división lemniscal de CI. El patrón de disparo predominante de las neuronas de las CxCI es de tipo ‘encendido’ y presentan latencias mayores que las neuronas de NCIC. También, las neuronas de la corteza dorsal y rostral del CI presentan arboles dendríticos amplios y desorientados, mientras que, las neuronas del NCCI están orientadas en láminas de isofrecuencias y presentan árboles dendríticos más pequeños (Malmierca et al., 1993; Malmierca et al., 1995b; Malmierca et al., 20119). La diferencia en el grado de SSA observada entre neuronas del CNCI y de las CxCI sugiere que tanto las propiedades intrínsecas de las neuronas (i.e., propiedades de membrana) y/o su patrón de conexiones neurales podrían contribuir significativamente en la generación de la SSA. De igual manera, es muy probable que neuronas con niveles parecidos de SSA compartan entradas sinápticas comunes y que formen grupos neuronales con propiedades fisiológicas similares. La observación de respuestas disminuidas a estímulos repetitivos y no a estímulos divergentes en registros de potenciales de campo en el CI refuerzan esta idea, ya que estos registros combinan la señal de las entradas sinápticas a grupos de neuronas dentro de un radio determinado (Patel et al., 2012).

También, otros estudios sugieren que las entradas sinápticas podrían estar jugando un papel fundamental en la generación y/o modulación de las respuestas de SSA (Eytan et al., 2003; Duque et al., 2012; Thomas et al., 2012). Por ejemplo, se ha observado que la magnitud de SSA no es evocada de manera homogénea por todas las frecuencias e intensidades que conforman el campo receptivo neuronal. Lo anterior sugiere que la SSA es modulada por la combinación de entradas aferentes que integra la neurona más que por sus propiedades intrínsecas (Duque et al., 2012).Estudios complementarios de microiontoforesis realizados en el CI (Pérez-González et al., 2012) y en el CGM de la rata (Duque et al., 2014) revelaron que las entradas inhibitorias mediadas por GABA modulan la SSA a través de un mecanismo de control de ganancia incrementando la excitabilidad global neuronal. Sin embargo, el bloqueo de los receptores GABAérgicos y glicinérgicos no extinguió la SSA por lo que es muy probable que otras y/o la combinación de entradas sinápticas adicionales puedan estar generando la SSA. A este respecto, se sabe que los sistemas neuromoduladores controlan el balance entre entradas excitatorias e inhibitorias

(Ranganath and Rainer, 2003; Thiele, 2013; Froemke, 2015) o que son capaces de generar efectos específicos a un estímulo repetitivo (Froemke, 2015). Por otro lado, un estudio de potenciales evocados en humanos (Moran et al., 2013) demostró que la aplicación sistémica de un inhibidor de la acetilcolinesterasa (enzima localizada en la hendidura sináptica y que degrada a la acetilcolina) atenúa la adaptación evocada por estímulos repetitivos conocida como supresión por repetición. Asimismo, otro estudio en humanos demostró que los niveles sistémicos de nicotina incrementan o disminuyen la detección de cambios en la estimulación de manera dependiente a los niveles basales de sensibilidad de cada sujeto (Knott et al., 2014). Considerando todo lo anterior, es plausible proponer que la adaptación neuronal en el CI refleja mecanismos de procesamiento que involucran entradas sinápticas específicas que convergen en las neuronas que exhiben SSA y no en otro tipo de neuronas del mismo núcleo.

2. Hipótesis

En el momento presente, se desconoce el mecanismo que genera la SSA. Como se mencionó anteriormente, una característica de la SSA a nivel de la A1 (Ulanovsky et al., 2003; Ulanovsky et al., 2004) y del tálamo auditivo (Antunes et al., 2010) y, que la distingue de otras formas de adaptación neuronal, es que la SSA ocurre a frecuencias de estimulación muy lenta. Se desconoce si la SSA también ocurre en el CI en el mismo orden temporal de segundos. La presencia de SSA en esta escala de tiempo sugiere que mecanismos como la fatiga neuronal o acomodación no participan, o al menos no totalmente, en la generación de la SSA. Por lo tanto, es más probable que mecanismos de plasticidad a corto plazo, tales como, depresión sináptica (Friauf et al., 2015) estén ocurriendo de manera específica en las entradas sinápticas que están siendo estimuladas de manera repetitiva sin provocar una adaptación generalizada de la neurona (Eytan et al., 2003; Grill-Spector et al., 2006; Nelken, 2014). De manera similar, la distribución de respuestas extremas de SSA en las divisiones corticales no-lemniscales del CI y del CGM (Malmierca et al., 2009; Antunes et al., 2010; Duque et al., 2012) sugiere que circuitos neuronales comunes a esas subdivisiones pueden participar en la generación de la SSA. Por otro lado, conviene subrayar que la separación de la vía auditiva en una división lemniscal y no-lemniscal emerge en el CI (Lee and Sherman, 2011) por lo que si la SSA depende de las naturaleza de microcircuitos específicos a esas divisiones, está también aparecería por primera vez en el CI. Esta cuestión no ha sido resuelta puesto que la presencia de SSA en núcleos auditivos previos al CI no ha sido explorada.

Estudios del papel de las entradas sinápticas sobre la SSA, indican que la inhibición modula pero no genera la SSA en el CI (Pérez-González et al., 2012) y CGM (Duque et al., 2014). De tal manera, que otras sustancias neuroactivas pueden estar participando en esta adaptación no generalizada de la respuesta. La acetilcolina (ACh) podría ser un candidato muy probable ya que se sabe que participa en fenómenos de plasticidad a corto plazo y que genera cambios específicos en las curvas de sintonización de neuronas auditivas (Metherate and Weinberger, 1989; Froemke et al., 2007; Froemke et al., 2013; Froemke, 2015). También, se sabe que ACh afecta la detección de novedad sensorial en humanos (Moran et al., 2013).

Considerando todo lo mencionado anteriormente, planteamos las siguientes hipótesis:

I. Las neuronas del CI son capaces de detectar estímulos discrepantes que ocurren en un orden temporal de segundos, así mismo, su sensibilidad a frecuencias de sonido se correlaciona con el grado de SSA en su respuesta.

II. Las neuronas con alto grado de SSA están restringidas a las cortezas del CI y reciben diferentes entradas sinápticas que aquellas neuronas que no muestran SSA. Por lo tanto, la SSA es una propiedad observadas en circuitos neuronales específicos y no una respuesta común observada en todos los niveles de la vía auditiva.

III. Las entradas sinápticas colinérgicas afectan la SSA en neuronas del CI.

3. Objetivos

En base a las hipótesis plantadas anteriormente, proponemos los siguientes objetivos:

I. Determinar si las neuronas del CI exhiben SSA en la escala temporal de segundos.

II. Describir el grado en que la sensibilidad para discriminar frecuencias de sonido refleja el grado de SSA y cómo la discriminación neural es afectada por el contexto de estimulación.

III. Determinar si la SSA es una propiedad común a diferentes núcleos de la vía auditiva por debajo del CI.

IV. Determinar las fuentes de proyecciones aferentes hacías las neuronas del CI que exhiben SSA.

V. Explorar si las entradas colinérgicas afectan la SSA en la respuesta de neuronas del CI.

4. Resumen de los resultados

Estudio 1. Discriminación a frecuencias de sonido y detección de novedad sensorial en el colículo inferior y núcleo coclear.

Objetivo: Determinar si la discriminación a frecuencias de sonido de neuronas del CI y de los núcleos cocleares (NC) depende del contexto de estimulación y hasta qué punto esta capacidad de discriminación refleja el grado de SSA que estas neuronas exhiben.

Metodología: Se registró la actividad extracelular unitaria de neuronas del CI y de los NC en la rata anestesiada. Se analizó la respuesta neuronal a estímulos estándar y discrepantes presentados en diferentes contextos de estimulación donde se varió la probabilidad de ocurrencia y el contraste físico entre las frecuencias de sonido. La sensibilidad neuronal se estimó en términos de probabilidad de disparo usando métodos de la teoría de detección de señales.

Resultados: Las neuronas del CI exhiben diferentes grados de SSA, mientras que, las neuronas de los NC no muestran SSA en sus respuestas. Además, se encontró que la discriminación de frecuencias de sonido de las neuronas del CI se mejora cuando se varía la probabilidad de presentación de los estímulos, mientas que, la discriminación de las neuronas de los NC es insensible al contexto probabilístico de estimulación.

Conclusiones: La SSA no es una propiedad ubicua y generalizada en neuronas de los NC y, por lo tanto, no es común a todos los niveles de la vía auditiva. También, los resultados de este estudio sugieren que la SSA mejora la sensibilidad a frecuencias de sonido de neuronas auditivas mucho más allá de lo esperado en base a sus curvas de sintonización.

Estudio 2. Adaptación a estímulos específicos y detección de novedad sensorial en el colículo inferior.

Objetivo: Determinar si las neuronas del CI exhiben SSA en su respuesta a estímulos presentados en el orden de los segundos.

Metodología: Se registró la respuesta extracelular unitaria de neuronas del CI de la rata anestesiada a estímulos estándar y discrepantes con diferente contraste de frecuencias y presentados a intervalos inter-estímulos de 500, 1000 y 2000 ms. Se cuantifico la magnitud de disparo así como la latencia de las respuestas a ambos estímulos.

Resultados: Las neuronas del CI son capaces de responder de manera diferencial a estímulos estándar y discrepantes aun cuando estos sean muy similares entre sí y presentados a muy bajas frecuencias de estimulación. Esta respuesta diferencial refleja la SSA que estas neuronas exhiben y, que también afecta a la latencia de sus respuestas.

Conclusiones: La SSA en núcleos subcorticales puede contribuir a procesos de detección de novedad sensorial con dinámicas de larga duración y que se reflejan en la actividad de potenciales de campo. La persistencia de SSA en la escala de los segundos sugiere que mecanismos tales como fatiga neuronal no generan del todo este tipo de respuestas.

Estudio 3. Diferencias en la densidad de proyecciones corticales y de núcleos del tallo cerebral hacia neuronas del colículo inferior que exhiben o no SSA.

Objetivo: Determinar si las neuronas que exhiben o que carecen de SSA en su respuesta forman parte de un mismo microcircuito neuronal en el CI.

Metodología: Se registró la respuesta de neuronas aisladas a la presentación de estímulos estándar y discrepantes en diferentes subdivisiones del CI. Posteriormente, se inyectó por iontoforesis un volumen minúsculo de un trazador retrogrado (fluorogold al 2%) en la zona de registro para correlacionar las zonas de proyección con el sitio de registro. Se realizaron técnicas histológicas para reconstruir los sitios de registro y determinar las neuronas que envían proyecciones a las zonas de registro en el CI.

Resultados: Las neuronas con SSA en su respuesta se localizaron en las CxCI mientras que las neuronas que no se adaptaron ante un estímulo repetitivo se localizaron en el NCCI. Además, estos dos grupos de neuronas mostraron propiedades espectrales y patrones de disparo diferentes. Los lugares de registro de neuronas con SSA están inervados densamente y/o exclusivamente por neuronas localizadas en la corteza auditiva primaria así

como en áreas corticales más dorsales y ventrales. Por el contrario, los lugares de registro de neuronas sin SSA recibieron principalmente y/o exclusivamente proyecciones de neuronas de núcleos del tronco del encéfalo. Estas proyecciones se organizaron de manera tonotópica.

Conclusiones: Nuestros resultados sugieren que las neuronas con SSA están inervadas principalmente por neuronas corticales y, que a su vez, éstas pueden estar formando dominios sinápticos, es decir, grupos de neuronas con propiedades de respuesta similares y que comparten entradas sinápticas similares. Así mismo, debido a su patrón de entradas sinápticas, estas neuronas podrían integrar información provenientes de centros superiores de procesamiento auditivo o multimodal con información auditiva proveniente de circuitos locales dentro del propio CI.

Estudio 4. Modulación colinérgica de la adaptación a estímulos específicos en el colículo inferior.

Objetivo: Determinar si la SSA en neuronas del CI está modulada por acetilcolina y, en su caso, describir la participación de los dos grupos de receptores colinérgicos.

Metodología: Se realizaron registros de la actividad extracelular de neuronas aisladas del CI en ratas anestesiadas antes, durante y después de la aplicación a nivel sináptico de ACh. Se utilizó la técnica de microiontoforesis para la liberación local y controlada de volúmenes muy reducidos de ACh, así como la liberación de antagonistas de los receptores nicotínicos y muscarínicos. Al finalizar el registro electrofisiológico, se realizaron lesiones electrolíticas en los sitios de registro para posteriormente determinar la localización de las neuronas en las diferentes divisiones del CI.

Resultados: La aplicación de ACh disminuyó los niveles de SSA al incrementar selectivamente la respuesta al estímulo estándar. La magnitud de efecto de la ACh sobre la SSA fue dependiente de los niveles de SSA que estas neuronas exhibieron en la condición control. La respuesta de las neuronas con niveles extremos de SSA, así como la respuesta de aquellas neuronas que no mostraron SSA, no fue afectada por ACh. También, se

demostró que la modulación colinérgica sobre la SSA esta mediada principalmente por los receptores muscarínicos. Tanto la ACh, como los antagonistas de los receptores colinérgicos afectaron únicamente el componente sostenido del curso temporal de la adaptación al estímulo estándar, sin afectar al componente de decaimiento rápido o lento de la misma. Neuronas sensibles a ACh se localizaron en tres divisiones del CI; la corteza rostral, lateral y el núcleo central.

Conclusiones: El neuromodulador ACh aumenta la sensibilidad de neuronas con niveles intermedios de SSA a los estímulos estándar. Este incremento en la representación de los estímulos repetitivos podría contribuir a un aumento generalizado en la sensibilidad del sistema auditivo a la estimulación continua.

Estudio 5. Detección de desviaciones en la estimulación en estructuras auditivas subcorticales: ¿qué podemos aprender de su neuroquímica y de su conectividad neuronal?

El objetivo de este estudio fue presentar una revisión de la SSA en núcleos auditivos subcorticales, haciendo énfasis específicamente en el colículo inferior y en el cuerpo geniculado medial del tálamo. Se discutió la distribución de receptores así como los patrones de conexiones neurales de las divisiones de estos núcleos en las que se concentran neuronas con altos niveles de SSA. Asimismo, se discuten las semejanzas y diferencias entre la SSA, respuestas de potenciales de campo y de potenciales evocados de media y larga latencia. Una característica común a las áreas donde se observan respuestas sensibles al contexto de estimulación es que reciben entradas sinápticas de más de una modalidad sensorial y exhiben una rápida adaptación a la estimulación repetitiva. Este trabajo propone que la identificación de similitudes en la respuesta, conectividad e inmunocitoquímica de estos núcleos auditivos y no auditivos sensibles contribuirá a revelar los posibles mecanismos que subyacen a la detección de cambios y novedad sensorial.

Estudio 6. Adaptación a estímulos específicos en el colículo inferior: el papel de las entradas sinápticas excitatorias, inhibitorias y moduladoras.

El objetivo fue comparar el papel de receptores glutamatérgicos, GABAérgicos y colinérgicos en la modulación de la SSA en neuronas del colículo inferior de la rata anestesiada. Se compara el efecto de diferentes agonistas y antagonistas de los mencionados receptores sobre la magnitud de disparo, latencia de respuesta e índices de SSA. Los datos indicaron que tanto las entradas excitatorias como inhibitorias modulan la SSA a través de un mecanismo de control de ganancia modificando la excitabilidad general de las neuronas, mientras que las entradas colinérgicas ejercen un efecto más selectivo sobre la respuesta a estímulos estándar. Estos resultados sugieren que las entradas sinápticas mediadas por los tres sistemas de neurotransmisión modulan de manera complementaria la SSA pero no la generan.

5. Conclusiones

I. La SSA está presente en las respuestas de neuronas del colículo inferior a bajas frecuencias de estimulación del orden de segundos, mientras que, las neuronas de los núcleos cocleares no muestran SSA incluso a altas frecuencias de estimulación de estímulos repetitivos.

II. La persistencia de la SSA durante frecuencias de estimulación bajas sugiere que la SSA puede contribuir a la segregación y percepción de componentes de estímulos auditivos complejos (Nelken y Ulanovsky, 2007; Winkler et al., 2009).

III. Las neuronas que exhiben SSA extrema están localizadas en las divisiones no-lemniscales del colículo inferior. Es muy probable que estas neuronas formen dominios sinápticos de neuronas con una amplia sintonización a frecuencias de sonido y con árboles dendríticos amplios y desorientados.

IV. Existe una segregación en las fuentes de proyecciones aferentes hacía las neuronas del CI que exhiben SSA o que carecen de ella, sugiriendo la existencia de un microcircuito único que genera la SSA.

V. Las neuronas que exhiben SSA muestran un patrón consistente de proyecciones aferentes, esto es, proyecciones densas provenientes de áreas corticales auditivas y muy pocas proyecciones o prácticamente inexistentes desde núcleos del tronco del encéfalo.

VI. La acetilcolina incrementa específicamente la respuesta a los estímulos estándar. El ajuste en la sensibilidad de las neuronas del CI mediado por la acetilcolina podría contribuir a favorecer la transmisión de la información sensorial proveniente de los órganos periféricos y que converge en el tálamo auditivo en ruta hacia la corteza.

VII. La acetilcolina disminuye la SSA en neuronas del CI principalmente a través de la activación de los receptores muscarínicos.

10. Publications

frontiers in
NEURAL CIRCUITS

ORIGINAL RESEARCH ARTICLE
published: 14 January 2013
doi: 10.3389/fncir.2012.00119

Frequency discrimination and stimulus deviance in the inferior colliculus and cochlear nucleus

Yaneri A. Ayala[1], David Pérez-González[1], Daniel Duque[1], Israel Nelken[2] and Manuel S. Malmierca[1,3]*

[1] Auditory Neurophysiology Laboratory, Institute of Neuroscience of Castilla y León, University of Salamanca, Salamanca, Spain
[2] Department of Neurobiology, Institute of Life Sciences, The Interdisciplinary Center for Neural Computation and the Edmond and Lily Safra Center for Brain Sciences, The Hebrew University of Jerusalem, Jerusalem, Israel
[3] Department of Cell Biology and Pathology, Faculty of Medicine, University of Salamanca, Salamanca, Spain

Edited by:
Eric D. Young, Johns Hopkins University, USA

Reviewed by:
Sarah L. Pallas, Georgia State University, USA
Edward L. Bartlett, Purdue University, USA

****Correspondence:***
Manuel S. Malmierca, Laboratory for the Neurobiology of Hearing, Auditory Neurophysiology Unit (Lab 1), Institute of Neuroscience of Castilla y León, University of Salamanca, C/ Pintor Fernando Gallego 1, 37007 Salamanca, Spain. e-mail: msm@usal.es

Auditory neurons that exhibit stimulus-specific adaptation (SSA) decrease their response to common tones while retaining responsiveness to rare ones. We recorded single-unit responses from the inferior colliculus (IC) where SSA is known to occur and we explored for the first time SSA in the cochlear nucleus (CN) of rats. We assessed an important functional outcome of SSA, the extent to which frequency discriminability depends on sensory context. For this purpose, pure tones were presented in an oddball sequence as standard (high probability of occurrence) or deviant (low probability of occurrence) stimuli. To study frequency discriminability under different probability contexts, we varied the probability of occurrence and the frequency separation between tones. The neuronal sensitivity was estimated in terms of spike-count probability using signal detection theory. We reproduced the finding that many neurons in the IC exhibited SSA, but we did not observe significant SSA in our CN sample. We concluded that strong SSA is not a ubiquitous phenomenon in the CN. As predicted, frequency discriminability was enhanced in IC when stimuli were presented in an oddball context, and this enhancement was correlated with the degree of SSA shown by the neurons. In contrast, frequency discrimination by CN neurons was independent of stimulus context. Our results demonstrated that SSA is not widespread along the entire auditory pathway, and suggest that SSA increases frequency discriminability of single neurons beyond that expected from their tuning curves.

Keywords: SSA, deviant sensitivity, change detection, mismatch negativity, non-lemniscal pathway, ROC analysis

INTRODUCTION

Auditory neurons displaying stimulus-specific adaptation (SSA) decrease their response to high probability stimuli (standards) while maintaining responsiveness to rare ones (deviants, Ulanovsky et al., 2003). SSA is correlated with behavioral habituation (Netser et al., 2011; Gutfreund, 2012) and it has been proposed to underlie sensory memory for stimulation history (Ulanovsky et al., 2004). Neurons showing SSA have been found in the mammalian auditory pathway from the inferior colliculus (IC) up to the cortex (Ulanovsky et al., 2003; Pérez-González et al., 2005; Anderson et al., 2009; Malmierca et al., 2009; von der Behrens et al., 2009; Yu et al., 2009; Antunes et al., 2010; Lumani and Zhang, 2010; Reches et al., 2010; Taaseh et al., 2011; Zhao et al., 2011; Ayala and Malmierca, 2012; Duque et al., 2012; Anderson and Malmierca, 2013) as well as in bird midbrain and forebrain (Reches and Gutfreund, 2008, 2009). Originally, SSA was suggested to emerge in the auditory cortex and to be transmitted downstream to subcortical nuclei through the corticofugal pathway (Nelken and Ulanovsky, 2007), as subcortical SSA is mostly confined to the non-lemniscal regions (Malmierca et al., 2009; Antunes et al., 2010; Duque et al., 2012), the main target of the corticofugal projections (Malmierca and Ryugo, 2011). However, it has been recently shown that cortical deactivation does not affect SSA neither in the non-lemniscal auditory thalamus (Antunes and Malmierca, 2011) nor in the IC (Anderson and Malmierca, 2013), while SSA in lemniscal regions is minimal (Malmierca et al., 2009; Antunes et al., 2010; Bäuerle et al., 2011). Thus, SSA may be computed independently in the non-lemniscal pathway and in primary auditory cortex. Thus far, the existence of SSA has not been explored in auditory nuclei below the IC, where the lemniscal and non-lemniscal divisions first emerge.

Frequency discrimination has been widely explored in psychoacoustics (Nelson and Kiester, 1978; Sinnott et al., 1985; Syka et al., 1996; Talwar and Gerstein, 1998, 1999; Shofner, 2000; Witte and Kipke, 2005; Walker et al., 2009), but few studies tested the detection of frequency deviants by single neurons (Ulanovsky et al., 2003; Malmierca et al., 2009; von der Behrens et al., 2009). SSA has already been shown to result in a change in frequency discrimination performance by single neurons (Ulanovsky et al., 2003; Malmierca et al., 2009) but this relationship has not been thoroughly explored.

The main goal of our study is to compare the relationships between frequency discrimination and SSA in two neuronal populations; one at the IC that it is already known to exhibit SSA

and the other at a lower auditory structure, the cochlear nucleus (CN) where SSA has not been explored thus far. For this purpose we assessed whether the probabilistic context affects frequency discrimination as judged by signal detection theory (Green and Swets, 1966) based on distributions of spike counts, and to what extent changes in frequency discriminability reflect the degree of SSA in these two stations. We show that SSA and the enhancement in neurometric frequency discrimination in the IC are strongly correlated and that both depend on the frequency separation and deviant probability in similar ways. Our results also demonstrated that SSA and context-dependent neuronal sensitivity are not present in CN supporting the hypothesis that SSA first emerge in non-lemniscal IC.

MATERIALS AND METHODS

SURGICAL PROCEDURES

Experiments were performed on 71 adult female rats (*Rattus norvergicus*, Rj: Long–Evans) with body weights between 160 and 270 g. All experimental procedures were carried out at the University of Salamanca with the approval of, and using methods conforming to the standards of, the University of Salamanca Animal Care Committee. Anesthesia was induced (1.5 g/kg, i.p., 20% solution) and maintained (0.5 g/kg, i.p. given as needed) with urethane. Urethane was chosen as an anesthetic because of its effects on multiple aspects of neural activity, including inhibition and spontaneous firing, are known to be less than those of barbiturates and other anesthetic drugs (Hara and Harris, 2002). The respiration was maintained artificially (SAR-830/P Ventilator) monitoring the end-tidal CO_2 level (CapStar-100). For this purpose, the trachea was cannulated and atropine sulfate (0.05 mg/kg, s.c.) was administered to reduce bronchial secretions. Body temperature was maintained at 38 ± 1°C by means of a heating blanket. Details of surgical procedures have been described previously (Hernández et al., 2005; Pérez-González et al., 2005; Malmierca et al., 2009; Antunes et al., 2010). The animal was placed inside a sound-attenuated room in a stereotaxic frame in which the ear bars were replaced by a hollow speculum that accommodated a sound delivery system.

ACOUSTIC STIMULI AND ELECTROPHYSIOLOGICAL RECORDING

Extracellular single unit responses were recorded from neurons in the IC and CN in two separate sets of experiments. For the IC recordings, a craniotomy was performed to expose the cerebral cortex overlying the IC and a tungsten electrode (1 – 2 MΩ) (Merrill and Ainsworth, 1972) was lowered through the cortex by means of a piezoelectric microdrive (Burleigh 6000 ULN). Neuron identification in the IC was based on stereotaxic coordinates, physiological criteria of tonotopicity, and response properties (Rees et al., 1997; LeBeau et al., 2001; Malmierca et al., 2003; Hernández et al., 2005; Pérez-González et al., 2005, 2006). An electrode dorsoventral penetration (with an angle of 20° from the frontal plane) through the central nucleus of the IC is identified by the stepwise progression from low to high frequencies (Malmierca et al., 2008) and by the constant presence of tonically firing units (Rees et al., 1997). Typical responses of the neurons in the cortices of the IC (i.e., dorsal, lateral, and rostral) are characterized by longer response latencies, predominantly on-phasic firing patterns and weaker tonic firing than those from the central nucleus. Cortical IC neurons commonly display broadly tuned, W-shaped, or other complex tuning curves (Lumani and Zhang, 2010; Geis et al., 2011; Duque et al., 2012) and a clear topographic organization of the frequencies along the dorsal cortex is not present (Malmierca et al., 2008; Lumani and Zhang, 2010). For the recording of CN neurons, part of the cerebellum was carefully aspirated to visually localize the dorsal cochlear nucleus (DCN). Glass micropipettes filled with 2 M NaCl (15 – 25 MΩ) or tungsten electrodes (1 – 2 MΩ) were advanced into the DCN. For some IC experiments and most of the CN recordings, an electrolytic lesion (10 – 15 μA for 10 – 15 s) was applied for subsequent histological verification of the recording site. Brains were fixed using a mixture of 1% paraformaldehyde and 1% glutaraldehyde diluted in 0.4 M phosphate buffer saline (0.5% $NaNO_3$ in PBS). After fixation, tissue was cryoprotected in 30% sucrose and sectioned in the coronal or sagital plane at a thickness of 40 μm on a freezing microtome. Slices were Nissl stained with 0.1% cresyl violet to facilitate identification of cytoarchitectural boundaries. The CN units were assigned to one of the two main divisions (dorsal or ventral) of the nucleus using as reference the standard sections from a rat brain atlas (Paxinos and Watson, 2007).

Acoustic stimuli were delivered through a sealed acoustic system (Rees, 1990; Rees et al., 1997) using two electrostatic loudspeakers (TDT-EC1) driven by two TDT-ED1 modules. Search stimuli were pure tones or noise bursts monaurally delivered under computer control using TDT System 2 hardware (Tucker-Davis Technologies) and custom software (Faure et al., 2003; Pérez-González et al., 2005, 2006; Malmierca et al., 2008). The output of the system at each ear was calibrated *in situ* using a ¼ inch condenser microphone (Brüel and Kjær 4136, Nærum, Denmark) and a DI-2200 spectrum analyzer (Diagnostic Instruments Ltd., Livingston, Scotland, UK). The maximum output of the TDT system was flat from 0.3 to 5 kHz (∼100 ± 7 dB SPL) and from 5 to 40 kHz (90 ± 5 dB SPL). The highest frequency produced by this system was limited to 40 kHz. The second and third harmonic components in the signal were 40 dB or more below the level of the fundamental at the highest output level (Hernández et al., 2005; Malmierca et al., 2009).

Action potentials were recorded with a BIOAMP amplifier (TDT), the 10× output of which was further amplified and bandpass-filtered (TDT PC1; f_c: 0.5 – 3 kHz) before passing through a spike discriminator (TDT SD1). Spike times were logged at one microsecond resolution on a computer by feeding the output of the spike discriminator into an event timer (TDT ET1) synchronized to a timing generator (TDT TG6). Stimulus generation and on-line data visualization were controlled with custom software. Spike times were displayed as dot rasters sorted by the acoustic parameter varied during testing.

Once a neuron was isolated, the monoaural frequency response area (FRA), i.e., the combination of frequencies and intensities capable of evoking a response, was obtained by an automated procedure with 5 stimulus repetitions at each frequency (from 0.5 to 40 kHz, in 20 – 30 logarithmic steps) and intensity step (steps of 10 dB) presented randomly at a repetition

rate of 4 Hz. The stimuli used to generate the tuning curves were pure tones with duration of 75 ms. The neuronal response to the combination of frequencies and intensities was plotted using MATLAB software (Mathworks, Inc.) and the best frequency (BF) and threshold for each neuron were identified.

STIMULUS PRESENTATION PARADIGMS

For all neurons, stimuli were presented in an oddball paradigm similar to that used to record mismatch negativity responses in human studies (Näätänen, 1992), and more recently in the cat auditory cortex (Ulanovsky et al., 2003, 2004), rat IC (Malmierca et al., 2009; Pérez-González et al., 2012) and auditory thalamus (Antunes et al., 2010; Antunes and Malmierca, 2011). Briefly, we presented two stimuli consisting of pure tones at two different frequencies (f_1 and f_2), that elicited a similar firing rate and response pattern at the same level of 10 – 40 dB SPL above threshold. Both frequencies were within the excitatory response area previously determined for the neuron. A train of 400 stimulus presentations containing both frequencies was delivered in three different sequences (**Figure 1**). The repetition rate of the train of stimuli for the IC neurons was 4 Hz, as it has been previously demonstrated to be suitable to elicit SSA in IC neurons of the rat (Malmierca et al., 2009). In the CN recordings, we explored repetitions rates of 4, 8, 12, and 20 Hz. Due to the different repetition rates used, the duration of the pure tones was 75 ms for the IC recordings (Hernández et al., 2005) and 25 ms for the CN recordings (in a few recordings at 4 and 8 Hz, tones lasted 75 ms as well), including a 5 ms rise/fall ramp for both cases.

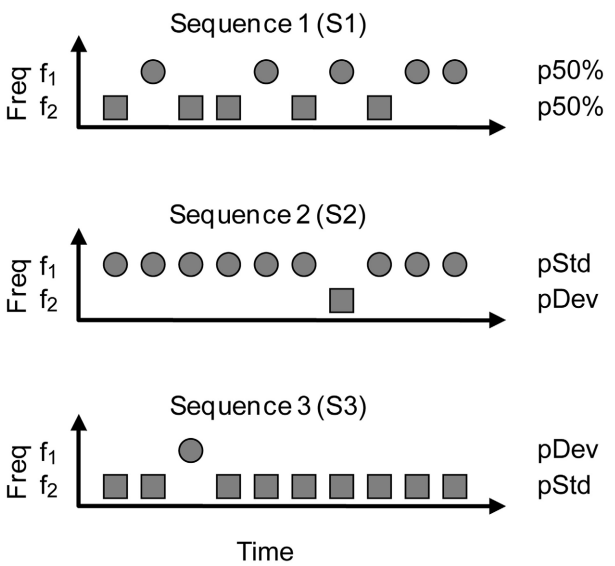

FIGURE 1 | The oddball stimulation paradigm. Two frequencies (f_1, f_2) were presented pseudo-randomly with different probabilities of occurrence. In Sequence 1 (S1), f_1, and f_2 occurred with equal probability (p50%), which served as a control condition. This condition is useful to see the neuron's tuning to the frequencies chosen. For the oddball condition, the probability of the frequencies was modified such that one frequency (f_1, circles) was the standard tone, occurring with high probability, and the other (f_2, squares) was the deviant tone, with low probability of occurrence (Sequence 2, S2). The probabilities of f_1 and f_2 were reversed in Sequence 3 (S3) in order to have each frequency presented as deviant and standard. We tested two probabilities for the deviant tone (pDev), 30 and 10%, so the corresponding probabilities for the standard (pStd) were 70 and 90%, respectively.

As shown in **Figure 1**, in Sequence 1 (S1) both frequencies were presented with the same probability of occurrence (equiprobable condition; $p(f_1) = p(f_2) = 50\%$). In Sequence 2 (S2), one frequency (f_1) was presented as the standard (i.e., high probability within the sequence: 90 or 70%); interspersed randomly among the standards were the deviant stimuli (i.e., low probability: 10 or 30%, respectively) at the second frequency (f_2). After obtaining one data set, the relative probabilities of the two stimuli were reversed, with f_2 as the standard and f_1 as the deviant (S3). Sequences 2 and 3 constitute what we refer to as an oddball condition. The responses to the standard and deviant stimuli were normalized to spikes per stimulus, to account for the different number of presentations in each condition, because of the different probabilities. We tested several frequency separations between f_1 and f_2, expressed as frequency contrast $\Delta f = (f_2 - f_1)/(f_2 \times f_1)^{1/2}$ (Ulanovsky et al., 2003). As the frequency pairs were chosen to evoke similar firing rates in responses to both tones, Δf ranged from 0.02 to 3. The Δf values were grouped into three intervals: $\Delta f \leq 0.07$, $0.07 < \Delta f \leq 0.2$ and $\Delta f > 0.2$ (≤ 0.101, $0.101 < \Delta f \leq 0.288$ and $\Delta f > 0.288$ octaves, respectively), in order to approximate to the values used in other studies, i.e., $\Delta f = 0.04$, 0.10, and 0.37 (Ulanovsky et al., 2003, 2004; Malmierca et al., 2009). The same paradigm was repeated changing the probability of the deviant tone (pDev = 10%, 30%) or the Δf. For the CN experiments, we only tested pDev = 10% and $\Delta f = 0.1$. The presentation of sequences at different deviant probabilities and at different repetition rates was randomized.

DATA ANALYSIS

We measured the sharpness of the FRA of IC neurons calculating the bandwidth (BW) and Q-values at 10 and 40 dB SPL above the threshold as in our previous work (Hernández et al., 2005; Malmierca et al., 2009). The BW at n dB expresses the difference in kHz between the lower (F_L) and upper (F_U) frequencies of the FRA ($BW_n = F_U - F_L$). The Q-value is calculated as the characteristic frequency (CF) divided by the BW at n dB above threshold ($Q_n = CF/BW$).

The amount of SSA was quantified by two indices that have been used in previous studies (Ulanovsky et al., 2003, 2004; Malmierca et al., 2009; Antunes et al., 2010; Antunes and Malmierca, 2011; Pérez-González et al., 2012). The first index was the Frequency-Specific SSA Index (SI) defined as: $SI(f_i) = [d(f_i) - s(f_i)]/[d(f_i) + s(f_i)]$, where $i = 1$ or 2 and $d(f_i)$ and $s(f_i)$ are responses (as normalized spike counts) to frequency f_i when it was deviant or standard, respectively. The second one was the Common-SSA Index (CSI) defined as $CSI = [d(f_1) + d(f_2) - s(f_1) - s(f_2)]/[d(f_1) + d(f_2) + s(f_1) + s(f_2)]$, where $d(f)$ and $s(f)$ are responses to each frequency f_1 or f_2 when they were the deviant (d) or standard (s) stimulus, respectively. These indices reflect the extent to which the neuron responds more strongly to the frequencies when they are deviant compared to when they are standard. The possible SI and CSI values range from −1 to +1,

being positive if the response to the deviant stimulus is greater and negative if the response to the standard stimulus is greater.

To estimate the neuronal sensitivity we performed a receiver operating characteristic (ROC) analysis (Tanner and Swets, 1954; Cohn et al., 1975; Fawcett, 2006; for a review of the use of ROC in psychometric and neurometric data analysis, see Stüttgen et al., 2011). This analysis has been previously used to measure the ability of CN units to signal changes in intensity (Shofner and Dye, 1989) and the sensitivity of IC units to interaural-time differences and binaural correlation (Skottun et al., 2001; Shackleton et al., 2003, 2005; Gordon et al., 2008). It is assumed that when different stimuli elicit different firing rates the response of a neuron provides the basis for discriminating between them. However, there is also a substantial variability in the responses to each stimulus, so the distributions of firing rates to similar stimuli overlap, and thus discrimination based upon firing rate will only be correct on a proportion of trials. The ROC analysis allows us to calculate the performance of the best possible discriminator between the two frequencies which is based on spike counts only. This discriminator is a function of the two probability distributions of spike counts in response to the two stimuli.

The ROC plots the probability of correct detection of f_2 against the probability of "false alarm" detection of f_2 when f_1 occurred. Since detection is assumed to be based on spike counts only, trials have to be classified to one or the other frequency based solely on the evoked spike count. Thus, any discriminator between the two frequencies consists, in practice, of a list of spike counts that are assigned to frequency f_1, with all other spike counts assigned to frequency f_2 (we do not need to consider so-called "randomized rules" here, because we are only interested in the integral of the ROC, see below). In many studies, ROCs are calculated by a threshold on spike counts: all spike counts below the threshold are assigned to one frequency, and those above the threshold to the other. However, the lemma of Neyman and Pearson (Maris, 2012) requires spike counts to be assigned to frequencies based on their likelihoods, the ratio $p(n|f_2)/p(n|f_1)$. For an optimal decision rule, a threshold is selected, and all spike counts whose likelihood is larger than that threshold are assigned to f_2 (with the others assigned to f_1). The probabilities of correct decision and false alarm for this decision rule can then be calculated in a straightforward manner. The ROC is obtained by calculating these probabilities while varying the threshold.

Then, we calculated the area under the ROC curve (AUC) as an estimate of the neural discriminability of frequency. The AUC corresponds to the probability of correct stimulus detection expected from an ideal observer in a two-alternative forced-choice psychophysical task (Green and Swets, 1966; Fawcett, 2006). Thus, sensitivity measured as AUC varies between 0.5 and 1, where 0.5 occurs when the spike count distributions for frequencies f_1 and f_2 are identical, and 1 indicates complete separation of the distributions. To compensate for sampling bias, we corrected each AUC value by performing 10,000 permutations of the original spike count distributions, assigned randomly to either f_1 or f_2, calculated the corresponding AUCs, and subtracted their mean value from the original AUC. Due to this correction some of the AUC values we report are smaller than 0.5. We also used the permutations test to estimate the probability of the AUC being significantly larger than 0.5. This way, we obtained one AUC value for the equiprobable condition (S1) and two AUC values for the oddball conditions (S2, S3). We used the mean AUC of S2 and S3 for the analyses instead of the maximum value as in previous works (Ulanovsky et al., 2003; Malmierca et al., 2009), in order to avoid an upward bias.

The CSI values were tested against zero by bootstrapping (1000 samples) in order to estimate a 95% confidence interval. Typically, CSI values smaller than 0.1 were not statistically different from zero (85% of all cases with CSI < 0.1 and 15% of the cases with CSI > 0.1). Thus, CSI values within the range of -0.1 to 0.1 were considered be due to random fluctuations in spike counts. This procedure provided a CSI cutoff comparable to other values previously set with different criteria (e.g., CSI $= 0.18$ for auditory thalamus of the rat; Antunes et al., 2010). It may be somewhat smaller than the cutoff in thalamus because of the lower variability in the responses of IC neurons (e.g., Chechik et al., 2006).

RESULTS

To investigate how frequency sensitivity is affected by the stimulation context we recorded the response of 224 well isolated single units in the IC and 51 units in the CN using an oddball paradigm. The frequency contrast ($\Delta f \leq 0.07$, $0.07 < \Delta f \leq 0.2$, $\Delta f > 0.2$) and probability of the deviant tone (pDev = 30% or 10%) were varied in IC recordings, and the repetition rate (4, 8, 12, and 20 Hz) in the CN. Additionally, an equiprobable context ($p(f_1) = p(f_2) = 50\%$) was tested as control condition in both sets of experiments.

NEURONS IN THE IC SHOW DIFFERENT DEGREES OF SSA AND STIMULUS DISCRIMINABILITY

As might be expected from our previous studies (Pérez-González et al., 2005; Malmierca et al., 2009), neurons in the IC exhibited different degrees of SSA. **Figure 2** shows the distribution of the CSI under different stimulus conditions in the current sample. The distributions of CSI are skewed toward positive values, and their medians are significantly different from zero (Signed Rank Test; $p < 0.05$) regardless of the condition tested (**Figure 2**). Positive CSI values reflect a stronger response to the deviant tone than to the standard one. The effects of frequency separation and deviant probability were tested using a Two-Way ANOVA on $\Delta f \times$ probability. There was a main effect of Δf ($F_{(2,\,489)} = 18$, $p = 0$) and of probability condition [$F_{(1,\,489)} = 39$, $p = 0$]. The interaction just failed to reach significance [$F_{(2,\,489)} = 2.5$, $p = 0.08$]. *Post-hoc* comparisons showed that the most positive CSI values were observed for deviant probability of 10% at the two highest frequency contrast intervals; $0.07 < \Delta f \leq 0.2$ and $\Delta f > 0.2$. For the 10% probability condition, the CSIs increased significantly with increased frequency separation: $\mathrm{CSI}_{10\%/\Delta f>0.2} > \mathrm{CSI}_{10\%/0.07<\Delta f\leq 0.2} > \mathrm{CSI}_{10\%/\Delta f\leq 0.07}$. On the other hand, the *post-hoc* comparisons did not show a significant difference between the average CSIs in the 30% condition and different frequency separations. There was also a significant difference due to changes in deviant probability for the two highest frequency separation intervals: $\mathrm{CSI}_{10\%/0.07<\Delta f\leq 0.2} > \mathrm{CSI}_{30\%/0.07<\Delta f\leq 0.2}$; $\mathrm{CSI}_{10\%/\Delta f>0.2} > \mathrm{CSI}_{30\%/\Delta f>0.2}$. This trend was emphasized by

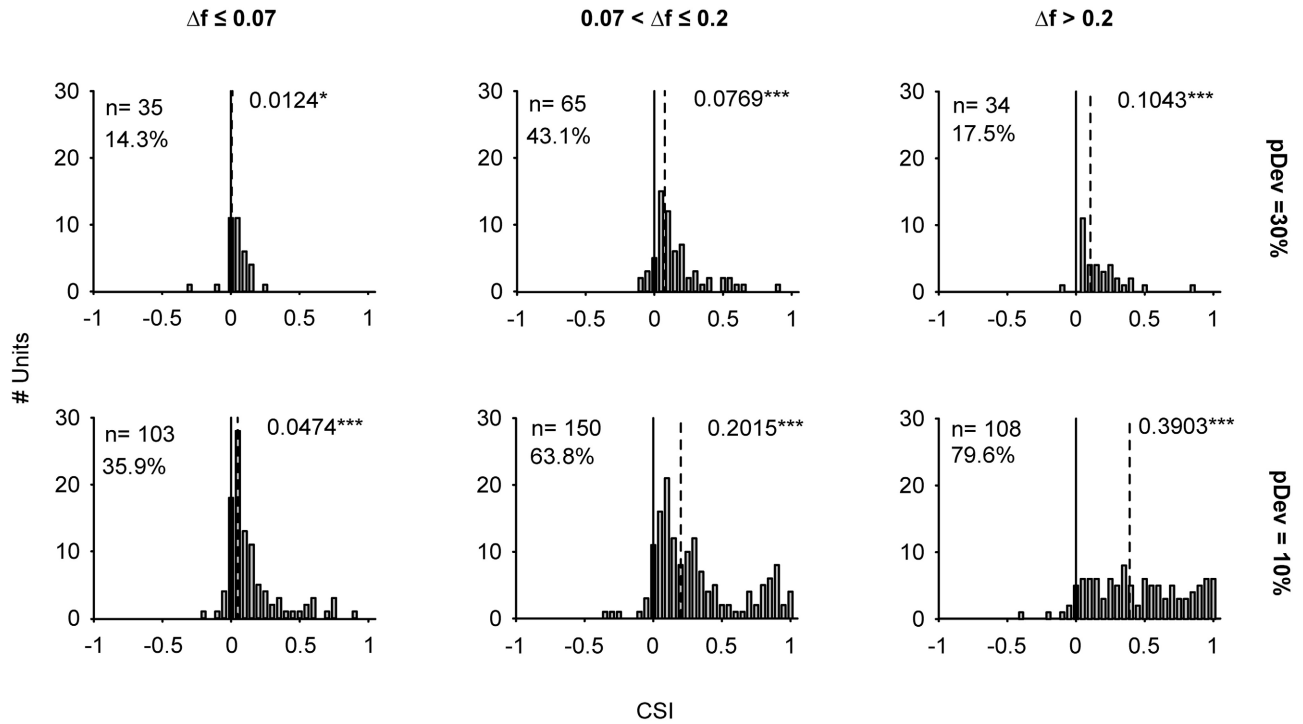

FIGURE 2 | Distribution of stimulus-specific adaptation indices of IC neurons. Histograms of the common SSA index (CSI) displayed according to the frequency separation intervals (columns: $\Delta f \leq 0.07$, $0.07 < \Delta f \leq 0.2$, $\Delta f > 0.2$) and the probability of the deviant tone (rows: pDev = 30 and 10%). The CSI was calculated from the responses recorded in S2 and S3. A CSI = 0 indicates an equal neuronal response when the tones were presented as deviant or standard, while positive and negative values represent higher firing rates when the tones were deviant or standard, respectively. For each stimulus condition the CSI values were tested against zero (solid line). The numbers next to the dashed line indicate the value of the median and the statistical significance (Signed Rank Test; $^*p < 0.05$, $^{***}p < 0.001$). The distributions moved toward positive values when Δf was larger and pDev smaller. The percentages indicate the amount of neurons with CSI > 0.1.

the higher percentage of neurons with CSI values larger than 0.1 when deviant probability was 10% compared to 30% (percentages indicated in **Figure 2**). From the six groups, only seven neurons (3.1%) showed CSI ≤ -0.1.

Examples of individual IC neurons exhibiting different CSI values are shown in **Figures 3–5**. The deviant probability for the three cases was 10% and the frequencies tested (f_1, f_2) in these examples were separated by 0.144 octaves ($\Delta f = 0.1$) around its BF at an intensity of 10 – 50 dB above threshold.

Figure 3 illustrates a neuron with a CSI not significantly different from zero (CSI = 0.04; $p > 0.05$). This neuron had a narrow FRA with a narrow bandwidth both at 10 and 40 dB SPL above its threshold (BF = 8.8 kHz, $Q_{10} = 5.62$ and $Q_{40} = 1.22$) (**Figure 3A**). It had an onset firing pattern (**Figure 3B**) and showed a mixed/complex rate-level function (**Figure 3C**). The responses elicited in the equiprobable condition (S1) and oddball condition (S2 and S3) are shown as dot rasters (**Figure 3D**) as well as the peristimulus time histograms (PSTH) (**Figure 3E**). **Figure 3F** displays the corresponding spike-count distributions and the ROC curve is shown in **Figure 3G**. This neuron displayed a very robust and reliable response across the 400 stimulus presentations. In consequence, its spike count distributions were very different from Poisson distributions: while the average spike count is about 1, the probability of having zero spike counts is much smaller than that of either frequency evoking a single spike (for a Poisson distribution, these two probabilities should be approximately equal when the mean spike count is close to 1). The spike-count distributions for f_1 and f_2 were very similar, overlapping almost completely (**Figure 3F**), although the average spike count was slightly larger for f_2 than for f_1. The large overlap between these distributions resulted in AUC values very close to 0.5, but the very low variability resulted in an AUC that was significantly larger than 0.5 in the equiprobable condition. When f_2 was the deviant, this difference was maintained, but when f_1 was the deviant, the average spike count in response to f_2 decreased slightly, enough to render the AUC not significantly different from 0.5 (AUC(S1) = 0.55, $p = 0$; AUC(S2) = 0.55, $p = 0.01$; AUC(S3) = 0.49, $p = 0.65$). Thus, the frequency discrimination capability of this neuron was poor in an equiprobable context and did not improve in an oddball stimulation context, consistent with its low CSI.

By contrast, neurons with high CSI values fired significantly differently in response to deviant and standard tones in the oddball condition. The neuron illustrated in **Figure 4** had a CSI = 0.88 ($p < 0.05$). It was tuned to a wide range of frequencies (**Figure 4A**) reflected by its low Q-values (BF = 10 kHz, $Q_{10} = 0.74$ and $Q_{40} = 0.27$). This neuron also had an onset firing pattern, although it showed a large variability of first

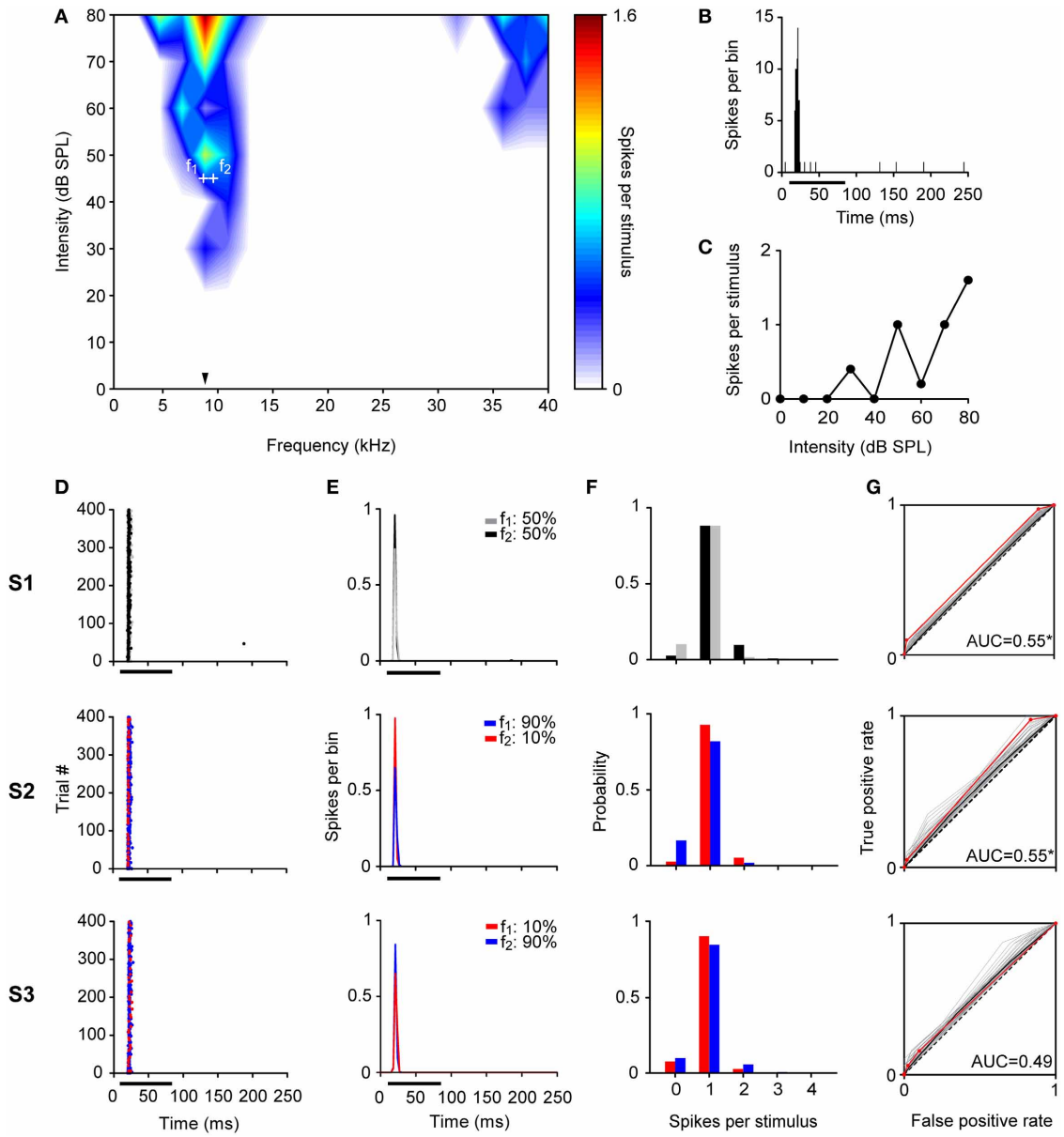

FIGURE 3 | Example of a non-adapting neuron in the IC. (A) Narrow FRA in color code for response magnitude. The tested frequencies (f_1: 8.7 kHz, f_2: 9.6 kHz, white crosses) were chosen around the BF (8.8 kHz) (arrowhead), at 45 dB SPL. **(B)** PSTH of the accumulated response to all the frequencies (0.5 – 40 kHz) and intensities (0 – 80 dB SPL) presented (1 ms bins). **(C)** Rate-level function at BF. **(D–G)** The responses of the neuron for each pair of stimuli for each of the three sequences (S1, S2, S3) are shown as dot raster plots **(D)**, PSTH (3 ms bins) **(E)**, spike probability distributions **(F)**, and ROC curves **(G)**. In the dot raster each dot represents the occurrence of a spike. The black bar under the PSTH and dot raster plots indicates the duration of the stimulus (75 ms). The probability of each frequency for each sequence is indicated on the upper left of the **(E)** panels. In the ROC curves **(G)** the dashed line corresponds to random guessing or no stimulus discrimination (AUC = 0.5), indicating complete overlap of the spike probability distributions. The red line represents the ROC curve calculated using the recorded data, the curves plotted in gray were obtained with the permutation method of the original spike count distributions, and the black line is represents the mean ROC curve of permutations. A total of 10,000 permutations were calculated, but for visual clarity only 100 curves are displayed. For each ROC curve, the area under the ROC curve (AUC) is shown corresponding to the original AUC value minus the mean AUC from permutations, as well as, the significance value for AUC > 0.5 (Permutation test; $^*p < 0.05$). The repetition rate was 4 Hz and the frequency separation was 0.141 octaves. This neuron did not show SSA (CSI = 0.04, Bootstrapping; $p > 0.05$), displaying a very similar response to f_1 and f_2 across the three sequences regardless the probability of each tone.

spike latency (FSL) (**Figure 4B**) and had a non-monotonic rate-level function (**Figure 4C**). During the equiprobable presentation of the tones (S1), this neuron adapted its response to both frequencies, and had a very low probability to respond at all ($P_{\geq 1sps} = 0.005$). In the oddball condition, responses to the standard tone remained extremely sparse, but deviant trials did evoke a few spikes with higher probability. Thus, the overlap between the spike-count distributions was reduced

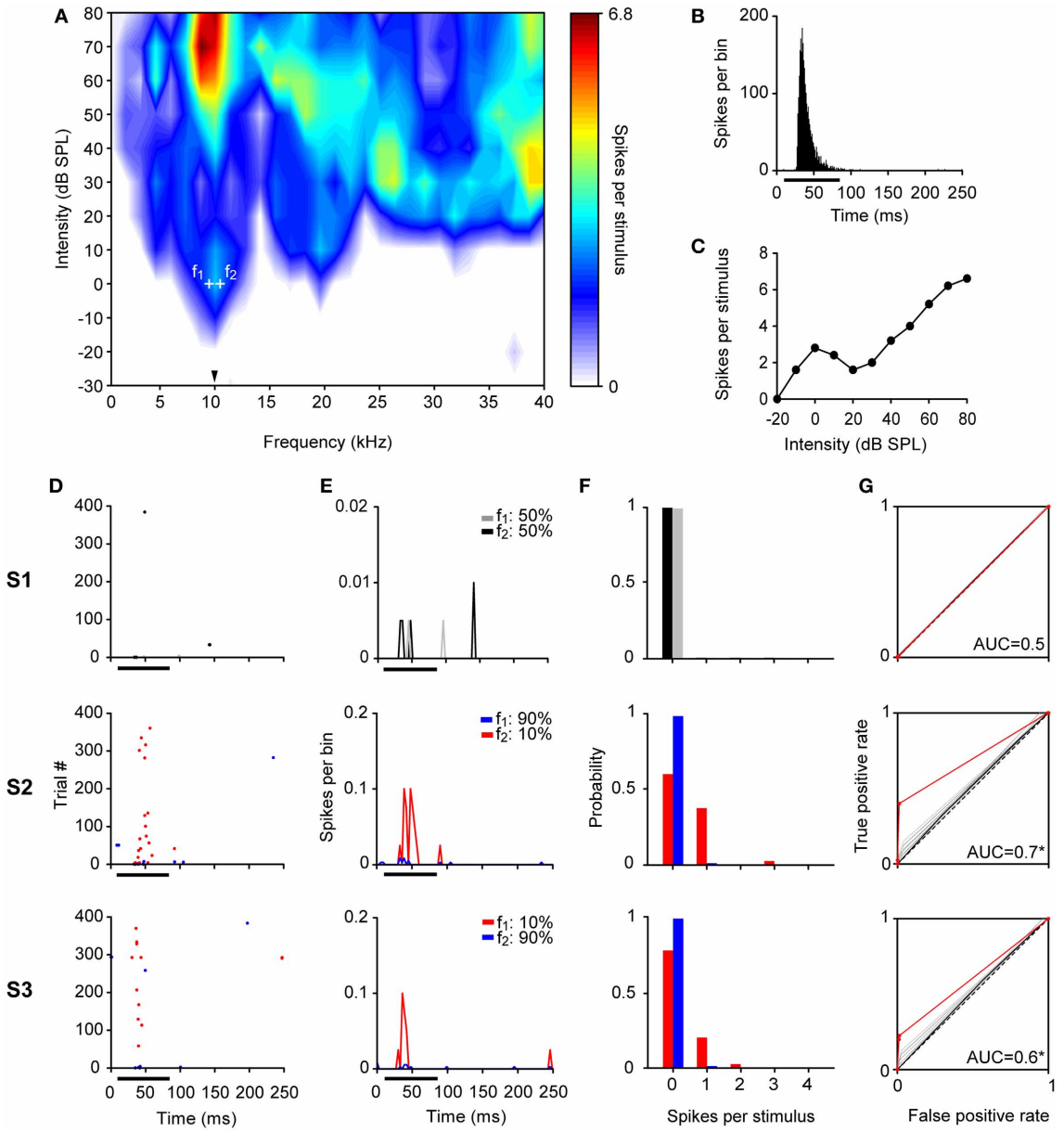

FIGURE 4 | Example of an adapting neuron in the IC. (A) FRA of a broadly tuned neuron with a BF of 10 kHz (arrowhead). The frequencies tested are indicated by the white crosses around the BF (f_1: 9.5 kHz, f_2: 9.6 kHz), at 0 dB SPL. **(B–G)** Same format as in **Figure 3**. This neuron showed strong SSA (CSI = 0.88, Bootstrapping; $p < 0.05$) reducing its firing to the high probability tone in S2 and S3 while still responding to the low probability one across most stimulus presentations. This differential firing is reflected in an AUC larger than 0.5 (Permutation test; $^*p < 0.05$) in oddball sequences (S2 and S3).

substantially (probability of firing $\geq$ 1 sps in response to the deviant/standard was 0.4/0.017 and 0.23/0.014 for S2 and S3, respectively). As a result, the AUCs for the oddball conditions were higher than for the equiprobable condition [AUC(S1) = 0.5, $p = 0.5$; AUC(S2) = 0.7, $p = 0$; AUC(S3) = 0.6, $p = 0$].

The examples shown in **Figures 3** and **4** are extreme cases, and neurons in the IC showed a continuous distribution of SSA as depicted in **Figure 2**. For example, **Figure 5** illustrates a partially-adapting neuron (CSI = 0.5; $p < 0.05$) tuned to high frequencies (**Figure 5A**) and with a non-monotonic rate-level function (**Figure 5C**). The bandwidth of the FRA increased between 10 and 40 dB above threshold, respectively (BF = 29.9 kHz, $Q_{10} = 7.81$ and $Q_{40} = 2.25$). This neuron showed a poor, although significant discrimination capability at the equiprobable condition [AUC(S1) = 0.57, $p = 0$] which improved in the oddball condition [AUC(S2) = 0.61, $p = 0$; AUC(S3) = 0.76, $p = 0$].

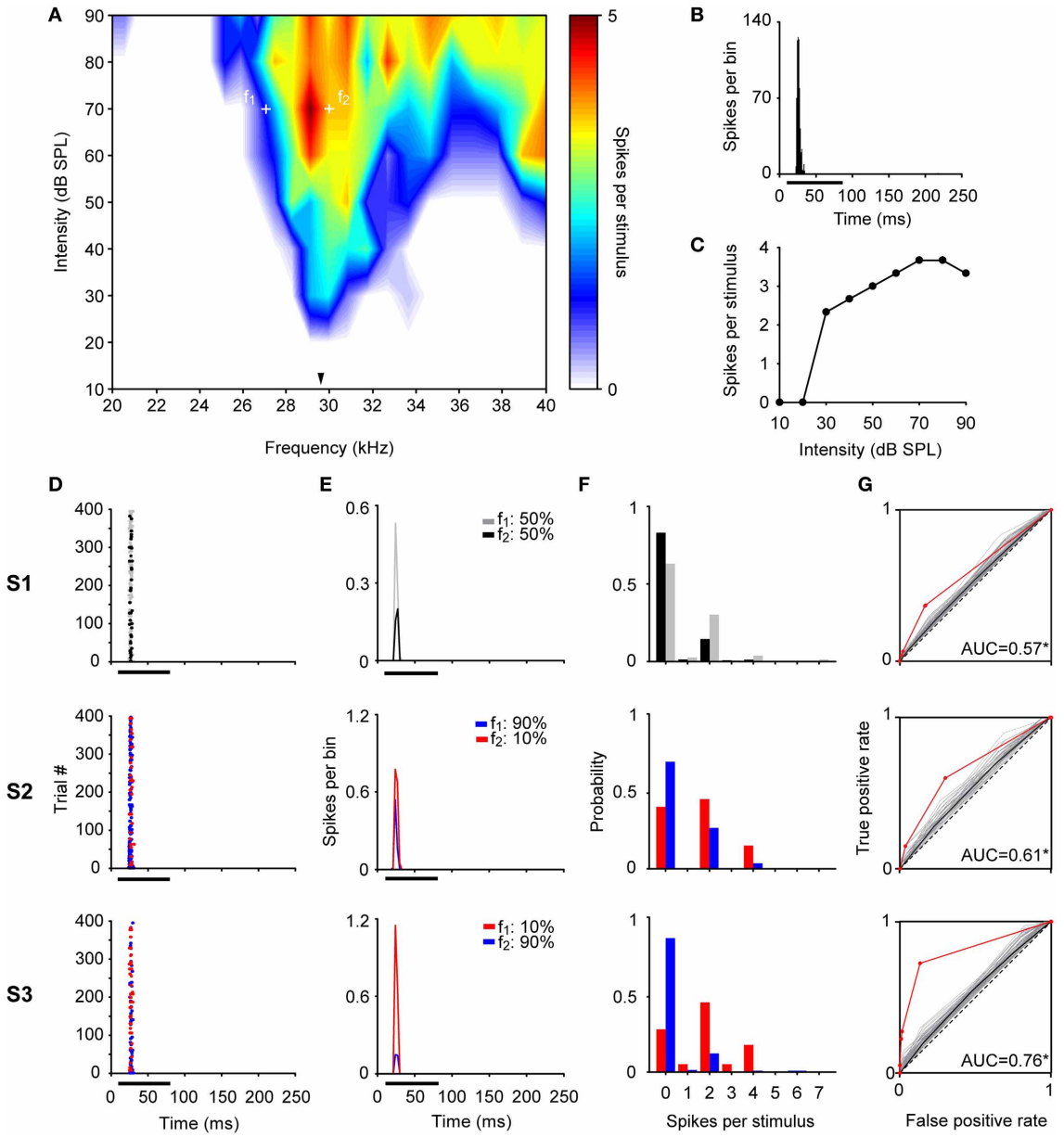

FIGURE 5 | Example of a partially-adapting neuron in the IC. (A) FRA from a neuron with a BF of 29.9 kHz (arrowhead). The frequencies tested were f_1: 27.1 kHz and f_2: 30 kHz, at 70 dB SPL. **(B–G)** Same format as in **Figure 3**. This neuron displayed a significant level of SSA (CSI = 0.5, Bootstrapping; $p < 0.05$), responding to both tones across the 400 stimulus trials. Although, the neuron displayed significant discriminability in the equiprobable condition (S1, AUC = 0.57) (Permutation test; $^*p < 0.05$), this was improved under the oddball sequences (S2, AUC = 0.61; S3, AUC = 0.76).

FREQUENCY DISCRIMINABILITY DEPENDS ON STIMULUS CONTEXT IN THE IC

IC neurons were able to discriminate very similar frequencies even when both tones had the same probability of occurrence ($p(f_1) = p(f_2) = 50\%$). The tested frequencies were selected online to evoke similar response magnitudes. Nevertheless, the noise in the estimation of response rates resulted in some imbalance between the responses to the two frequencies, leading to significant discriminability between them. The discriminability elicited under the equiprobable condition ($AUC_{50\%}$) across the three Δf intervals significantly differed from a mere random discrimination (AUC = 0.5, Signed Rank Test; $p < 0.001$) (**Figure 6A**). Furthermore, more than half of the neurons from each frequency separation group had $AUC_{50\%}$ significantly larger than 0.5 ($p < 0.05$) (**Figure 6A**, indicated in percentage). In a substantial number of cases, $AUC_{50\%}$ exceeded 0.71 (24.1, 23.2, and 41.6% for the three Δf groups), the generally accepted definition of a threshold (Green and Swets, 1966). Neurons with AUCs above this threshold for the smallest frequency contrast interval ($\Delta f \leq 0.07$) had narrower bandwidths ($Q_{10} = 6.23 \pm 5.43$)

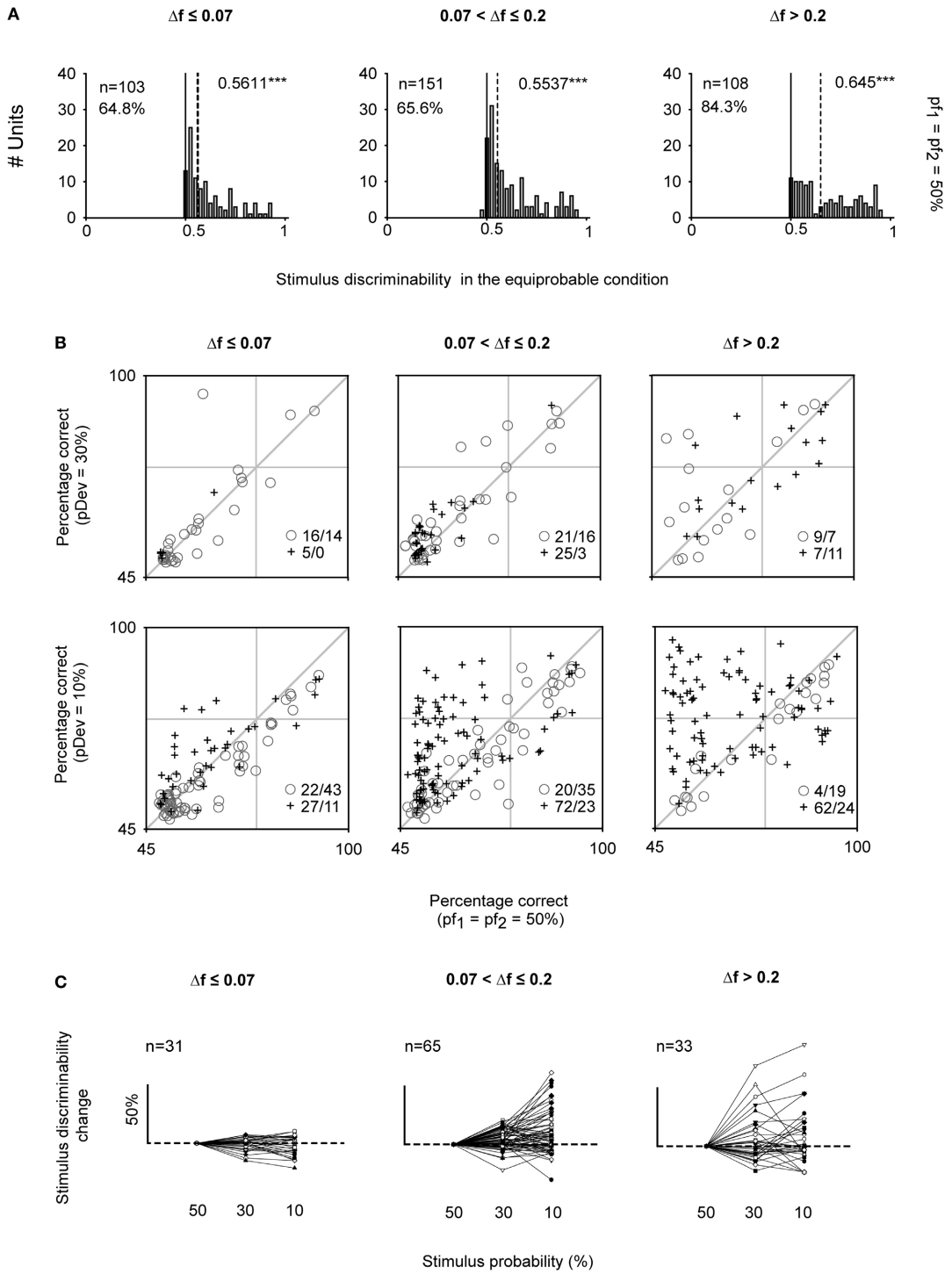

FIGURE 6 | Neurometric performance under equiprobable and oddball conditions of IC neurons. (A) Distributions of the AUC values for the equiprobable condition ($AUC_{50\%}$) indicating the median (dashed line) significantly differs from 0.5 (Signed Rank Test; $^{***}p < 0.001$). The percentage of neurons whose $AUC_{50\%}$ was higher than 0.5 is indicated for each panel (Permutation test; $p < 0.05$). **(B)** Scatter plots showing the neurometric performance for frequency discrimination expressed as percentage correct under the oddball condition (rows: pDev = 30, 10%) versus the equiprobable condition ($pf_1 = pf_2 = 50\%$), for each frequency contrast interval (columns: $\Delta f \leq 0.07$, $0.07 < \Delta f \leq 0.2$, $\Delta f > 0.2$). Separately are represented the neurons with CSI ≤ 0.1 (gray circles) and CSI > 0.1 (dark crosses). For the oddball condition, the percentage correct corresponds to the mean AUC value obtained from S2 and S3. The number of neurons above and below the diagonal line (equal performance in both conditions) is indicated by the inset on the bottom right of each panel. **(C)** Sensitivity curves of individual neurons expressed as percentage of change elicited when pDev = 10% and 30% regarding the $pf_1 = pf_2 = 50\%$ condition.

that the rest of neurons ($Q_{10} = 3.53 \pm 5.47$) (Signed Rank Test; $p < 0.05$).

To address the central question of this paper, **Figure 6B** compares the percent correct (as estimated by AUC) in the oddball and equiprobable condition for each neuron. For the oddball condition, we used the mean discriminability ($AUC_{oddball}$) from the values elicited in the two oddball sequences since there was not significant difference in the AUC values elicited in S2 and S3 (Rank Sum Test; $p > 0.05$). Neurons whose discriminability was unaffected in the oddball condition fell along the diagonal line. Neurons under the diagonal line showed a better discriminability in the equiprobable condition. By contrast, neurons that improved their discriminability in the oddball paradigm were located above the diagonal. Neurons with CSI > 0.1 are marked by crosses, the others are marked by circles. When pDev = 10%, there was a larger proportion of neurons with CSI > 0.1 than neurons with CSI ≤ 0.1 that showed improved discriminability in the oddball condition ($\chi^2 = 58.6$, df = 1, $p < 0.001$), but these proportions did not depend on frequency separation ($\chi^2 = 5.4$, df = 2, $p = 0.07$). For this probability condition, the AUCs of neurons with CSI ≤ 0.1 were slightly, although significantly, smaller in the oddball than in the equiprobable condition ($^{46}/_{96}$, neurons above and below the bisecting line, respectively, for all frequency separation classes together). This effect was due presumably to the poorer sampling of the spike count histograms for the deviant stimuli in the oddball condition. On the other hand, $AUC_{oddball}$ increased substantially for neurons with CSI > 0.1 ($^{161}/_{59}$ neurons above and below the bissecting line, respectively). The increase resulted in many neurons whose frequency discrimination was below threshold in the equiprobable condition ($AUC_{50\%} < 0.71$) and that exceed threshold in the oddball conditions ($AUC_{oddball} > 0.71$). Within this subset of neurons, there are cases in which the neurometric performance reached values close to 100% correct in the oddball condition. Such cases were much more common at the largest frequency contrasts ($0.07 < \Delta f \leq 0.2$ and $\Delta f > 0.2$). For pDev = 30%, the discriminability did not change consistently relative to the equiprobable condition, and proportions of neurons with slight increase or decrease in discriminability were as common in the different frequency difference classes ($\chi^2 = 5.4$, df = 2, $p = 0.07$) and among CSI classes ($\chi^2 = 3.9$, df = 1, $p = 0.05$).

In order to verify whether the same trend was observed at the level of single neurons, we obtained the individual "sensitivity curves" for the neurons that were tested under all probabilities conditions (50, 30, and 10%) and for the same frequency pairs (**Figure 6C**). The discriminability increment was expressed as the percentage of change in $AUC_{oddball}$ relative to the discriminability displayed under the equiprobable condition ($AUC_{50\%}$). These sensitivity curves revealed a considerable diversity in the neuronal performance. Both neuron identity and stimulus probability had a significant effect on the discrimination capability for the intermediate Δf interval [Two-Way ANOVA on stimulus probability × neuron, significant main effect of stimulus probability: $F_{(2, 128)} = 7.7$, $p < 0.001$], but for the smallest and largest Δf the main effect of stimulus probability was not significant.

Since some neurons under the equiprobable condition showed significant discriminability values that exceeded a mere random response (**Figure 6A**), we took into account this neuron-specific tuning. We calculated the *discriminability enhancement index* (DEI) as the difference between the discriminability elicited in the oddball condition and that elicited in the equiprobable one ($DEI = AUC_{oddball} - AUC_{50\%}$). DEI ranges from −0.5 to 0.5, with positive values indicating an improvement in discriminating two stimuli under an oddball context. The comparison of the mean population values of DEI across all stimulus combinations (Two-Way ANOVA, stimulus probability × Δf) demonstrated that it was affected by the frequency separation [$F_{(2, 489)} = 5.72$, $p < 0.01$] but not by stimulus probability [$F_{(1, 489)} = 3.71$, $p = 0.055$], with no interaction between those factors [$F_{(2, 489)} = 2.1$, $p = 0.12$] (**Figure 7**).

IC NEURONS WITH HIGH SSA SHOWED A GREATER DISCRIMINABILITY ENHANCEMENT UNDER ODDBALL CONDITIONS

Finally, we analyzed the relationship between the two metrics used to quantify the neuronal responses in order to explore whether or not the change in stimulus discrimination can be predicted by their SSA index. This analysis demonstrated a strong positive correlation between the degree of adaptation (CSI) and the enhancement in the frequency discriminability (DEI) shown by neurons under the condition with the lowest deviant probability, that is, when pDev = 10% (Spearman's rho; $p < 0.001$) (**Figure 8**). The great majority of neurons with CSI < 0.1 had discrimination indices clustered around the origin (gray circles). By contrast, most neurons with CSI > 0.1 (crosses) had a positive DEI, indicating that adapting neurons had better frequency

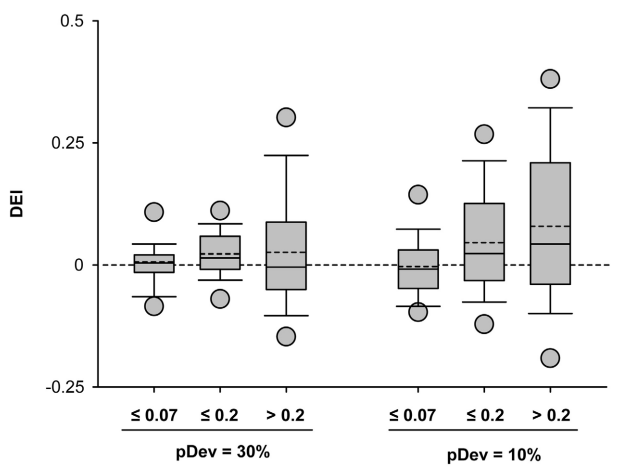

FIGURE 7 | Stimulus discriminability enhancement of IC neurons across different stimulus conditions. Box plots of the discriminability enhancement under the oddball condition (DEI) showing the mean (dashed line) and the median (solid line) values, as well as, the 5th and 95th outliers. All the mean values were positive (except for the $^{10\%}/_{\Delta f \leq 0.07}$ condition), reflecting a better stimulus discrimination when one of the frequencies is presented as a deviant tone, that is, with low probability of ocurrence (30 or 10%). The DEIs were only affected by the frequency separation [$F_{(2, 489)} = 5.72$, $p < 0.01$] (Two-Way ANOVA, deviant probability × frequency separation).

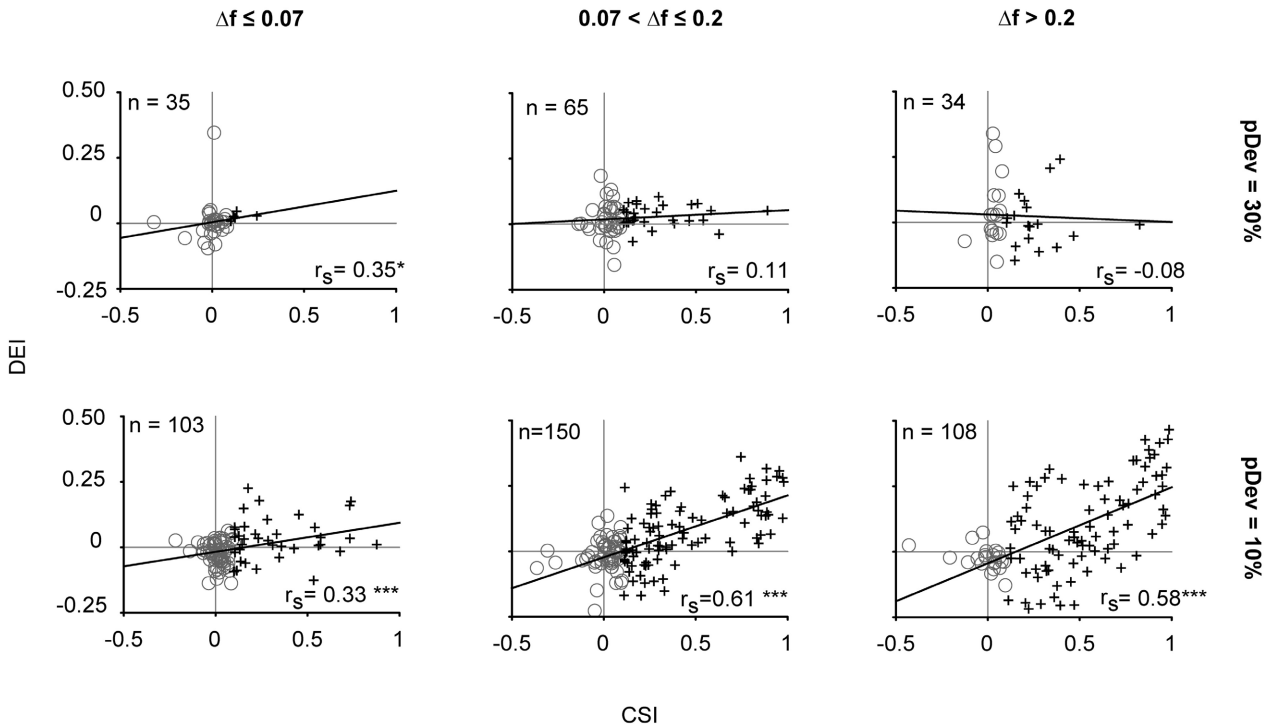

FIGURE 8 | The stimulus discriminability reflects the degree of stimulus-specific adaptation exhibited by IC neurons. Correlation of the stimulus discriminability enhancement (DEI) and the SSA index (CSI). In gray circles are represented the neurons with CSI $\leq$ 0.1 and in dark crosses those with CSI > 0.1. The linear correlation was reflected by the Spearman's correlation coefficient (r_s), whose strength varied according to the frequency contrast (columns) and probability of the deviant tone (rows). $^{*}p < 0.05$, $^{***}p < 0.001$.

discrimination for oddball sequences, and furthermore, there was a tendency for larger CSI values to be associated with larger DEI values.

RELATION BETWEEN THE WIDTH OF FREQUENCY TUNING AND THE SSA OR DISCRIMINABILITY EXHIBITED BY IC NEURONS

Previous reports demonstrated a differential expression of SSA through the lemniscal and non-lemniscal subdivisions of the IC (Pérez-González et al., 2005; Malmierca et al., 2009; Ayala and Malmierca, 2012; Duque et al., 2012) and medial geniculate body (MGB) (Antunes et al., 2010) of the rat. Neurons in the cortical regions of the IC exhibit broader FRAs than the ones from the central nucleus and the broader the response area is, the higher the SSA levels are (Duque et al., 2012). In order to test whether or not this relationship is found in our neuronal sample, we analyzed the width of response areas as a function of the level of SSA.

Figure 9A displays the bandwidths at 10 and 40 dB SPL above threshold ($BW_{10,40}$, respectively) for the lowest deviant probability (pDev = 10%) as a function of the CSI. The group of CSI $\leq$ 0.1 included all neurons that were considered to lack SSA. The other CSI cutoffs were selected to have approximately equal-size groups. It is interesting to note that there were neurons with very broad bandwidth already at 10 dB above threshold. We performed an analysis of covariance of BW, with level above threshold (10 or 40 dB SPL) and frequency separation as qualitative factors and CSI as a continuous factor. We found a highly significant effect of CSI [$F_{(1,688)} = 37.5$, $P = 0$]. The slope of the dependence of BW on CSI indicated that BW increased on average by 6.6 kHz as CSI increased from zero to one. The main effect of frequency separation was not significant, [$F_{(2,688)} = 0.54$, $p = 0.6$], while the level above threshold had, as expected, a significant effect on BW [$F_{(1,688)} = 77.4$, $p = 0$]. There was a significant interaction between the CSI slope and level above threshold [$F_{(1,688)} = 5.8$, $p = 0.01$], and *post-hoc* comparison indicated that CSI slopes at 10 and 40 dB above threshold were significantly different ($p < 0.05$).

As expected from the positive correlation between DEI and CSI (**Figure 8**), a significant effect of DEI on BW was also found [$F_{(1,688)} = 26.7$, $p = 0$] (**Figure 9B**). In consequence, a greater neuronal discriminability in the oddball condition is associated with a wider frequency integration range. DEI also had significant interaction with level above threshold [$F_{(1,688)} = 3.9$, $p = 0.048$] (analysis of covariance of BW with level, frequency separation, and now with DEI as a continuous factor).

In selected cases, we made electrolytic lesions in the IC and determined that we recorded neurons from central nucleus ($n = 9$) and from cortical regions ($n = 16$). Within this very limited sample, the central nucleus neurons had a CSI of 0.11 $\pm$ 0.21 and a DEI of -0.001 ± 0.12 (median $\pm$ SD). For the cortical neurons, the CSI and DEI were of 0.34 $\pm$ 0.3 and of 0.03 $\pm$ 0.13, respectively. However, this number of histological localizations was insufficient to guarantee a reliable study to correlate SSA

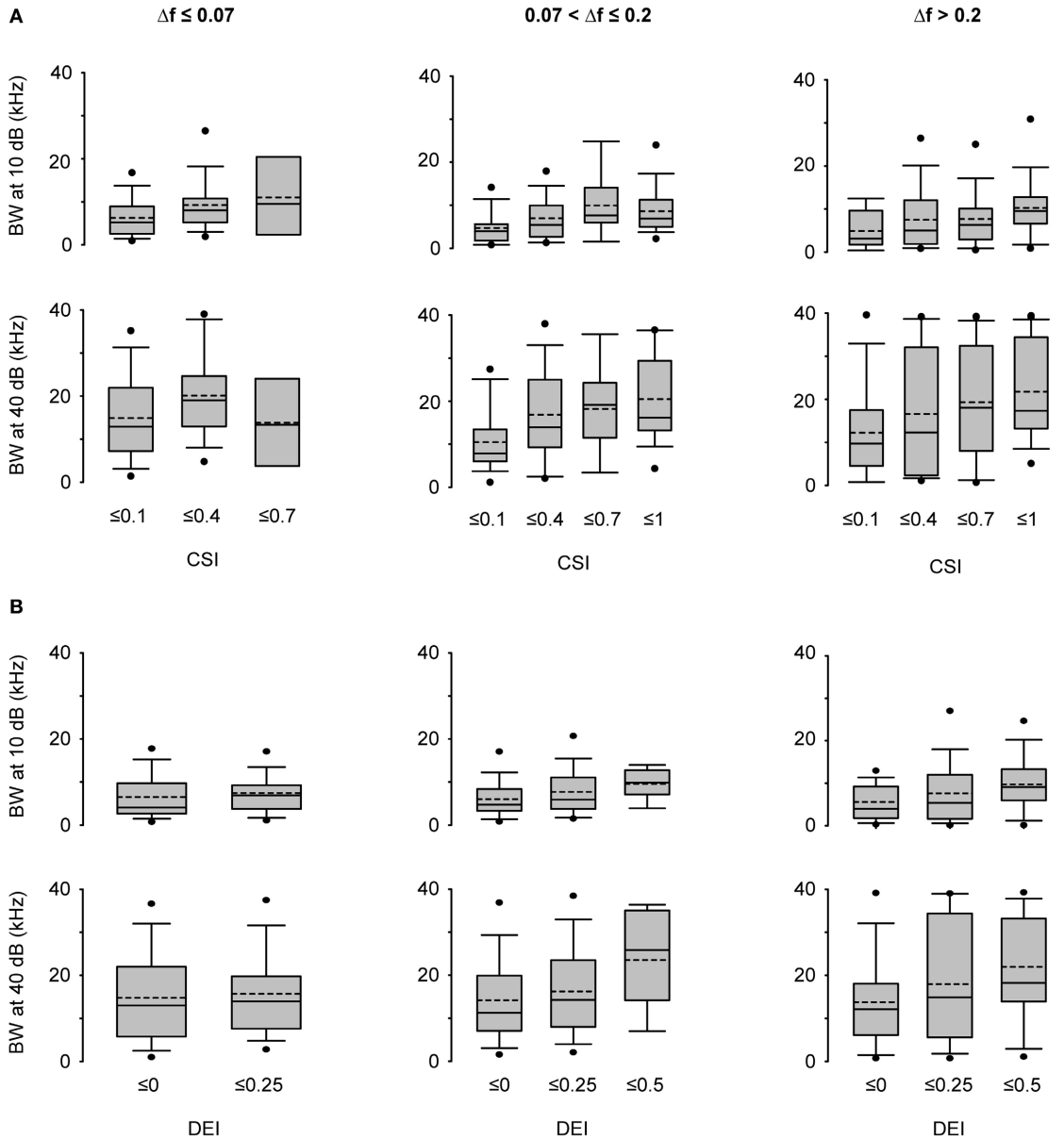

FIGURE 9 | Bandwidth of frequency response areas and SSA level of IC neurons. (A) Box plots of the bandwidth (BW) values grouped into CSI ranges for the three Δf intervals with the mean (dashed line) and median values (solid line) indicated, as well as, the 5th and 95th outliers. There is an increment in the bandwidths as neurons have higher CSI [$F_{(1,688)} = 37.5$, $P = 0$] and as the level increased [$F_{(1,688)} = 77.4$, $p = 0$] (Analysis of covariance of BW with level, Δf and CSI as factors). **(B)** Box plots of BW values grouped into DEI ranges. The BW increases for neurons that displayed higher discriminability improvement under the oddball condition [$F_{(1,688)} = 26.7$, $p = 0$]. Same format as panel **(A)**. (Analysis of covariance of BW with level, Δf and DEI as factors).

and discriminability degree across the different subdivisions of the IC. **Figure 10A** showed an example of a typical lesion located in the lateral cortex of the IC (Loftus et al., 2008; Malmierca et al., 2011).

CN NEURONS DO NOT EXHIBIT SSA AND THEIR FREQUENCY DISCRIMINABILITY IS NOT SENSITIVE TO A PROBABILITY CONTEXT

Since SSA is present in the IC, we wanted to explore whether SSA is already ubiquitously expressed earlier. We recorded 51 CN neurons to test whether SSA is exhibited by single-units and if so, whether adaptation strength correlates with neuronal sensitivity as shown for the IC neurons.

A total of 44 neurons out of 51 were localized and assigned to the ventral cochlear nucleus (VCN) ($n = 10$) or DCN ($n = 34$). The histological reconstruction for the remaining 7 neurons was not possible. **Figure 10B** shows the electrolytic lesion in a Nissl-stained section, illustrating the recording site of the neuron displayed in **Figure 11** and located in the DCN. Another example of

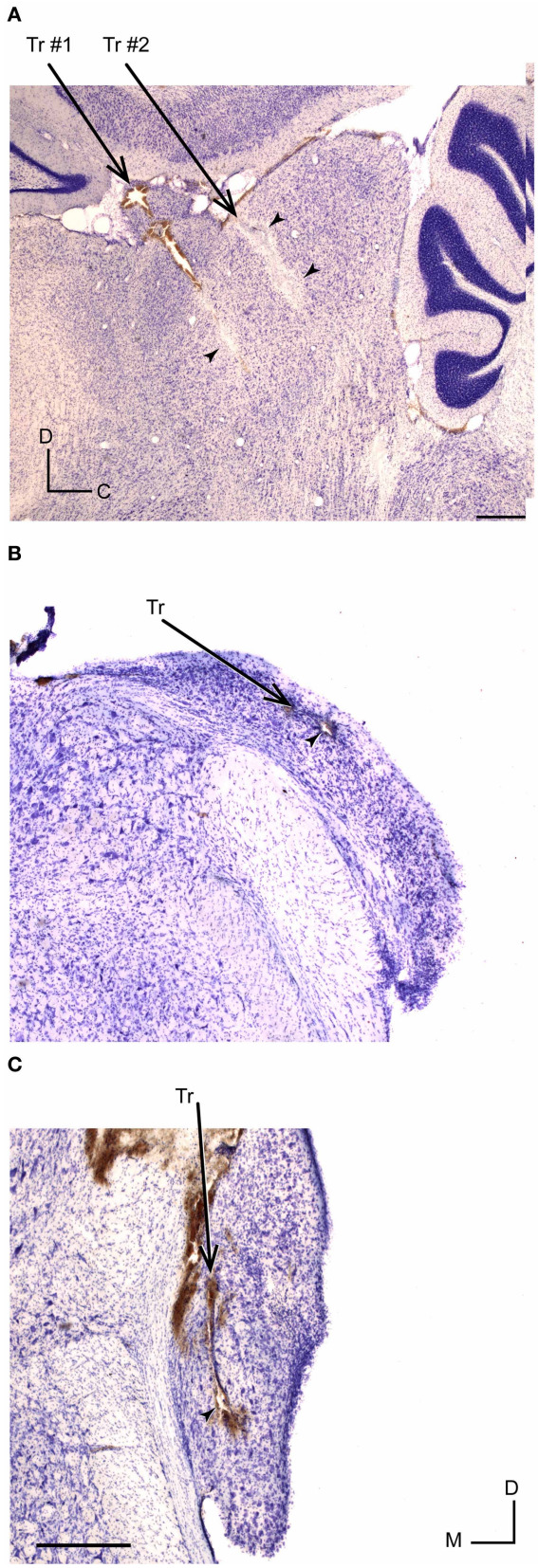

FIGURE 10 | Continued

FIGURE 10 | Histological identification of recording sites of IC and CN neurons. (A) Example of recording sites marked with an electrolytic lesion (arrowheads) in the lateral cortex of the IC at 1.9 mm lateral, according to Paxinos and Watson (2007). Two different tracts are indicated by Tr #1 and Tr #2. **(B,C)** Recording sites (arrowheads) and tracts (Tr) located in DCN (at 11.52 mm from bregma) and VCN (at 11.04 mm from bregma), respectively. The slices were Nissl stained and cut at 40 μm in a sagital **(A)** and coronal plane **(B,C)**. Scale bars of 500 μm. D, dorsal; C, caudal; M, medial.

recording site, in the VCN, is shown in **Figure 10C**. The recorded neurons had a wide variety of firing patterns and rate-level functions, as have been described in detail before (Stabler et al., 1996). More than the half of neurons in the DCN (21/34) displayed non-monotonic rate-level functions (5/10 in the VCN). Our sample of DCN neurons included chopper ($n = 13$), primary like ($n = 10$), pause/build ($n = 6$), and onset ($n = 5$) firing patterns. In the VCN, all firing patterns except the choppers were present (primary like, $n = 5$; pause/build, $n = 2$; onset, $n = 3$). **Figure 11** shows the response of a DCN neuron with a typical V-shaped FRA with a low-frequency tail. The evoked activity was robust across the 400 trials of the equiprobable (S1) and deviant sequences (S2, S3). The neuron showed significant discriminability under the equiprobable condition (AUC(S1) = 0.6, $p < 0.05$) which did not greatly improve under the oddball sequences (AUC(S2) = 0.62, AUC(S3) = 0.53, $p < 0.05$). This neuron failed to show SSA at a repetition rate of 4 Hz, as well as at faster stimuli presentation rates of 8 and 20 Hz (CSI = 0, $p > 0.05$).

SSA was not present in the neuronal population recorded in CN (**Figure 12**). We used faster repetition rates than in the IC since SSA seems to increase monotonically with stimulation rate (Malmierca et al., 2009; Antunes et al., 2010; Zhao et al., 2011; Patel et al., 2012). Regardless of the extreme repetitions rates, the strength of the neuronal response was equal for deviants and for standards stimuli (Signed Rank Test; $p > 0.05$) (**Figure 12A**) resulting in SI values clustered around zero (**Figure 12B**). There were no differences between the CSIs elicited by VCN and DCN neurons for any repetition rate tested (Rank Sum Test; $p > 0.05$). FSL is also affected by probability condition in IC, being shorter to the deviant stimulus regardless of the frequency tested (f_1 or f_2) (Malmierca et al., 2009; Pérez-González and Malmierca, 2012; Pérez-González et al., 2012). For CN neurons, the vast majority of FSL to deviant and to standard was almost equal and no differences in the median FSL between them was observed (Signed Rank Test; $p > 0.05$) (**Figure 12C**). The median of the FSLs was 9.62 ± 4.9 ms (range: 3.4 – 29.5 ms) and 9.82 ± 4.7 ms (range: 3.9 – 28.2 ms) for deviant and standard tone, respectively. These latencies are clearly shorter than the latencies of IC neurons (FSL to deviant: 26.1 ± 13.2 ms; range: 7.5 – 72 ms, FSL to standard: 29.6 ± 13.2 ms, range: 7.3 – 74.5 ms; from Malmierca et al., 2009). Although some neurons showed significant CSI > 0.1 (0.11 – 0.28) at 4 ($n = 3$), 8 ($n = 4$), 12 ($n = 2$), and 20 Hz ($n = 5$) (most of them from the DCN, $n = 5$), the average SSA indices were not significantly different from zero (Signed Rank Test; $p > 0.05$) nor they were sensitive to the rate of stimulation (Kruskal–Wallis Test; $p > 0.05$) (**Figure 12D**). Finally, CSI was not affected by increasing the frequency separation from

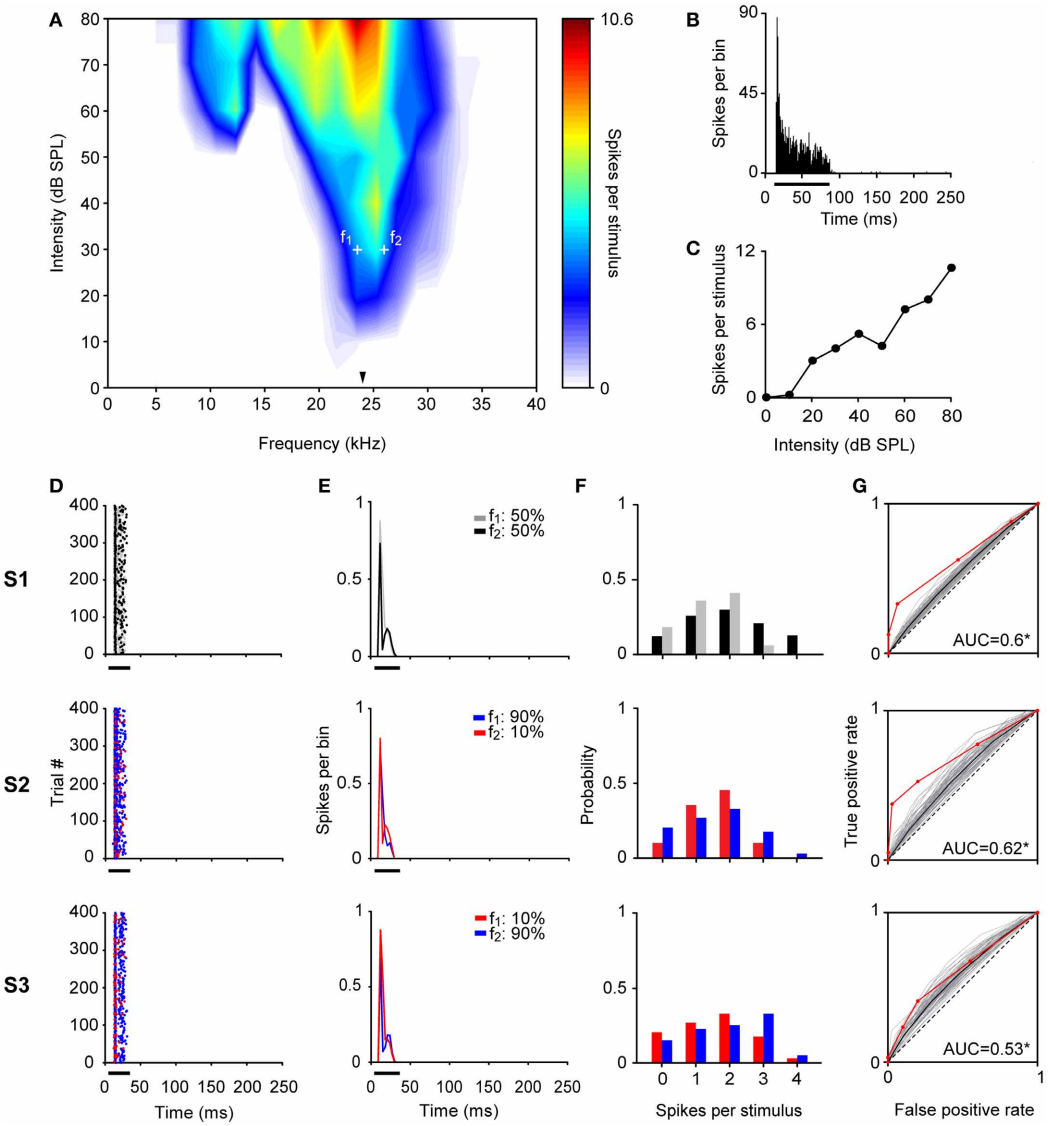

FIGURE 11 | Example of a CN neuron. The format for all panels is the same as in **Figures 3–5**. **(A)** The BF was 23.4 kHz (indicated by the arrowhead) and the tested frequencies ($f_1 = 23.4$ kHz and $f_2 = 25.9$ kHz, white crosses) differ by 0.144 octaves. The PSTH of the accumulated response to all the frequencies (0.5 – 40 KHz) and intensities (0 – 80 dB SPL) presented (1 ms bins), as well as, the rate-level function at BF are shown in **(B)** and **(C)**, respectively. The neuron exhibited a low CSI = 0.1 (Bootstrapping; $p > 0.05$) with a robust response across trials **(D,E)** and its frequency discriminability was not sensitive to the oddball condition **(F,G)**. The AUC values in all conditions were slightly higher than 0.5 (Permutation test; $^*p < 0.05$).

$\Delta f = 0.1$ to $\Delta f \geq 0.2$ $(0.2 - 0.37)$ (Signed Rank Test; $p > 0.05$) (**Figure 12E**).

In parallel with the lack of SSA, frequency discrimination was not affected by changes in tone probability in this neuronal population. The estimated correct detection in the oddball condition remained very similar to that elicited in the equiprobable one for most of the CN neurons (**Figure 13A**), and no improvement in frequency discriminability was elicited at the population level for any repetition rate group (Signed Rank Test; $p > 0.05$) (**Figure 13B**). Thus, the DEI was essentially zero and insensitive to increments in the repetition rate (Kruskal–Wallis Test; $p > 0.05$) (**Figure 13C**). As expected, it was not correlated with the SSA index (Spearman's correlation) (**Figure 13D**).

DISCUSSION

Our study demonstrates that sensitivity to frequency in IC neurons but not in CN neurons depends on probability context. Changes in frequency discriminability in IC neurons reflected the level of SSA they exhibit. Both the CSI and DEI values increased with frequency separation and DEI tended to be positive (**Figures 7** and **8**). The lack of effect of probability context in CN was related to the lack of SSA in the neuronal sample we recorded from (**Figure 12**).

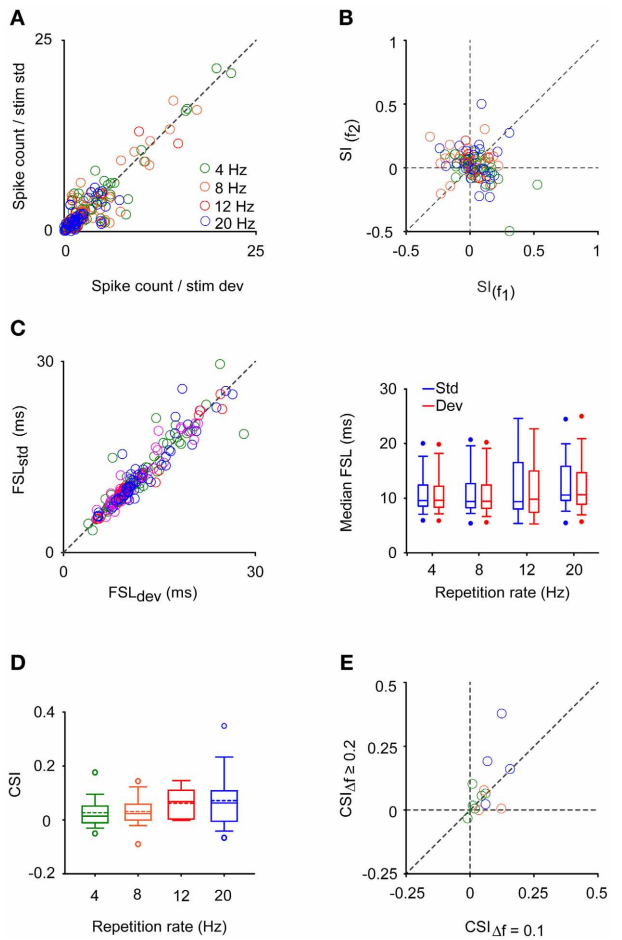

FIGURE 12 | CN neurons do not exhibit SSA. (A) Spike count to deviant (dev) and to standard (std) stimuli elicited at different repetition rates represented in a color code. This color code is the same for **(B–E)** panels. (4 Hz, $n = 47$; 8 Hz, $n = 29$; 12 Hz, $n = 9$; 20 Hz, $n = 26$) **(B)** Scattergraph of the Frequency-Specific SSA indices (SI) for f_1 and f_2 presented at different repetitions rates. This index reflects the normalized spikes counts elicited when each frequency was the deviant tone regarding the response evoked when it was the standard one. **(C)** Scattergraph of the median first spike latency (FSL) for f_1 and f_2 when they were the deviant (FSL_{dev}) or the standard (FSL_{std}) stimulus. In the right column, are displayed the box plots of the median FSL for the population of neurons to deviant (red) and to standard (blue) stimulus across repetition rates. The n for this panel is the double of the number of neurons tested, since two frequencies were tested as deviant and as standard stimulus for each neuron. **(D,E)** Box plots of the Common–SSA index (CSI) when increasing the rate of stimulation and scattergraph of CSI when varying the frequency separation factor (Δf), respectively.

STRONG SSA IS EXHIBITED BY IC NEURONS BUT NOT BY CN NEURONS

The strength of SSA reported here is similar to that reported previously by Malmierca et al. (2009) for IC neurons. This is not surprising, since we used a similar experimental preparation including animal model, parameters, and paradigm of stimulation (presentation rate: 4 Hz; tone duration: 75 ms; random presentation of tones). Other studies also have examined SSA in the IC, although as these studies have used different stimulation paradigms (e.g., Pérez-González et al., 2005; Lumani and Zhang, 2010), different metrics to quantify SSA (Pérez-González et al., 2005) or different stimulus repetition rates (Zhao et al., 2011), a quantitative comparison is difficult. According to the sample of histological verifications of the recording sites (**Figure 10A**) and taking into account the distribution of CSI (**Figure 2**), we recorded neurons from the central nucleus, as well as from the cortical non-lemniscal regions of IC. SSA varies as a continuum throughout the entire IC and it is strong and widespread in the non-lemniscal regions of the IC (Malmierca et al., 2009; Duque et al., 2012) and MGB (Antunes et al., 2010), being low or almost absent in the lemniscal subdivisions, the central nucleus of the IC and ventral MGB. Also, the neurons in the cortex of the IC exhibit broader response areas than those from the central nucleus (Malmierca et al., 2008, 2009; Geis et al., 2011; Duque et al., 2012). In agreement with these results, we show here that neurons with wider bandwidths (values as high as 30–40 kHz) showed the strongest SSA (**Figure 9**). Thus, the convergence of ascending, narrowly tuned frequency inputs with different frequency selectivity could be a major mechanism underlying SSA. In support to this idea, Taaseh et al. (2011) and Mill et al. (2011) showed that individual inputs showing simple fatigue could result in SSA. Beyond this mechanism, SSA could be further refined through the local inhibitory circuits and descending inputs from higher auditory centers. In this respect, a modulatory role of postsynaptic $GABA_A$ receptors in shaping SSA in the IC has already been demonstrated (Pérez-González and Malmierca, 2012; Pérez-González et al., 2012).

Considering that (1) the IC is the locus of convergence for most inputs originating at lower auditory brainstem nuclei and the locus where the lemniscal and non-lemniscal pathways appears (Malmierca et al., 2003; Lee and Sherman, 2010, 2011), and that (2) our results demonstrated the lack of widespread SSA at the CN (**Figure 12**), it is tempting to suggest that cells exhibiting strong SSA in the subcortical pathways first emerge in the non-lemniscal IC. Two possible confounds currently limit this hypothesis. First, a decrease in the responsiveness and changes in the response variability of auditory cortical neurons caused by the anesthesia (Kisley and Gerstein, 1999; Harris et al., 2011) could also result in the absence of strong SSA in CN. This would be the case, for example, if SSA in the CN were dependent on descending projections for its generation. However, this possibility seems unlikely since previous studies have demonstrated that SSA at the IC (Anderson and Malmierca, 2013) and MGB (Antunes and Malmierca, 2011) persist even if the corticofugal pathway is reversibly deactivated. Second, the CN has multiple distinct physiological response types which are well-correlated with anatomical and cellular characteristics. While neurons were recorded in both VCN and DCN, currently there is no detailed classification of CN neurons in the anesthetized rat. Therefore, we cannot rule out that we recorded from all response types in this study. Indeed, because across-frequency integration seems to be important in SSA, CN neuronal types that show frequency convergence and that project to the IC, e.g., some multipolar cells or small cells from the cap area (Winter and Palmer, 1995; Jiang et al., 1996; Palmer et al., 1996; Malmierca et al., 2002; Cant and Benson, 2003) might potentially be capable of showing high levels

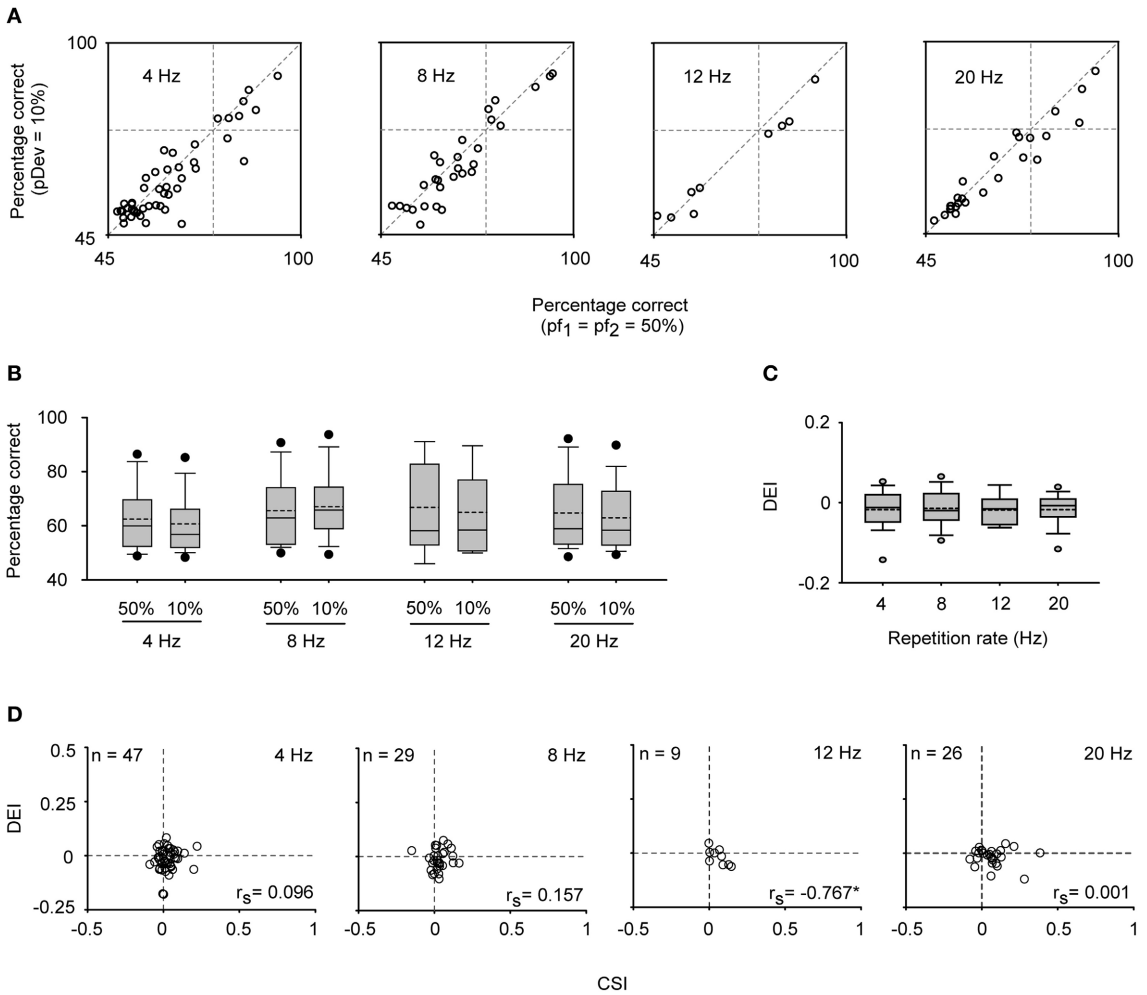

FIGURE 13 | Stimulus sensitivity in CN neurons. (A) Neurometric boxes displaying the percentage of correct identifications in the equiprobable and oddball condition (pDev = 10%) for different repetitions rates (4, 8, 12, and 20 Hz). **(B)** Box plots indicating that no improvement was elicited under the oddball condition regarding the equiprobable one (Signed Rank Test; $p > 0.05$). **(C)** Box plots that indicate that the discrimination enhancement indexes (DEI) remained at zero and did not change across repetition rate (Kruskal–Wallis Test; $p > 0.05$). **(D)** No positive correlation between the CSI and DEI was found (Spearman's correlation coefficient, r_s; $^*p < 0.05$).

of SSA as well. To rule out this possibility a detailed morphological and physiological study is necessary in the future. Finally, the presence of SSA in brainstem nuclei between the CN and IC also remains to be tested.

NEURONAL SENSITIVITY OF IC

We show here that the vast majority of IC neurons discriminate between nearby tones around BF even when they occur with equal probability (**Figures 6A,B**; upper left quadrants). While many of the AUCs were significantly larger than 0.5, they also tended to be smaller than 0.71, the standard definition of a psychophysical threshold. Note that other pairs of frequencies within the FRA with the same frequency difference could give rise to larger AUCs. Thus, our results for the equiprobable case should be seen as a lower bound on the frequency discrimination capabilities of IC neurons. Even with the biased selection of frequencies to test, a small population reached AUC > 0.71 for frequency separations as small as $\Delta f = 0.07$, very close to the psychophysical thresholds of rats (e.g., Talwar and Gerstein, 1998, 1999). Interestingly, these neurons also showed narrower bandwidths than the rest. The narrow bandwidth could result in large changes in firing rates for nearby frequencies, leading to the high AUCs (Gordon et al., 2008). Such narrowly-tuned inputs could also account for the hyperacuity of MGB and cortical neurons in oddball conditions, as previously reported (Ulanovsky et al., 2003; von der Behrens et al., 2009).

Frequency discrimination in IC depended on context, being larger when the stimuli had decreased probability (**Figures 6B,C** and **7**). Robust increases in discrimination in the oddball conditions occurred for the lower deviant probability (pDev = 10%) and the larger frequency separations ($\Delta f > 0.07$). Note that we used here the mean AUC across the two oddball sequences, rather than the maximal one as used previously (Ulanovsky et al., 2003; Malmierca et al., 2009). The mean AUC is

a more conservative estimate of frequency discriminability, and its use may explain why we did not observe extreme discrimination performance as reported previously in IC (Malmierca et al., 2009 their **Figure 7**, neurons in the upper left corner). Either way, these results emphasize the influence of context on sensory processing as early as in the IC as has been demonstrated before for the processing of interaural phase (Spitzer and Semple, 1991, 1993, 1998; McAlpine et al., 2000), level differences (Sanes et al., 1998), monaural frequency transitions (Malone and Semple, 2001) and simulated motion (Wilson and O'Neill, 1998).

FREQUENCY DISCRIMINABILITY ENHANCEMENT REFLECTS THE DEGREE OF SSA

We found a strong correlation between the discriminability enhancement and the degree of SSA, but only for the condition with the lowest deviant probability (pDev = 10%) and larger frequency separation ($\Delta f > 0.07$) (**Figure 8**). These are also the conditions that had higher CSI. This positive correlation is expected from the design of the experiment. The two frequencies were selected to evoke equivalent responses in the equiprobable condition, and in the oddball condition they were expected to evoke different responses. In consequence, we expected a substantial overlap between the spike count distributions in the equiprobable condition, but a decreasing overlap in the oddball condition. Indeed, DEI depended on deviant probability and frequency separation very similarly to CSI (**Figure 7**). Finally, the absence of SSA and null enhancement in deviant detectability by CN neurons reinforced the notion that deviant discriminability is a functional consequence of SSA (**Figures 12** and **13**).

Nevertheless, we also found that neurons with CSI ≤ 0.1 showed a significant decrease in AUC in the oddball condition (**Figure 6B**). This decrease was due to larger corrections for the AUCs obtained under the oddball condition than to the AUCs under the equiprobable one. This trend should be seen as a negative bias in the estimation of the AUC under oddball conditions. Given that as a rule AUC increased with decreasing deviant probability, our conclusions should be considered as conservative.

FUNCTIONAL SIGNIFICANCE

Neuronal responses in auditory cortex are plastic at many different time scales (Condon and Weinberger, 1991; Kilgard and Merzenich, 1998, 2002; Fritz et al., 2003; Ulanovsky et al., 2003; Froemke et al., 2007). Here we demonstrate that neurons in IC show some sort of short-term plasticity under similar conditions to neurons in MGB and A1. As previously suggested (Antunes et al., 2010), the non-lemniscal regions of the IC could transmit SSA to the non-lemniscal MGB neurons, which in turn would project to the superficial layers of AC (Cetas et al., 1999; Huang and Winer, 2000; Anderson et al., 2009). Neurons in the medial division of the MGB have large-diameter axons that are known to terminate primarily in layer I of the auditory cortex in both primary and secondary cortical fields. For example, in the somatosensory cortex Cauller and Connors (1994) observed strong excitatory effects on pyramidal cells present in layers II, III and V to be mediated by long horizontal axons located in layer I. Further experiments are required in order to check this possibility. Thus, at all levels of the auditory pathways, context-dependence of the responses could serve for adjusting the neural code to match the statistics of the input signal to produce an efficient representation of auditory scene. Similarly, the changes in responses as a function of tone probability could serve in the processes of auditory scene analysis. Indeed, auditory stream segregation is also sensitive to frequency separation and presentation rate (e.g., Fishman et al., 2004; Fishman and Steinschneider, 2010). Moreover, there is evidence suggesting the involvement of pre-attentive neural process in auditory stream segregation (Winkler et al., 2003). Thus, SSA in IC may increase the saliency of low-probability signals, helping to segregate them by reducing the ambiguity of the neuronal representations for downstream read-out mechanisms.

Interestingly, our results suggest that the initial locus for the computation of SSA is not at the very first stations of the auditory pathway, e.g., the CN. Thus, the picture of the auditory system that emerges here reinforces the idea that the initial coding of sounds is purely based on their short-term physical characteristics, and sensitivity to longer contexts that is required for higher-order processing, efficient coding, and auditory scene analysis appears only later.

AUTHOR CONTRIBUTIONS

Manuel S. Malmierca and David Pérez-González designed research; Yaneri A. Ayala performed research; Yaneri A. Ayala, Daniel Duque, David Pérez-González and Israel Nelken analyzed data; Yaneri A. Ayala, David Pérez-González, Israel Nelken and Manuel S. Malmierca wrote the paper.

ACKNOWLEDGMENTS

Financial support was provided by the Spanish MEC (BFU2009-07286), EU (EUI2009-04083, in the framework of the ERA-NET NEURON Network of European Funding for Neuroscience Research) to Manuel S. Malmierca. Israel Nelken was supported by a grant from the Israeli Ministry of Health in the framework of the ERA-NET Network. Daniel Duque held a fellowship from the Spanish MINECO (BES-2010-035649). David Pérez-González held a postdoctoral fellowship from the Botín Foundation. We thank Drs. Alan Palmer and Trevor M. Shackleton for their constructive comments on a previous version.

REFERENCES

Anderson, L. A., Christianson, G. B., and Linden, J. F. (2009). Stimulus-specific adaptation occurs in the auditory thalamus. *J. Neurosci.* 29, 7359–7363.

Anderson, L. A., Izquierdo, M. A., Antunes, F. M., and Malmierca, M. S. (2009). A monosynaptic pathway from dorsal cochlear nucleus to auditory cortex in rat. *Neuroreport* 20, 462–466.

Anderson, L. A., and Malmierca, M. S. (2013). The effect of auditory cortical deactivation on stimulus-specific adaptation in the inferior colliculus of the rat. *Eur. J. Neurosci.* 37, 52–62.

Antunes, F. M., and Malmierca, M. S. (2011). Effect of auditory cortex deactivation on stimulus-specific adaptation in the medial geniculate body. *J. Neurosci.* 31, 17306–17316.

Antunes, F. M., Nelken, I., Covey, E., and Malmierca, M. S. (2010). Stimulus-specific adaptation in the auditory thalamus of the anesthetized rat. *PLoS ONE* 5:e14071. doi: 10.1371/journal.pone.0014071

Ayala, Y. A., and Malmierca, M. S. (2012). Stimulus-specific adaptation and deviance detection in the inferior colliculus. *Front. Neural Circuits* 6:89. doi: 10.3389/fncir.2012.00089

Bäuerle, P., von der Behrens, W., Kössl, M., and Gaese, B. H. (2011). Stimulus-specific adaptation in the gerbil primary auditory thalamus is the result of a fast frequency-specific habituation and is regulated by the corticofugal system. *J. Neurosci.* 31, 9708–97022.

Cant, N. B., and Benson, C. G. (2003). Parallel auditory pathways: projection patterns of the different neuronal populations in the dorsal and ventral cochlear nuclei. *Brain Res. Bull.* 60, 457–474.

Cauller, L. J., and Connors, B. W. (1994). Synaptic physiology of horizontal afferents to layer I in slices of rat SI neocortex. *J. Neurosci.* 14, 751–762.

Cetas, J. S., de Venecia, R. K., and McMullen, N. T. (1999). Thalamocortical afferents of Lorente de Nó: medial geniculate axons that project to primary auditory cortex have collateral branches to layer I. *Brain Res.* 830, 203–208.

Chechik, G., Anderson, M. J., Bar-Yosef, O., Young, E. D., Tishby, N., and Nelken, I. (2006). Reduction of information redundancy in the ascending auditory pathway. *Neuron* 51, 359–368.

Cohn, T. E., Green, D. G., and Tanner, W. P. Jr. (1975). Receiver operating characteristic analysis. Application to the study of quantum fluctuation effects in optic nerve of Rana pipiens. *J. Gen. Physiol.* 66, 583–616.

Condon, C. D., and Weinberger, N. M. (1991). Habituation produces frequency-specific plasticity of receptive fields in the auditory cortex. *Behav. Neurosci.* 105, 416–430.

Duque, D., Pérez-González, D., Ayala, A. Y., Palmer, A. R., and Malmierca, M. S. (2012). Topographic distribution, frequency and intensity dependence of stimulus specific adaptation in the inferior colliculus of the rat. *J. Neurosci.* 32, 17762–17774.

Faure, P. A., Fremouw, T., Casseday, J. H., and Covey, E. (2003). Temporal masking reveals properties of sound-evoked inhibition in duration-tuned neurons of the inferior colliculus. *J. Neurosci.* 23, 3052–3065.

Fawcett, T. (2006). An introduction to ROC analysis. *Pattern Recognit. Lett.* 27, 861–874.

Fishman, Y. I., Arezzo, J. C., and Steinschneider, M. (2004). Auditory stream segregation in monkey auditory cortex: effects of frequency separation, presentation rate, and tone duration. *J. Acoust. Soc. Am.* 116, 1656–1670.

Fishman, Y. I., and Steinschneider, M. (2010). "Formation of auditory streams," in *The Oxford Handbook of Auditory Science: the Auditory Brain,* ed D. R. Moore (New York, NY: Oxford UP), 215–245.

Fritz, J., Shamma, S., Elhilali, M., and Klein, D. (2003). Rapid task-related plasticity of spectrotemporal receptive fields in primary auditory cortex. *Nat. Neurosci.* 6, 1216–1223.

Froemke, R. C., Merzenich, M. M., and Schreiner, C. E. (2007). A synaptic memory trace for cortical receptive field plasticity. *Nature* 450, 425–429.

Geis, H. R., van der Heijden, M., and Borst, J. G. (2011). Subcortical input heterogeneity in the mouse inferior colliculus. *J. Physiol.* 589, 3955–3967.

Gordon, N., Shackleton, T. M., Palmer, A. R., and Nelken, I. (2008). Responses of neurons in the inferior colliculus to binaural disparities: insights from the use of Fisher information and mutual information. *J. Neurosci. Methods* 169, 391–404.

Green, D. M., and Swets, J. A. (1966). *Signal Detection Theory and Psychophysics*. New York, NY: Wiley.

Gutfreund, Y. (2012). Stimulus-specific adaptation, habituation and change detection in the gaze control system. *Biol. Cybern*. 106, 657–668.

Huang, C. L., and Winer, J. A. (2000). Auditory thalamocortical projections in the cat: laminar and areal patterns of input. *J. Comp. Neurol.* 427, 302–331.

Hara, K., and Harris, R. A. (2002). The anesthetic mechanism of urethane: the effects on neurotransmitter-gated ion channels. *Anesth. Analg.* 94, 313–318.

Harris, K. D., Bartho, P., Chadderton, P., Curto, C., De La Rocha, J., Hollender, L., et al. (2011). How do neurons work together? Lessons from auditory cortex. *Hear. Res.* 271, 37–53.

Hernández, O., Espinosa, N., Pérez-González, D., and Malmierca, M. S. (2005). The inferior colliculus of the rat: a quantitative analysis of monaural frequency response areas. *Neuroscience* 132, 203–217.

Jiang, D., Palmer, A. R., and Winter, I. M. (1996). Frequency extent of two-tone facilitation in onset units in the ventral cochlear nucleus. *J. Neurophysiol.* 75, 380–395.

Kilgard, M. P., and Merzenich, M. M. (1998). Plasticity of temporal information processing in the primary auditory cortex. *Nat. Neurosci.* 1, 727–731.

Kilgard, M. P., and Merzenich, M. M. (2002). Order-sensitive plasticity in adult primary auditory cortex. *Proc. Natl. Acad. Sci. U.S.A.* 99, 3205–3209.

Kisley, M. A., and Gerstein, G. L. (1999). Trial-to-trial variability and state-dependent modulation of auditory-evoked responses in cortex. *J. Neurosci.* 19, 10451–10460.

LeBeau, F. E., Malmierca, M. S., and Rees, A. (2001). Iontophoresis *in vivo* demonstrates a key role for GABA(A) and glycinergic inhibition in shaping frequency response areas in the inferior colliculus of guinea pig. *J. Neurosci.* 21, 7303–7312.

Lee, C. C., and Sherman, S. M. (2010). Topography and physiology of ascending streams in the auditory tectothalamic pathway. *Proc. Natl. Acad. Sci. U.S.A.* 107, 372–377.

Lee, C. C., and Sherman, S. M. (2011). On the classification of pathways in the auditory midbrain, thalamus, and cortex. *Hear. Res.* 276, 79–87.

Loftus, W. C., Malmierca, M. S., Bishop, D. C., and Oliver, D. L. (2008). The cytoarchitecture of the inferior colliculus revisited: a common organization of the lateral cortex in rat and cat. *Neuroscience* 154, 196–205.

Lumani, A., and Zhang, H. (2010). Responses of neurons in the rat's dorsal cortex of the inferior colliculus to monaural tone bursts. *Brain Res.* 1351, 115–129.

Malmierca, M. S., Blackstad, T. W., and Osen, K. K. (2011). Computer-assisted 3-D reconstructions of Golgi-impregnated neurons in the cortical regions of the inferior colliculus of rat. *Hear. Res.* 274, 13–26.

Malmierca, M. S., Cristaudo, S., Pérez-González, D., and Covey, E. (2009). Stimulus-specific adaptation in the inferior colliculus of the anesthetized rat. *J. Neurosci.* 29, 5483–5493.

Malmierca, M. S., Hernández, O., Falconi, A., Lopez-Poveda, E. A., Merchan, M., and Rees, A. (2003). The commissure of the inferior colliculus shapes frequency response areas in rat: an *in vivo* study using reversible blockade with microinjection of kynurenic acid. *Exp. Brain Res.* 153, 522–529.

Malmierca, M. S., Izquierdo, M. A., Cristaudo, S., Hernández, O., Pérez-González, D., Covey, E., et al. (2008). A discontinuous tonotopic organization in the inferior colliculus of the rat. *J. Neurosci.* 28, 4767–4776.

Malmierca, M. S., Merchán, M. A., Henkel, C. K., and Oliver, D. L. (2002). Direct projections from cochlear nuclear complex to auditory thalamus in the rat. *J. Neurosci.* 22, 10891–10897.

Malmierca, M. S., and Ryugo, D. K. (2011). "Descending connections of auditory cortex to the midbrain and brainstem," in *The Auditory Cortex*, eds J. A. Winer and C. E. Schreiner (New York, NY: Springer), 189–208.

Malone, B. J., and Semple, M. N. (2001). Effects of auditory stimulus context on the representation of frequency in the gerbil inferior colliculus. *J. Neurophysiol.* 86, 1113–1130.

Maris, E. (2012). Statistical testing in electrophysiological studies. *Psychophysiology* 49, 549–565.

McAlpine, D., Jiang, D., Shackleton, T. M., and Palmer, A. R. (2000). Responses of neurons in the inferior colliculus to dynamic interaural phase cues: evidence for a mechanism of binaural adaptation. *J. Neurophysiol.* 83, 1356–1365.

Merrill, E. G., and Ainsworth, A. (1972). Glass-coated platinum-plated tungsten microelectrodes. *Med. Biol. Eng.* 10, 662–672.

Mill, R., Coath, M., Wennekers, T., and Denham, S. L. (2011). A neurocomputational model of stimulus-specific adaptation to oddball and Markov sequences. *PLoS Comput. Biol.* 7:e1002117. doi: 10.1371/journal.pcbi.1002117

Näätänen, R. (1992). *Attention and Brain Function*. Hillsdale, NJ: Lawrence Erlbaum.

Nelken, I., and Ulanovsky, N. (2007). Mismatch negativity and stimulus-specific adaptation in animal models. *J. Psychophysiol.* 21, 214–223.

Nelson, D. A., and Kiester, T. E. (1978). Frequency discrimination in the chinchilla. *J. Acoust. Soc. Am.* 64, 114–126.

Netser, S., Zahar, Y., and Gutfreund, Y. (2011). Stimulus-specific adaptation: can it be a neural correlate of behavioral habituation? *J. Neurosci.* 31, 17811–17820.

Palmer, A. R., Jiang, D., and Marshall, D. H. (1996). Responses of ventral cochlear nucleus onset and chopper units as a function of signal bandwidth. *J. Neurophysiol.* 75, 780–794.

Patel, C. R., Redhead, C., Cervi, A. L., and Zhang, H. (2012). Neural sensitivity to novel sounds in the rat's dorsal cortex of the inferior colliculus as revealed by evoked local field potentials. *Hear. Res.* 286, 41–54.

Paxinos, G., and Watson, C. (2007). *The Rat Brain in Stereotaxic Coordinates*. Burlington, VT: Elsevier-Academic.

Pérez-González, D., Hernández, O., Covey, E., and Malmierca, M. S. (2012). GABA(A)-mediated inhibition modulates stimulus-specific adaptation in the inferior

colliculus. *PLoS ONE* 7:e34297. doi: 10.1371/journal.pone.0034297

Pérez-González, D., and Malmierca, M. S. (2012). Variability of the time course of stimulus-specific adaptation in the inferior colliculus. *Front. Neural Circuits* 6:107. doi: 10.3389/fncir.2012.00107

Pérez-González, D., Malmierca, M. S., and Covey, E. (2005). Novelty detector neurons in the mammalian auditory midbrain. *Eur. J. Neurosci.* 22, 2879–2885.

Pérez-González, D., Malmierca, M. S., Moore, J. M., Hernández, O., and Covey, E. (2006). Duration selective neurons in the inferior colliculus of the rat: topographic distribution and relation of duration sensitivity to other response properties. *J. Neurophysiol.* 95, 823–836.

Reches, A., and Gutfreund, Y. (2008). Stimulus-specific adaptations in the gaze control system of the barn owl. *J. Neurosci.* 28, 1523–1533.

Reches, A., and Gutfreund, Y. (2009). Auditory and multisensory responses in the tectofugal pathway of the barn owl. *J. Neurosci.* 29, 9602–9613.

Reches, A., Netser, S., and Gutfreund, Y. (2010). Interactions between stimulus-specific adaptation and visual auditory integration in the forebrain of the barn owl. *J. Neurosci.* 30, 6991–6998.

Rees, A. (1990). A close-field sound system for auditory neurophysiology. *J. Physiol.* 430, 2.

Rees, A., Sarbaz, A., Malmierca, M. S., and Le Beau, F. E. (1997). Regularity of firing of neurons in the inferior colliculus. *J. Neurophysiol.* 77, 2945–2965.

Sanes, D. H., Malone, B. J., and Semple, M. N. (1998). Role of synaptic inhibition in processing of dynamic binaural level stimuli. *J. Neurosci.* 18, 794–803.

Shackleton, T. M., Arnott, R. H., and Palmer, A. R. (2005). Sensitivity to interaural correlation of single neurons in the inferior colliculus of guinea pigs. *J. Assoc. Res. Otolaryngol.* 6, 244–259.

Shackleton, T. M., Skottun, B. C., Arnott, R. H., and Palmer, A. R. (2003). Interaural time difference discrimination thresholds for single neurons in the inferior colliculus of guinea pigs. *J. Neurosci.* 23, 716–724.

Shofner, W. P. (2000). Comparison of frequency discrimination thresholds for complex and single tones in chinchillas. *Hear. Res.* 149, 106–114.

Shofner, W. P., and Dye, R. H. Jr. (1989). Statistical and receiver operating characteristic analysis of empirical spike-count distributions: quantifying the ability of cochlear nucleus units to signal intensity changes. *J. Acoust. Soc. Am.* 86, 2172–2184.

Sinnott, J. M., Petersen, M. R., and Hopp, S. L. (1985). Frequency and intensity discrimination in humans and monkeys. *J. Acoust. Soc. Am.* 78, 1977–1985.

Skottun, B. C., Shackleton, T. M., Arnott, R. H., and Palmer, A. R. (2001). The ability of inferior colliculus neurons to signal differences in interaural delay. *Proc. Natl. Acad. Sci. U.S.A.* 98, 14050–14054.

Spitzer, M. W., and Semple, M. N. (1991). Interaural phase coding in auditory midbrain: influence of dynamic stimulus features. *Science* 254, 721–724.

Spitzer, M. W., and Semple, M. N. (1993). Responses of inferior colliculus neurons to time-varying interaural phase disparity: effects of shifting the locus of virtual motion. *J. Neurophysiol.* 69, 1245–1263.

Spitzer, M. W., and Semple, M. N. (1998). Transformation of binaural response properties in the ascending auditory pathway: influence of time-varying interaural phase disparity. *J. Neurophysiol.* 80, 3062–3076.

Stabler, S. E., Palmer, A. R., and Winter, I. M. (1996). Temporal and mean rate discharge patterns of single units in the dorsal cochlear nucleus of the anesthetized guinea pig. *J. Neurophysiol.* 76, 1667–1688.

Stüttgen, M. C., Schwarz, C., and Jakel, F. (2011). Mapping spikes to sensations. *Front. Neurosci.* 5:125. doi: 10.3389/fnins.2011.00125

Syka, J., Rybalko, N., Brozek, G., and Jilek, M. (1996). Auditory frequency and intensity discrimination in pigmented rats. *Hear. Res.* 100, 107–113.

Taaseh, N., Yaron, A., and Nelken, I. (2011). Stimulus-specific adaptation and deviance detection in the rat auditory cortex. *PLoS ONE* 6:e23369. doi: 10.1371/journal.pone.0023369

Talwar, S. K., and Gerstein, G. L. (1998). Auditory frequency discrimination in the white rat. *Hear. Res.* 126, 135–150.

Talwar, S. K., and Gerstein, G. L. (1999). A signal detection analysis of auditory-frequency discrimination in the rat. *J. Acoust. Soc. Am.* 105, 1784–1800.

Tanner, W. P. Jr., and Swets, J. A. (1954). A decision-making theory of visual detection. *Psychol. Rev.* 61, 401–409.

Ulanovsky, N., Las, L., Farkas, D., and Nelken, I. (2004). Multiple time scales of adaptation in auditory cortex neurons. *J. Neurosci.* 24, 10440–10453.

Ulanovsky, N., Las, L., and Nelken, I. (2003). Processing of low-probability sounds by cortical neurons. *Nat. Neurosci.* 6, 391–398.

von der Behrens, W., Bäuerle, P., Kossl, M., and Gaese, B. H. (2009). Correlating stimulus-specific adaptation of cortical neurons and local field potentials in the awake rat. *J. Neurosci.* 29, 13837–13849.

Walker, K. M., Schnupp, J. W., Hart-Schnupp, S. M., King, A. J., and Bizley, J. K. (2009). Pitch discrimination by ferrets for simple and complex sounds. *J. Acoust. Soc. Am.* 126, 1321–1335.

Wilson, W. W., and O'Neill, W. E. (1998). Auditory motion induces directionally dependent receptive field shifts in inferior colliculus neurons. *J. Neurophysiol.* 79, 2040–2062.

Winkler, I., Sussman, E., Tervaniemi, M., Horvath, J., Ritter, W., and Naatanen, R. (2003). Preattentive auditory context effects. *Cogn. Affect. Behav. Neurosci.* 3, 57–77.

Winter, I. M., and Palmer, A. R. (1995). Level dependence of cochlear nucleus onset unit responses and facilitation by second tones or broadband noise. *J. Neurophysiol.* 73, 141–159.

Witte, R. S., and Kipke, D. R. (2005). Enhanced contrast sensitivity in auditory cortex as cats learn to discriminate sound frequencies. *Brain Res. Cogn. Brain Res.* 23, 171–184.

Yu, X. J., Xu, X. X., He, S., and He, J. (2009). Change detection by thalamic reticular neurons. *Nat. Neurosci.* 12, 1165–1170.

Zhao, L., Liu, Y., Shen, L., Feng, L., and Hong, B. (2011). Stimulus-specific adaptation and its dynamics in the inferior colliculus of rat. *Neuroscience* 181, 163–174.

Conflict of Interest Statement: The authors declare that the research was conducted in the absence of any commercial or financial relationships that could be construed as a potential conflict of interest.

Received: 10 September 2012; accepted: 19 December 2012; published online: 14 January 2013.

*Citation: Ayala YA, Pérez-González D, Duque D, Nelken I and Malmierca MS (2013) Frequency discrimination and stimulus deviance in the inferior colliculus and cochlear nucleus. Front. Neural Circuits **6**:119. doi: 10.3389/fncir.2012.00119*

frontiers in
NEURAL CIRCUITS

REVIEW ARTICLE
published: 17 January 2013
doi: 10.3389/fncir.2012.00089

Stimulus-specific adaptation and deviance detection in the inferior colliculus

Yaneri A. Ayala*[1] *and Manuel S. Malmierca*[1,2]

[1] *Laboratory for the Neurobiology of Hearing, Auditory Neurophysiology Unit, Institute of Neuroscience of Castilla y León, University of Salamanca, Salamanca, Spain*
[2] *Department of Cell Biology and Pathology, Faculty of Medicine, University of Salamanca, Salamanca, Spain*

Edited by:
Eric D. Young, Johns Hopkins University, USA

Reviewed by:
Adrian Rees, Newcastle University, UK
Eric D. Young, Johns Hopkins University, USA

****Correspondence:***
Manuel S. Malmierca, Auditory Neurophysiology Unit (Lab. 1), Institute of Neuroscience of Castilla y León, University of Salamanca, Laboratory for the Neurobiology of Hearing, C/ Pintor Fernando Gallego, 1, 37007 Salamanca, Spain.
e-mail: msm@usal.es

Deviancy detection in the continuous flow of sensory information into the central nervous system is of vital importance for animals. The task requires neuronal mechanisms that allow for an efficient representation of the environment by removing statistically redundant signals. Recently, the neuronal principles of auditory deviance detection have been approached by studying the phenomenon of stimulus-specific adaptation (SSA). SSA is a reduction in the responsiveness of a neuron to a common or repetitive sound while the neuron remains highly sensitive to rare sounds (Ulanovsky et al., 2003). This phenomenon could enhance the saliency of unexpected, deviant stimuli against a background of repetitive signals. SSA shares many similarities with the evoked potential known as the "mismatch negativity," (MMN) and it has been linked to cognitive process such as auditory memory and scene analysis (Winkler et al., 2009) as well as to behavioral habituation (Netser et al., 2011). Neurons exhibiting SSA can be found at several levels of the auditory pathway, from the inferior colliculus (IC) up to the auditory cortex (AC). In this review, we offer an account of the state-of-the art of SSA studies in the IC with the aim of contributing to the growing interest in the single-neuron electrophysiology of auditory deviance detection. The dependence of neuronal SSA on various stimulus features, e.g., probability of the deviant stimulus and repetition rate, and the roles of the AC and inhibition in shaping SSA at the level of the IC are addressed.

Keywords: auditory, non-lemniscal pathway, frequency deviance, change detection, GABA-mediated inhibition, corticofugal modulation, mismatch negativity

THE AUDITORY SYSTEM IS HIGHLY SENSITIVE TO DEVIANT STIMULI

An animal's behavioral responses to unexpected changes in the continuous flow of sensory, including acoustic, information are critical for its survival. These responses depend on the ability to detect deviancy in an ongoing stimulus. In order for the nervous system to determine whether a sound is deviant, there must be an ongoing storage of information about the sounds that have already occurred, as well as a comparison of new sounds with previous ones.

Auditory deviance detection has been widely explored in human electroencephalogram (EEG) studies (for a review see Grimm and Escera, 2012). Those studies have shown that the waveform elicited by a deviant (low probability) stimulus differs from that elicited by a predictable (high probability) stimulus. Deviance detection has been associated with a particular evoked potential derived from the human EEG, namely the "mismatch negativity" (MMN; Näätänen et al., 1978; for recent review, see Näätänen et al., 2007). The MMN is measured as the difference between the evoked potential elicited to a sequentially repeated (high probability) stimulus, referred to as the "standard," and that elicited by a rarely occurring (low probability) sound referred to as the "deviant" that differs in any of its attributes such as location, pitch, intensity, or duration (**Figure 1A**). The MMN usually peaks at 150–200 ms from the onset of a change. It has a frontocentral scalp distribution, with positive voltages at electrode positions below the Sylvian fissure, indicating generator sources located bilaterally on the supratemporal plane of the auditory cortex (AC) (Huotilainen et al., 1998) with an additional prefrontal contribution (Shalgi and Deouell, 2007). The MMN is useful for the study of deviance detection in humans because (1) it provides a reliable signal of auditory change detection (e.g., Escera et al., 2000), and (2) it can be recorded passively, i.e., with no specific instruction given to the subjects, which makes it suitable for studying non-cooperative populations, such as patients with cerebral lesions, neurodegenerative diseases, or psychiatric disorders (e.g., Duncan et al., 2009; Luck et al., 2011), as well as newborns (Carral et al., 2005a) and fetuses (Draganova et al., 2005).

Because deviance detection requires information storage and comparison over time, it could be thought of as a form of cognitive processing, or "primitive intelligence" (Näätänen et al., 2001). For this reason, it has been commonly assumed that deviance detection must be accomplished at the level of the cortex. This assumption has persisted not only for theoretical reasons, but also because it is difficult to pinpoint the site at which EEG waveforms are generated, especially in the case of subcortical structures. However, the fact that the MMN persists during sleep or anesthesia suggests that it is "preattentive" in origin (Tiitinen et al., 1994)

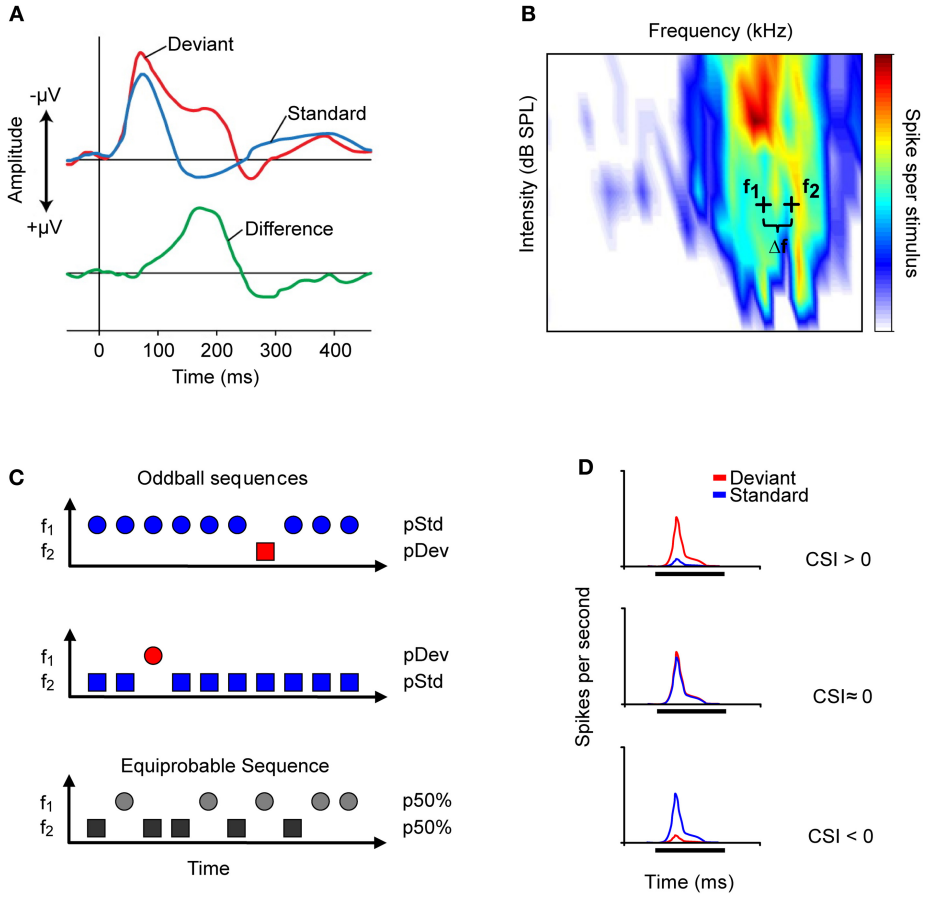

FIGURE 1 | Auditory change detection is studied by recording the evoked potentials of populations of neurons or the responses of single-units. (A) Schematic representation of the evoked potential known as the mismatch negativity (MMN) recorded through an electroencephalogram. The MMN is associated with the detection of deviant auditory events. It is measured as the difference (green line) between the potential elicited by a sequentially repeated stimulus (standard, blue line), and that elicited by a sound "deviating" in any of its attributes (deviant, red line). The peak of the MMN wave usually occurs at 150–200 ms from the onset of the deviant stimulus. **(B)** Frequency response area (FRA, combination of frequencies and intensities capable of evoking a response) of an IC neuron. Based on the FRA, the experimenter chooses a pair of frequencies (f_1 and f_2, black crosses) with a fixed physical separation (Δf) and at the same level to present in the oddball paradigm. Usually, in studies of the IC, a Δf of 0.058, 0.144, or 0.53 octaves is used. **(C)** Representation of the oddball paradigm used to study the detection of frequency deviance. In one oddball sequence (top), one frequency (f_1) is presented as the standard stimulus with a high probability of occurrence (blue symbol), while the second (f_2) is the rarely occurring deviant stimulus (red symbol), interspersed randomly among the standards. In a second oddball sequence (middle), the relative probabilities of the two stimuli are reversed, with f_2 as the standard (blue) and f_1 as the deviant (red). As a control (bottom), both frequencies are presented with the same probability of occurrence [equiprobable condition; $p(f_1) = p(f_2) = 50\%$]. **(D)** The common-SSA index (CSI) is a widely used metric to quantify the extent of SSA in the neuronal responses. The three PSTHs represents the response to deviant (red) and to standard (blue) tone of neurons exhibiting different values of CSI. The CSI compares the responses to deviant and to standard stimuli from the two oddball sequences by normalizing the responses in terms of spikes per stimulus (see text). The normalization corrects for the different number of presentations of the standard and deviant stimuli in each sequence. The possible values of the CSI range from +1 to −1, with positive values indicating that the response magnitude to the deviant is higher than that to the standard stimulus (upper PSTH); zero indicating that the two stimuli elicit equal responses (middle PSTH); and negative values indicating that the response to the standard stimulus is greater than that to the deviant stimulus (bottom PSTH).

and therefore could originate subcortically. This idea was largely untested and controversial until recently, as deviant occurrence is also reflected in the middle latency response (MLR) range of the evoked-activity, indicating that auditory change detection already occurs in early stages of human auditory processing (Slabu et al., 2010, 2012; Grimm et al., 2011).The MLR is a sequence of waveforms in the range of 12–50 ms from sound onset that precedes the well-studied MMN and it is generated by activation of subcortical areas as well as primary and secondary cortical areas (Grimm and Escera, 2012). Moreover, Slabu et al. (2012) showed that the human auditory brainstem is able to encode regularities in the recent auditory past that could be used for comparison to deviant events, and confirmed multiple anatomical and temporal scales of human deviance detection.

Finally, it is worth mentioning that MMN-like auditory-evoked potentials have also been recorded in laboratory animals in the AC (Javitt et al., 1994; Ruusuvirta et al., 1998; Eriksson and Villa, 2005; Astikainen et al., 2006, 2011; Tikhonravov et al., 2008; Nakamura et al., 2011) and subcortical structures: thalamus of the guinea pig (Kraus et al., 1994; King et al., 1995) and

inferior colliculus (IC) of the rat (Patel et al., 2012). Overall, these studies suggest that deviance detection may be a basic property of the functional organization of the auditory system occurring on multiples levels along the auditory pathway (Grimm et al., 2011; Grimm and Escera, 2012). Nevertheless, identification of the neuronal microcircuits and functional mechanisms underlying deviance detection remains a challenge in auditory neuroscience.

STIMULUS-SPECIFIC ADAPTATION: A NEURAL MECHANISM FOR DETECTION OF DEVIANT STIMULI

A decade ago, Nelken and colleagues (Ulanovsky et al., 2003) published a pioneering study that described a phenomenon similar to MMN and occurring at the cellular level in the mammalian AC. The single-neuron phenomenon was referred to as stimulus-specific adaptation (SSA) [a term originally coined by Movshon and Lennie (1979)] and it is proposed to be a neuronal mechanism that could be contributing to auditory deviance detection (Ulanovsky et al., 2003; Jääskeläinen et al., 2007). SSA is the reduction in the responsiveness of a neuron to a common or repetitive sound while the response decrement does not generalize to others sounds that are rarely presented. In this sense, SSA is a phenomenon of neuronal adaptation to the history of the stimulus rather than to the activity of the neuron (Nelken and Ulanovsky, 2007; Netser et al., 2011; Gutfreund, 2012). Although, MMN and SSA share several features such as their dependence on stimulation rate, they also greatly differ in their latencies and level of the neural structures involved (Nelken and Ulanovsky, 2007; Grimm and Escera, 2012). In addition, MMN is elicited by deviant stimuli immersed in complex forms of regularities (Carral et al., 2005b; Cornella et al., 2012; Recasens et al., 2012) that remained to be tested in single-unit recordings.

SSA is a widespread phenomenon in the brain exhibited by neurons of the visual (Woods and Frost, 1977; Sobotka and Ringo, 1994; Müller et al., 1999), somatosensory (Katz et al., 2006) and auditory (Ulanovsky et al., 2003; Malmierca et al., 2009a; Reches and Gutfreund, 2008; Anderson et al., 2009; Antunes et al., 2010) systems.

Auditory neurons that exhibit SSA for frequency deviance have been described in the IC (Pérez-González et al., 2005; Reches and Gutfreund, 2008; Malmierca et al., 2009a; Lumani and Zhang, 2010; Netser et al., 2011; Zhao et al., 2011), medial geniculate body (MGB) (Anderson et al., 2009; Yu et al., 2009; Antunes et al., 2010; Baüerle et al., 2011), and primary AC (Ulanovsky et al., 2003, 2004; Von Der Behrens et al., 2009; Taaseh et al., 2011). In the brainstem, SSA has been recently explored in the ventral and dorsal cochlear nucleus of the rat and the results suggest that all cochlear nucleus neurons tested lack SSA (Ayala et al., 2012). Thus, the IC is the earliest center where SSA has been described (Malmierca et al., 2009a), although it remains to be tested whether or not other brainstem nuclei located in between the cochlear nucleus and IC show some degree of SSA. In this review, we will focus on a description of SSA occurring at the IC, which is the major auditory station in the midbrain for the integration of ascending, descending, intrinsic, and commissural inputs (Malmierca, 2003; Malmierca et al., 2003, 2005a,b, 2009b; Cant and Benson, 2006; Loftus et al., 2010; Malmierca and Hackett, 2010; Malmierca and Ryugo, 2011).

STIMULUS-SPECIFIC ADAPTATION IN SINGLE-NEURON RESPONSE

Most of the studies of SSA in the IC have been carried out in the anesthetized rat (Pérez-González et al., 2005, 2012; Malmierca et al., 2009a; Lumani and Zhang, 2010; Zhao et al., 2011; Patel et al., 2012). Initially, Pérez-González et al. (2005) found that cortical IC neurons of the rat show adaptation to the repetitive stimulation of an acoustic parameter, but they resume firing if the sound parameter was changed. Responses similar to those reported by Pérez-González and colleagues were originally described in the midbrain of frogs (Bibikov, 1977; Bibikov and Soroka, 1979).

More recent studies have explored sensitivity to frequency deviance using an "oddball paradigm," similar to that used to record MMN responses in human studies (Näätänen, 1992). In this paradigm two tones are selected within the frequency response area of the neuron (**Figure 1B**) and randomly presented with different probabilities of occurrence. The high probability tone is usually referred to as the standard stimulus; interspersed among the standard stimuli are the low probability or deviant stimuli. In a second sequence of stimulation, the relative probabilities are reversed so that both frequencies are presented as standard and deviant. Usually, the neuronal responses are also recorded under an equiprobable condition, in which both frequencies have the same probability of occurrence (**Figure 1C**).

The amount of SSA is quantified by an index that reflects the extent to which a neuron responds to tones when they are presented as the deviant stimulus compared to when they are presented as the standard stimulus. This index is referred as the common SSA index (CSI) defined as $\mathrm{CSI} = [d(f_1) + d(f_2) - s(f_1) - s(f_2)]/[d(f_1) + d(f_2) + s(f_1) + s(f_2)]$, where $d(f)$ and $s(f)$ are responses measured as spike rate to frequencies f_1 or f_2 used as either the deviant (d) or standard (s) stimulus. The CSI values range from -1 to $+1$, being positive when the response to the deviant stimulus is stronger, and negative when the standard stimulus evokes more spikes (**Figure 1D**).

SSA to frequency deviance has been found to be stronger in the non-lemninscal regions, i.e., in the dorsal (DCIC), rostral (RCIC), and lateral cortices (LCIC), than in the central nucleus (CNIC) (Pérez-González et al., 2005; Malmierca et al., 2009a, 2011; Lumani and Zhang, 2010; Duque et al., 2012) (**Figure 2**). Studies of specific adaptation have also been reported in the awake barn owl (Reches and Gutfreund, 2008; Netser et al., 2011) and bat (Thomas et al., 2012).

Sensitivity to intensity and duration deviance has been observed in the AC (Ulanovsky et al., 2003; Farley et al., 2010) but it is not as robust as frequency deviance. These other stimulus features, i.e., intensity and duration, have not been tested under the oddball paradigm in the IC, but it seems likely that subcortical neurons that show SSA to frequency may also be able to detect deviance in other stimulus dimensions, as occurs with neurons of the midbrain of avians. Neurons in the optic tectum (analogous to the superior colliculus of mammals) of the barn owl exhibit SSA to sound frequencies, amplitude, and interaural time and level difference (Reches and Gutfreund, 2008).

The great majority of neurons with high levels of SSA display transient onset responses and have low or absent spontaneous

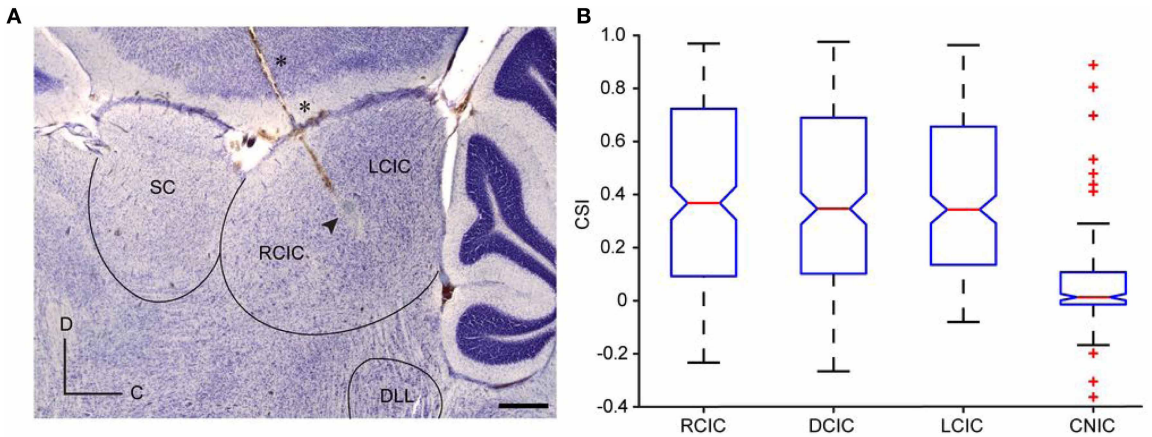

FIGURE 2 | Anatomical location of SSA in the IC. (A) Photomicrography showing a sagittal section of the IC with a typical electrode track (asterisks) and the electrolytic lesion generated (arrowhead). Scale bar = 500 μm. C, caudal; D, dorsal. **(B)** Box plot with the median value (red line) of CSI sorted by anatomic regions. The blue box delimits the 25th and 75th percentile and dashed lines show the most extreme data points not considered outliers. Red crosses indicate outliers. Cortical regions (RCIC, DCIC, and LCIC) are significantly different from the CNIC (Kruskal–Wallis test, $p < 0.001$). Reproduced from Duque et al. (2012).

activity in anesthetized rats (Pérez-González et al., 2005, 2012; Malmierca et al., 2009a; Lumani and Zhang, 2010; Duque et al., 2012). This finding is consistent with a higher incidence of SSA in the non-lemniscal IC since a large proportion of neurons in the dorsal regions of the IC have onset responses (Reetz and Ehret, 1999; LeBeau et al., 1996). Moreover, for adapting neurons with other types of responses, i.e., on-sustained and on-off (Rees et al., 1997), the largest difference between responses to deviant and standard stimuli is signaled by the onset component (Malmierca et al., 2009a; Duque et al., 2012).

Another feature of neurons that exhibit SSA is their broad frequency response area (Malmierca et al., 2009a; Duque et al., 2012). In the IC of the rat, neurons in the DCIC and RCIC regions possess widespread dendritic arbors (Malmierca et al., 1993, 1995, 2011), and broader frequency tuning than the CNIC (Syka et al., 2000; Duque et al., 2012). A possible functional consequence of neurons with large dendritic arbors is the integration of inputs over a broad frequency range. Among cortical IC neurons the broader the frequency response area the higher the level of SSA observed (Duque et al., 2012). In the bat IC, SSA is present in a subset of non-specialized neurons which are broadly tuned to frequency and non-selective for spectrotemporal pattern (Thomas et al., 2012) suggesting a complex input processing. Furthermore, SSA is not a property homogeneously distributed throughout the neuron's frequency response area. Duque et al. (2012) compared the degree of SSA at multiple combinations of frequencies and intensities in single-unit recordings in the IC of the anesthetized rat. They found that adapting neurons exhibit stronger SSA at the high frequency edge of the response area and low sound intensities (**Figure 3**). This study concluded that SSA is not constant within the neuronal receptive field, and therefore is not a characteristic property of the neuron, instead the neuron's inputs contribute to its generation.

In addition to encoding deviance by spike count, IC neurons can also encode deviance information through their spike timing. In neurons that exhibit SSA, the first spike latency (FSL) in the response evoked by the deviant tone is shorter than that evoked by the standard tone (Malmierca et al., 2009a; Zhao et al., 2011; Duque et al., 2012). This phenomenon is known as "latency adaptation" and seems to be a unique feature of subcortical neurons (Malmierca et al., 2009a; Antunes et al., 2010; Duque et al., 2012). The neurons in the DCIC that show SSA have much longer FSLs than neurons in the CNIC (Lumani and Zhang, 2010). Thus, temporal coding appears to play a key role in the signaling of deviance.

STIMULUS-SPECIFIC ADAPTATION AND ITS RELATIONSHIP TO STIMULATION PARAMETERS

A hallmark of SSA in the different auditory areas is its sensitivity to a variety of stimulus parameters such as the deviant probability, the frequency separation, and the time interval (stimulation rate) between stimuli (Ulanovsky et al., 2003; Malmierca et al., 2009a; Yu et al., 2009; Von Der Behrens et al., 2009; Antunes et al., 2010; Zhao et al., 2011). This dependency is also present for the processing of other stimulus features such as interaural time- and level-differences and amplitude deviants (Ulanovsky et al., 2003; Reches and Gutfreund, 2008).

The manipulation of the probability of occurrence of the deviant and, consequently, of the standard stimulus has a strong effect on the extent of SSA observed (Malmierca et al., 2009a; Patel et al., 2012). Deviant probabilities of 30 and 10% have been explored; SSA increases as the deviant probability decreases. Thus, neurons are sensitive to stimulus probability with greater sensitivity to tones that are less likely to occur (Malmierca et al., 2009a).

The sensitivity to deviance increases proportionally with the extent of physical separation between tones. The frequency contrast is expressed as $\Delta f = (f_2 - f_1)/(f_2 \times f_1)^{1/2}$; where f_2 and f_1 correspond to the frequencies tested (Ulanovsky et al., 2003) (**Figure 1B**). Most studies of SSA have employed pure tones

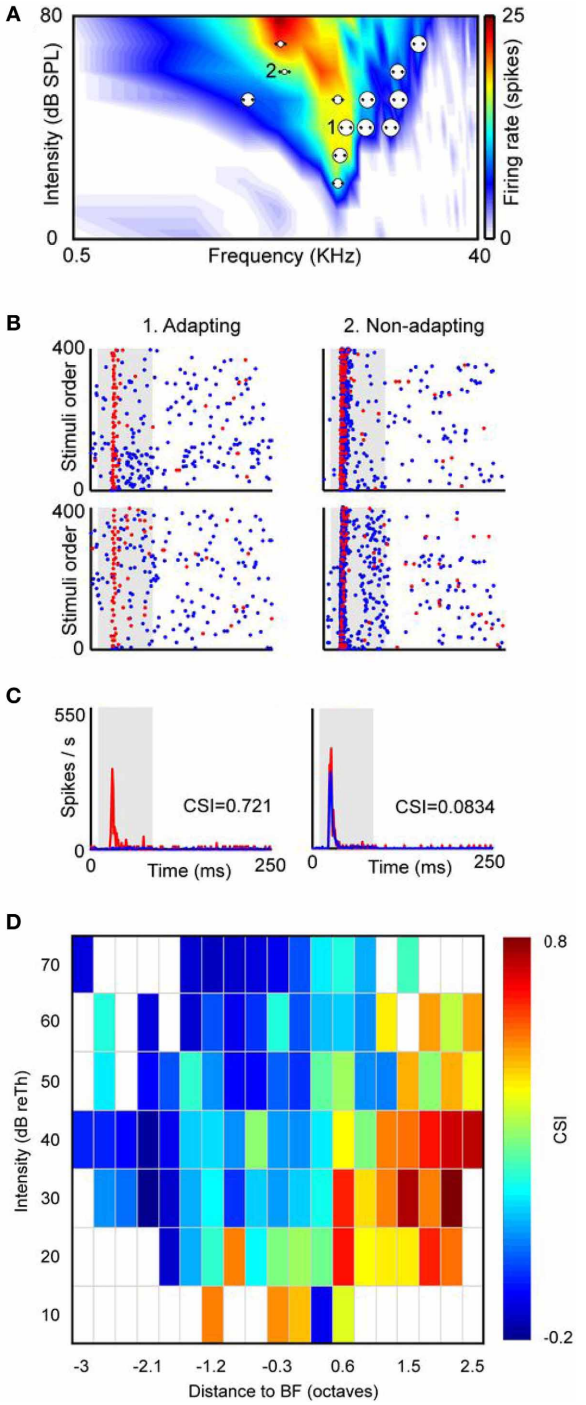

FIGURE 3 | SSA is not homogeneously distributed within the frequency response area of IC neurons. (A) Example of a neuron with a broad V-shaped response area and the distribution of the several pairs of frequencies presented under the oddball paradigm (dots). Each pair of dots is associated to a circle the size of which is proportional to the level of CSI evoked. An example of an adapting pair of frequencies (i.e., frequencies that elicited SSA) is marked as 1 and another example of a non-specifically adapting pair of frequencies is marked as 2. **(B)** Dot raster plots obtained with the adapting pair (left panels) and with the non-specifically adapting (right panels) pair of frequencies. The blue dots represent spikes evoked by *(Continued)*

FIGURE 3 | Continued
the standard stimulus (90% probability), while the red dots represent those evoked by the deviant stimulus (10% probability). Stimulus presentations are accumulated in the temporal domain along the vertical axis. In the adapting examples red dots are more visible because of the specific decrease of the response to the standard stimulus. The upper panels are the ones obtained when f_1 was the standard tone and f_2 was the deviant, and the bottom panels represent the response when the relative probabilities were inversed, that is, f_1 was the deviant and f_2 the standard. **(C)** Averaged PSTH for both frequencies when deviant (red) or standard (blue). CSI values obtained in each pair of frequencies are showed as insets in the PSTH. The shaded backgrounds in the dot raster and PSTH plots indicate the duration of the stimulus. **(D)** Distribution of the CSI values sorted relatively to the best frequency (BF) and the threshold (Th) of the response area of a sample of IC neurons (almost 80% are from the cortical region, $n = 124$). Higher CSI values are confined to the high-frequency edge and at low sound intensities. Reproduced from Duque et al. (2012).

centered on the best (Malmierca et al., 2009a; Pérez-González et al., 2012) or characteristic frequency (Zhao et al., 2011) of the neurons. The differential adaptation of the responses to deviant and standard stimuli is more prominent when Δf increases from 0.04 to 0.1 to 0.37 (0.058, 0.144, and 0.531 octaves, respectively) (Malmierca et al., 2009a). Neurons with strong SSA in the IC, as in the MGB and primary AC, show hyperacuity, that is, a strong and highly sensitive adaptation for frequency ratios as small as 4% ($\Delta f = 0.04$). This frequency ratio is smaller than the width of their frequency response areas (Ulanovsky et al., 2004; Moshitch et al., 2006; Malmierca et al., 2009a).

The highest levels of SSA are elicited by IC neurons at an ISI of 250 ms with a deviant probability of 10% compared to shorter (125 ms) or longer ISIs (500 ms) (Malmierca et al., 2009a). Few studies have explored SSA at very long ISIs. It has been reported that IC neurons are still capable of detecting frequency deviants at ISIs up to 1 s (repetition rate of 1 Hz) (Pérez-González et al., 2005; Reches and Gutfreund, 2008; Zhao et al., 2011). Indeed, we have recorded neurons that exhibit SSA at even slower repetition rates (ISI = 2000 ms) (Malmierca et al., 2010). **Figure 4** illustrates an example of the response of an IC neuron that exhibits SSA in the anesthetized rat. This neuron was very broadly tuned with a complex non-monotonic rate-level function and a transient onset firing pattern (**Figures 4A–C**). For this neuron, a pair of frequencies (black crosses; f_1 and f_2) with a physical separation of 0.216 octaves ($\Delta f = 0.15$) was chosen for presentation in the oddball paradigm with an ISI of either 2000 or 1000 ms. **Figures 4D,E** depict the responses to the deviant and standard stimuli as dot rasters and the corresponding peri-stimulus time histogram (PSTH) obtained with 0.5 and 1 Hz repetition frequencies, respectively. Under these conditions, the neuron showed SSA (CSI: 0.3–0.4), resulting in higher-evoked spiking to the deviant frequency (red color). **Figure 5A** shows the average PSTHs of a subset of neurons recorded with ISIs of 2000, 1000, and 500 ms. It is evident that there is an increasing difference between responses to deviant and standard tones as the frequency separation is increased (insets). Under these extreme stimulation rates, the FSLs evoked by the deviant tone were earlier than those evoked by the same tone when it was used as the standard, suggesting that the cellular mechanisms that discriminate between

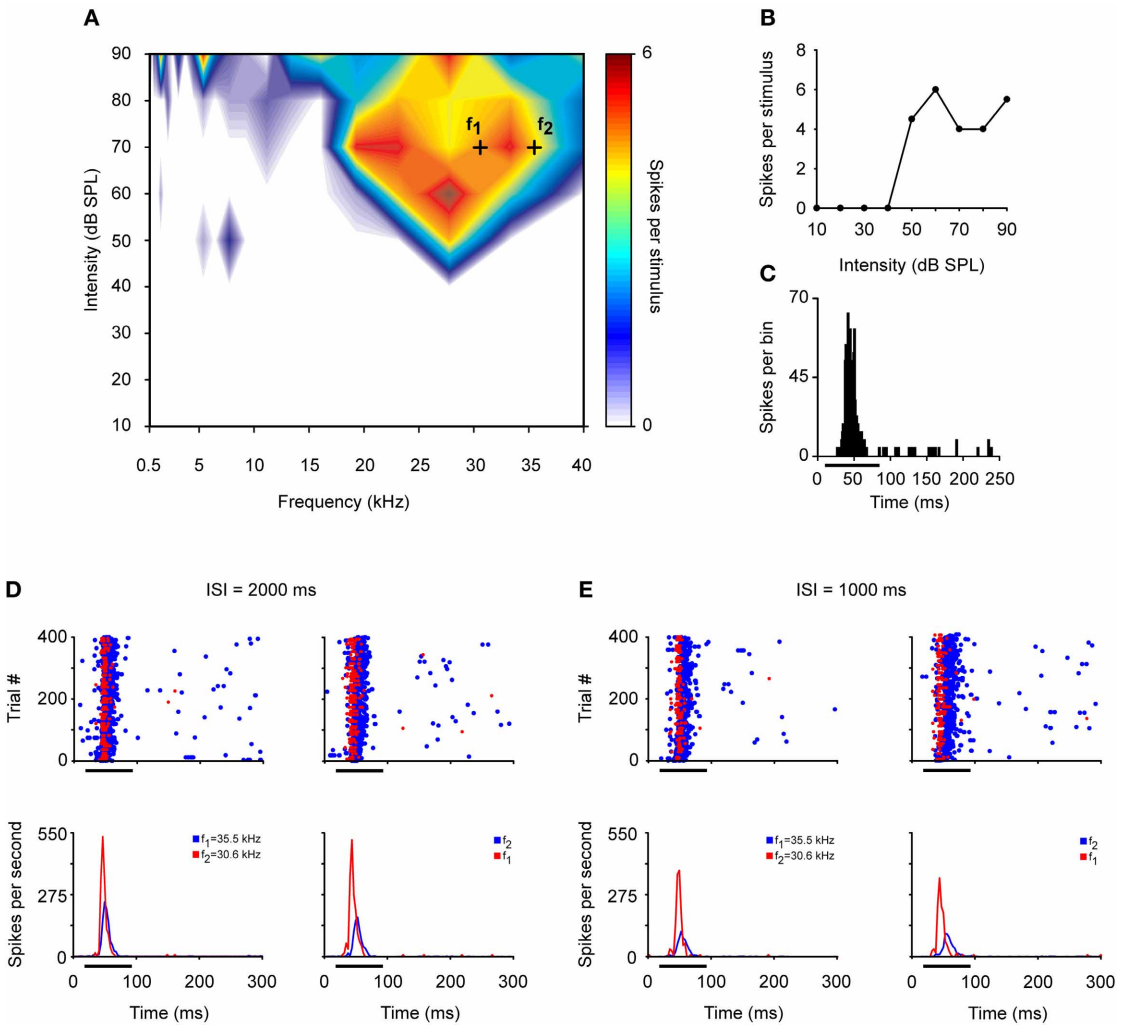

FIGURE 4 | Example of an IC neuron that exhibits SSA at low repetition frequencies. (A) Broad frequency response area displayed in color code according to the strength of the response. Black crosses represent a frequency pair—f_1 (30.6 kHz) and f_2 (35.5 kHz)—with a physical separation of 0.216 octaves ($\Delta f = 0.15$) at 70 dB SPL. **(B)** The neuron exhibits a non-monotonic rate-level function at its best frequency (27.1 kHz). **(C)** PSTH of the accumulated responses to all the frequencies (0.5–40 kHz) and intensities (10–90 dB SPL) presented (1 ms bins). **(D)** Top panels. Dot rasters of the response to oddball sequences of 400 stimulus presentations with a repetition rate of 0.5 Hz (ISI = 2000 ms). The frequencies used as the deviant stimulus (probability of 10%, red dots) and the standard or repetitive stimulus (probability of 90%, blue dots) are reversed in the left and right panels. The bottom panels show the corresponding normalized PSTHs to deviant (red line) and standard (blue line) stimuli. **(E)** Response to the oddball sequences presented at a higher repetition rate of 1Hz (ISI = 1000 ms). Format same as for panel **(D)**.

deviant and standard responses are functional at the temporal scale of seconds (**Figures 5B,C**). As highlighted by Nelken and Ulanovsky (2007), the neuronal mechanisms for deviance detection become more important at more extreme stimulation values, e.g., slow stimulation rates and very similar stimulus frequencies.

Long interstimulus intervals affect the long-term dynamics of SSA, prolonging the time course of adaptation from several seconds at ISI of 125 ms, to tens of seconds when ISI is increased to 1000 ms. The frequency resolution of neurons is also modified by the repetition rate (Malmierca et al., 2009a; Antunes et al., 2010; Zhao et al., 2011). Frequencies separated by $\Delta f = 0.04$ do not elicit SSA in the IC or in the MGB of the rat (Antunes et al., 2010) when tested with the longest ISI of 2000 ms. Together these data indicate that the timing between stimuli affect both the extent and frequency resolution of SSA.

SSA at the time scale of 2000 ms has been found in primary AC, but cortical neurons do not adapt at ISIs longer than 2000 ms (Ulanovsky et al., 2003). SSA also occurs at an ISI of 2000 ms in the MGB, a mandatory processing station between the IC and the AC (Antunes et al., 2010). The presence of SSA in subcortical structures such as the IC and MGB on a time scale of the magnitude of seconds, similar to the time scale of cognition (Ulanovsky et al., 2003, 2004; Nelken and Ulanovsky, 2007), suggests that deviance detection at these early neuronal stages could be contributing to the perceptual organization of the

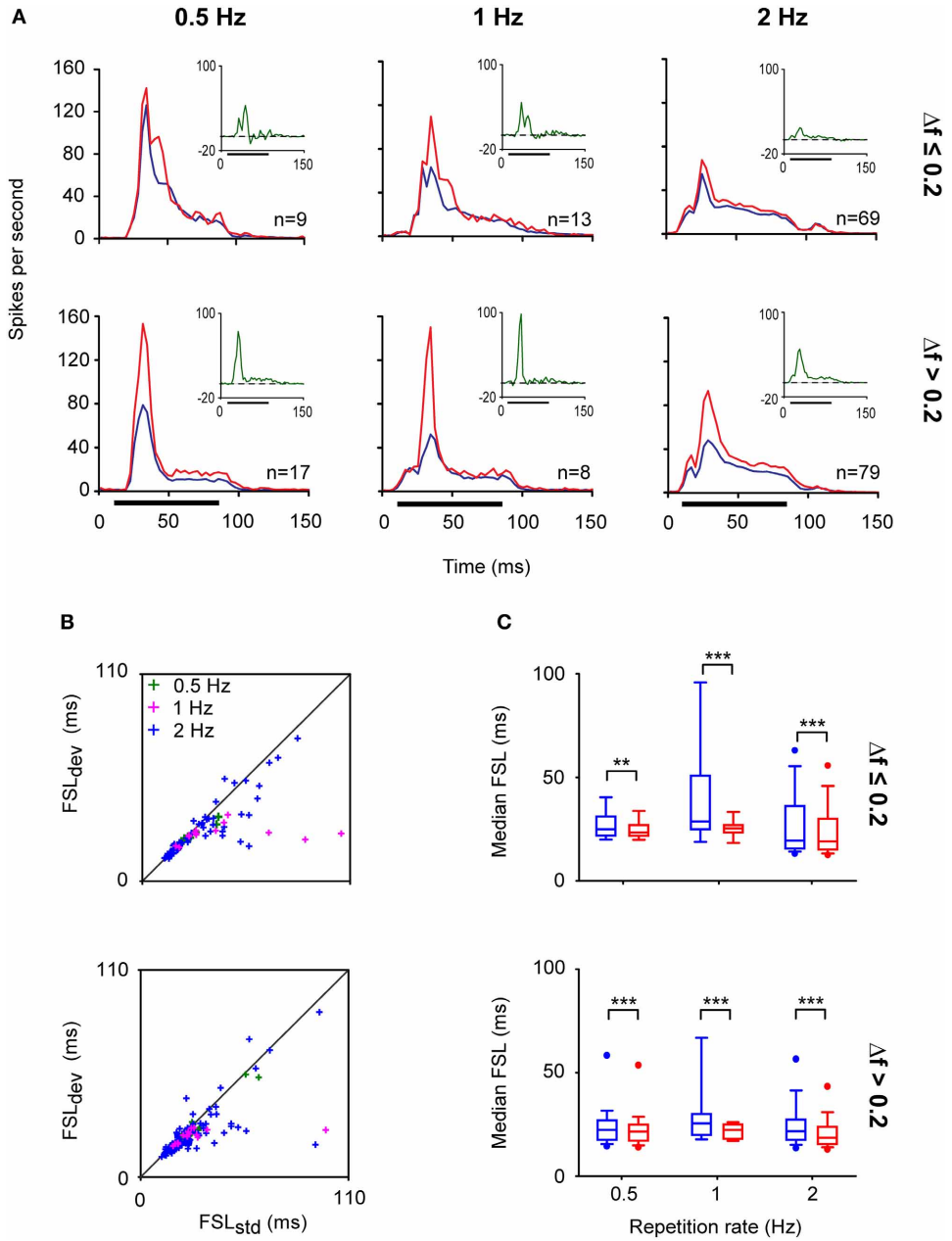

FIGURE 5 | IC neurons exhibit SSA even at very low repetition rates. **(A)** Population PSTHs of the IC neuronal responses to a deviant (red line) and to a standard (blue line) stimulus presented at different repetition rates; 0.5 (ISI = 2000 ms), 1 (ISI = 1000 ms), and 2 Hz (ISI = 500 ms). The physical separations between frequencies were grouped into $\Delta f \leq 0.2$ ($\leq$ 0.288 octaves) (top panels) and $\Delta f > 0.2$ (bottom panels). The firing rates of individual neurons were averaged and normalized to account for the different number of stimulus presentations due to the different probabilities of the tones (deviant; 10%, standard; 90%). The insets shown in the right upper quadrants of each graph correspond to the averaged difference between the responses to the deviant and standard stimuli (green lines). The horizontal black bars indicate the duration of the stimulus. **(B)** Scatter plots of the first spike latency (FSL) of the neuronal responses evoked by f_1 and f_2 when they were the deviant (FSL_{dev}) or the standard (FSL_{std}) stimulus according to their frequency separation ($\Delta f \leq 0.2$ and $\Delta f > 0.2$) and across different repetition rates (0.5, 1, and 2 Hz). **(C)** Box plots of the population FSL indicating that even at very low repetition rates the FSLs evoked by the deviant tone (red boxes) are shorter than those evoked by the standard stimulus (blue boxes). (Signed-Rank Test; $^{**}p < 0.01$, $^{***}p < 0.001$).

components of complex auditory stimuli (Winkler et al., 2009) and to the change detection recorded in local field potentials (Slabu et al., 2010; Grimm et al., 2011). This temporal scale is consistent with the duration of sensory (echoic) memory in monkeys and humans, which is estimated to be in the order of a few seconds (Javitt et al., 1994; Näätänen and Escera, 2000).

The same systematic dependence on deviant probability, frequency contrast, and repetition rate seen in single neurons is

also present in the activity of ensembles of neurons in the IC (**Figure 6**). In a recent study the evoked local field potentials of DCIC neurons of the rat were recorded while stimulating with tone bursts under an oddball paradigm (Patel et al., 2012). The auditory response is a waveform with a relatively small positive deflection (D_P) followed by a large negative reflection (D_N) (**Figure 6A**). The degree of SSA is quantified by comparing the amplitude of the waves evoked by the deviant and standard stimuli using an amplitude-based, frequency-specific, SSA index for D_P and D_N ($SSAI_{Am}$). As expected, the amplitude of the local field potential is larger to a tone burst presented as deviant than as standard, and the difference is greater when the deviant stimulus is less likely to occur (deviant probability of 10% rather than 30%) (**Figures 6B,C**). The difference between responses to deviant and standard tones occurs after the initial rising phase of the dominant deflection (D_N), and no difference is elicited at the beginning of the response in D_P. Overall, the results by Patel et al. (2012) suggest that frequency deviance coding is detectable in ensembles or neuronal microcircuits of subcortical neurons as an evoked response with a larger amplitude and longer peak latency. There are some differences, however, compared to the SSA observed in single-units. The frequency separation required to elicit SSA is greater ($\Delta f = 0.37$ rather than $\Delta f = 0.1$); the strongest SSA

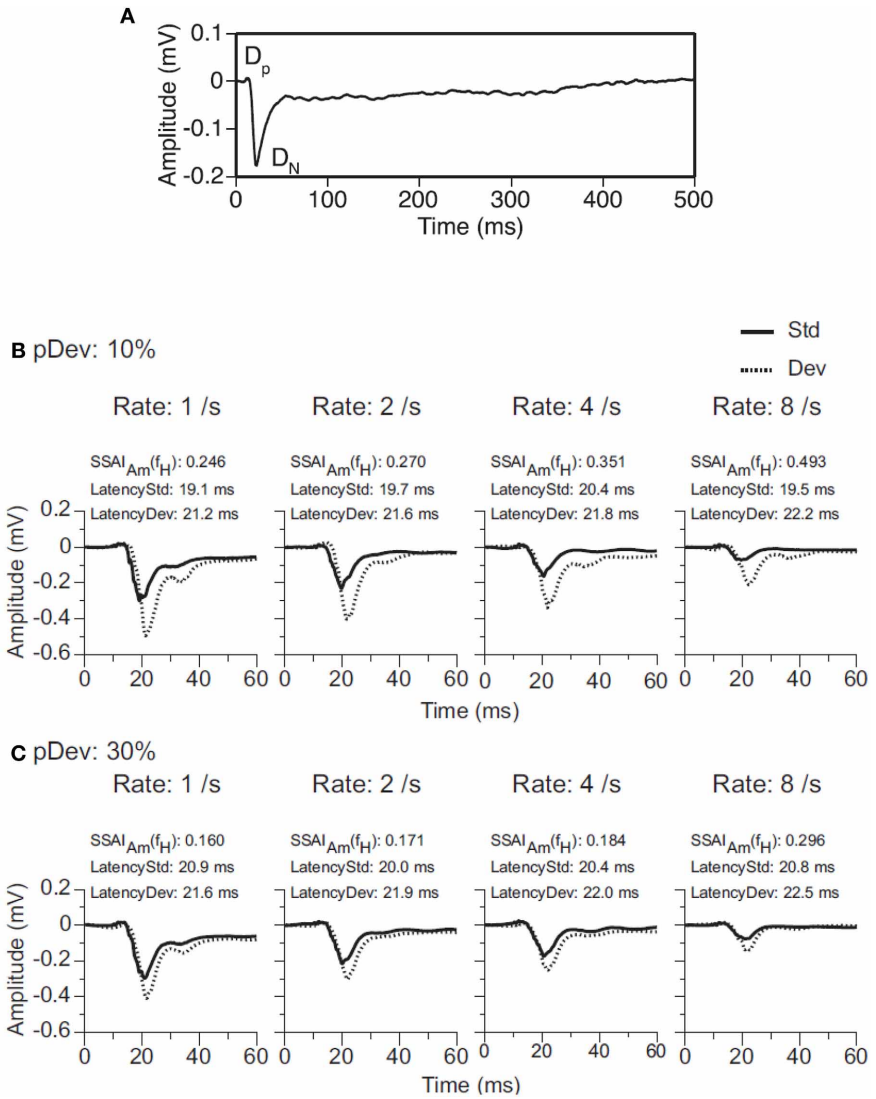

FIGURE 6 | Evoked local field potentials (LFP) recorded in the DCIC. (A) An average LFP is a waveform with a relatively small positive deflection (D_P) followed by a large negative deflection (D_N). Together, the two deflections are about 40 ms in total duration. (**B,C**) Evoked LFPs in response to a tone burst presented as standard stimulus (Std, solid line) or deviant stimulus (Dev, dotted line) in a pair of oddball sequences with probabilities of occurrence of the deviant of 10% (panel **B**) or 30% (panel **C**). Data were obtained for pairs of tones ($f_1 = 2.25$ kHz and $f_2 = 3.24$ kHz.) separated by a $\Delta f = 0.37$ and presented at 1, 2, 4 and 8 Hz. The BF of the recording site was 2.7 kHz. An amplitude-based, frequency-specific, stimulus-specific adaptation index [$SSAI_{Am}(f_X)$], along with the peak latencies of the responses evoked by the sound as standard and deviant stimuli, is shown at the top of each graph. Reproduced from Patel et al. (2012).

is elicited with a higher repetition rate (8 Hz); and the peak latency of the response to standard tone bursts is shorter than that to the deviant tone burst (contrary to the shorter latencies for deviants in single-unit recordings). As the authors suggested, these differences may be attributed to the fact that an evoked local field potential reflects a weighted average of voltage changes generated by multiple excitatory and inhibitory events in the vicinity of the recording electrode so that individual differences among neurons are largely averaged out. The short latency of responses in subcortical nuclei suggests that these responses could contribute to the earliest components of the evoked potential associated with the occurrence of a deviant acoustic event (Pa waveform in the MLR; peak at about 30 ms) (Grimm and Escera, 2012).

CORTICOFUGAL MODULATION

It was originally proposed that auditory SSA has a cortical origin and is propagated to subcortical nuclei through direct corticofugal projections (Ulanovsky et al., 2003; Nelken and Ulanovsky, 2007). Indeed, in the IC and MGB, the strongest SSA has been described in the extralemniscal regions (cortical regions of the IC: Malone et al., 2002; Pérez-González et al., 2005; Malmierca et al., 2009a; Lumani and Zhang, 2010; medial division of the MGB: Antunes et al., 2010), which operate under strong cortical control (Loftus et al., 2008; He and Yu, 2010; Lee and Sherman, 2011; Malmierca and Ryugo, 2011).

In a recent study, Anderson and Malmierca (2013) addressed whether SSA in the IC is dependent upon the AC for its generation. The authors reversibly deactivated the AC by cooling through a cryoloop device (Lomber et al., 1999; Lomber and Malhotra, 2008) and recorded the changes in SSA sensitivity exhibited by IC neurons. This technique has been successfully used to study the influence of the corticofugal system in the auditory system, including a study of sensitivity in IC neurons to cues for spatial position (Nakamoto et al., 2008) and sensitivity to deviance in the MGB (Antunes and Malmierca, 2011).

The neuronal responses to the oddball paradigm (with a deviant probability of 10% and a frequency separation between deviant and standard stimuli of 0.531 octaves) were recorded before, during and after the cooling of the AC. At the population level, the main finding was that deactivation of the ipsilateral AC did not eliminate SSA exhibited by IC neurons. A decrease in firing rate to both the deviant and standard stimuli was observed during the cooling condition, but the response was still higher to the deviant stimulus (**Figure 7A**). Thus, the deviant salience in the IC was preserved even after the deactivation of cortical inputs. Interestingly, at the single-neuron level Anderson and Malmierca identified IC neurons that showed SSA and were insensitive to the cooling of the AC (**Figure 7B**). Those neurons exhibited different levels of SSA covering the full CSI spectrum, from zero to one. On the other hand, the adaptive properties of about half of the IC neurons with SSA (52%) were differentially affected throughout the period of cortical cooling, increasing (**Figure 7C**) or decreasing (**Figure 7D**) their SSA sensitivity. Examples of single neurons are shown in **Figures 8** and **9**. During the cooling period, the neuron displayed in **Figure 8** increased its response area (**Figure 8A**), and its spontaneous and evoked firing rate. The increase was greater in response to the standard presentations (by a factor of seven) (**Figures 8B–D**, blue) than to the deviant ones (by a factor of three) (**Figures 8B–D**, red), resulting in a drop of its CSI (**Figure 8D**). On the other hand, the neuronal response illustrated in **Figure 9** exhibited a disproportionately decrease in the firing rate with an almost extinguished response to the standard stimulus, thus, increasing its CSI. The

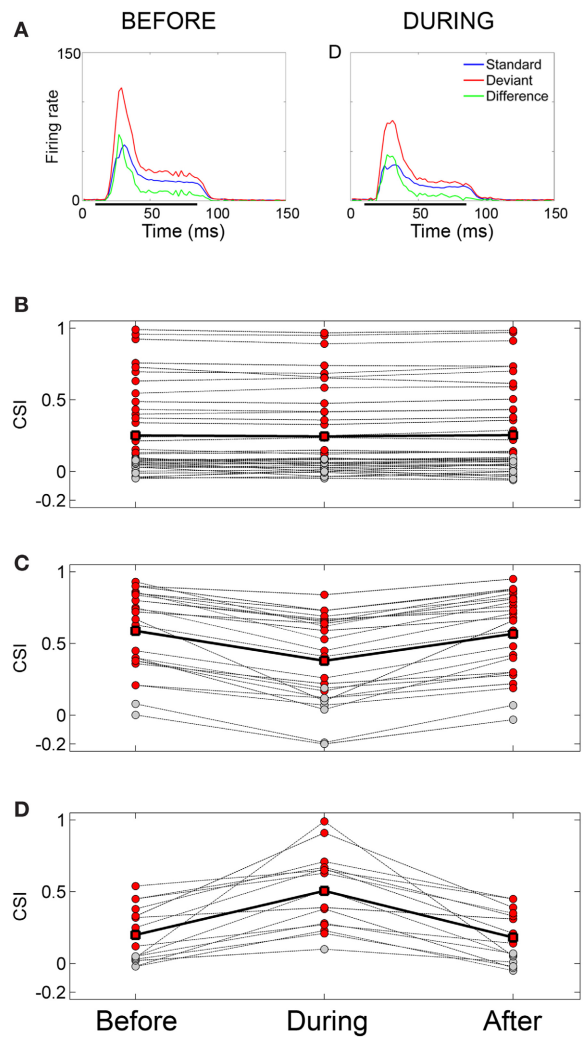

FIGURE 7 | Effect of cortical deactivation on SSA exhibited by IC neurons. (A) Mean population PSTHs from IC recordings ($n = 82$) in response to tones presented as standard (blue) or deviant (red) before and during cooling the ipsilateral AC. The difference between the two is plotted in green. Deactivation of the auditory cortex does not eliminate the deviant saliciency in the averaged signal. **(B)** Population of neurons which showed no significant change in SSA during cooling, red circles indicate significant SSA, those in gray indicate non-significant CSI values. The solid line connected with square symbols indicates the mean CSI values for the three conditions. **(C)** Population which shows a decrease in SSA during cooling. Note that on cooling some neurons cease to show significant SSA. **(D)** Population which shows an increase in SSA during cooling. Note that on cooling some neurons which previously did not show significant SSA now become significant. Figure layout in **(C)** and **(D)** is the same as in **(A)**. Reproduced from Anderson and Malmierca (2013).

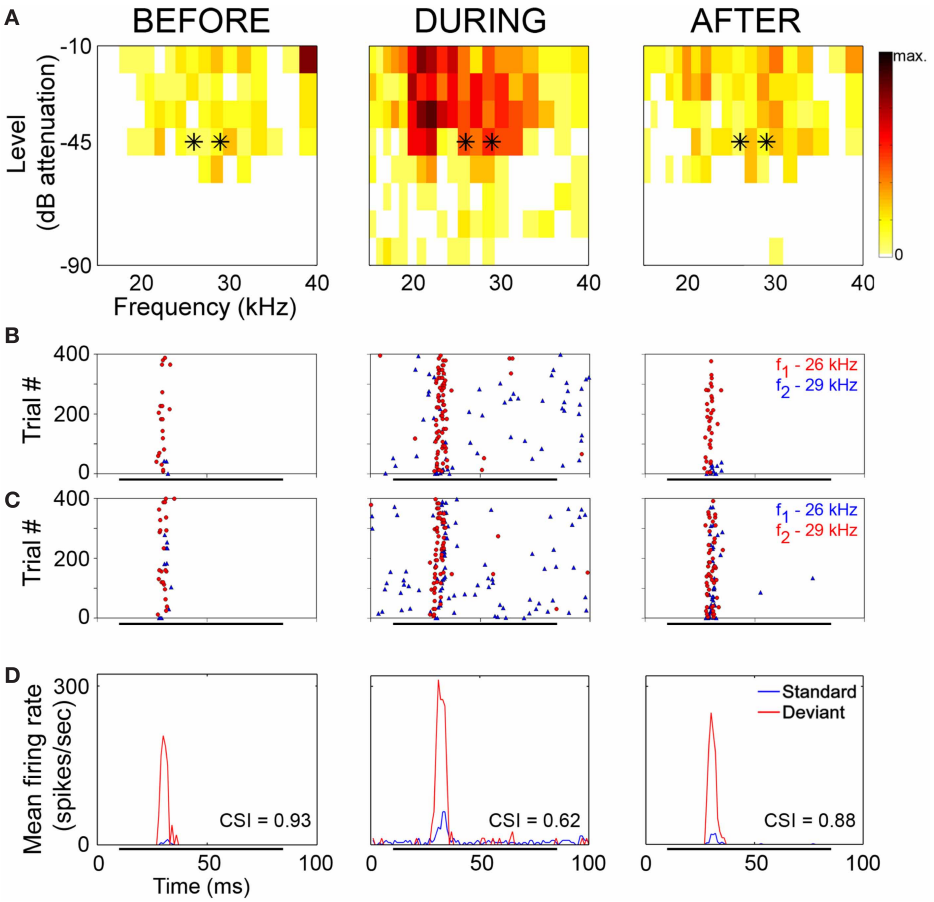

FIGURE 8 | Example of an IC neuron which shows a decrease in its adaptive properties with cooling. (A) Frequency response areas recorded before (left), during (middle), and after (right) cooling. Black asterisks indicate the frequencies used in the oddball paradigm, firing rate (spikes/sec) indicated by the color scale which applies to all response areas in this figure. **(B)** Raster plots showing response to f_1 (lower frequency) as deviant (red circles) and f_2 (higher frequency) as standard (blue triangles). **(C)** Raster plots showing response to f_1 as standard (blue triangles) and f_2 as deviant (red circles). **(D)** PSTH showing mean response to standard (blue) and deviant (red) stimuli. CSI values for each period are superimposed onto the relevant PSTH. Reproduced from Anderson and Malmierca (2013).

authors suggest that the disproportionate changes in the neuron's firing rate to standard or deviant stimulus caused by the cortical inactivation may indicate the occurrence of a gain control modulation similar to that observed in the MGB under a similar manipulation (Antunes and Malmierca, 2011) and elicited by $GABA_A$-mediated inhibition in the IC (Pérez-González and Malmierca, 2012; Pérez-González et al., 2012) which is clearly compatible with the "iceberg effect" notion described by, e.g., Isaacson and Scanziani (2011, see below).

Overall, a decrease in SSA was the predominant response, although the majority of IC neurons continued to show significant SSA after the deactivation of the cortical inputs. The extreme effects of cortical cooling were exhibited by (1) IC neurons that lost their pre-existing deviance sensitivity during the cooled condition and (2) non-adapting neurons that began to exhibit SSA. The existence of sets of IC neurons differentially affected by the AC deactivation suggests that the ipsilateral AC may relay SSA to a small group of neurons, but that corticofugal inputs do not account significantly for the SSA exhibited by the majority of adapting neurons. Using the same cooling technique, Antunes and Malmierca (2011) demonstrated that SSA persisted in the MGB neurons regardless of the lack of functional corticofugal feedback, suggesting that SSA is inherited through lower input channels in a bottom-up manner and/or generated *de novo* at each level of the auditory pathway. Pharmacological manipulation in the IC suggests that local circuits may operate intrinsically to shape SSA at this neuronal station (Pérez-González and Malmierca, 2012; Pérez-González et al., 2012; see below).

ROLE OF INHIBITORY INPUTS IN SHAPING SSA AND POSSIBLE MECHANISMS UNDERLYING SSA IN THE IC

It is well known that the IC integrates ascending and descending inputs from multiple sources (Malmierca, 2003; Malmierca and Ryugo, 2011) and possesses a dense and complex microcircuitry of local connections (Malmierca et al., 2003, 2005a, 2009b; Malmierca and Hackett, 2010). The IC is a major center for the convergence of both excitatory and inhibitory inputs and for combination of information across frequency-specific channels,

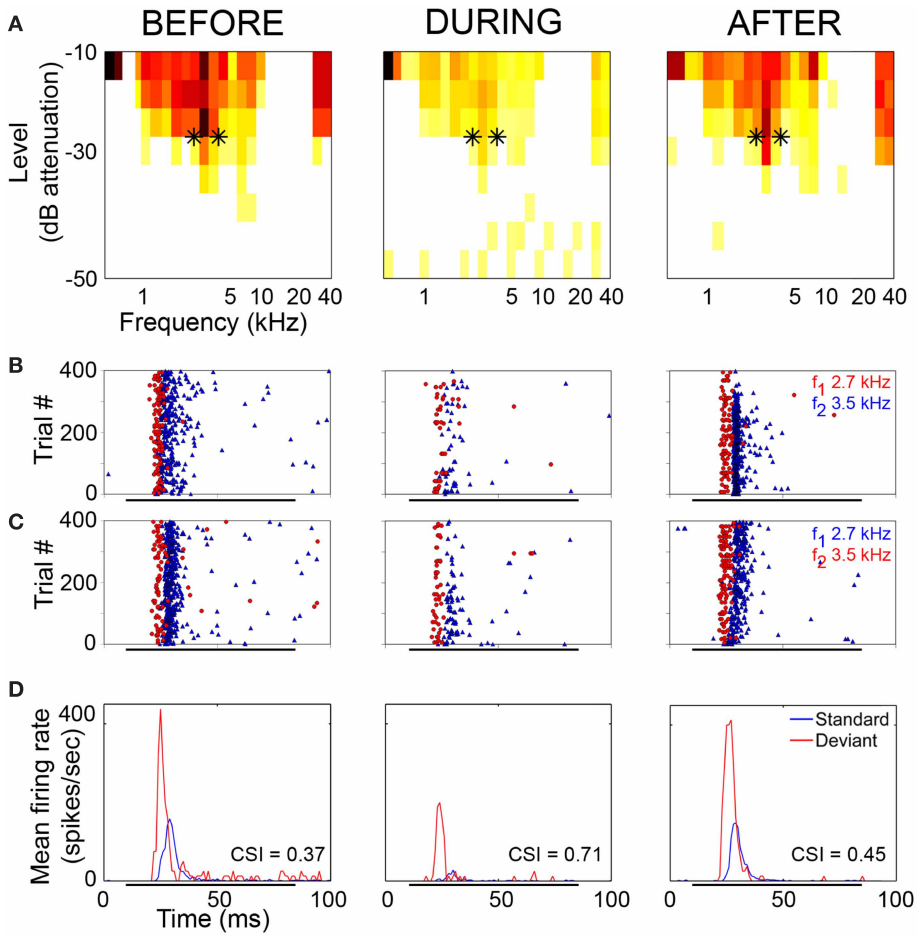

FIGURE 9 | Example of an IC neuron which shows stimulus-specific adaptation under normal conditions and increased SSA during the period of cortical cooling. (A) Frequency response areas recorded before (left), during (middle) and after (right) cooling of AC. Black asterisks indicate the frequencies used in the oddball paradigm and the firing rate (spikes/sec) are indicated by the same colour scale that appears in **Figure 8A**. **(B)** Raster plots showing response to f_1 (lower frequency) as deviant (red circles) and f_2 (higher frequency) as standard (blue triangles). **(C)** Raster plots showing response to f_1 as standard (blue triangles) and f_2 as deviant (red circles). **(D)** PSTH showing mean response to standard (blue) and deviant (red) stimuli. CSI values for each period are superimposed onto the relevant PSTH. Reproduced from Anderson and Malmierca (2013).

especially in the non-lemnical regions (Malmierca et al., 2011). Inhibitory neurotransmission in the IC is mediated by GABAergic and glycinergic receptors (Palombi and Caspary, 1996; Caspary et al., 2002; Sivaramakrishnan et al., 2004; Ingham and McAlpine, 2005; Hernández et al., 2005; Malmierca et al., 2005a; Merchán et al., 2005). GABAergic inputs come from several sources, including bilateral projections from the dorsal nucleus of the lateral lemniscus and ipsilateral projections from the ventral nucleus of the lateral lemniscus as well as intrinsic and commissural GABAergic IC neurons (Hernández et al., 2005; Malmierca et al., 2003, 2005a). Glycinergic inputs originate from the ipsilateral lateral superior olive and from the ipsilateral ventral nucleus of the lateral lemiscus (Kelly and Li, 1997; Moore et al., 1998; Riquelme et al., 2001). Pharmacological manipulation of inhibitory neurotransmitters has strong effects on neuronal response area (LeBeau et al., 2001), firing rate (Palombi and Caspary, 1996), temporal response properties (LeBeau et al., 1996), tuning for sound duration (Casseday et al., 1994, 2000) as well as for frequency (Koch and Grothe, 1998) and amplitude modulation (Caspary et al., 2002).

Recently, in a first attempt to study the role of GABAergic neurotransmission in the generation and/or modulation of SSA, gabazine an antagonist of $GABA_A$ receptors was applied microiontophoretically, and the firing rate of neurons exhibiting SSA was recorded before, during and after the drug injection (**Figures 10A–C**; Pérez-González et al., 2012). The response magnitude (**Figure 10D**), discharge pattern and latency remained distinct for the deviant and standard stimuli. The main finding was that the blockade of $GABA_A$ receptors modified the temporal dynamics of SSA but did not abolish it completely, although the CSI index was generally reduced. Adaptation to the standard stimulus still occurred in the absence of $GABA_A$-mediated inhibition but it was slower, especially at the beginning of stimulation.

The time course of the adaptation to the standard stimulus has a rapid- and a slow-decay component, after which the

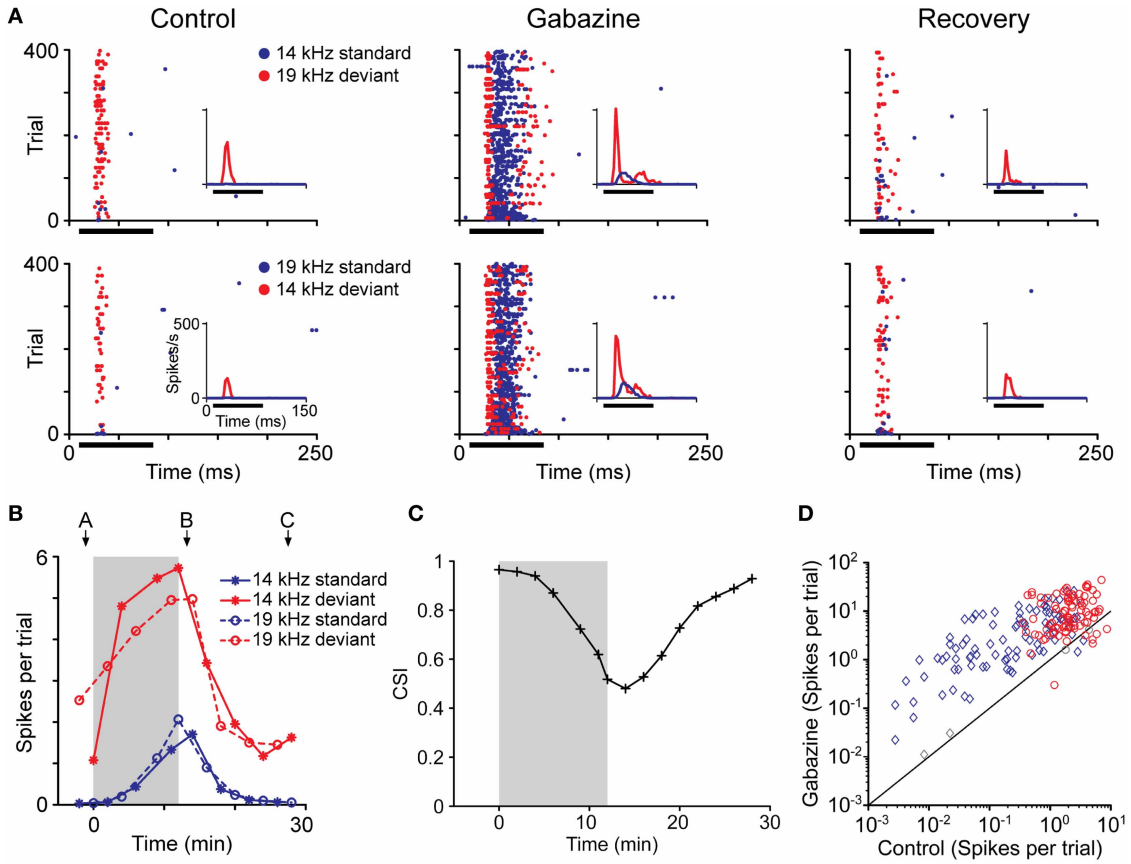

FIGURE 10 | Effect of the blockade of $GABA_A$ receptors on the response magnitude for deviant and for standard stimuli. (A) Dot rasters showing the effect of gabazine blockade of $GABA_A$ receptors on the responses of a neuron with SSA. The frequencies tested in the oddball paradigm were 14 kHz and 19 kHz ($\Delta f = 0.3$, 0.43 octaves). The insets show a PSTH of the response (3 ms bin size); the horizontal black bar indicates the duration of the stimulus. Before the application of gabazine, this neuron responded much more strongly to both frequencies when they were presented as the deviant than when they were presented as the standard stimulus, resulting in a CSI of 0.965. The application of gabazine for 12 min increased the response to both types of stimuli, but the relative increment was larger for the standards, causing the CSI to drop to 0.480. Fifteen minutes after the end of gabazine application, the neuron's response recovered to the control level, and the CSI increased to 0.926. **(B)** Evolution of the response magnitude of the neuron (mean spikes per trial) shown in **(A)** in response to standards (blue lines) and deviants stimulus (red lines). Note that the changes are similar for both frequencies (asterisk and circles) and the main differences are due to the probability condition. The shaded background represents the application of gabazine, which starts at $T = 0$. The arrows indicate the times corresponding to the dot rasters in **(A)**. **(C)** Evolution of CSI during the experiment. The symbols indicate the time at the end of a testing oddball sequence, so all times at or before 0 represent recordings completed before the start of the injection. **(D)** Effect of gabazine on response magnitude in the population of neurons. Gabazine increased the response (spikes per trial) of almost all neurons recorded, but the effect was different for standards (blue diamonds) than for deviants (red circles). Each symbol corresponds to one of the pair of stimuli for each neuron. Colored symbols indicate that the effect of gabazine was significant (Bootstrapping, 95% ci). Gray symbols represent changes that were not statistically significant. Reproduced from Pérez-González et al. (2012).

response reaches a steady-state (**Figures 11A–F**). Both decay components are faster for the neurons exhibiting higher levels of SSA (CSI > 0.5) than for the neurons with less SSA (CSI < 0.5). The blockade of the $GABA_A$ receptors slowed down both components and GABA inhibits more profoundly the steady-state component of the response of the neurons with the highest levels of SSA. As expected from previous results (Malmierca et al., 2009a; Zhao et al., 2011), Pérez-González et al. (2012) also found that the deviant-related activity did not decrease, showing a linear time course across the trials. The authors concluded that $GABA_A$-mediated inhibition acts as a gain control mechanism that enhances SSA by controlling the neuron's gain and responsiveness. Thus, synaptic inhibition via $GABA_A$ receptors seems to increase the saliency of the deviant stimulus (**Figure 12**). The role of inhibition in shaping contrast between stimuli has been described in detail in what is referred to as "the iceberg effect." Briefly, the iceberg effect describes the observation whereby a neuron's spike output is more sharply tuned than the underlying membrane potential since only the strongest excitatory input sufficiently depolarizes the membrane to reach threshold for spike generation (Isaacson and Scanziani, 2011).

The results by Pérez-González and colleagues suggest that other factors must be involved in the generation of SSA, leading to an interest in exploring the role of $GABA_B$ and glycinergic-mediated inhibition as well as neuromodulatory influences. $GABA_B$ receptors may be key players in shaping SSA. These

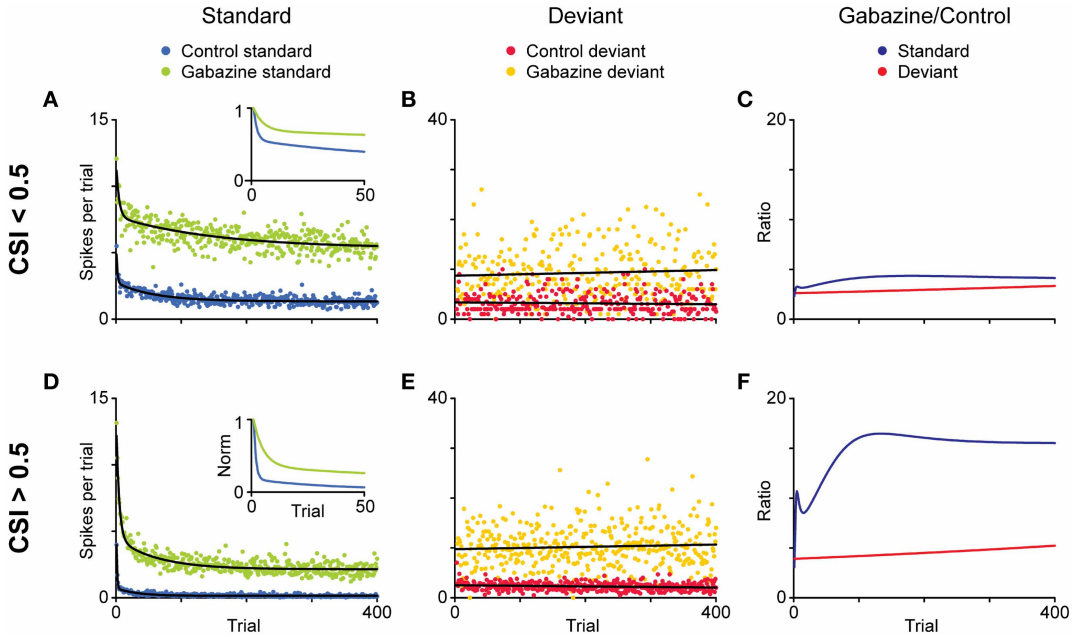

FIGURE 11 | Effect of the blockade of $GABA_A$ receptors on the time course of adaptation and a model of SSA modulation by inhibition. (A,B; D,E) Average discharge across the population of neurons for each position (trial) in the oddball sequence, separately for standard **(A,D)** and deviant **(B,E)** stimuli. The minimally adapting neurons (**A–C**; CSI < 0.5 in the control condition) and the highly adapting ones (**D,E**; CSI.0.5 in the control condition) were analyzed separately. Then the time course of habituation in the control condition and during application of gabazine was compared. The data for standard stimuli were fitted by a double exponential function (black lines), and the data for deviant stimuli, by a linear function. The insets show a magnified view of the normalized functions during the first 50 trials. Note the different ordinate scales for standard and deviant. **(C,F)** Ratio of gabazine/control for each type of stimulus during gabazine application. Reproduced from Pérez-González et al. (2012).

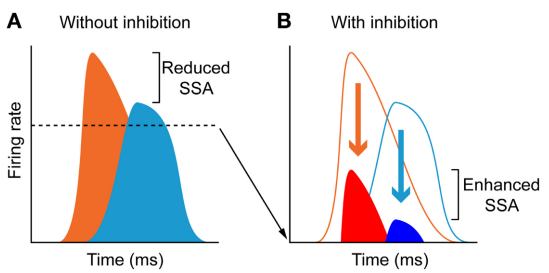

FIGURE 12 | The iceberg effect. (A) Schematic representation of a model of the iceberg effect indicating that in the absence of inhibition, neurons respond to deviants (orange) and standards (light blue) with high firing rates, and thus the deviant to standard ratio is small. **(B)** Inhibition reduces the responses to both deviants (red) and standards (dark blue) increasing the deviant to standard ratio and thus enhancing SSA. The dashed line in **(A)**, delimit the amount of activity (bottom area of the histograms) that decreases due to inhibition. Reproduced from Pérez-González et al. (2012).

receptors seem to be involved in the processing of novel visual stimuli in the superior colliculus (Binns and Salt, 1997) and they regulate the release of glutamate from excitatory terminals in the DCIC through presynaptic mechanisms (Scanziani, 2000; Sun and Wu, 2009). Then, both pre- and postsynaptic mechanisms are likely to contribute to a reduction in the membrane depolarization after initial excitation. To dissect the interplay of synaptic excitation and inhibition is also necessary to understand the cellular and network mechanisms underlying SSA. Previously, Binns and Salt (1995) demonstrated that the activity mediated by the NMDA and AMPA/Kainate receptors modulates response habituation in the superior colliculus. Hitherto, no attempt has been made to determine whether SSA in single-unit activity in the IC depends on local glutamatergic neurotransmission.

Since the level of SSA varies within the neuronal frequency response area (Duque et al., 2012), it is likely that the mechanisms underlying SSA act at the sites of synaptic inputs on the IC neuron. The specific decrement to repetitive stimuli seen in neurons exhibiting SSA could be explained by adaptation occurring at frequency-segregated input channels (Eytan et al., 2003). The persistence of SSA at long ISI suggests that it is not merely a result of mechanisms such as synaptic fatigue (e.g., reduction in neuronal responses independently of the stimulus due to depletion of neurotransmitter vesicles). This is less likely to occur at very long interstimulus gaps. Delayed synaptic inhibition might account for the specific response suppression to a highly repetitive stimulus. This idea is supported by intracellular recording suggesting that excitation in neurons throughout the IC is often followed by long-lasting hyperpolarization, possibly due to synaptic inhibition (Covey et al., 1996; Syka et al., 2000; Wehr and Zador, 2005). This could also explain why the neurons with the highest SSA levels (Duque et al., 2012) exhibit onset response patterns to sound stimulation. Another possibility is short-term plasticity occurring at the sites of synaptic integration in IC neurons. These possibilities are not mutually exclusive and it could be that they operate

in conjunction. It is plausible to think that the neuronal adaptation in the IC reflects high level network computations with strong participation of local inhibitory circuits (Pérez-González and Malmierca, 2012; Pérez-González et al., 2012), and with a modulatory control on SSA exerted by corticofugal projections (Anderson and Malmierca, 2013). Multidisciplinary efforts that will combine histological, electrophysiological, computational, and behavioral methods (Garagnani and Pulvermuller, 2011; Mill et al., 2011) will be necessary to unveil the basic mechanisms that generate SSA at each level along the auditory system.

CONCLUDING REMARKS AND FUTURE DIRECTIONS

In this review, we have attempted to offer an account of the current state of SSA studies in the IC because of the growing interest on the single-neuron electrophysiology of auditory deviance detection. The dependence of neuronal SSA on various stimulus features, such as deviant probability and repetition rate, and the role of AC and of inhibition in shaping SSA at this auditory stage have been addressed.

Among the questions to be resolved in the study of auditory deviance detection are whether SSA is present along the entire auditory pathway or whether it is a regionalized phenomenon to certain structures and how the deviance coding is modified by bottom-up and top-down processes that take place at each station. The localization of the most strongly adapting neurons to frequencies in the non-lemniscal portions of the subcortical nuclei opens interesting question about the neuronal circuits involved since these parts of the auditory pathway process more complex acoustic features. To address these issues, it is necessary to record neurons in the brainstem nuclei (especially those that exhibit cross-frequency integration), to track the common input sources to neurons with strong SSA, as well as, their projections, and to make simultaneous recordings at two or more connected sites. Since stimuli in a natural scene vary in multiple features, another open question is whether neurons sensitive to frequency deviants are also deviance detectors for more complex sound patterns and whether the same neurons are capable of detecting deviant stimulus immersed in more complex forms of regularity (Cornella et al., 2012; Grimm and Escera, 2012). These and other questions await future studies.

ACKNOWLEDGMENTS

We thank Dr. Nell B. Cant and Monty A. Escabí for their critical and constructive suggestions. Financial support was provided by the Spanish MEC (BFU2009-07286) and EU (EUI2009-04083, in the framework of the ERA-NET Network of European Funding for Neuroscience Research) to Manuel S. Malmierca. The funders had no role in study design, data collection and analysis, decision to publish, or preparation of the manuscript.

REFERENCES

Anderson, L. A., Christianson, G. B., and Linden, J. F. (2009). Stimulus-specific adaptation occurs in the auditory thalamus. *J. Neurosci.* 29, 7359–7363.

Anderson, L. A., and Malmierca, M. S. (2013). The effect of auditory cortical deactivation on stimulus-specific adaptation in the inferior colliculus of the rat. *Eur. J. Neurosci.* 37, 52–62.

Antunes, F. M., and Malmierca, M. S. (2011). Effect of auditory cortex deactivation on stimulus-specific adaptation in the medial geniculate body. *J. Neurosci.* 31, 17306–17316.

Antunes, F. M., Nelken, I., Covey, E., and Malmierca, M. S. (2010). Stimulus-specific adaptation in the auditory thalamus of the anesthetized rat. *PLoS ONE* 5:e14071. doi: 10.1371/journal.pone.0014071

Astikainen, P., Ruusuvirta, T., Wikgren, J., and Penttonen, M. (2006). Memory-based detection of rare sound feature combinations in anesthetized rats. *Neuroreport* 17, 1561–1564.

Astikainen, P., Stefanics, G., Nokia, M., Lipponen, A., Cong, F., Penttonen, M., et al. (2011). Memory-based mismatch response to frequency changes in rats. *PLoS ONE* 6:e24208. doi: 10.1371/journal.pone.0024208

Ayala, Y. A., Pérez-González, D., Duque, D., Nelken, I., and Malmierca, M. S. (2012). Frequency discrimination and stimulus deviance in the inferior colliculus and cochlear nucleus. *Front. Neural Circuits* 6:119. doi: 10.3389/fncir.2012.00119

Baüerle, P., Von Der Behrens, W., Kossl, M., and Gaese, B. H. (2011). Stimulus-specific adaptation in the gerbil primary auditory thalamus is the result of a fast frequency-specific habituation and is regulated by the corticofugal system. *J. Neurosci.* 31, 9708–9722.

Bibikov, N. G. (1977). 'Novelty' neurons in the frog auditory system. *Zh. Vyssh. Nerv. Deiat. Im. I P Pavlova* 27, 1075–1082.

Bibikov, N. G., and Soroka, S. K. (1979). Structure of the neurons in the midbrain auditory center in the frog, *Rana ridibunda*. *Zh. Evol. Biokhim. Fiziol.* 15, 608–616.

Binns, K. E., and Salt, T. E. (1995). Excitatory amino acid receptors modulate habituation of the response to visual stimulation in the cat superior colliculus. *Vis. Neurosci.* 12, 563–571.

Binns, K. E., and Salt, T. E. (1997). Different roles for $GABA_A$ and $GABA_B$ receptors in visual processing in the rat superior colliculus. *J. Physiol.* 504(Pt 3), 629–639.

Cant, N. B., and Benson, C. G. (2006). Organization of the inferior colliculus of the gerbil (*Meriones unguiculatus*): differences in distribution of projections from the cochlear nuclei and the superior olivary complex. *J. Comp. Neurol.* 495, 511–528.

Carral, V., Huotilainen, M., Ruusuvirta, T., Fellman, V., Naatanen, R., and Escera, C. (2005a). A kind of auditory 'primitive intelligence' already present at birth. *Eur. J. Neurosci.* 21, 3201–3204.

Carral, V., Corral, M. J., and Escera, C. (2005b). Auditory event-related potentials as a function of abstract change magnitude. *Neuroreport* 16, 301–305.

Caspary, D. M., Palombi, P. S., and Hughes, L. F. (2002). GABAergic inputs shape responses to amplitude modulated stimuli in the inferior colliculus. *Hear. Res.* 168, 163–173.

Casseday, J. H., Ehrlich, D., and Covey, E. (1994). Neural tuning for sound duration: role of inhibitory mechanisms in the inferior colliculus. *Science* 264, 847–850.

Casseday, J. H., Ehrlich, D., and Covey, E. (2000). Neural measurement of sound duration: control by excitatory-inhibitory interactions in the inferior colliculus. *J. Neurophysiol.* 84, 1475–1487.

Cornella, M., Leung, S., Grimm, S., and Escera, C. (2012). Detection of simple and pattern regularity violations occurs at different levels of the auditory hierarchy. *PLoS ONE* 7:e43604. doi:10.1371/journal.pone.0043604

Covey, E., Kauer, J. A., and Casseday, J. H. (1996). Whole-cell patch-clamp recording reveals subthreshold sound-evoked postsynaptic currents in the inferior colliculus of awake bats. *J. Neurosci.* 16, 3009–3018.

Draganova, R., Eswaran, H., Murphy, P., Huotilainen, M., Lowery, C., and Preissl, H. (2005). Sound frequency change detection in fetuses and newborns, a magnetoencephalographic study. *Neuroimage* 28, 354–361.

Duncan, C. C., Barry, R. J., Connolly, J. F., Fischer, C., Michie, P. T., Näätänen, R., et al. (2009). Event-related potentials in clinical research: guidelines for eliciting, recording, and quantifying mismatch negativity, P300, and N400. *Clin. Neurophysiol.* 120, 1883–1908.

Duque, D., Pérez-González, D., Ayala, A. Y., Palmer, A. R., and Malmierca, M. S. (2012). Topographic distribution, frequency and intensity dependence of stimulus-specific adaptation in the inferior colliculus of the rat. *J. Neurosci.* 32, 17762–17774.

Eriksson, J., and Villa, A. E. (2005). Event-related potentials in an auditory oddball situation in the rat. *Biosystems* 79, 207–212.

Escera, C., Alho, K., Schroger, E., and Winkler, I. (2000). Involuntary attention and distractibility as

evaluated with event-related brain potentials. *Audiol. Neurootol.* 5, 151–166.

Eytan, D., Brenner, N., and Marom, S. (2003). Selective adaptation in networks of cortical neurons. *J. Neurosci.* 23, 9349–9356.

Farley, B. J., Quirk, M. C., Doherty, J. J., and Christian, E. P. (2010). Stimulus-specific adaptation in auditory cortex is an NMDA-independent process distinct from the sensory novelty encoded by the mismatch negativity. *J. Neurosci.* 30, 16475–16484.

Garagnani, M., and Pulvermuller, F. (2011). From sounds to words: a neurocomputational model of adaptation, inhibition and memory processes in auditory change detection. *Neuroimage* 54, 170–181.

Grimm, S., and Escera, C. (2012). Auditory deviance detection revisited: evidence for a hierarchical novelty system. *Int. J. Psychophysiol.* 85, 88–92.

Grimm, S., Escera, C., Slabu, L., and Costa-Faidella, J. (2011). Electrophysiological evidence for the hierarchical organization of auditory change detection in the human brain. *Psychophysiology* 48, 377–384.

Gutfreund, Y. (2012). Stimulus-specific adaptation, habituation and change detection in the gaze control system. *Biol. Cybern.* 106, 657–668.

He, J., and Yu, Y. (2010). "Role of descending control in the auditory pathway," in *The Oxford Handbook of Auditory Science: The Auditory Brain*, eds A. Rees and A. R. Palmer (New York, NY: OUP), 247–268.

Hernández, O., Espinosa, N., Pérez-González, D., and Malmierca, M. S. (2005). The inferior colliculus of the rat: a quantitative analysis of monaural frequency response areas. *Neuroscience* 132, 203–217.

Huotilainen, M., Winkler, I., Alho, K., Escera, C., Virtanen, J., Ilmoniemi, R. J., et al. (1998). Combined mapping of human auditory EEG and MEG responses. *Electroencephalogr. Clin. Neurophysiol.* 108, 370–379.

Ingham, N. J., and McAlpine, D. (2005). GABAergic inhibition controls neural gain in inferior colliculus neurons sensitive to interaural time differences. *J. Neurosci.* 25, 6187–6198.

Isaacson, J. S., and Scanziani, M. (2011). How inhibition shapes cortical activity. *Neuron* 72, 231–243.

Jääskeläinen, I. P., Ahveninen, J., Belliveau, J. W., Raij, T., and Sams, M. (2007). Short-term plasticity in auditory cognition. *Trends Neurosci.* 30, 653–661.

Javitt, D. C., Steinschneider, M., Schroeder, C. E., Vaughan, H. G. Jr., and Arezzo, J. C. (1994). Detection of stimulus deviance within primate primary auditory cortex: intracortical mechanisms of mismatch negativity (MMN) generation. *Brain Res.* 667, 192–200.

Katz, Y., Heiss, J. E., and Lampl, I. (2006). Cross-whisker adaptation of neurons in the rat barrel cortex. *J. Neurosci.* 26, 13363–13372.

Kelly, J. B., and Li, L. (1997). Two sources of inhibition affecting binaural evoked responses in the rat's inferior colliculus: the dorsal nucleus of the lateral lemniscus and the superior olivary complex. *Hear. Res.* 104, 112–126.

King, C., McGee, T., Rubel, E. W., Nicol, T., and Kraus, N. (1995). Acoustic features and acoustic changes are represented by different central pathways. *Hear. Res.* 85, 45–52.

Koch, U., and Grothe, B. (1998). GABAergic and glycinergic inhibition sharpens tuning for frequency modulations in the inferior colliculus of the big brown bat. *J. Neurophysiol.* 80, 71–82.

Kraus, N., McGee, T., Littman, T., Nicol, T., and King, C. (1994). Nonprimary auditory thalamic representation of acoustic change. *J. Neurophysiol.* 72, 1270–1277.

LeBeau, F. E., Malmierca, M. S., and Rees, A. (2001). Iontophoresis *in vivo* demonstrates a key role for $GABA_A$ and glycinergic inhibition in shaping frequency response areas in the inferior colliculus of guinea pig. *J. Neurosci.* 21, 7303–7312.

LeBeau, F. E., Rees, A., and Malmierca, M. S. (1996). Contribution of GABA- and glycine-mediated inhibition to the monaural temporal response properties of neurons in the inferior colliculus. *J. Neurophysiol.* 75, 902–919.

Lee, C. C., and Sherman, S. M. (2011). On the classification of pathways in the auditory midbrain, thalamus, and cortex. *Hear. Res.* 276, 79–87.

Loftus, W. C., Bishop, D. C., and Oliver, D. L. (2010). Differential patterns of inputs create functional zones in central nucleus of inferior colliculus. *J. Neurosci.* 30, 13396–13408.

Loftus, W. C., Malmierca, M. S., Bishop, D. C., and Oliver, D. L. (2008). The cytoarchitecture of the inferior colliculus revisited: a common organization of the lateral cortex in rat and cat. *Neuroscience* 154, 196–205.

Lomber, S. G., and Malhotra, S. (2008). Double dissociation of 'what' and 'where' processing in auditory cortex. *Nat. Neurosci.* 11, 609–616.

Lomber, S. G., Payne, B. R., and Horel, J. A. (1999). The cryoloop: an adaptable reversible cooling deactivation method for behavioral or electrophysiological assessment of neural function. *J. Neurosci. Methods* 86, 179–194.

Luck, S. J., Mathalon, D. H., O'Donnell, B. F., Hamalainen, M. S., Spencer, K. M., Javitt, D. C., et al. (2011). A roadmap for the development and validation of event-related potential biomarkers in schizophrenia research. *Biol. Psychiatry* 70, 28–34.

Lumani, A., and Zhang, H. (2010). Responses of neurons in the rat's dorsal cortex of the inferior colliculus to monaural tone bursts. *Brain Res.* 1351, 115–129.

Malmierca, M. S. (2003). The structure and physiology of the rat auditory system: an overview. *Int. Rev. Neurobiol.* 56, 147–211.

Malmierca, M. S., Blackstad, T. W., and Osen, K. K. (2011). Computer-assisted 3-D reconstructions of Golgi-impregnated neurons in the cortical regions of the inferior colliculus of rat. *Hear. Res.* 274, 13–26.

Malmierca, M. S., Blackstad, T. W., Osen, K. K., Karagulle, T., and Molowny, R. L. (1993). The central nucleus of the inferior colliculus in rat: a Golgi and computer reconstruction study of neuronal and laminar structure. *J. Comp. Neurol.* 333, 1–27.

Malmierca, M. S., Cristaudo, S., Pérez-González, D., and Covey, E. (2009a). Stimulus-specific adaptation in the inferior colliculus of the anesthetized rat. *J. Neurosci.* 29, 5483–5493.

Malmierca, M. S., Hernández, O., Antunes, F. M., and Rees, A. (2009b). Divergent and point-to-point connections in the commissural pathway between the inferior colliculi. *J. Comp. Neurol.* 514, 226–239.

Malmierca, M. S., and Hackett, T. A. (2010). "Structural organization of the ascending auditory pathway," in *The Oxford Handbook of Auditory Science: The Auditory Brain,* ed D. R. Moore (New York, NY: OUP), 9–41.

Malmierca, M. S., Hernández, O., Antunes, F. M., Pérez-González, D., Izquierdo, M. A., and Covey, E. (2010). "$GABA_A$ receptors mediate stimulus-specific adaptation (SSA) in the auditory midbrain," in *33rd Midwinter Meeting of the Association for Research in Otolaryngology: ARO abstr 786.* (Anaheim, CA).

Malmierca, M. S., Hernández, O., Falconi, A., Lopez-Poveda, E. A., Merchán, M., and Rees, A. (2003). The commissure of the inferior colliculus shapes frequency response areas in rat: an *in vivo* study using reversible blockade with microinjection of kynurenic acid. *Exp. Brain Res.* 153, 522–529.

Malmierca, M. S., Hernández, O., and Rees, A. (2005a). Intercollicular commissural projections modulate neuronal responses in the inferior colliculus. *Eur. J. Neurosci.* 21, 2701–2710.

Malmierca, M. S., Saint Marie, R. L., Merchán, M. A., and Oliver, D. L. (2005b). Laminar inputs from dorsal cochlear nucleus and ventral cochlear nucleus to the central nucleus of the inferior colliculus: two patterns of convergence. *Neuroscience* 136, 883–894.

Malmierca, M. S., and Ryugo, D. K. (2011). "Descending connections of auditory cortex to the midbrain and brainstem," in *The Auditory Cortex*, eds J. A. Winer and C. E. Schreiner (New York, NY: Springer), 189–208.

Malmierca, M. S., Seip, K. L., and Osen, K. K. (1995). Morphological classification and identification of neurons in the inferior colliculus: a multivariate analysis. *Anat. Embryol. (Berl.)* 191, 343–350.

Malone, B. J., Scott, B. H., and Semple, M. N. (2002). Context-dependent adaptive coding of interaural phase disparity in the auditory cortex of awake macaques. *J. Neurosci.* 22, 4625–4638.

Merchán, M., Aguilar, L. A., Lopez-Poveda, E. A., and Malmierca, M. S. (2005). The inferior colliculus of the rat: quantitative immunocytochemical study of GABA and glycine. *Neuroscience* 136, 907–925.

Mill, R., Coath, M., Wennekers, T., and Denham, S. L. (2011). Abstract stimulus-specific adaptation models. *Neural Comput.* 23, 435–476.

Moore, D. R., Kotak, V. C., and Sanes, D. H. (1998). Commissural and lemniscal synaptic input to the gerbil inferior colliculus. *J. Neurophysiol.* 80, 2229–2236.

Moshitch, D., Las, L., Ulanovsky, N., Bar-Yosef, O., and Nelken, I. (2006). Responses of neurons in primary auditory cortex (A1) to pure tones in the halothane-anesthetized cat. *J. Neurophysiol.* 95, 3756–3769.

Movshon, J. A., and Lennie, P. (1979). Pattern-selective adaptation in visual cortical neurones. *Nature* 278, 850–852.

Müller, J. R., Metha, A. B., Krauskopf, J., and Lennie, P. (1999). Rapid adaptation in visual cortex to the

structure of images. *Science* 285, 1405–1408.

Näätänen, R. (1992). *Attention and Brain Function*. Hillsdale, NJ: Lawrence Erlbaum.

Näätänen, R., and Escera, C. (2000). Mismatch negativity: clinical and other applications. *Audiol. Neurootol.* 5, 105–110.

Näätänen, R., Gaillard, A. W., and Mantysalo, S. (1978). Early selective-attention effect on evoked potential reinterpreted. *Acta Psychol. (Amst.)* 42, 313–329.

Näätänen, R., Paavilainen, P., Rinne, T., and Alho, K. (2007). The mismatch negativity (MMN) in basic research of central auditory processing: a review. *Clin. Neurophysiol.* 118, 2544–2590.

Näätänen, R., Tervaniemi, M., Sussman, E., Paavilainen, P., and Winkler, I. (2001). "Primitive intelligence," in the auditory cortex. *Trends Neurosci.* 24, 283–288.

Nakamoto, K. T., Jones, S. J., and Palmer, A. R. (2008). Descending projections from auditory cortex modulate sensitivity in the midbrain to cues for spatial position. *J. Neurophysiol.* 99, 2347–2356.

Nakamura, T., Michie, P. T., Fulham, W. R., Todd, J., Budd, T. W., Schall, U., et al. (2011). Epidural auditory event-related potentials in the rat to frequency and duration deviants: evidence of mismatch negativity? *Front. Psychology* 2:367. doi: 10.3389/fpsyg.2011.00367

Nelken, I., and Ulanovsky, N. (2007). Mismatch negativity and stimulus-specific adaptation in animal models. *J. Psychophysiol.* 21, 214–223.

Netser, S., Zahar, Y., and Gutfreund, Y. (2011). Stimulus-specific adaptation: can it be a neural correlate of behavioral habituation? *J. Neurosci.* 31, 17811–17820.

Palombi, P. S., and Caspary, D. M. (1996). GABA inputs control discharge rate primarily within frequency receptive fields of inferior colliculus neurons. *J. Neurophysiol.* 75, 2211–2219.

Patel, C. R., Redhead, C., Cervi, A. L., and Zhang, H. (2012). Neural sensitivity to novel sounds in the rat's dorsal cortex of the inferior colliculus as revealed by evoked local field potentials. *Hear. Res.* 286, 41–54.

Pérez-González, D., Hernández, O., Covey, E., and Malmierca, M. S. (2012). $GABA_A$-mediated inhibition modulates stimulus-specific adaptation in the inferior colliculus. *PLoS ONE* 7:e34297. doi: 10.1371/journal.pone.0034297

Pérez-González, D., and Malmierca, M. S. (2012). Variability of the time course of stimulus-specific adaptation in the inferior colliculus. *Front. Neural Circuits* 6:107. doi: 10.3389/fncir.2012.00107

Pérez-González, D., Malmierca, M. S., and Covey, E. (2005). Novelty detector neurons in the mammalian auditory midbrain. *Eur. J. Neurosci.* 22, 2879–2885.

Recasens, M., Grimm, S., Capilla, A., Nowak, R., and Escera, C. (2012). Two sequential processes of change detection in hierarchically ordered areas of the human auditory cortex. *Cereb. Cortex* doi: 10.1093/cercor/bhs295. [Epub ahead of print].

Reches, A., and Gutfreund, Y. (2008). Stimulus-specific adaptations in the gaze control system of the barn owl. *J. Neurosci.* 28, 1523–1533.

Rees, A., Sarbaz, A., Malmierca, M. S., and Le Beau, F. E. (1997). Regularity of firing of neurons in the inferior colliculus. *J. Neurophysiol.* 77, 2945–2965.

Reetz, G., and Ehret, G. (1999). Inputs from three brainstem sources to identified neurons of the mouse inferior colliculus slice. *Brain Res.* 816, 527–543.

Riquelme, R., Saldana, E., Osen, K. K., Ottersen, O. P., and Merchán, M. A. (2001). Colocalization of GABA and glycine in the ventral nucleus of the lateral lemniscus in rat: an *in situ* hybridization and semiquantitative immunocytochemical study. *J. Comp. Neurol.* 432, 409–424.

Ruusuvirta, T., Penttonen, M., and Korhonen, T. (1998). Auditory cortical event-related potentials to pitch deviances in rats. *Neurosci. Lett.* 248, 45–48.

Scanziani, M. (2000). GABA spillover activates postsynaptic $GABA_B$ receptors to control rhythmic hippocampal activity. *Neuron* 25, 673–681.

Shalgi, S., and Deouell, L. Y. (2007). Direct evidence for differential roles of temporal and frontal components of auditory change detection. *Neuropsychologia* 45, 1878–1888.

Sivaramakrishnan, S., Sterbing-D'Angelo, S. J., Filipovic, B., D'Angelo, W. R., Oliver, D. L., and Kuwada, S. (2004). $GABA_A$ synapses shape neuronal responses to sound intensity in the inferior colliculus. *J. Neurosci.* 24, 5031–5043.

Slabu, L., Escera, C., Grimm, S., and Costa-Faidella, J. (2010). Early change detection in humans as revealed by auditory brainstem and middle-latency evoked potentials. *Eur. J. Neurosci.* 32, 859–865.

Slabu, L., Grimm, S., and Escera, C. (2012). Novelty detection in the human auditory brainstem. *J. Neurosci.* 32, 1447–1452.

Sobotka, S., and Ringo, J. L. (1994). Stimulus specific adaptation in excited but not in inhibited cells in inferotemporal cortex of macaque. *Brain Res.* 646, 95–99.

Sun, H., and Wu, S. H. (2009). The physiological role of pre- and postsynaptic $GABA_B$ receptors in membrane excitability and synaptic transmission of neurons in the rat's dorsal cortex of the inferior colliculus. *Neuroscience* 160, 198–211.

Syka, J., Popelar, J., Kvasnak, E., and Astl, J. (2000). Response properties of neurons in the central nucleus and external and dorsal cortices of the inferior colliculus in guinea pig. *Exp. Brain Res.* 133, 254–266.

Taaseh, N., Yaron, A., and Nelken, I. (2011). Stimulus-specific adaptation and deviance detection in the rat auditory cortex. *PLoS ONE* 6:e23369. doi: 10.1371/journal.pone.0023369

Thomas, J. M., Morse, C., Kishline, L., O'Brien-Lambert, A., Simonton, A., Miller, K. E., et al. (2012). Stimulus-specific adaptation in specialized neurons in the inferior colliculus of the big brown bat, *Eptesicus fuscus*. *Hear. Res.* 291, 34–40.

Tiitinen, H., May, P., Reinikainen, K., and Näätänen, R. (1994). Attentive novelty detection in humans is governed by pre-attentive sensory memory. *Nature* 372, 90–92.

Tikhonravov, D., Neuvonen, T., Pertovaara, A., Savioja, K., Ruusuvirta, T., Näätänen, R., et al. (2008). Effects of an NMDA-receptor antagonist MK-801 on an MMN-like response recorded in anesthetized rats. *Brain Res.* 1203, 97–102.

Ulanovsky, N., Las, L., Farkas, D., and Nelken, I. (2004). Multiple time scales of adaptation in auditory cortex neurons. *J. Neurosci.* 24, 10440–10453.

Ulanovsky, N., Las, L., and Nelken, I. (2003). Processing of low-probability sounds by cortical neurons. *Nat. Neurosci.* 6, 391–398.

Von Der Behrens, W., Bauerle, P., Kossl, M., and Gaese, B. H. (2009). Correlating stimulus-specific adaptation of cortical neurons and local field potentials in the awake rat. *J. Neurosci.* 29, 13837–13849.

Wehr, M., and Zador, A. M. (2005). Synaptic mechanisms of forward suppression in rat auditory cortex. *Neuron* 47, 437–445.

Winkler, I., Denham, S. L., and Nelken, I. (2009). Modeling the auditory scene: predictive regularity representations and perceptual objects. *Trends Cogn. Sci.* 13, 532–540.

Woods, E. J., and Frost, B. J. (1977). Adaptation and habituation characteristics of tectal neurons in the pigeon. *Exp. Brain Res.* 27, 347–354.

Yu, X. J., Xu, X. X., He, S., and He, J. (2009). Change detection by thalamic reticular neurons. *Nat. Neurosci.* 12, 1165–1170.

Zhao, L., Liu, Y., Shen, L., Feng, L., and Hong, B. (2011). Stimulus-specific adaptation and its dynamics in the inferior colliculus of rat. *Neuroscience* 181, 163–174.

Conflict of Interest Statement: The authors declare that the research was conducted in the absence of any commercial or financial relationships that could be construed as a potential conflict of interest.

Received: 19 August 2012; accepted: 02 November 2012; published online: 17 January 2013.

Citation: Ayala YA and Malmierca MS (2013) Stimulus-specific adaptation and deviance detection in the inferior colliculus. Front. Neural Circuits ***6****:89. doi: 10.3389/fncir.2012.00089*

SCIENTIFIC REPORTS

OPEN

Differences in the strength of cortical and brainstem inputs to SSA and non-SSA neurons in the inferior colliculus

Received: 30 January 2015
Accepted: 10 April 2015
Published: 20 May 2015

Yaneri A. Ayala[1], Adanna Udeh[2], Kelsey Dutta[2], Deborah Bishop[2], Manuel S. Malmierca[1,2,3] & Douglas L. Oliver[2]

In an ever changing auditory scene, change detection is an ongoing task performed by the auditory brain. Neurons in the midbrain and auditory cortex that exhibit stimulus-specific adaptation (SSA) may contribute to this process. Those neurons adapt to frequent sounds while retaining their excitability to rare sounds. Here, we test whether neurons exhibiting SSA and those without are part of the same networks in the inferior colliculus (IC). We recorded the responses to frequent and rare sounds and then marked the sites of these neurons with a retrograde tracer to correlate the source of projections with the physiological response. SSA neurons were confined to the non-lemniscal subdivisions and exhibited broad receptive fields, while the non-SSA were confined to the central nucleus and displayed narrow receptive fields. SSA neurons receive strong inputs from auditory cortical areas and very poor or even absent projections from the brainstem nuclei. On the contrary, the major sources of inputs to the neurons that lacked SSA were from the brainstem nuclei. These findings demonstrate that auditory cortical inputs are biased in favor of IC synaptic domains that are populated by SSA neurons enabling them to compare top-down signals with incoming sensory information from lower areas.

Animals, including humans are immersed in an ever-changing auditory scene. In order to detect unexpected events, the responses of some auditory neurons adapts to frequent sounds while they retain their excitability to rare sounds[1]. This neuronal phenomenon is called stimulus-specific adaptation (SSA) and has been thought to enhance the response to infrequent sounds and to reduce acoustic information redundancy[2]. SSA may contribute to evoked potentials related to deviance detection[3–5] and to focus attention on the changes in the incoming stream of sensory information[2]. SSA responses are apparent in many neurons of the primary auditory cortex (Au1)[1], medial geniculate body[6,7], and inferior colliculus (IC)[8–10].

The IC may be a site of dynamic control for the flow of biologically important acoustic information since it is a center for convergence of both ascending and descending auditory and non-auditory information[11]. The lemniscal pathway emerges from the central nucleus of the IC and projects to the core auditory cortex via the ventral division of the medial geniculate body. The non-lemniscal pathways originate from the cortex of the IC and the lateral tegmental system to project to the belt auditory cortex via the dorsal division of the medial geniculate body[12,13]. Interestingly, the non-lemniscal pathways in the midbrain have stronger inputs from the neocortex than those of the central nucleus of the IC[14,15].

[1]Auditory Neurophysiology Laboratory. Institute of Neuroscience of Castilla Y León, University of Salamanca, C/ Pintor Fernando Gallego, 1, 37007 Salamanca, Spain. [2]Department of Neuroscience, University of Connecticut Health Center, Farmington, CT 06030-3401, USA. [3]Department of Cell Biology and Pathology, Faculty of Medicine, University of Salamanca, Campus Miguel de Unamuno, 37007 Salamanca, Spain. Correspondence and requests for materials should be addressed to M.S.M. (email: msm@usal.es) or D.L.O. (email: doliver@neuron.uchc.edu)

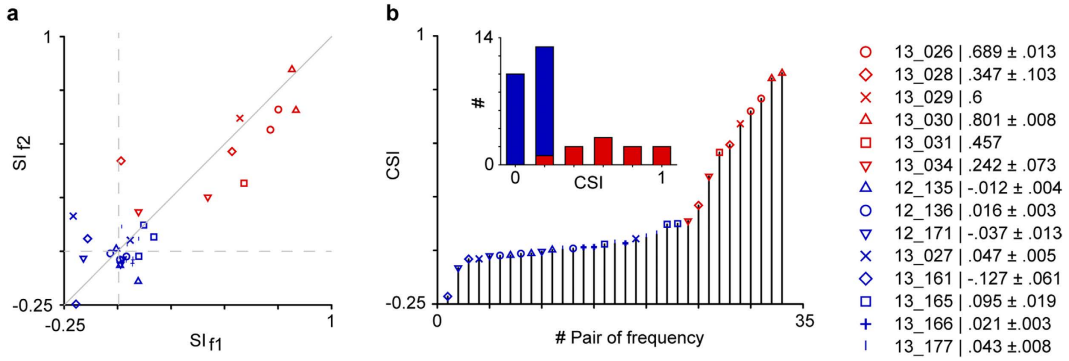

Figure 1. SSA indices of the response of neurons that exhibit SSA (red) and of those non-SSA neurons that lack SSA (blue). From one to four pairs of frequencies were presented for each neuron (symbols). (**a**) The Frequency-Specific Index (SI) was similar for both frequencies (f1, f2) presented under the oddball paradigm resulting in SI values aligned along the diagonal line (Wilcoxon Signed Rank Test, $p = 0.08$). (**b**) The non-SSA neurons had Common-SSA Index (CSI) values lower than 0.18 for all the pair of frequency tested. The SSA neurons had CSI values higher than 0.18 for most of the pair of frequency tested (9/10). The CSI = 0.18 was used as cutoff value to separate SSA from non-SSA neurons. The differential distribution of the CSI values for the SSA and non-SSA group is shown in the inset. The right inset showed the neuron number and the mean ± s.e.m. CSI value for each neuron when two or more frequencies were presented.

Previous studies suggest that neurons with SSA are primarily located in the non-lemniscal subdivisions of the IC[9,16,17].

Although the neurophysiology of SSA has been studied in great deal at the single neuron level in the IC[9,16–18], rigorous attempts to correlate the anatomy of the auditory inputs and the physiology of SSA neurons are lacking. Here, we test whether neurons exhibiting SSA and those without are part of the same networks in the IC. We studied neurons exhibiting or lacking SSA in the IC and then marked the sites of these neurons with a retrograde tracer to correlate the source of the inputs with the physiological response. This approach is designed to detangle the connectivity of the so-called network for auditory deviance detection[4].

Results

Since the main goal of this study was to determine the inputs to regions of IC that contain neurons that either exhibit significant SSA or lack SSA, first we recorded the extracellular single-unit responses to the oddball paradigm from 14 IC neurons (one per animal) and then made a minute injection of FG at the recording site. Two to four pairs of frequencies were used in the majority of neurons (12/14), and these elicited SI values ranging from −0.246 to 0.846 (Fig. 1a) and CSI values ranging from −0.214 to 0.827 (Fig. 1b). Neurons were classified as showing SSA when the CSI value exceeded 0.18 as in previous studies[7,16,17]. Thus, six neurons in our sample exhibited significant SSA levels (SSA cases), while eight neurons responded similarly to the deviant and standard tones across trials and, therefore, lacked SSA. The latter non-SSA neurons were used for comparison. Importantly, these two groups of neurons are easily distinguishable based solely on the presence or absence of SSA regardless of other response properties. The sizes of the FG injections were similar across the cases as well as the quality of the retrograde labeling of the neurons.

In the following results, we will first present the physiology and anatomy of two SSA cases; one with a low frequency BF and the other with a high frequency BF that are typical and representative of the whole sample. Then, we will compare these to the responses and inputs to the recording sites of two other neurons that lack SSA and that also showed low- and high-frequency BFs.

SSA Cases. We show two representative neurons from the six cases with significant SSA levels. The first neuron had a low BF at 2.52 kHz at 80 dB SPL and a complex FRA tuned to a wide spectrum of frequencies (Fig. 2a). Its broad bandwidth was similar at different intensity levels ($Q_{10} = 0.51$, $Q_{30} = 0.56$). The neuron showed a transient response and an irregular firing pattern at BF (CV = 1.27, Fig. 2b). Sensitivity to SSA was demonstrated by the adaptation of firing in response to the standard tone. This resulted in a CSI = 0.67 for a closely spaced pair of frequencies ($\Delta f = 0.144$ octaves, Fig. 2c,d). When the frequency contrast increased to $\Delta f = 0.531$ octaves, the CSI also increased to 0.71 (Fig. 2e,f). The latency of the neuronal response to the deviant stimulus was shorter (FSL = 26.568 ms ± 10.07, red) than to the standard one (FSL = 30.92 ms ± 12.52, blue) for both frequency contrast (Mann-Whitney Rank Sum Test, $p = 0.016$).

In this case, the injection of the region containing the recorded neuron resulted in extensive retrograde labeling in the auditory cortex but little labeling in the brainstem. The FG injection was confined

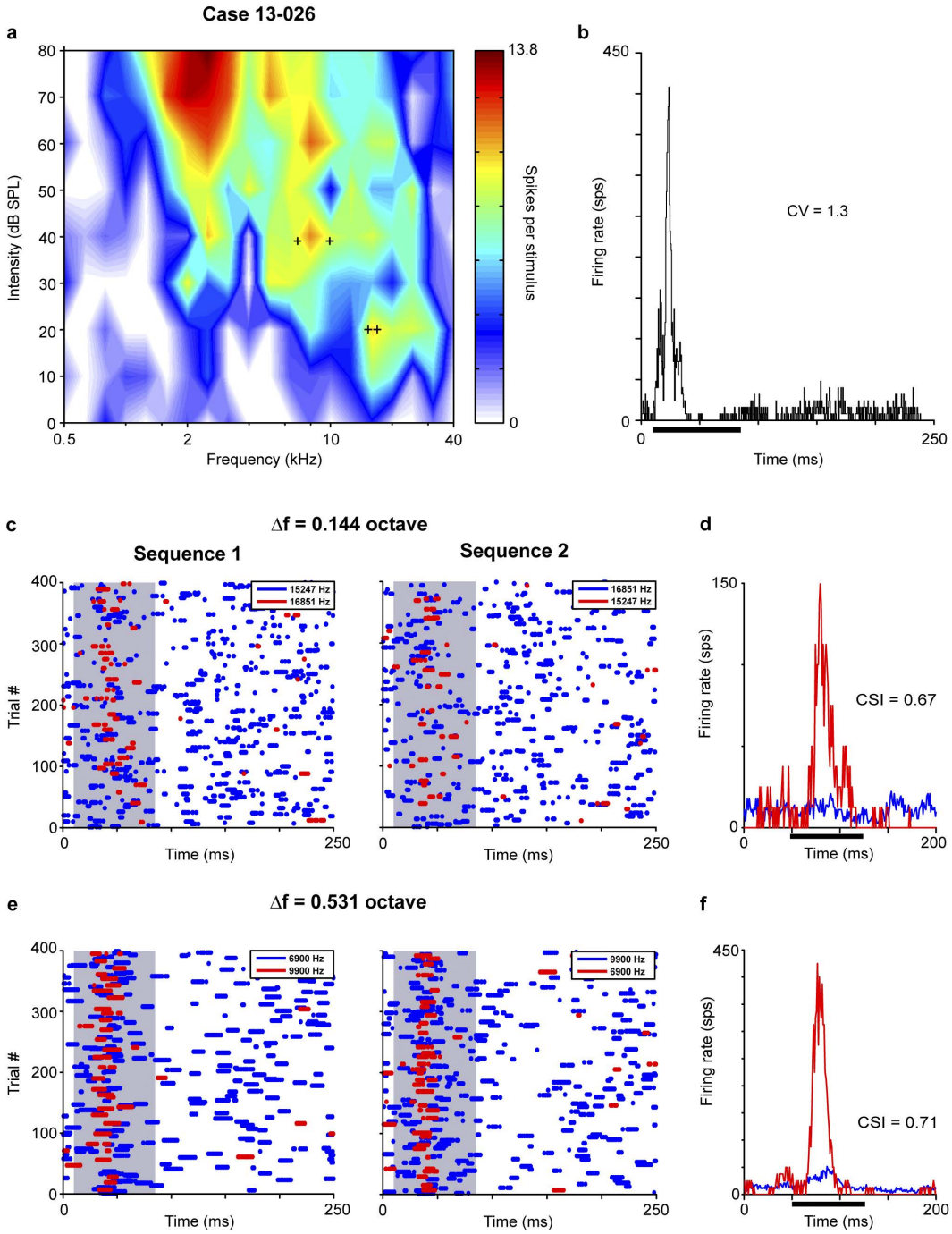

Figure 2. Low-frequency neuron with SSA. The adaptation to the standard tone was reflected by positive SSA index in this low-frequency SSA neuron. (**a**) Broadly-tuned frequency response area with a characteristic frequency of 2.52 kHz. (**b**) Transient and irregular firing pattern to the characteristic frequency. Dot rasters (**c**,**e**) and normalized PSTH (**d**,**f**) for two pairs of tested frequencies with separations of 0.144 and 0.531 octave. The pairs of frequencies are indicated within the frequency response area (+). The PSTHs (**d**,**f**) represent the mean response from both oddball sequences (1 and 2) showing a higher neuronal response to the deviant tone (red) than to the standard (blue). Case 13-026. PSTH bin size = 1 ms. CV, coefficient of variation; CSI, common SSA index. sps, spikes per second. Tone duration represented by bar and shaded areas.

to the lateral cortex with a 350 μm-wide center (Fig. 3a, section 760, black; the box indicates the photomicrograph illustrated in Fig. 4a), and it followed the dorsal to ventral electrode track. This orientation matches that of the recording pipette which was tilted 20° in a rostro-caudal direction and advanced from dorsal to ventral. It was primarily confined to the small-cell middle layer and the deepest layer of large

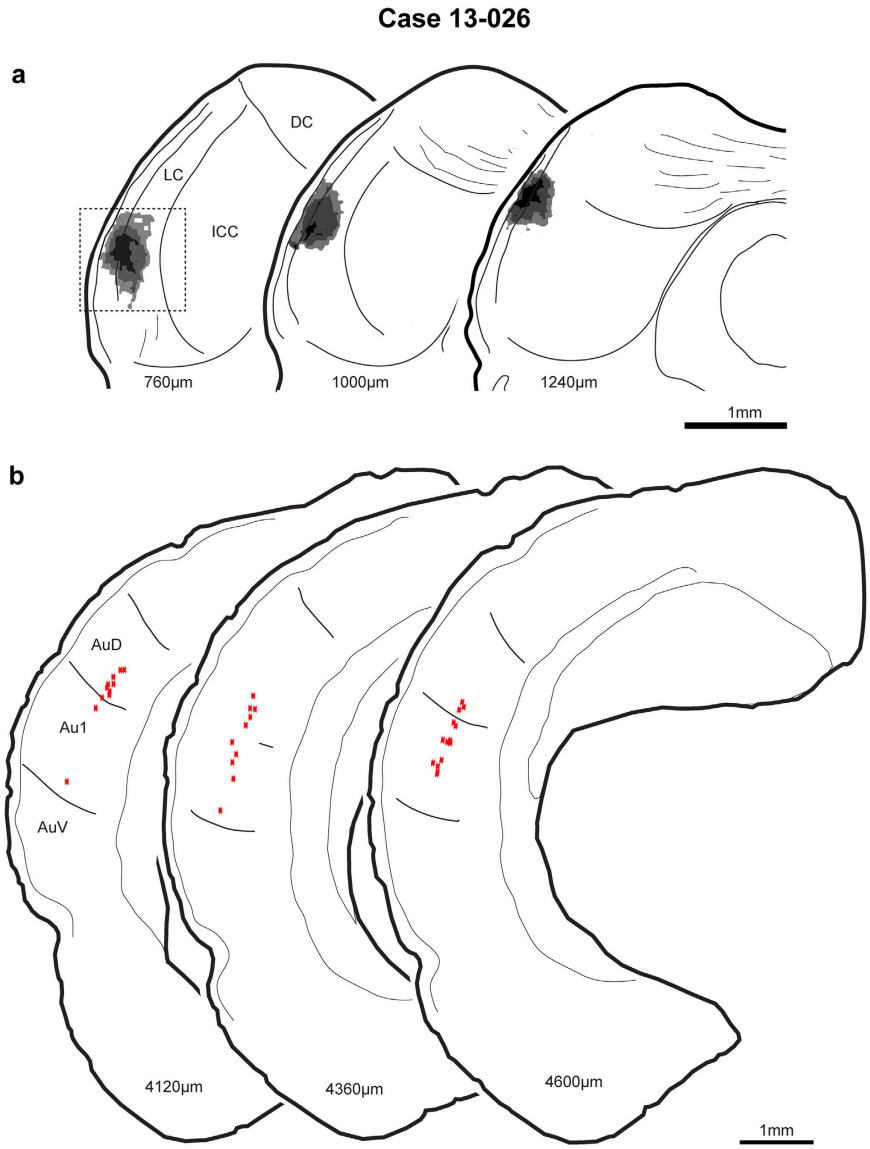

Figure 3. Injection site of SSA neuron and retrograde labelling for case 13-026. The injection site for the high-frequency SSA neuron was confined to the lateral cortex of the IC (**a**) and labeled neurons (◆) were only found in auditory cortices including primary and non-primary areas (**b**). Section distance is relative to caudal-most section of IC. LC, lateral cortex of IC; DC, dorsal cortex of IC; ICC, central nucleus of IC; Au1, primary auditory neocortex; AuD, dorsal auditory area; AuV, ventral auditory area.

cells[19]. No brainstem labelling was found, but heavily labeled neurons were found through the auditory cortices including areas Au1 and AuD (Fig. 3b). Those cortical neurons were mostly found at a similar depth of about 700−880 μm and displayed the morphology of layer 5 pyramidal cells. In all cases, there was labeling in the ICC apart from the injection site that we interpret as retrograde labeling.

The second typical case also had a neuron exhibiting strong SSA. The neuron had a broad frequency response area ($Q_{10} = 1.03$, $Q_{30} = 0\ 1.02$) and was tuned to high frequencies around 10 kHz and above. It showed a non-monotonic rate level response to both the BF (15.853 kHz, MI = 0.53) and CF (31.915 kHz, MI = 0.6) (Fig. 5a). The response to the BF at 60 dB SPL was transient and irregular (CV = 0.62) with a suppression in the spontaneous activity that lasted more than 100 ms (Fig. 5b). In terms of SSA, the neuron´s differential response to the deviant and to the standard tone produced a high CSI value for pairs of frequencies separated by 0.144 octave (CSI = 0.81) (Fig. 5c,d) and 0.531octave (CSI = 0.79) (Fig. 5e,f).

The site of this neuron received extensive inputs from the neocortex but only sparse input from the superior olive. The injection site was rostral and lateral in the cortex of the IC with a center of 280 μm at its maximum extent (Fig. 6a, section 1920 μm, black; the box indicates the photomicrograph illustrated in Fig. 4b). In the most rostral sections (Fig. 6a, 2160 μm), two tracer deposits were found but the upper one had the heaviest labelling. Very few FG-labeled somata were located in the brainstem. Single labeled neurons were found in the superior periolivary nucleus (SPO), medial superior olive and medial region

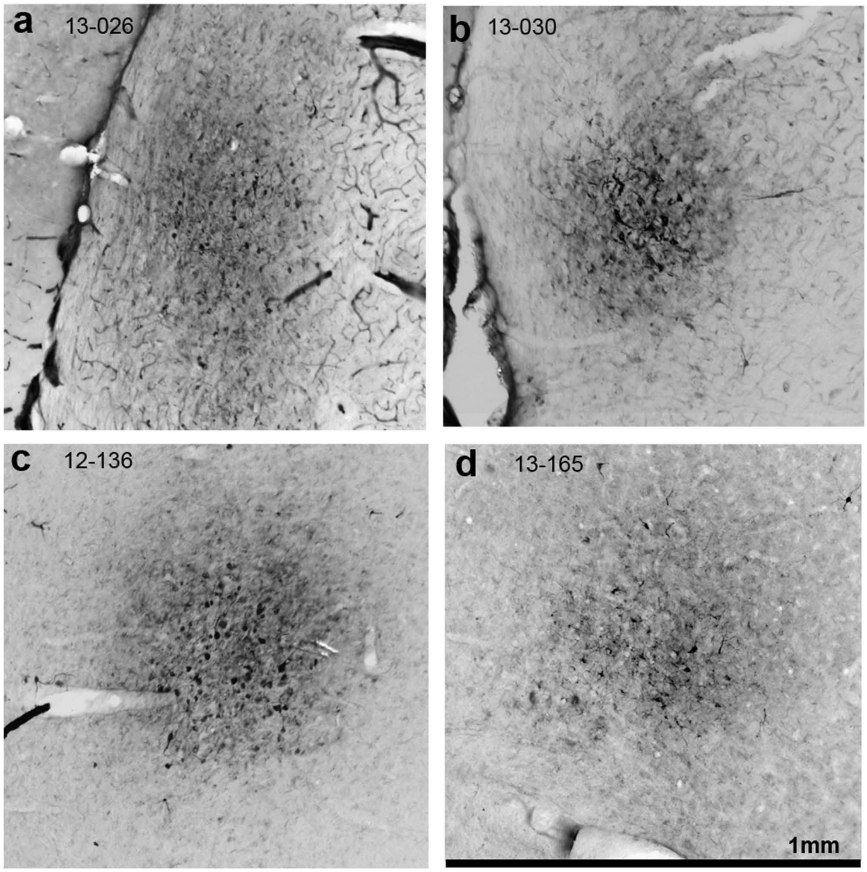

Figure 4. Photomicrographs showing the injection site for SSA cases 13-026 (**a**) and 13-030 (**b**) and non SSA cases 12-136 (**c**) and 13-165 (**d**). Each photomicrograph showing the injection site is identified with a box in the illustration of each case (cf. Figs. 3, 6, 8, and 10).

of the lateral superior olive (Fig. 6b). The location of the labeled neurons in the medial superior olive and lateral superior olive indicated that the retrograde labelling pattern corresponded well with the high frequency tuning of the IC recorded neuron. On the other hand, the neocortical labelling pattern was similar and more abundant than the previous SSA case (Fig. 3). Retrogradely labelled cortical neurons extended to very rostral sections (5760 μm) and were distributed throughout the dorsoventral axis in areas AuV, Au1 and AuD. The highest density of labeled neurons were those clustered in AuD area of auditory cortex (Fig. 6c).

Non-SSA Cases. Neurons that lack SSA were used to compare both physiological and anatomical data. The first example neuron had a low BF with a narrow V-shaped FRA (Fig. 7a), and a monotonic rate intensity function (MI = 1). The temporal response to the BF (2.61 kHz) showed an on-sustained response type (Fig. 7b). In this neuron, we stimulated with two pairs of frequencies, one with a Δf of 0.144 octave (Fig. 7c,d), and the other with a Δf of 0.531 octave (Fig. 7e–f). The neuronal responses to the deviant and standard tone presentations during the two oddball sequences are illustrated by dot rasters (Fig. 7c–e) and the corresponding mean peri-stimulus time histogram (PSTH, Fig. 7d,f). This neuron did not show SSA since its response strength and pattern to the deviant and standard tone was very similar regardless of the frequency separation between tones. This lack of adaptation in the response was reflected by its very low CSI value, 0.01 and −0.025 for Δf = 0.144 and 0.531, respectively.

In this case, the small region around the neuron received extensive brainstem inputs. The center of the injection site was rostral and lateral in the central nucleus of the IC and reached a maximum diameter of 450 μm (Fig. 8a; the box on section 1080 μm indicates the photomicrograph illustrated in Fig. 4c). The injection also extended into the adjacent lateral cortex of IC (Fig. 8a). The resulting retrograde labelling in the brainstem nuclei was typical with many labeled neurons in the ipsilateral superior olivary complex, ipsilateral ventral nucleus of the lateral lemniscus (LL), and contralateral cochlear nucleus (CN) (Fig. 8b). Labeling was prominent in the ipsilateral medial and lateral superior olives and ipsilateral SPO. Little labeling was seen in the contralateral superior olivary complex. Labeling in the nuclei of the LL was concentrated ventrally in the ventral nucleus and very little in the intermediate and dorsal nuclei of the LL. Dense clusters of labeled neurons were found in the contralateral dorsal CN and anteroventral CN

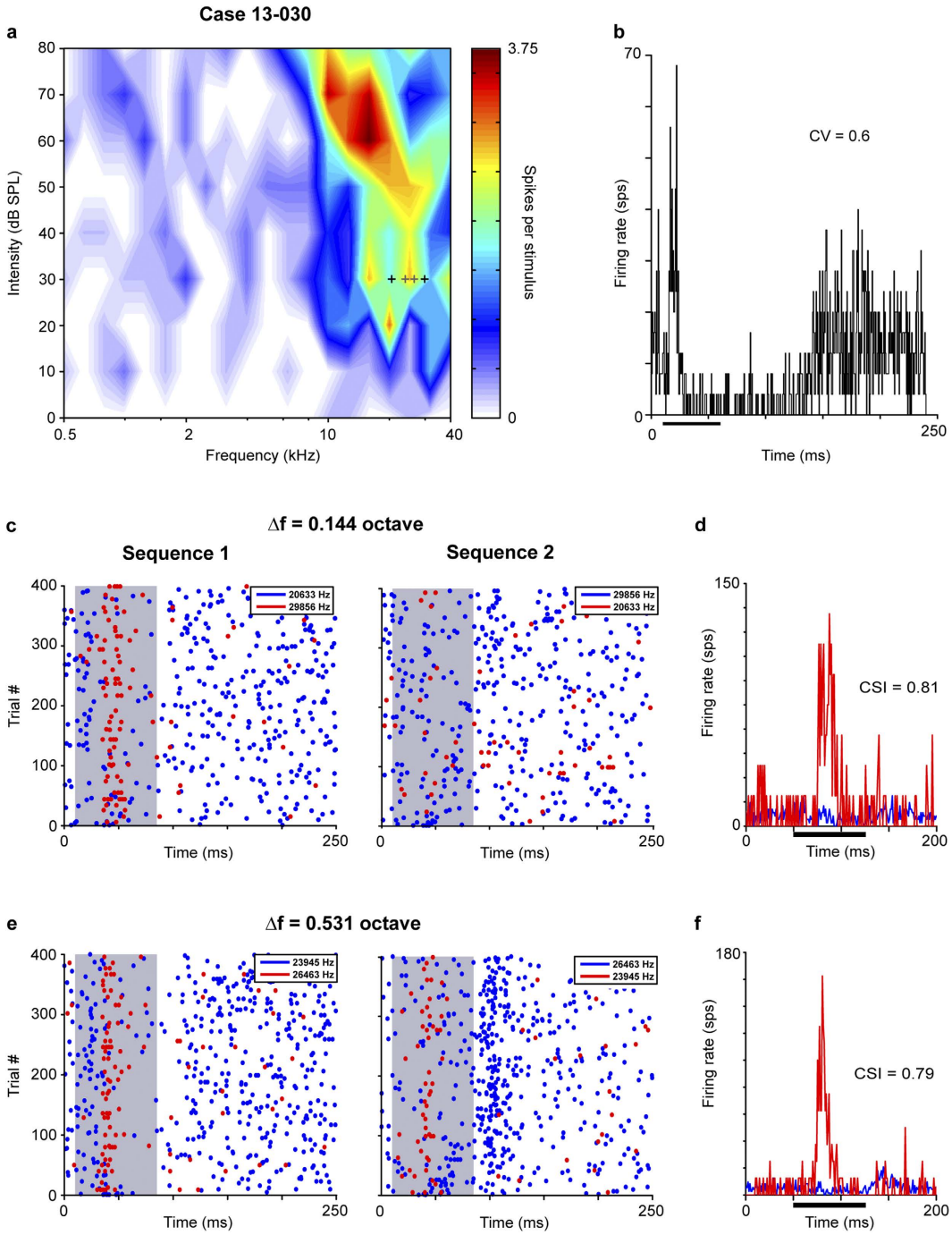

Figure 5. High-frequency neuron with SSA. The significant SSA level exhibited by this neuron was reflected by the stronger response to the deviant tone and the faint response to the standard tone. (**a**) Frequency response area tuned to high frequencies with a low threshold. (**b**) The irregular response and spontaneous discharge to best frequency (15.853 kHz) was evident in the PSTH. Dot rasters (**c**,**e**) and normalized PSTH (**d**,**f**) for two pairs of tested frequencies as deviant (red) and standard (blue) with separations of 0.144 and 0.531 octave. Case 13-030. Abbreviations as in Fig. 2.

(Fig. 8b). In contrast to the robust labelling displayed by the brainstem nuclei, only two labeled neurons were found in the neocortex, and these were located in Au1 (Fig. 8c).

The second non-SSA neuron had a high BF, a narrow FRA (2.36 and 2.75 for the Q_{10} and Q_{30}, respectively) flanked by an inhibitory area at the low frequency region, and a non-monotonic rate intensity function (MI = 0.66) (Fig. 9a). At the BF of 32.13 kHz (at 40 dB SPL), this neuron had an onset response with a short first spike latency (7.495 ms ± 0.5861) across trials (Fig. 9b). Despite the difference in the BF, FRA, rate level function, and temporal patterns compared to the first non-SSA neuron, the strength

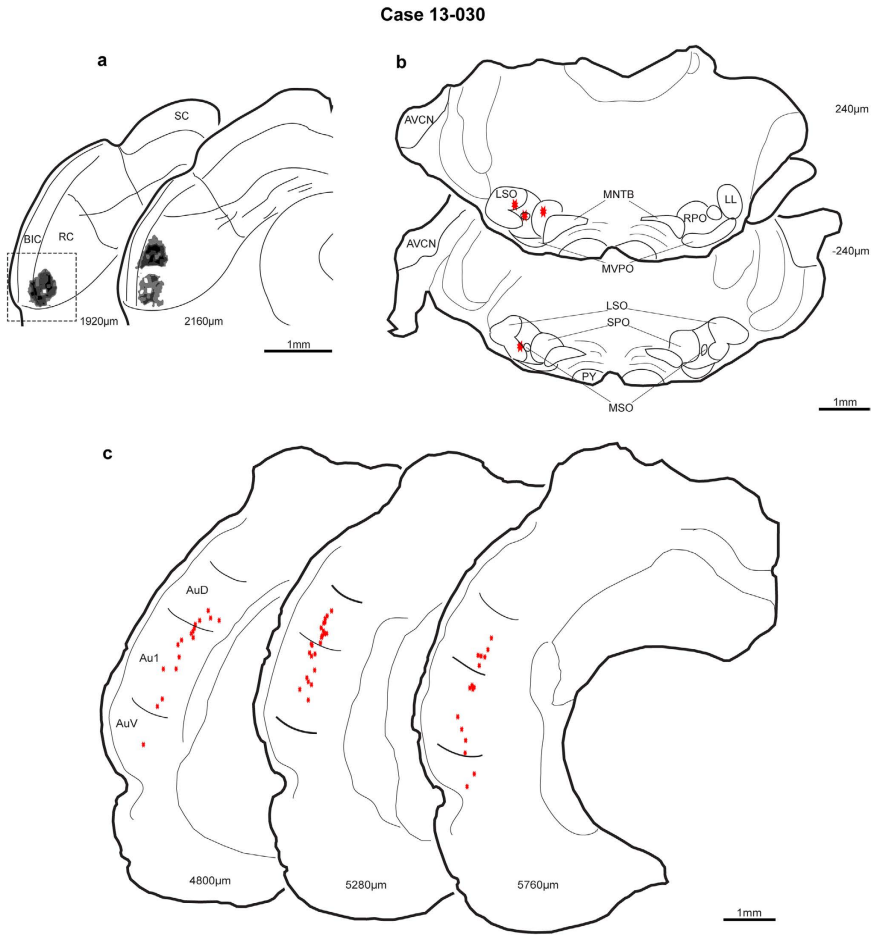

Figure 6. Injection site and retrograde labelling for case 13-030. (**a**) The injection site in the ventral lateral and rostral cortex of IC. Rostrally, two tracer deposits appeared. (**b**) Sparse brainstem labelling (◆). (**c**) Numerous labeled neurons throughout the auditory cortex. SC, superior colliculus; BIC, brachium inferior colliculus; RC, rostral cortex of the IC; AVCN, anteroventral cochlear nucleus; LSO, lateral superior olive; MNTB, medial nucleus of the trapezoid body; LL, lateral lemniscus; MVPO, medioventral periolivary nucleus; SPO, superior periolivary nucleus; MSO, medial superior olive; RPO, rostral periolivary region; PY, pyramidal tract. Other abbreviations as in Fig. 3.

and timing of the response to the deviant and standard stimulus was still very similar as observed in the rasters (Fig. 9c,e) and PSTHs (Fig. 9d,f) obtained from two pair of tested frequencies. The CSIs ranged from 0.03 for 0.144 octave separation to 0.13 for $\Delta f = 0.29$ octave.

Similar to the first non-SSA case, most inputs to the region of the neuron were in the brainstem. As predicted from the high BF, the recording site was located in the ventral central nucleus and reached a maximum diameter of 350 µm (Fig. 10a; the box on section 2320 µm indicates the photomicrograph illustrated in Fig. 4c). The most prominent labelling was throughout the ventral nucleus of the LL and SPO (Fig. 10b). As expected from the high BF in the recording site, the medial, high frequency lateral superior olive was retrogradely labeled bilaterally and labeled neurons were found in the middle and dorsal anteroventral CN. A tonotopic organization for the modest labeling in the periolivary nuclei of superior olivary complex was less obvious. At the level of the midbrain, the three ipsilateral nuclei of the LL (dorsal, intermediate, and ventral) contained labeled neurons as did the contralateral dorsal and intermediate LL (not shown). Scattered labelling was also found in the central nucleus and lateral cortex at the level of the injection site. As in the previous non-SSA case, the cortical labelling was very modest with only one labeled neuron located in Au1 (Fig. 10c).

Characteristics of All Sampled Neurons. A clear difference between neurons that exhibit SSA and those neurons without SSA was the bandwidth of their response areas. SSA neurons were characterized by their broadband tuning, whilst most non-SSA neurons had V-shaped FRAs ($n = 5$) according to the receptive field classification previously suggested[20,21]. The remaining non-SSA neurons had V-shaped FRAs but non-monotonic at CF ($n = 1$) and narrow response areas ($n = 2$). The differential spectral sensitivity between both groups was reflected in the population BW and Q-values (Fig. 11a, b). At 10 dB

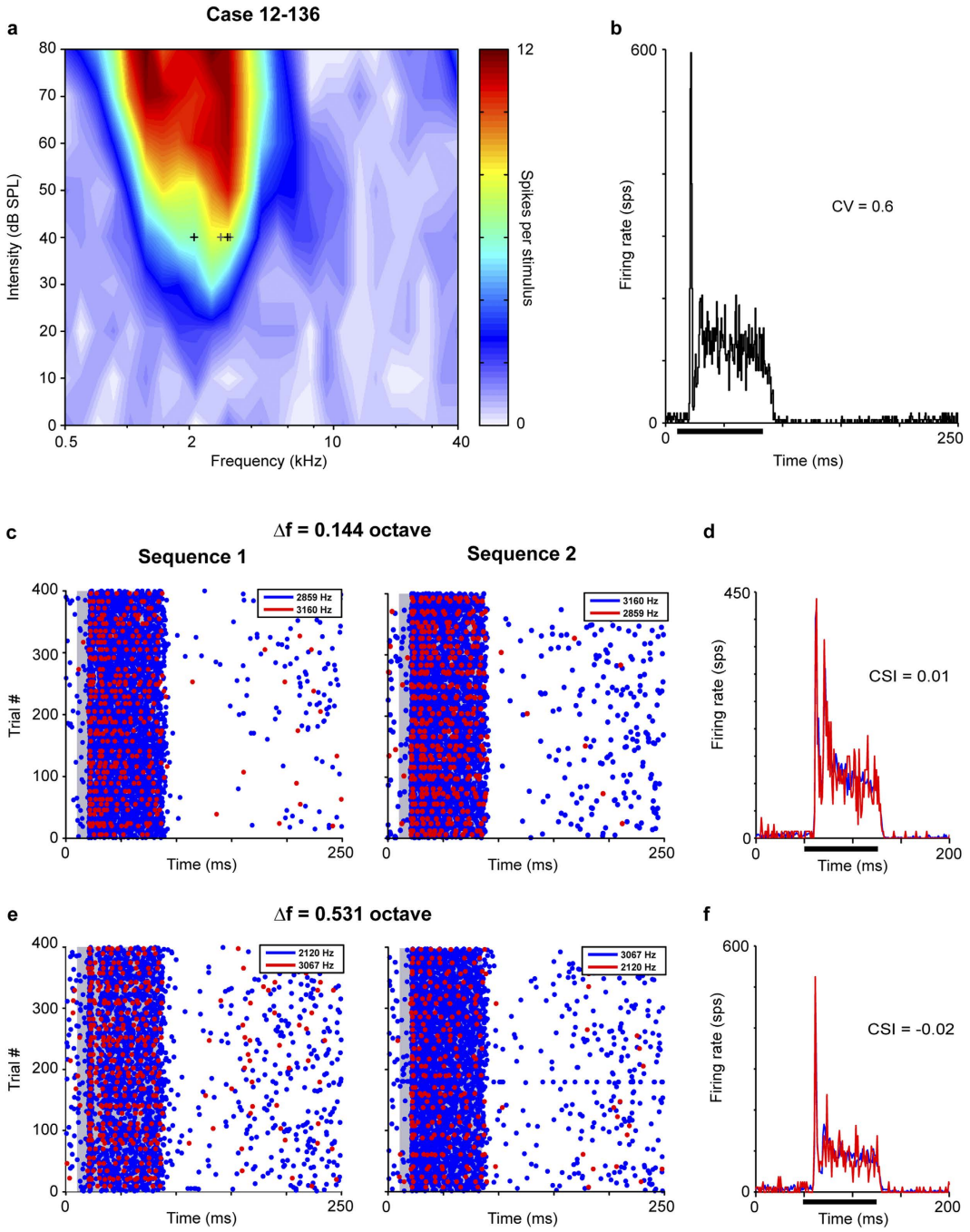

Figure 7. Low-frequency neuron without SSA. Typical V-shaped frequency response area and lack of SSA in a low-frequency neuron. (**a**) This neuron is tuned to low frequencies (best frequency and characteristic frequency = 2.61 kHz). (**b**) On-sustained response to the best frequency. Lack of SSA in sequence 1 and 2 with 0.114 octave separation shown in raster (**c**; standard, blue; deviant, red) and normalized PSTH (**d**). Similar lack of SSA with 0.531 octave separation (**e**,**f**). Case 12-136. Abbreviations as in Fig. 2.

SPL above threshold, the SSA neurons already had a bandwidth of 30.889 ± 14.929 kHz that remained similar at higher intensities (29.952 ± 14.017 kHz) (Paired t-test, $t = -1.546$, $p = 0.183$).

SSA and non-SSA groups did not differ in their monotonicity (MI = 1 ± 0.136, 1 ± 0.18 for non-SSA and SSA group, respectively), firing regularity (CV = 0.75 ± 0.295, 1.271 ± 0.652), frequency tuning (CF = 20.67 ± 13.87, 17.993 ± 12.104 kHz) or thresholds (20 ± 15.119, 35 ± 16.733 dB SPL) (For all parameters, Mann-Whitney Rank Sum Test, $p > 0.05$). Sample of SSA and non-SSA neurons included both the low and high extremes of the rat audiogram. Moreover, the neuronal thresholds (Fig. 11c) were within, or very close to, the average limens of the audiogram[22]. There was no correlation between the CF

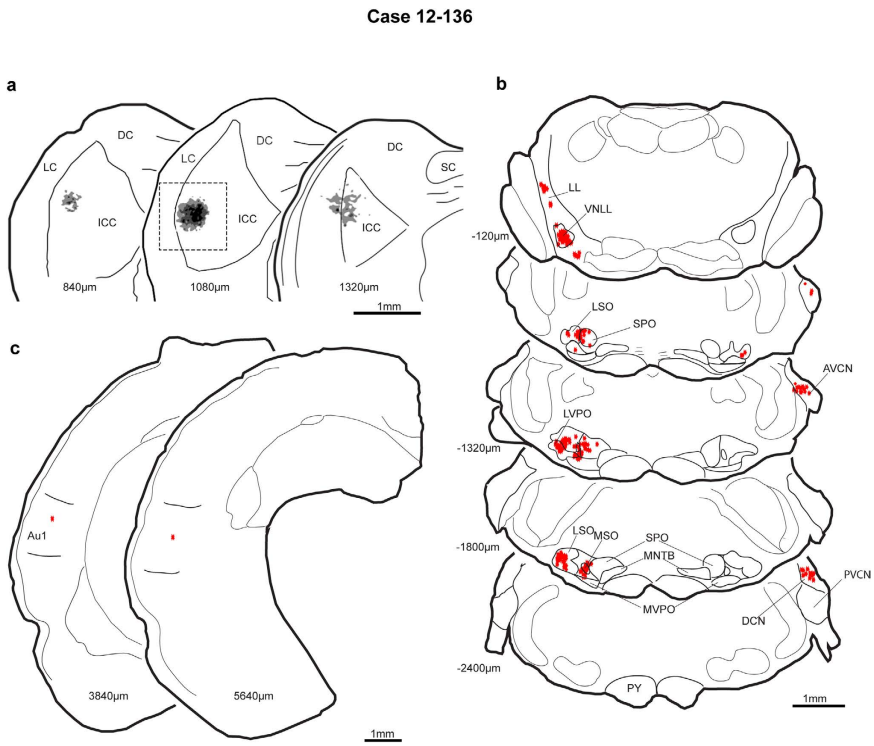

Figure 8. Central nucleus injection site and retrograde labelling of the brainstem and auditory cortices of the non-SSA case 12-136 (**a**) Injection site in IC in rostral central nucleus and adjacent lateral cortex. (**b**) Numerous labeled neurons (◆) in brainstem but sparse label in the auditory cortices (**c**). Case 12-136. DCN, dorsal cochlear nucleus; LVPO, lateroventral periolivary nucleus; PVCN, posterioventral cochlear nucleus; VNLL, ventral nucleus of lateral lemniscus. Other abbreviations as in Figs. 3 and 6.

and the CSI for either SSA (Spearman Rank Order Correlation Coefficient = 0.242, $p > 0.05$) or non-SSA neurons (Coefficient = 0.182, $p > 0.05$) (Fig. 11d).

Obviously, there was a significant difference in the amount of SSA between SSA (CSI = 0.546 ± 0.172) and non-SSA groups (CSI = 0.0195 ± 0.102) (t-test, $t = -7.744$, $P < 0.001$). Since the majority of the recorded neurons exhibited spontaneous discharge (7.7656 ± 5.3142 spikes per second, n = 13 neurons) and this affects the CSI measurement[23], we recalculated the CSI by subtracting the mean spontaneous discharge from the responses to the deviant and standard tones. After subtraction, the median population CSI values changed slightly (SSA, CSI = 0.576 ± 0.205; non-SSA, CSI = −0.00491 ± 0.141). Consistent with the population CSI, the median spike count was higher in response to the deviant tone (1.625 ± 1.5963) than to the standard tone (0.3222 ± 0.5141) for the SSA group (Wilcoxon Signed Rank Test, $Z = -4.107$, $p < 0.001$) (Fig. 11e); while the response to both tones was similar in the non-SSA group (4.15 ± 2.987 and 4.5972 ± 3.0487 for deviant and standard stimulus, respectively) (Wilcoxon Signed Rank Test, Z = −0,464, p = 0.646). The temporal dynamics of the response of the SSA neurons to the standard tone (Fig. 11f, bottom plot) followed a double exponential function ($r^2 = 0.6754$, SSE: 5.048) indicating that the strength of the response rapidly decays during the first presentations of the standard tones as described previously[24]. On the contrary, the response of the non-SSA neurons to the standard tone (Fig. 11f, upper plot) did not suffered an strong decay reflected by a poor fit to the same function ($r^2 = 0.2613$, SSE: 6.54).

In all cases, there was a good correlation between the neuronal response properties and the morphology. The SSA neurons were localized in the lateral (n = 3) and rostral cortex of IC (n = 3). On the other hand, the sites of the non-SSA neurons were confined to the dorsolateral (n = 2), ventrolateral (n = 3), middle (n = 2) and very rostral (n = 1) regions of the central nucleus.

Discussion

We show a segregation of cortical and brainstem inputs to the sites where SSA and non-SSA neurons are located in the IC. Consistent with previous studies, SSA neurons were located in the cortex of the IC, whilst the IC neurons that do not exhibit SSA were confined to the central nucleus of the IC[9,16,17]. The injection sites in the SSA cases received heavy inputs from Au1 as well as from areas dorsal and ventral to Au1, while the non-SSA cases were strongly innervated by brainstem inputs. Since these results show that regions in IC containing neurons with SSA have a pattern of inputs that differs from regions without SSA, it suggests a unique network organization to generate SSA in the IC.

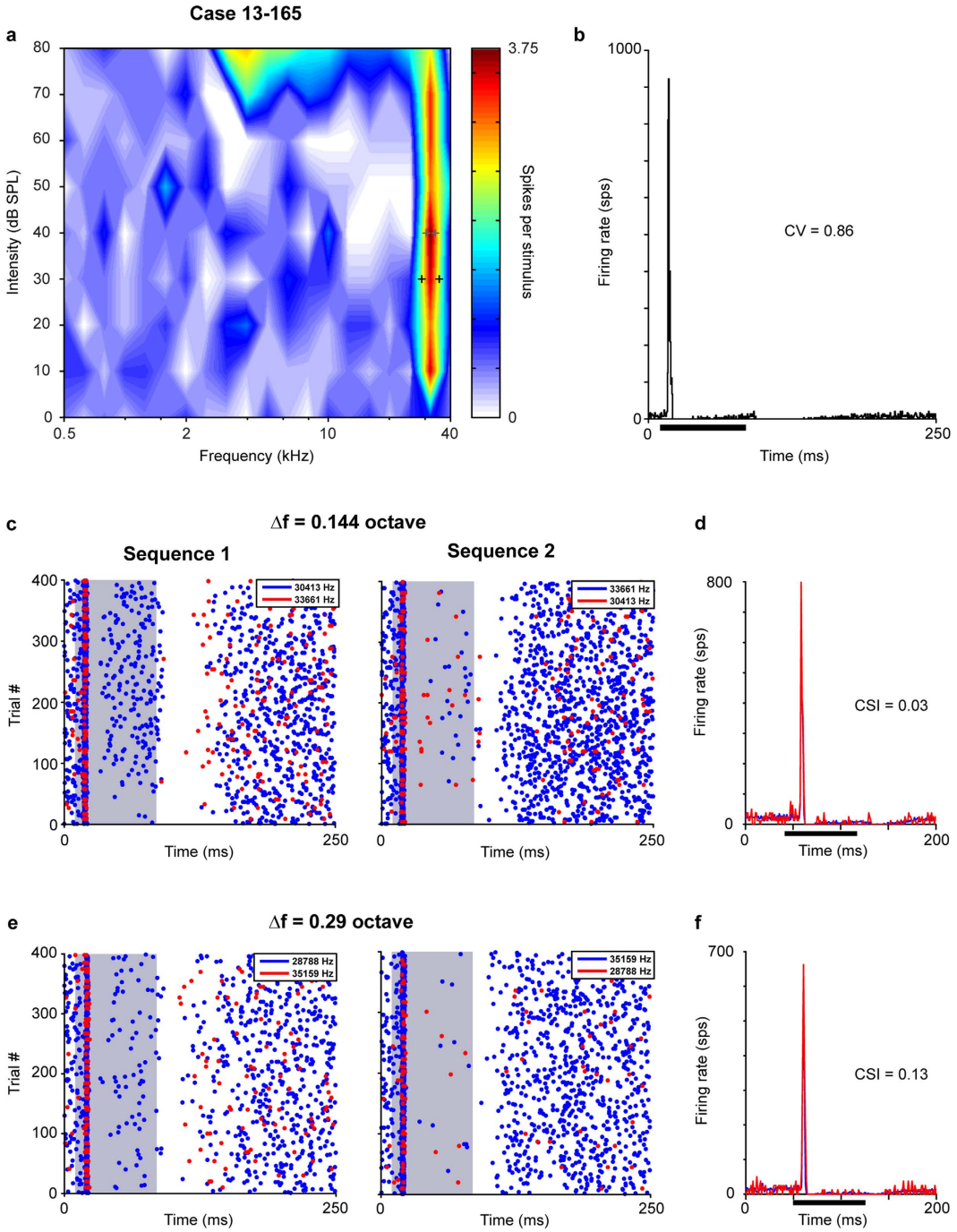

Figure 9. High-frequency neuron without SSA. This neuron had a very narrow frequency response area (**a**) and an onset response pattern to its characteristic frequency (**b**). The neuron did not show SSA in its response to the oddball paradigm for two pairs of frequencies (standard, blue; deviant, red) with different separation; 0.144 octave (**c**,**d**) and 0.29 octave (**e**,**f**). Case 13-165. Abbreviations as in Fig. 2.

Sources of inputs to regions with and without SSA. All SSA cases showed a consistent pattern of afferent projections, *i.e.*, strong inputs from the auditory cortex and very poor or even absent projections from the brainstem nuclei. Thus, one of the main sources of input to neurons exhibiting SSA in the IC is the auditory cortex. The distribution of the retrogradely labeled neurons in the cortex covered not only the Au1 area, but it also included other high-order auditory cortical areas that may be involved in deviance detection as suggested by recent studies[25]. In addition to the cortical input, the injection sites in the lateral cortex of IC invariably labeled neurons in ICC with retrograde transport. This may provide important auditory inputs to SSA neurons. However, with the methods used here it is difficult to separate ICC neurons labeled due to fibers of passage from those with direct inputs to SSA neurons. The projections

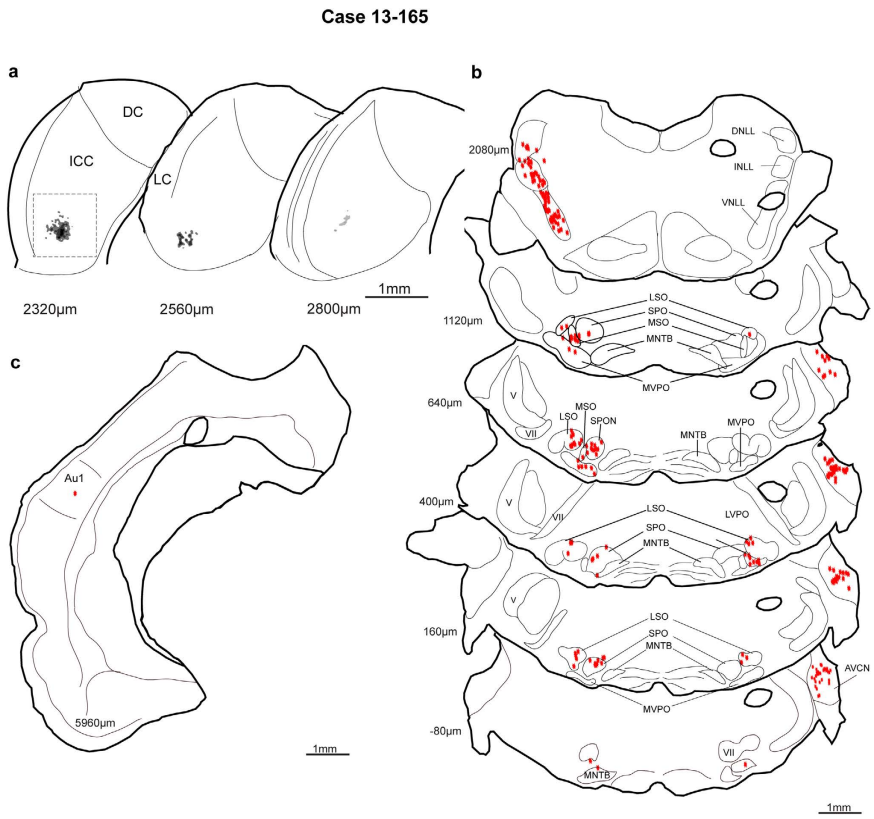

Figure 10. IC injection site and retrograde labelling for case 13-165. (**a**) Injection site in the ventromedial central nucleus. (**b**) Strong labelling in the brainstem sections corresponding to the high frequencies areas of the superior olivary complex and nucleus of the trapezoid body. (**c**) Weak auditory cortex labelling. DNLL, dorsal nucleus of lateral lemniscus; INLL, intermediate nucleus of lateral lemniscus. V, trigeminal tract; VII, facial nerve. Other abbreviations as in Figs. 3, 6, 8.

from ICC to the LC were documented earlier with autoradiographic anterograde transport methods that are not subject to the fiber of passage artifact[26]. So, it is certain that collateral axons from ICC neurons may terminate in the LC in route to the brachium of the IC and the medial geniculate body[27–29].

Neurons that lacked SSA differed markedly from SSA neurons in their source of inputs. The major sources of input to the non-SSA cases were from brainstem nuclei, *i.e.*, CN, nuclei of the superior olivary complex and LL, consistent the notion that ICC neurons mainly integrate ascending excitatory and inhibitory information. The distribution of the labeled neurons followed the general tonotopic arrangement described for the ascending projections to the recordings sites within the central nucleus[30,31]. The weak cortical projections seen after non-SSA injections were distinct from those in the SSA cases. Furthermore, the few retrograde labeled neurons found in the auditory cortex were restricted to Au1. This is consistent with previous reports of weaker projections from auditory cortex to ICC than to LC or DC[14,15].

The injections in this study were intentionally designed to produce local minute deposits of tracer and used micropipettes with tips that allowed good isolation of single units. Because of the small size of the injections, relatively small numbers of neurons were labeled in each case, and some could be missed. Not all of the neurons known to project to the ICC or LC were found in every case, e.g., neurons from the CN[32,33], the medial superior olive[34,35], the SPO[32,36], the LL[37], and the contralateral IC[28,38].

The retrogradely labeled neurons identify the sources of projections to a small region in the vicinity of the recorded neuron consistent with a small functional zone. Despite the small size of the injection, the diffusion of the FG from the tip of the electrode undoubtedly extends beyond the dendritic field of the single neuron under study. Presumably, all the neurons in the small region around the neuron in the injection site share the same input sources. While this does not rule out exclusive projections to SSA or non-SSA neurons that are side by side, it is consistent with the notion that neurons with SSA are organized into functional zones at least as small as the injection sites. Synaptic domains, *i.e.*, small groups of neurons that share the same subset of synaptic inputs[39–41] have been identified in ICC. In the present context, the consistent pattern of cortical labelling may reflect common projections to synaptic domains

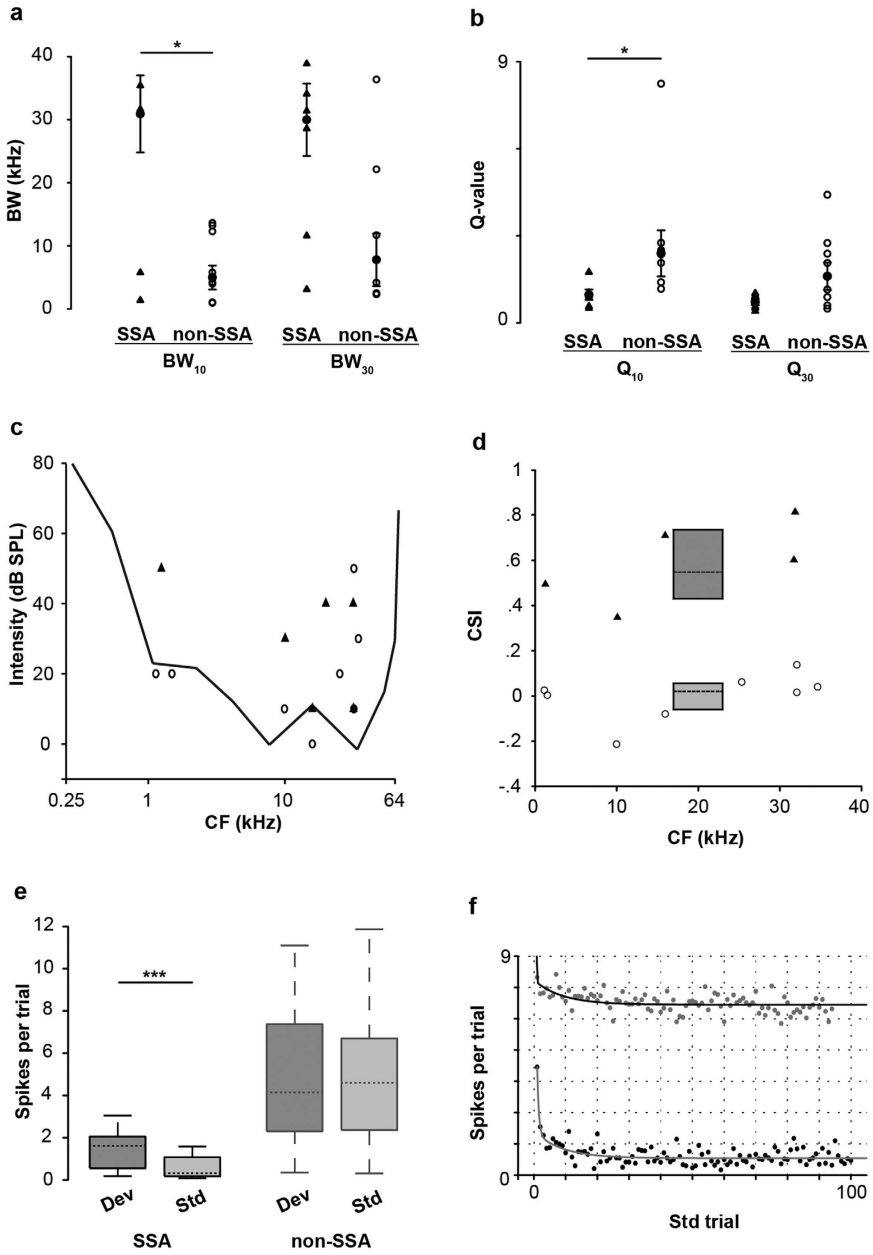

Figure 11. SSA and non-SSA neurons differed in frequency response areas, deviant sensitivity and response strength, but not in threshold. (**a**) Distribution and median ± s.e.m. of bandwidth (BW) of SSA and non-SSA neurons at 10 and 30 dB SPL above threshold. (**b**) Distribution and median ± s.e.m. of Q values at 10 dB and 30 dB SPL above threshold. SSA neurons had broader frequency tuning at 10 dB SPL above threshold (Wilcoxon Signed Rank Test, * $p < 0.05$). (**c**) Distribution of the characteristic frequencies (CF) for SSA (▲) and non-SSA (○) neurons relative to rat audiogram. (**d**) Box plot of the SSA indices (CSI) of the SSA (▲) and non-SSA (○) groups (median value, dashed lines). (**e**) Box plots of the population spike rates for SSA and non-SSA neurons to deviant (Dev) and standard (Std) stimuli. The dashed lines within each box represent the median values, the edges of the box delimit the 25th and 75th percentiles and the whiskers bars indicate the 10th and 90th percentiles. The firing response to the deviant and standard tone only differs in the SSA group (Wilcoxon Signed Rank Test, *** $p < 0.001$). (**f**) Fit of the population response to the standard tone for SSA (•) and non-SSA (∗) neurons to a double exponential function. There is a rapid and pronounce decay from the first standard trial in the response of SSA neurons but not in non-SSA neurons.

for SSA neurons in the cortex of IC. Those synaptic domains may account for other physiological properties exhibited by SSA neurons.

Relationship of inputs to neuronal function. The injection sites confirmed that SSA neurons are confined to the non-lemniscal subdivisions of the IC, *i.e.,* lateral and rostral cortices[13]. A broad spectral sensitivity and a lower driven rate characterize the response properties of auditory neurons of the non-lemniscal pathway[13,42]. In contrast, the response features of non-SSA neurons match those described for the lemniscal auditory pathway[13,42,43]. The location and frequency tuning of the recorded neurons in ICC was well-matched to the tonotopic organization of the central nucleus[44]. The non-SSA neurons were very sharply tuned (Fig. 11a,b) and responded to the occurrence of the deviant and standard tones with a similar and constant response strength along all the stimulus presentations (Fig. 11e,f).

The pattern of connections described above is also consistent with the function of the corticocollicular projections on SSA responses in IC as demonstrated by the inactivation of the auditory cortex[45]. The corticofugal projection exert mainly gain control over the SSA response and affected both the response to the deviant and to the standard tone without abolishing the difference between them. The cortical inactivation elicited changes in the SSA index in either direction; increasing or decreasing the CSI. However, very few SSA responses were generated *de novo* or abolished completely by the inactivation of the cortical inputs. The diverse effects of cortical manipulation on SSA responses might be explained by cortical inputs to synaptic domains in IC that contain neurons with different SSA sensitivities. More likely, SSA domains might receive inputs from different areas of auditory cortex. Diverse cortical effects might be indirect since cholinergic neurons of the tegmental nucleus that project directly to IC also receive inputs from auditory cortex[46].

Functional significance. The theory of predictive coding relies in the comparison between the incoming bottom-up sensory input and the memory trace formation in top-down fashion[47]. Then, a higher order center of processing sends predictions to the level below, which reciprocate bottom-up signals. These signals are prediction errors that report discrepancies between top-down predictions and representations at each level[48] without requiring attentional processing of the stimulus or cognitive control of the predictions[49,50]. While current studies of predictive coding consider mostly cortical processing[51], here we proposed that SSA neurons in the IC participate in this processing through corticofugal projections[52–54].

Our results support the notion that SSA neurons generate an error signal by comparing ascending and descending inputs. The present data show that SSA neurons are in a position in the auditory pathway (*i.e.*, non-lemniscal subdivisions) to compare higher-level signals with incoming sensory information. We postulate that when the same stimulus evokes converging simultaneous excitatory inputs to the SSA neuron from the auditory cortex and the central nucleus of the IC, the SSA neuron adapts (as occurs in response to the common sound). However, when those inputs differ (as when a rare sound occurs), the SSA neuron fires generating an error signal. SSA neurons in the IC are in a suitable circuit to send the error signal to the neocortex by connections in the non-lemniscal pathways[55] driving neuronal activity in the belt auditory cortex to adjust and update the sensory representation[56]. The present data suggests a fast, top-down adjustment of IC activity is made possible by the feedback loop from the cortex. This is consistent with the corticofugal modulation of IC neurons that effects a short-term plastic reorganization in the frequency domain[52] and on SSA responses[45]. Thus, SSA neurons in the IC may be useful in the context of the continuous interaction between a top-down flow of sensory predictions and a bottom-up flow of the incoming sensory representation.

Methods

Subjects and surgical procedures. Experiments were performed on 14 female rats (*Rattus norvegicus*, Rj: Long-Evans) with body weights ranging 136–222 g. All surgery and recording procedures, tracer injections as well as perfusions were conducted at the University of Salamanca. The experimental protocols were approved by Animal Care Committees of the University of Salamanca and used methods conforming to the standards of the University of Salamanca Animal Care Committee and the European Union (Directive 2010/63/EU) for the use of animals in neuroscience research. Detailed procedures are given elsewhere[9,21,57]. Anesthesia was induced using a mixture of ketamine chlorohydrate (30 mg/kg, I.M., Imalgene 1000, Rhone Méreuse, Lyon, France) and xylazine chlorohydrate (5 mg/ Kg, Rompun, Bayer, Leverkusen, Germany). The animal was placed inside a sound-attenuated room in a stereotaxic frame in which the ear bars were replaced by a hollow speculum that accommodated a sound delivery system. Atropine sulphate (0.05 mg/kg, s.c., Braun, Barcelona, Spain) was administered to reduce bronchial secretions. During surgery and recording, the body temperature was monitored with a rectal probe and maintained at 38 °C with a thermostatically controlled electric blanket. A craniotomy was made in the caudal part of the left parietal bone to expose the cerebral cortex in order to gain access to the left IC.

Electrophysiological recordings and acoustical stimuli. Extracellular responses of a well-isolated neuron were recorded in the left IC of each animal with a glass micropipette (tip OD=4 μm, 3.5–5.5 MΩ) that was used for both recording and iontophoretic injections. Pipettes were filled with the 2% Fluorogold (FG, Fluorochrome, Denver, CO, USA) in a sterile saline solution (0.9% NaCl). The IC was approached from 20° relative to the frontal plane so that the electrode moved caudal and ventral during the penetration. The electrode was lowered into the brain with a piezoelectric microdrive (Burleigh 6000 ULN)

mounted on a stereotaxic manipulator to a depth between 3.5–5 mm where acoustically driven responses were found.

Search stimuli were pure tones or noise bursts delivered through a sealed acoustic system[43] using two electrostatic loudspeakers (TDT-EC1) driven by a TDT System 2 (TDT, Tucker-Davis Technologies, Florida, USA) that was controlled by custom software for stimulus generation and on-line data visualization. Action potentials were recorded with a TDT BIOAMP amplifier, the ×10 output of which was further amplified and bandpass-filtered (TDT PC1; fc: 0.5–3 kHz) before passing through a spike discriminator (TDT SD1). Spike times were logged at one microsecond resolution on a computer by feeding the output of the spike discriminator into an event timer (TDT ET1) synchronized to a timing generator (TDT TG6). Spike times were displayed as dot rasters sorted by the acoustic parameter varied during testing.

After a neuron was isolated, pure tone stimuli (75 ms with a 5 ms rise/fall time) were delivered to the ear contralateral to the recording site and the monaural frequency response area (FRA) was obtained. Specifically, the combination of frequencies and intensities capable of evoking a response, was obtained with an automated procedure consisting of 5 stimulus repetitions at each frequency (from 0.5 to 40 kHz, in 20–25 logarithmic steps) and intensity step (steps of 10 dB, from 0 to 80 dB SPL) presented randomly at a repetition rate of 4 Hz.

Stimulus presentation paradigm. Monaural stimuli to the contralateral ear were presented in an oddball paradigm similar to that used to record mismatch negativity responses in human studies[58] and more recently in animal studies of SSA in the auditory cortex[1] and auditory midbrain[6,7,9]. Briefly, this paradigm consists in a flip-flop design of two pure tones at two different frequencies (f1 and f2) that elicited a similar firing rate and response pattern at the same level of 10–40 dB SPL above threshold. Both frequencies were within the excitatory response area of the neuron. A train of 400 stimulus presentations containing both frequencies was delivered in two different sequences (sequence 1 and 2). The repetition rate of the train of stimuli was 4 Hz, as it has been previously demonstrated to be suitable to elicit SSA in IC neurons of the rat[9,10]. In sequence 1, the f1 frequency was presented as the standard (*i.e.*, high probability within the sequence: 90%); interspersed randomly among the standards were the f2 frequency deviant stimulus (*i.e.*, low probability: 10%, respectively). After obtaining one data set, the relative probabilities of the two stimuli were reversed, with f2 as the standard and f1 as the deviant in the sequence 2. These two sequences are a flip-flop design since the identity of the standard and deviant are reversed. The responses to the standard and deviant stimuli were normalized to spikes per stimulus, to account for the different number of presentations in each condition, because of the different probabilities. The frequency separations (Δf) between f1 and f2 varied between 0.14 octaves to 0.53 octaves since the frequency pairs were chosen to evoke similar firing rates in responses to both tones.

Once the electrophysiological recording was completed, FG was iontophoretically ejected from the recording pipette into the recording site with 0.5 μA current applied for 1 s to produce a small tracer deposit. Seven days after the surgery, the animals were deeply anesthetized with sodium pentobarbital (60 mg/kg, Dolethal, Vétoquinol, Madrid, Spain) and perfused transcardially with Ringer´s solution and 4% paraformaldehyde in 0.1 M phosphate buffer (PB, pH 7.4).

Analysis of neuronal responses. For each neuron, the amount of SSA was quantified by the Common-SSA Index (CSI) and the Frequency-Specific SSA Index (SI) used previously[1,7,9,24]. The CSI and SI reflect the normalized difference between the neuronal response to the deviant stimulus and the response to the standard one. The CSI is defined as

$$\mathrm{CSI} = [d(\mathrm{f1}) + d(\mathrm{f2}) - s(\mathrm{f1}) - s(\mathrm{f2})]/[d(\mathrm{f1}) + d(\mathrm{f2}) + s(\mathrm{f1}) + s(\mathrm{f2})]$$

where d(f) and s(f) are responses to each frequency f1 or f2 when they were the deviant (d) or standard (s) stimulus, respectively. The SI was separately calculated for each frequency and it is defined as

$$\mathrm{SI}(\mathrm{fi}) = [d(\mathrm{fi}) - s(\mathrm{fi})]/[d(\mathrm{fi}) + s(\mathrm{fi})]$$

where i = 1 or 2. The positive CSI and SI values indicate neurons respond more strongly to the frequencies when they were deviant compared to when they were standard. To study the contribution of the spontaneous activity on the estimation of the CSI, we calculated again the SSA indices from the evoked activity but with subtracted spontaneous activity bin by bin (evoked activity minus spontaneous activity in spikes/s). The spontaneous activity was estimated within a 50 ms window before each tone presentation in the oddball paradigm (50 ms x 400 trials = 20 s sample window) as previously used[23].

The best frequency (BF, frequency evoking the most spikes at high intensity levels), characteristic frequency (CF, frequency producing a response at the lowest intensity level) and the threshold were identified. To estimate the temporal response, the BF (100 ms with a 5 ms rise/fall time) was played 500 times at 4 Hz and the regularity of firing was measured by calculating the coefficient of variation (CV, *i.e.*, the ratio of the standard deviation to the mean of the interspike intervals) as a function of time over the neuronal response (binwidth=500 μs). A regular response was defined as CV < 0.5 as used by Rees *et al.*, 1997. Also, the monotonicity index (MI, *i.e.*, the ratio of the spike count at 80 dB SPL to the maximum

spike count) that refers to the degree of reduced spiking at higher intensities was calculated from the FRA measure[59]. Monotonic responses were those with a MI >0.75. Finally, we measured the sharpness of the frequency response area by calculating the bandwidth and Q-values at 10 and 30 dB SPL above the threshold as in our previous work[9,21]. The bandwidth at n dB expresses the difference in kHz between the lower and upper frequencies of the FRA (BWn = FU − FL). The Q-value was calculated as the characteristic frequency divided by the bandwidth at n dB above threshold (Qn = CF/BW). Results are reported as median ± standard deviation (s.d.) and represented in plots as median ± standard error (s.e.m.).

Histology and analysis of retrograde labeling. All histological procedures on the fixed brains from the experimental animals were carried out at the University of Connecticut Health Center. Brains were embedded in a gelatin/albumin matrix and transverse, frozen sections were cut at 40 μm thickness through the brainstem. Two series of sections at 240 μm intervals were stained for Nissl substance with cresyl violet and thionin (1:1). Another set of sections at 120 μm intervals was used for FG immunohistochemistry.

Immunohistochemical methods were used to reveal the neurons retrogradely labeled by FG. After 20 min in 0.5% H_2O_2 to remove endogenous peroxidase, sections were rinsed in 0.05 M phosphate buffered saline (PBS) and exposed to 10% goat serum with 0.5% Triton X-100 in PBS for 2 hr. Sections were then incubated in anti-FG antibody made in rabbit (Fluorochrome LLC, 1:50000) in the blocker at 4 °C overnight. Following PBS rinses, tissue was exposed to a biotinylated anti-rabbit secondary antibody made in goat (Vector Laboratories; 1:800) in 10% goat serum blocker for 2 hours at 4 °C. The biotinylated secondary antibody was visualized with the ABC-peroxidase method (ABC Elite, Vector Laboratories) performed 2 hr to overnight; and this was followed by preincubation in 0.05% diaminobenzidine with 0.02% cobalt chloride and 0.02% nickel ammonium sulfate (15 min) and the same solution with 0.005% H_2O_2 (15 min or less). Sections were dried onto subbed slides and coverslipped with Permount (Fisher Scientific, Pittsburgh, PA).

The injection site (Fig. 4) and retrograde labeling were localized relative to the cytoarchitecture of defined regions in the brainstem, midbrain, and cortex. A mosaic brightfield image was obtained for the complete IC section at the center of the FG injection on a Zeiss Axiovert 200M microscope using AxioVision Rel. 4.8 (Carl Zeiss Imaging Solutions) with a ×10/0.45 NA Planapo lens. An image processing routine was used to visualize the area of the injection site. The image was blurred over a 20 pixel radius, and the background and areas without labeling were removed. The remaining signal representing the FG labeling at the injection site was subdivided into thirds to produce three zones representing heavy, intermediate, and light FG labeling in the injection site. Contours representing those zones were superimposed on the original image and on plots of the relevant sections.

After the examination of all processed sections, Neurolucida (MBF Bioscience Inc., Williston, VT) was used to draw the section outlines and location of the injection sites and the retrogradely labeled neurons. Nissl-stained sections adjacent to the plotted sections were used to draw the cytoarchitectonic boundaries of IC subdivisions, the left auditory cortex, and the nuclei of the lower auditory brainstem. Nissl cytoarchitecture and plots were combined to illustrate the highest density labeling of each structure containing labeled neurons.

References

1. Ulanovsky, N., Las, L. & Nelken, I. Processing of low-probability sounds by cortical neurons. *Nat Neurosci.* **6,** 391–398 (2003).
2. Gutfreund, Y. Stimulus-specific adaptation, habituation and change detection in the gaze control system. *Biol. Cybern.* **106,** 657–668 (2012).
3. Nelken, I. & Ulanovsky, N. Mismatch negativity and simulus-specific adaptation in animal models. *J. Psychophysiol.* **21,** 214 –223 (2007).
4. Escera, C. & Malmierca, M. S. The auditory novelty system: an attempt to integrate human and animal research. *Psychophysiology* **51,** 111–123 (2014).
5. Malmierca, M. S., Sanchez-Vives, M. V., Escera, C. & Bendixen, A. Neuronal adaptation, novelty detection and regularity encoding in audition. *Front Syst. Neurosci.* **8,** 111 (2014).
6. Anderson, L. A., Christianson, G. B. & Linden, J. F. Stimulus-specific adaptation occurs in the auditory thalamus. *J Neurosci* **29,** 7359–7363 (2009).
7. Antunes, F. M., Nelken, I., Covey, E. & Malmierca, M. S. Stimulus-specific adaptation in the auditory thalamus of the anesthetized rat. *PLoS One* **5,** e14071 (2010).
8. Pérez-González, D., Malmierca, M. S. & Covey, E. Novelty detector neurons in the mammalian auditory midbrain. *Eur. J. Neurosci.* **22,** 2879–2885 (2005).
9. Malmierca, M. S., Cristaudo, S., Perez-Gonzalez, D. & Covey, E. Stimulus-specific adaptation in the inferior colliculus of the anesthetized rat. *J. Neurosci.* **29,** 5483–5493 (2009).
10. Ayala, Y. A. & Malmierca, M. S. Stimulus-specific adaptation and deviance detection in the inferior colliculus. *Front Neural Circuits* **6,** 89 (2013).
11. Malmierca, M. S. Auditory system. in *The rat nervous system* (ed. G. Paxinos) (Academic Press, Amsterdam, 2015).
12. Morest, D. K. The lateral tegmental system of the midbrain and the medial geniculate body: Study with Golgi and Nauta methods in cat. *J. Anat.* **99,** 611–634 (1965).
13. Lee, C. C. & Sherman, S. M. On the classification of pathways in the auditory midbrain, thalamus, and cortex. *Hear Res.* **276,** 79–87 (2011).
14. Winer, J. A. Three systems of descending projections to the inferior colliculus. in *The Inferior Colliculus* (ed. J. A. Winer & C. E. Schreiner) 231–247 (Springer, New York, 2005).

15. Malmierca, M. S. & Ryugo, D. K. Descending connections of auditory cortex to the midbrain and brainstem. in *The Auditory Cortex*. (ed. J. A. Winer & C. E. Schreiner) 189–208 (Springer, New York, 2011).
16. Duque, D., Perez-Gonzalez, D., Ayala, Y. A., Palmer, A. R. & Malmierca, M. S. Topographic distribution, frequency, and intensity dependence of stimulus-specific adaptation in the inferior colliculus of the rat. *J. Neurosci.* **32,** 17762–17774 (2012).
17. Ayala, Y. A., Perez-Gonzalez, D., Duque, D., Nelken, I. & Malmierca, M. S. Frequency discrimination and stimulus deviance in the inferior colliculus and cochlear nucleus. *Front Neural Circuits* **6,** 119 (2013).
18. Lumani, A. & Zhang, H. Responses of neurons in the rat's dorsal cortex of the inferior colliculus to monaural tone bursts. *Brain Res.* **1351,** 115–129 (2010).
19. Loftus, W. C., Malmierca, M. S., Bishop, D. C. & Oliver, D. L. The cytoarchitecture of the inferior colliculus revisited: a common organization of the lateral cortex in rat and cat. *Neuroscience* **154,** 196–205 (2008).
20. Palmer, A. R., Shackleton, T. M., Sumner, C. J., Zobay, O. & Rees, A. Classification of frequency response areas in the inferior colliculus reveals continua not discrete classes. *J. Physiol.* **591,** 4003–4025 (2013).
21. Hernandez, O., Espinosa, N., Perez-Gonzalez, D. & Malmierca, M. S. The inferior colliculus of the rat: a quantitative analysis of monaural frequency response areas. *Neuroscience* **132,** 203–217 (2005).
22. Heffner, H. E., Heffner, R. S., Contos, C. & Ott, T. Audiogram of the hooded Norway rat. *Hear Res.* **73,** 244–247 (1994).
23. Duque, D. & Malmierca, M. S. Stimulus-specific adaptation in the inferior colliculus of the mouse: anesthesia and spontaneous activity effects. *Brain Struct. Funct.* (2014).
24. Perez-Gonzalez, D., Hernandez, O., Covey, E. & Malmierca, M. S. GABA(A)-Mediated Inhibition Modulates Stimulus-Specific Adaptation in the Inferior Colliculus. *PLoS One* **7,** e34297 (2012).
25. Harms, L., *et al.* Mismatch Negativity (MMN) in Freely-Moving Rats with Several Experimental Controls. *PLoS One* **9,** e110892 (2014).
26. Kudo, M. & Niimi, K. Ascending projections of the inferior colliculus in the cat: an autoradiographic study. *J. Comp. Neurol.* **191,** 545–556 (1980).
27. Oliver, D. L., Kuwada, S., Yin, T. C., Haberly, L. B. & Henkel, C. K. Dendritic and axonal morphology of HRP-injected neurons in the inferior colliculus of the cat. *J. Comp. Neurol.* **303,** 75–100 (1991).
28. Saldana, E. & Merchan, M. A. Intrinsic and commissural connections of the rat inferior colliculus. *J. Comp. Neurol.* **319,** 417–437 (1992).
29. Malmierca, M. S., Seip, K. L. & Osen, K. K. Morphological classification and identification of neurons in the inferior colliculus: a multivariate analysis. *Anat Embryol (Berl)* **191,** 343–350 (1995).
30. Oliver, D. L. Dorsal cochlear nucleus projections to the inferior colliculus in the cat: a light and electron microscopic study. *J. Comp. Neurol.* **224,** 155–172 (1984).
31. Malmierca, M. S., Saint Marie, R. L., Merchan, M. A. & Oliver, D. L. Laminar inputs from dorsal cochlear nucleus and ventral cochlear nucleus to the central nucleus of the inferior colliculus: two patterns of convergence. *Neuroscience* **136,** 883–894 (2005).
32. Coleman, J. R. & Clerici, W. J. Sources of projections to subdivisions of the inferior colliculus in the rat. *J. Comp. Neurol.* **262,** 215–226 (1987).
33. Oliver, D. L., Ostapoff, E. M. & Beckius, G. E. Direct innervation of identified tectothalamic neurons in the inferior colliculus by axons from the cochlear nucleus. *Neuroscience* **93,** 643–658 (1999).
34. Oliver, D. L., Beckius, G. E. & Shneiderman, A. Axonal projections from the lateral and medial superior olive to the inferior colliculus of the cat: a study using electron microscopic autoradiography. *J. Comp. Neurol.* **360,** 17–32 (1995).
35. Winer, J. A., Larue, D. T. & Pollak, G. D. GABA and glycine in the central auditory system of the mustache bat: structural substrates for inhibitory neuronal organization. *J. Comp. Neurol.* **355,** 317–353 (1995).
36. Gonzalez-Hernandez, T., Mantolan-Sarmiento, B., Gonzalez-Gonzalez, B. & Perez-Gonzalez, H. Sources of GABAergic input to the inferior colliculus of the rat. *J. Comp. Neurol.* **372,** 309–326 (1996).
37. Malmierca, M. S., Leergaard, T. B., Bajo, V. M., Bjaalie, J. G. & Merchan, M. A. Anatomic evidence of a three-dimensional mosaic pattern of tonotopic organization in the ventral complex of the lateral lemniscus in cat. *J. Neurosci.* **18,** 10603–10618 (1998).
38. Malmierca, M. S., Hernandez, O., Antunes, F. M. & Rees, A. Divergent and point-to-point connections in the commissural pathway between the inferior colliculi. *J. Comp. Neurol.* **514,** 226–239 (2009).
39. Oliver, D. L. Ascending efferent projections of the superior olivary complex. *Microsc. Res. Tech.* **51,** 355–363 (2000).
40. Ito, T. & Oliver, D. L. Origins of Glutamatergic Terminals in the Inferior Colliculus Identified by Retrograde Transport and Expression of VGLUT1 and VGLUT2 Genes. *Front Neuroanat.* **4,** 135 (2010).
41. Loftus, W. C., Bishop, D. C. & Oliver, D. L. Differential patterns of inputs create functional zones in central nucleus of inferior colliculus. *J. Neurosci.* **30,** 13396–13408 (2010).
42. Hu, B. Functional organization of lemniscal and nonlemniscal auditory thalamus. *Exp. Brain Res.* **153,** 543–549 (2003).
43. Rees, A., Sarbaz, A., Malmierca, M. S. & Le Beau, F. E. Regularity of firing of neurons in the inferior colliculus. *J. Neurophysiol.* **77,** 2945–2965 (1997).
44. Malmierca, M. S., *et al.* A discontinuous tonotopic organization in the inferior colliculus of the rat. *J. Neurosci.* **28,** 4767–4776 (2008).
45. Anderson, L. A. & Malmierca, M. S. The effect of auditory cortex deactivation on stimulus-specific adaptation in the inferior colliculus of the rat. *Eur. J. Neurosci.* **37,** 52–62 (2012).
46. Schofield, B. R. Projections from auditory cortex to midbrain cholinergic neurons that project to the inferior colliculus. *Neuroscience* **166,** 231–240 (2010).
47. Friston, K. A theory of cortical responses. *Philos. Trans. R Soc. Lond B Biol. Sci.* **360,** 815–836 (2005).
48. Kiebel, S. J., Daunizeau, J. & Friston, K. J. Perception and hierarchical dynamics. *Front Neuroinform* **3,** 20 (2009).
49. Bendixen, A., SanMiguel, I. & Schroger, E. Early electrophysiological indicators for predictive processing in audition: a review. *Int. J. Psychophysiol.* **83,** 120–131 (2012).
50. Bendixen, A. Predictability effects in auditory scene analysis: a review. *Front Neurosci.* **8,** 60 (2014).
51. Cauller, L. Layer I of primary sensory neocortex: where top-down converges upon bottom-up. *Behav. Brain Res.* **71,** 163–170 (1995).
52. Bajo, V. M. & King, A. J. Cortical modulation of auditory processing in the midbrain. *Front Neural Circuits* **6,** 114 (2013).
53. Slater, B. J., Willis, A. M. & Llano, D. A. Evidence for layer-specific differences in auditory corticocollicular neurons. *Neuroscience* **229,** 144–154 (2013).
54. Stebbings, K. A., Lesicko, A. M. & Llano, D. A. The auditory corticocollicular system: molecular and circuit-level considerations. *Hear Res.* **314,** 51–59 (2014).
55. Malmierca, M. S., Merchan, M. A., Henkel, C. K. & Oliver, D. L. Direct projections from cochlear nuclear complex to auditory thalamus in the rat. *J. Neurosci.* **22,** 10891–10897 (2002).
56. Näätänen, R. & Winkler, I. The concept of auditory stimulus representation in cognitive neuroscience. *Psychol. Bull* **125,** 826–859 (1999).
57. Malmierca, M. S., Hernandez, O. & Rees, A. Intercollicular commissural projections modulate neuronal responses in the inferior colliculus. *Eur. J. Neurosci.* **21,** 2701–2710 (2005).

58. Näätänen, R. *Attention and brain function*. Hillsdale, NJ: Lawrence Erlbaum. (1992).
59. Watkins, P. V. & Barbour, D. L. Level-tuned neurons in primary auditory cortex adapt differently to loud versus soft sounds. *Cereb Cortex* **21,** 178–190 (2011).

Acknowledgements
This work was funded by the NIDCD grant R01-DC000189 to D.L.O. and the MINECO grant BFU201343608-P, JCYL grant (SA343U14), and USAL grant (Programa 1, 2014: KAQJ) to M.S.M. Y.A.A. held CONACyT (216106) and SEP fellowships.

Author Contributions
M.S.M. and D.L.O. designed the experiments, Y.A.A. performed the electrophysiological experiments and data analysis, A.U., K.D., D.B. and D.L.O. performed the histological experiments and data plotting, Y.A.A., M.S.M. and D.L.O. wrote the manuscript.

Additional Information
Competing financial interests: The authors declare no competing financial interests.

How to cite this article: Ayala, Y. A. *et al.* Differences in the strength of cortical and brainstem inputs to SSA and non-SSA neurons in the inferior colliculus. *Sci. Rep.* **5**, 10383; doi: 10.1038/srep10383 (2015).

Title Page

Title: Cholinergic modulation of stimulus-specific adaptation in the inferior colliculus

Abbreviated title: Cholinergic modulation of auditory SSA

Authors: Yaneri A. Ayala[1], Manuel S. Malmierca[1,2]

Affiliations:

[1]Auditory Neuroscience Laboratory. Institute of Neuroscience of Castilla Y León, University of Salamanca, C/Pintor Fernando Gallego, 1, 37007 Salamanca, Spain.

[2] Department of Cell Biology and Pathology, Faculty of Medicine, University of Salamanca, Campus Miguel de Unamuno, 37007 Salamanca, Spain.

Keywords: acetylcholine, SSA, auditory, attention, neuromodulators, micrioiontophoresis

Author Contribution

M.S.M. and Y.A.A. designed the experiments, Y.A.A. performed the electrophysiological experiments and data analysis, Y.A.A. and M.S.M. wrote the manuscript.

Corresponding author:

Manuel S. Malmierca

Department of Cell Biology and Pathology, Faculty of Medicine, University of Salamanca, Campus Miguel de Unamuno, 37007 Salamanca, Spain. Tel: +34 923 294 500, ext. 5333. Fax: +34 923 294 750. e-mail: msm@usal.es

Number of pages: 47

Number of figures: 6

Number of words for Abstract: 206; **Introduction**: 453; **Discussion:** 1542.

Acknowledgements

We thank Drs. Nell Cant, Raju Metherate and Adrian Rees, for their comments on a previous version of the manuscript and for their constructive criticisms. This project was funded by the MINECO grant BFU201343608-P and the JCYL grant SA343U14 to M.S.M. Y.A.A. held a CONACyT (216106) and a SEP fellowship. The authors declare no competing financial interests.

Abstract

Neural encoding of an ever-changing acoustic environment is a complex and demanding task that may depend on modulation by the animal´s attention. Some neurons of the inferior colliculus (IC) exhibit 'stimulus-specific adaptation (SSA)', *i.e.*, a decrease in their response to a repetitive sound but not to a rare one. Previous studies have demonstrated that acetylcholine (ACh) alters the frequency response areas of auditory neurons and therefore is important in the encoding of spectral information. Here, we address how microiontophretic application of ACh modulates SSA in the IC. We found that ACh decreased SSA in IC neurons by increasing the response to the repetititve tone. This effect was mainly mediated by muscarinic receptors. The strength of the cholinergic modulation depended on the baseline SSA level, exerting its greatest effect on neurons with intermediate SSA responses across cortical IC subdivisions. Our data demonstrates that ACh alters the sensitivity of partially-adapting IC neurons by switching neural discriminability to a more linear transmission of sounds. This change serves to increase ascending sensory-evoked afferent activity propagated through the thalamus *en route* to the cortex. Our results provide empirical support for the notion that high ACh levels may enhance attention to the environment, making neural circuits more responsive to external sensory stimuli.

Introduction

Neural encoding of an ever-changing acoustic environment is a complex and demanding task that may depend on modulation by an animal´s attention or by the demands of ongoing activity (Sarter et al., 2005; Thiel and Fink, 2008; Edeline, 2012). Neural mechanisms for detecting sensory changes engage a distributed network of neural circuits that are sensitive to stimulation history (Ranganath and Rainer, 2003; Grimm and Escera, 2012).

In the auditory brain, neurons that specifically decrease their response to a repeated sound but resume their firing when deviant stimuli are presented are found in the primary auditory cortex (AC, Ulanovsky et al., 2003; von der Behrens et al., 2009), auditory thalamus (Antunes et al., 2010) and inferior colliculus (IC, Perez-Gonzalez, 2005; Malmierca et al., 2009). This differential response to repeated versus rare sounds is referred to as 'stimulus-specific adaptation' (SSA) and might reflect a special type of short-term plasticity that transiently modulates neural responsiveness in an activity-dependent manner (Jääskeläinen et al., 2007; Nelken, 2014). SSA may contribute to the upstream encoding of mismatch signals to repeated and deviant sounds observed at larger spatial and temporal scales in electroencephalographic studies (Nelken and Ulanovsky, 2007; Escera and Malmierca 2014; Malmierca et al., 2014). In humans, the encoding of repeated and rare sounds is affected by top-down processing (Todorovic et al., 2011) and by the application of modulatory substances, such as cholinergic compounds, that are known to vary across vigilance and cognitive states (Knott et al., 2014; Moran et al., 2013; Grupe et al., 2013).

An augmentation of aceytlycholine (ACh) release occurs during attention-demanding tasks (Himmelheber et al., 2000; Passetti et al., 2000). The increase in ACh

52 modifies circuit dynamics in response to internal and external inputs (Sarter et al., 2005;
53 Hasselmo and McGaurghy, 2004; Picciotto et al., 2012). It has been suggested that
54 cholinergic modulation may shift brain activity from a discrimination mode to a detection
55 mode, thus favoring the encoding of ongoing stimulation (Sarter et al., 2005; Hasselmo and
56 McGaughy, 2004; Jääskeläinen et al., 2007). In the AC, ACh enhances responses to
57 afferent sensory input while decreasing intracortical processing (Metherate and Ashe, 1993;
58 Hsieh et al., 2000). Moreover, previous studies have demonstrated that cholinergic
59 modulation alters frequency response areas of auditory neurons and therefore is important
60 in the encoding of spectral representation (Ashe et al., 1989; Metherate and Weinberger,
61 1989, 1990; Metherate et al., 1990; Ma and Suga, 2005; IC: Ji et al., 2001).

62 The main goal of the present study was to analyse what role, if any, ACh plays in
63 generation or modulation of SSA. We employed microiontophretic application of ACh to
64 address how ACh affects the responses of IC neurons that exhibit SSA. Preliminary reports
65 have been presented elsewhere (Ayala and Malmierca, 2014, 2015).

66

Material and methods

Subjects and surgical procedures

Experiments were performed on 44 adult female rats (*Rattus norvegicus*, Rj: Long-Evans) with body weights ranging from 180–333 g (median ± SEM: 210 ± 0.76 g). All surgical, recording and histological procedures were conducted at the University of Salamanca, Spain. The experimental protocols were approved by Animal Care Committees of the University of Salamanca and followed the standards of the European Union (Directive 2010/63/EU) for the use of animals in neuroscience research. Detailed procedures are given elsewhere (Malmierca et al., 2003; Malmierca et al., 2009; Perez-Gonzalez et al., 2012). Anesthesia was induced using a mixture of ketamine chlorohydrate (30 mg/kg, I.M., Imalgene 1000, Rhone Méreuse, Lyon, France) and xylazine chlorohydrate (5 mg/ Kg, Rompun, Bayer, Leverkusen, Germany). Body temperature was monitored with a rectal probe and maintained at 38 ± 1ºC with a thermostatically controlled electric blanket. The trachea was cannulated and atropine sulphate (0.05 mg/kg, s.c., Braun, Barcelona, Spain) was administered to reduce bronchial secretions. The animals were connected to aventilator (SAR-830/P) and expired CO_2 was monitored using a capnograph (Capstar-100). A craniotomy was made in the caudal part of the left and right parietal bone, exposing the cerebral cortex, in order to gain access to the IC. To perform electrophysiological recordings from IC neurons, anesthesia was maintained with an initial i.p. injection of urethane (750 mg/kg, Sigma-Aldrich Corp., St Louis, MO, USA) and with booster doses of one-third of the initial amount.

Acoustic delivery and electrophysiological recording

Prior to surgery, auditory brainstem responses (ABRs) to clicks (100 μs, 10 Hz rate) delivered in 10 dB SPL ascending steps from 10 to 90 dB SPL were obtained to check that the animal had normal hearing with thresholds lower or at 30 dB SPL. ABR recordings were performed inside a sound-attenuated room, using a closed-field sound delivery system and a real-time signal processing system (Tucker-Davis Technologies System 3, Alachua, Florida, USA). Subcutaneous needle electrodes placed at the vertex (active electrode), the mastoid ipsilateral to the stimulated ear (reference electrode) and the mastoid contralateral to the stimulated ear (ground electrode) were used for the recordings. Evoked potentials were averaged from 500 presentations, and the final signal was filtered with a 500-Hz high-pass filter and a 3000-Hz low-pass filter with hearing thresholds determined visually. Afterwards, the animal was placed in a stereotaxic frame in which the ear bars were replaced by a hollow speculum that accommodated a sound delivery system (Rees, 1990) using two electrostatic loudspeakers (TDT-EC1). Search stimuli were pure tones or white noise driven by a TDT System 2 (TDT, Tucker-Davis Technologies, Florida, USA) that was controlled by custom software for stimulus generation and on-line data visualization (Faure et al., 2003; Pérez-González et al., 2005; Malmierca et al., 2008). Action potentials were recorded with a TDT BIOAMP amplifier, the ×10 output of which was further amplified and bandpass-filtered (TDT PC1; fc: 0.5–3 kHz) before passing through a spike discriminator (TDT SD1). Spike times were logged at one microsecond resolution on a computer by feeding the output of the spike discriminator into an event timer (TDT ET1) synchronized to a timing generator (TDT TG6). Extracellular single-unit responses were recorded in the left and/or right IC of each animal to contralateral stimulation. The IC was approached from 20° relative to the frontal plane so that the recording electrode moved

caudal and ventral during the penetration. The electrode was lowered into the brain with a piezoelectric microdrive (Burleigh 6000 ULN) mounted on a stereotaxic manipulator to a depth of 3.5–5 mm where acoustically driven responses were found. After a neuron was isolated, pure tone stimuli with a duration of 75 ms (5 ms rise/fall time) were delivered to obtain the monaural frequency response area (FRA), *i.e.,* the combination of frequencies and intensities capable of evoking a suprathreshold response. To do this, 5 stimulus repetitions at each frequency (from 0.5 to 40 kHz, in 20–25 logarithmic steps) and intensity step (steps of 10 dB, from 0 to 80 dB SPL) were presented randomly at a repetition rate of 4 Hz.

Stimulus presentation paradigm

Pure tones (75 ms, 5 ms rise/fall time) were presented in an oddball paradigm similar to that used to record mismatch negativity responses in human studies (Näätänen, 1992) and more recently in animal studies of SSA (Ulanovsky et al., 2003; Malmierca, et al., 2009, von der Behrens et al., 2010). Briefly, this paradigm consists of a flip-flop design employing two pure tones at two different frequencies (f1 and f2), both of which elicited similar firing rates and response patterns at a level of 10–40 dB SPL above threshold within the neural FRA. For most of the neurons (64%), the f1 and f2 tones were located around the characteristic frequency (CF, the sound frequency that produces a response at the lowest stimulus level) while the rest of the frequency pairs were both either lower (23%) or higher (13%) than the CF. The frequency separations (Δf) between f1 and f2 varied between 0.14 octaves and 0.53 octaves. A train of 300 or 400 stimulus presentations containing both frequencies was delivered in two different sequences (sequence 1 and 2). The repetition rate of the train of stimuli was 4 Hz, as this has been previously demonstrated to elicit SSA in

IC neurons of the rat (Malmierca et al., 2009; Ayala and Malmierca, 2013). In sequence 1, the f1 frequency was presented as the standard tone with a high probability of occurrence (90%) within the sequence. Interspersed randomly among the standard stimuli were the f2 frequency-deviant stimuli (10% probability). After the sequence 1 data set was obtained, the relative probabilities of the two stimuli were reversed, with f2 as the standard and f1 as the deviant in sequence 2. The responses to the standard and deviant stimuli were normalized to spikes per stimulus, to account for the different number of presentations in each condition.

Electrodes and iontophoresis

A tungsten electrode (1–2.5 MΩ, Merrill and Ainsworth, 1972) was used to record single-neuron activity. It was attached to a multibarrel borosilicate glass pipette that carried drugs to be delivered in the vicinity of the recorded neuron. The tip of the recording electrode protruded 15–25 μm from the pipette tip. The glass pipette consisted of five barrels in H-configuration (World Precision Instruments, 5B120F-4) with the tip broken to a diameter of 20–30 μm. The center barrel was filled with saline for current compensation (165 mM NaCl), while the others were filled with 1 M ACh chloride (Sigma, A6625), 0.5 M scopolamine hydrobromide (Sigma, S0929) or 0.5 M mecamylamine hydrochloride (Tocris, 2843). The drugs were dissolved in distilled water and their pH adjusted to 4–4.2. ACh chloride acts at both muscarinic and nicotinic receptors while the scopolamine and mecamylamine are non-selective antagonists of muscarinic and nicotinic receptors, respectively. These compounds have been used previously in the mammalian IC (Farley et al., 1983; Habbicht and Vater, 1996). The drugs were retained in the pipette with a –15 nA current and were ejected, when required, typically using 30–40 nA currents (Neurophore

BH-2 System, Harvard Apparatus). The duration of the drug ejection usually lasted 15–25 min but could be extended when no visual effect was observed in order to ensure the absence of effect. After the drug injection, we repeated the stimulation protocol until we observed recovery of firing.

Verification of the recording sites

Once the electrophysiological recordings were completed, electrolytic lesions (10–20 μA for 15 s) were applied for subsequent histological verification of the recording sites in 24 of the 44 animals. Brains were fixed using a mixture of 1% paraformaldehyde and 1% glutaraldehyde diluted in 0.4 M phosphate buffer saline (0.5% NaNO3 in PBS). After fixation, tissue was cryoprotected in 30% sucrose and sectioned in the coronal or sagital plane at a thickness of 50 μm on a freezing microtome. Slices were stained with 0.1% cresyl violet to facilitate identification of cytoarchitectural boundaries. The recorded units were assigned to one of the four main subdivisions of the IC (rostral, lateral and dorsal cortices or central nucleus, Loftus et al., 2008; Ayala et al., 2015) using as reference the standard sections from a rat brain atlas (Paxinos and Watson, 2005).

Analysis of neural responses

For each neuron, the degree of SSA was quantified by the Common-SSA Index (CSI) and the Frequency-Specific SSA Index (SI) reported previously (Ulanovsky et al., 2003; Malmierca et al., 2009; von der Behrens et al., 2009; Richardson et al., 2013). Both SSA indices reflect the normalized difference between the neural response to the deviant stimulus and the response to the standard, averaging (CSI) or quantifying separately (SI) the responses to f1 and f2. The CSI is defined as

$$CSI = [d(f1) + d(f2) - s(f1) - s(f2)] / [d(f1) + d(f2) + s(f1) + s(f2)]$$

where d(f) and s(f) are responses to each frequency f1 or f2 when they were the deviant (d) or standard (s) stimulus, respectively. The SI was separately calculated for each frequency and it is defined as

$$SI(fi) = [d(fi) - s(fi)] / [d(fi) + s(fi)]$$

where i = 1 or 2. Positive CSI and SI values indicate that the neurons responded more strongly to the frequencies when they were deviant compared to when they were standard. A CSI value of 0.1 was used as cutoff between neurons that exhibited or lacked SSA since it has been previously demonstrated that CSIs < 0.1 are not statistically different from zero and are due to random fluctuations in spike counts (Ayala et al., 2013).

To characterize the time course of adaptation, we averaged the response of all neurons to the standard tone (mean spikes per trial). This was done trial by trial for the total of stimulus presentations under the oddball paradigm. The mean response was plotted at their original trial-long time scale. Then, we performed a nonlinear least-square fit to this population mean curve to find the best-fitting double exponential function as follows:

$$f(t) = A_{ss} + A_r \cdot e^{-t/\tau(r)} + A_s \cdot e^{-t/\tau(s)},$$

where A_{ss}, A_r and A_s are the magnitudes of the steady state, and the rapid and slow components, respectively, and τ_r and τ_s are the time constants of the rapid and slow components (see details in Perez-Gonzalez et al., 2012).

The CF and threshold of each neuron was identified. The monotonicity index (MI = spike count at 80 dB SPL / maximum spike count) that refers to the degree of reduced

201 spiking at higher intensities was calculated from the FRA measure at the CF (Watkins and
202 Barbour, 2011). Monotonic responses were those with a MI > 0.75. Finally, we measured
203 the sharpness of the FRA by calculating the Q-value at 10 above the threshold as in
204 previous studies (Hernandez et al., 2005; Malmierca et al., 2009; Duque et al., 2012; Ayala
205 et al., 2013). The Q_{10}-value was calculated as the CF divided by the bandwidth which is the
206 difference in kHz between the lower and upper frequencies of the FRA. To test for
207 significant effects of the drugs on each individual neuron, the 95% confidence intervals
208 (C.Is.) for the baseline CSI were calculated using the bootstrapping method (1000
209 repetitions). The limits of 95% CIs were calculated using the 2.5 and 97.5 percentiles of the
210 CSI bootstrap distribution. An effect of the drug was considered to be significant when the
211 CSI value obtained under the injection condition was larger or smaller than the high or low
212 95% C.I., respectively.

213 To study the contribution of spontaneous activity on the SSA, we again calculated
214 the SSA indices from the evoked activity but with subtracted spontaneous activity bin by
215 bin (evoked activity minus spontaneous activity in spikes/s). Spontaneous activity was
216 estimated within a 50 ms window before each tone presentation in the oddball paradigm as
217 described previously (Duque and Malmierca, 2014). Unless otherwise stated, results are
218 presented as median ± SEM. To test for significant differences among medians,
219 distributions across baseline, drug application and recovery conditions we performed the
220 Friedman Repeated Measures Analysis of Variance on Ranks. Post hoc comparisons were
221 performed following Dunn's method and a $p < 0.05$ was considered statistically significant.
222 To measure the strength of association between variables we used the Spearman Rank
223 Order Correlation Coefficient. Analyses and figures were executed using SigmaPlot

Version 11 (Systat Software, Inc., Chicago, IL, USA) and Matlab 13 (MathWorks, Inc., Natick, MA, USA).

227 **Results**

228 To explore the influence of cholinergic neuromodulation on SSA in the IC of the rat, we
229 recorded the responses of 152 well-isolated single neurons to an oddball paradigm before,
230 during and after microiontophoretic application of ACh (n = 105), scopolamine (n = 19),
231 and mecamylamine (n = 28).

232 **The strength of the ACh effect depends on the baseline SSA level**

233 The recorded neurons had different temporal response patterns and exhibited (82 %) or
234 lacked SSA (18 %). Three example neurons are shown in Figure 1. The first neuron (Fig.
235 1A) responded with sustained firing of similar strength to both the deviant and standard
236 tones across all the tone presentations; therefore it lacks SSA ($CSI_{baseline}$ = 0.076).
237 Microiontophoretic application of ACh did not change either the temporal response pattern
238 or the ratio between the responses to the standard and deviant sound as estimated by its CSI
239 = 0.072 (Bootstrapping, 95% C.I., Fig. 1A,B). Figure 1C illustrates another neuron that
240 showed an onset response type and a high level of SSA as depicted by its CSI (0.974). It
241 was also unaffected by ACh, even after a long period of application (more than 2 hours;
242 Fig. 1C,D). In contrast, Figure 1E,F depicts the response of a third neuron, with an
243 intermediate CSI value (0.732), that was strongly affected by ACh. In this neuron, the firing
244 response increased (Fig. 1E) and the CSI (0.41, Fig. 1F) decreased significantly but
245 returned to baseline values during recovery (Fig. 1F).

246 Our data (n = 105) contains a wide range of CSI values from −0.063 to 0.994 (Fig.
247 2A) and thus includes neurons that lack or exhibit different levels of SSA. Across the entire
248 sample, the most remarkable finding was that ACh differentially affected only a subset of

249 IC neurons (54 out of 105, Bootstrapping, 95% C.I.), mainly by decreasing their CSI (36
250 out 54). The majority of neurons with intermediate CSI values were sensitive to the ACh
251 application ($0.1 < CSI < 0.9$, 43 out 62), whereas most of the neurons that exhibited low
252 ($CSI \leq 0.1$; 15 out 19) or high ($CSI \geq 0.9$, 17 out 24) values were unaffected by ACh (Fig.
253 2A). The different baseline CSI values of our sample of neurons were fitted by a Sigmoidal
254 curve ($r^2 = 0.99$, $p < 0.0001$, Fig. 2B, gray line). We found that the magnitude of the
255 absolute change exerted by ACh on the CSI followed a Gaussian distribution ($r^2 = 0.44$, p <
256 0001, Fig. 2B, black line). The tails of the Gaussian curve correspond to the weak or absent
257 effect exerted on neurons with low or extremely high CSI values, and the peak corresponds
258 to the maximum effect exerted on neurons with intermediate CSI values. These results
259 indicate a distinct dependence of the strength of the ACh effect on the baseline CSI. This
260 dependence was also evident in the normalized responses to each frequency (f1 or f2)
261 estimated by the SIs (Fig. 2C). There was no difference between the absolute change on SI1
262 and SI2 (Mann-Whitney Rank Sum Test, $p = 0.696$, $T = 11250$, $n = 105$), indicating that
263 ACh affected both frequencies similarly. Also, the absolute change exerted by ACh on the
264 CSI correlated with the changes elicited on SI1 (Spearman´s coefficient: 0.63, p = < 0.001,
265 $n = 210$) and SI2 (coefficient: 0.59, $p < 0.001$, $n = 210$, Fig. 2D). The magnitude of change
266 on SI was higher for the group of neurons with $0.1 < CSI < 0.9$ while for the neurons with
267 $CSI < 0.1$ and $CSI > 0.9$, this magnitude was similar (Kruskal-Wallis One Way ANOVA, p
268 < 0.001, $H = 38.759$, Dunn´s Method, $p < 0.05$, $n = 210$). Hence, we can safely conclude
269 that ACh decreased both the CSI and SI at the population level. The CSI decreased from
270 0.57 ± 0.034 to 0.452 ± 0.035 (Friedman test, $p = 0.01$, $Xi^2 = 8.9$, $n = 105$) and the SI from
271 0.574 ± 0.025 to 0.443 ± 0.025 (Friedman test, $p = 0.009$, $Xi^2 = 9.36$, $n = 210$, Fig. 2E). The

recovery values for most neurons were virtually identical to the baseline cases (CSI_{rec} = 0.522 ± 0.036, SI_{rec} = 0.535 ± 0.027). Twelve neurons that were manipulated with ACh (11% of the sample) were lost before the full recovery (crosses in Figure 2A). Nevertheless, those 12 neurons were distributed along the whole spectrum of CSI values in the sample and followed the same trend. They were similarly affected by ACh as other neurons with a similar baseline CSI (Figure 2A, crosses). Furthermore, ACh increased the spontaneous rate (from 0.17 ± 0.49 to 0.28 ± 0.97 spikes per second) of those IC neurons with partial levels of CSI ($0.1 < CSI < 0.9$, Wilcoxon Signed Rank Test, W = 476, Z-statics = 2.441, $p = 0.015$, n = 62) but did not affect the spontaneous discharge of those with low ($CSI \leq 0.1$, $p = 0.232$, n = 19) or high CSI values ($CSI \geq 0.9$, $p = 0.375$, n = 24). Based on this result we subtracted the spontaneous rate from the evoked response and recalculated the SSA indices of all neurons in order to validate that the changes we observed were due to an ACh effect on the driven responses. Under this manipulation, the SSA indices across the baseline, ACh and recovery condition were increased, but the ACh still decreased the CSI (Friedman test, $p = 0.01$, $Xi^2 = 9.31$, n = 210) and SI (Friedman test, $p = 0.002$, $Xi^2 = 12.04$, n = 210, Fig. 2E) indicating a genuine cholinergic effect on the evoked responses.

Acetylcholine differentially modulates the responses to deviant- and standard tones

In terms of spike count (spikes per trial), positive CSI values reflect smaller spike count to the standard tone than to the deviant one. In agreement with this, the spike count to the standard sound was negatively correlated with the CSI (Spearman´s coefficient = −0.932, $p < 0.001$, n = 105), while the response to the deviant sound elicited a weaker correlation (−0.512, $p < 0.001$, n = 105). The firing rate of the neural responses was significantly affected by the ACh (Friedman test, $Xi^2 = 405.112$, $p < 0.001$). The post hoc analysis

295 indicated that the spike count to the deviant was higher (1.05 ± 0.106 spikes per trial) than
296 to the standard tone (0.262 ± 0.102 spikes per trial) in the baseline condition as expected,
297 since our sample was biased to positive CSI values ($p < 0.05$). ACh increased the spike
298 count to both the deviant and standard tones to 1.188 ± 0.133 and 0.421 ± 0.128 spikes per
299 trial, respectively ($p < 0.05$) without eliminating the difference between them (Fig. 3A,B).
300 In the recovery condition, the ACh effect on the neural firing was completely abolished and
301 the response decreased to baseline values; 1.125 ± 0.122 and 0.246 ± 0.116 for the deviant
302 and standard tone, respectively ($p < 0.05$). Since ACh did not affect all neurons with
303 different CSI values equally, we explored the change in the spike count of those partially
304 adapting neurons whose CSI was significantly changed by ACh application ($n = 43$). Most
305 notably, for this group of neurons we found that ACh only increased the response to the
306 standard tone (Friedman test, $Xi^2 = 204.847$, $p < 0.001$, Fig. 3C,D). Moreover, the
307 differential effect exerted by ACh on the response to the standard stimulus was also
308 apparent for all neurons with a significant change in their CSI ($n = 54$, Friedman test, $Xi^2 =$
309 232.583, $p < 0.001$).

310 We analyzed the effect of ACh on the time course of the response to the standard
311 tone for those partially adapting neurons with a significant change in their CSI. The
312 dynamics of the response to the standard tone was fit well by a double exponential function
313 under the baseline ($r^2 = 0.7871$) and ACh ($r^2 = 0.7767$) condition, displaying a rapid and a
314 slow decay as well as a steady-state component (Fig. 3E). ACh increased the response
315 during the steady-state component of the response from 0.6343 spikes per trial (95% C.Is.:
316 0.6246, 0.6441) to 0.9932 (0.9825, 1.004) (Fig. 3E) without affecting either the timing or
317 the magnitude of the fast (baseline: $\tau_r = 0.6165$ trial, $A_r = 4.973$ spikes per trial; ACh: $\tau_r =$

318 0.596, $A_r = 6.536$) and slow (baseline: $\tau_s = 29.15$, $A_s = 0.4969$; ACh: $\tau_s = 26.7$, $A_s = 0.5197$)
319 components of the adaptation.

320 The differential effect exerted by ACh on the response to the standard and deviant
321 tone was also reflected by the strength of correlation between the change in the CSI
322 ($CSI_{ACh} - CSI_{baseline}$) and spike count. The change in the CSI was correlated stronger with
323 the normalized change in the mean spiking response to f1 and f2 when presented as
324 standard ($r^2 = -0.7$, $p < 0.001$, $n = 105$) than with the change in the response to f1 and f2
325 when presented as deviant tone ($r^2 = -0.3$, $p < 0.001$, Fig. 3F,G). We explored the effect of
326 ACh on the first spike latency (FSL) of the response to the deviant and standard tone. As
327 expected from previous IC studies (Malmierca et al., 2009), the FSL of the deviant (15.55 ±
328 0.43 ms) was shorter than the FSL of the standard response (16.2 ± 0.67 ms, $p < 0.05$) in
329 the baseline condition. ACh did not affect the FSL; the response latency to the deviant tone
330 remained shorter during the injection (deviant: 15.2 ± 0.46 ms; standard: 15.87 ± 0.64 ms)
331 and recovery conditions (deviant: 15.61 ± 0.54 ms; standard: 15.71 ± 0.75 ms) (Friedman
332 test $Xi^2 = 68.064$, $p < 0.001$).

333 Next, to assure that the lack of effect on the CSI we observed in some neurons was
334 not due to a failed iontophoretic release of ACh, we measured the CF, MI and threshold of
335 most of the neuronal FRAs (96 out 105) before and during the ACh application. We found
336 that the threshold was affected (Wilcoxon Signed Rank Test, $W = -747$, Z-statics = −4.037,
337 $p < 0.001$, $n = 96$) while the CF (Wilcoxon Signed Rank Test, $W = -168$, Z-statics =
338 −0.836, $p = 0.406$, $n = 96$) and MI (Wilcoxon Signed Rank Test, $W = 211$, Z-statics =
339 0.934, $p = 0.353$, $n = 96$) remained unchanged by ACh. Moreover, the threshold of both
340 groups of neurons, *i.e.*, neurons with significant change in their CSI (Wilcoxon Signed

341 Rank Test, W = −226, Z-statics = −2.973, p = 0.003, n = 50) as well as those whose CSI
342 was unaffected by ACh (Wilcoxon Signed Rank Test, W = −158, Z-statics = −2.747, p =
343 0.006, n = 46) was lowered from 30 to 20 dB SPL. These results demonstrate that the
344 differential effects elicited by ACh on the CSI were genuine and not an artifact.

345 **The effect of the ACh on SSA responses is mainly mediated by the mAChRs**

346 Two major classes of cholinergic receptors (muscarinic and nicotinic) are distributed
347 throughout the IC (Morley and Kemp, 1981; Clarke et al., 1985; Kelly and Caspary, 2005).
348 To examine whether the ACh effects described above are mediated by the muscarinic
349 and/or nicotinic receptors, we recorded 47 additional neurons before, during and after the
350 microiontophoretic application of their respective antagonists; *i.e.*, scopolamine and
351 mecamylamine. The application of scopolamine affected the CSI of 15 out 19 neurons (Fig.
352 4A) while the mecamylamine affected 16 out 28 neurons (Fig, 4B, Bootstrapping, 95%
353 C.I.). The majority of the significantly affected neurons showed an increase in their CSI
354 under the blockade of the muscarinic (n = 12 out of 15, Fig. 4A) and nicotinic (n = 12 out
355 of 16, Fig. 4B) receptors. The magnitude of the effect of both antagonists exhibited the
356 same dependence on baseline CSI value as with ACh. The greatest changes elicited by the
357 scopolamine and mecamylamine were on neurons with intermediate CSI values and the
358 absolute changes followed a Gaussian distribution ($r^2 = 0.52$, p = 0.003 and $r^2 = 0.756$, p <
359 0.0001, respectively, Fig. 4A,B).

360 At the population level, only scopolamine significantly increased the CSI
361 (Friedman test, $Xi^2 = 7$, p = 0.03, n = 19, Fig. 4C). Mecamylamine application did not
362 significantly increase the CSI of the whole population (Friedman test, $Xi^2 = 1.52$, p = 0.468,

363 n = 28, Fig. 4D) neither for the group of neurons with intermediate CSI values that were
364 most affected at the single-neuron analysis (0.1 < CSI < 0.9) (Friedman test, $Xi^2 = 5.286$, p
365 = 0.071, n = 17). Likewise, the SI was affected by scopolamine (Friedman test, $Xi^2 = 7.357$,
366 p = 0.025, n = 38, Fig, 4E,F) but not by mecamylamine (Friedman test, p = 0.364, $Xi^2 =$
367 2.02, n = 56, Fig. 4E,G). The blockade of the cholinergic receptors decreased the response
368 only to the deviant tone (Friedman test, p < 0.001). The driving response changed from
369 1.171 ± 0.166 to 0.95 ± 0. 111 spikes per trial under the scopolamine injection (Friedman
370 test $Xi^2 = 66.375$, p < 0.001, Dunn´s Method, p < 0.05, n = 38) and from 1.283 ± 0.132 to
371 0.95 ± 0.139 spikes per trial (Friedman test $Xi^2 = 148.844$, p < 0.001, Dunn´s Method, p <
372 0.05, n = 56) under the mecamylamine application. Although the mean population response
373 to the standard tone was not significantly affected, we observed a clear change in the
374 temporal course of adaptation elicited by the muscarinic and nicotinic blockade (Fig. 4H,I).
375 The standard responses of those neurons with intermediate (0.1 < CSI < 0.9) and significant
376 change in their CSI under the scopolamine ($r^2 = 0.66$) and mecamylmine application ($r^2 =$
377 0.61) were fitted by the double exponential function previously described for ACh. We
378 found that scopolamine caused a greater decrease in the response during the steady-state in
379 comparison with mecamylamine effect. The response showed a 53% change from 0.6084
380 spikes per trial (C.I. 95%: 0.59, 0.6268) to 0.2857 (0.2733, 0.2981) with application of
381 scopolamine (Fig. 4H) while the change was only 29%, from 0.5043 (0.487, 0.5216) to
382 0.3565 (0.3448, 0.3682) with mecamylamine application (Fig. 4I). The magnitude and
383 timing of the rapid and slow decay of the response to the standard were not affected by
384 cholinergic blockade.

385 **Anatomical and physiological correlates of the ACh effect**

We determined the location of the majority of the recorded neurons (64 out 105) across IC subdivisions. Most of the neurons were located in the RCIC (n = 34) and the remaining neurons were distributed in the LCIC (n = 17) and CNIC (n = 13). The baseline SSA was higher in the cortical subdivisions (RCIC: 0.62 ± 0.058; LCIC: 0.72 ± 0.076) than in the central nucleus (0.13 ± 0.069) (Kruskal-Wallis One Way ANOVA, H = 12.983, p = 0.002; Fig. 5A). Interestingly, the magnitude of change exerted on the CSI by ACh in RCIC and LCIC neurons followed the same Gaussian distribution as the whole population depicted in Figure 2B ($r^2 = 0.47$, $p < 0.0001$ and $r^2 = 0.47$, p = 0.011, respectively) (Fig. 5B) while the sample of neurons from the CNIC showed a weak effect that was not Gaussianly distributed (p = 1, Fig. 5C).

Finally, we wished to test whether any other response feature in addition to the baseline CSI correlates with the presence or absence of ACh effect on SSA. We found that the MI of the group of neurons whose CSI was affected by the ACh (1 ± 0.0229, n = 54) was slightly higher than the MI of the group of neurons with non-affected CSIs (0.929 ± 0.0322, n = 51) (Mann-Whitney Rank Sum Test, U-statics = 996.5, T = 2322.5, p = 0.037), but in both cases the MIs were monotonic. Neither group differed in other parameters such as the response duration (67.55 ± 3.466 and 42 ± 3.634 ms for affected and unaffected groups, respectively, Mann-Whitney Rank Sum Test, p =0.614), threshold (30 ± 1.879, 30 ± 2.008 dB SPL, p = 0.263), Q_{10} (1.426 ± 0.123, 1.556 ± 1.204, p = 0.601) or CF (11.245 ± 1.026, 11.199 ± 0.998 kHz, p = 0.605). The CF (Spearman´s coefficient = 0.806, p = 0.003, Fig. 5D) as well as the response duration (Spearman´s coefficient = −0.612, p = 0.053, Fig. 5E) correlated with the CSI at the baseline condition, *i.e.* neurons with higher CSI are tuned to higher frequencies and have shorter response durations. Then, the median CF and

409 reponse duration of the group of unaffected neurons may have been averaged out
410 explaining the lack of difference between the group of neurons whose CSI was or not
411 affected by ACh.

412

413 **DISCUSSION**

414 We have demonstrated that application of ACh decreases the SSA of IC neurons by
415 increasing the response to the standard tone and that this effect is mainly mediated by
416 muscarinic receptors. Moreover, we have found that the strength of the cholinergic
417 modulation depends on the baseline SSA level, exerting its greatest effect on neurons with
418 intermediate SSA responses. To the best of our knowledge, this is the first study
419 demonstrating that auditory SSA is sensitive to cholinergic modulation.

420 A selective effect of ACh on frequency processing has been described in AC
421 neurons. A repeated single-frequency stimulus simultaneously paired with the iontophoretic
422 application of ACh produced a highly specific change in the response to the paired
423 frequency rather than a general change in excitability (Metherate and Weinberger, 1989).
424 The effect was mediated by muscarinic receptors. Similar mechanisms may underly the
425 selective change in the response to the standard tone that we observed (Fig. 3C,D), since
426 this tone was repeated many more times than the deviant tone under ACh application. The
427 observed decrease in the adaptation to the standard tones agrees with diminished spike-
428 frequency adaptation exerted by ACh in other sensory areas (Metherate et al., 1992;
429 McCormick, 1993; Martin-Cortecero and Nunez, 2014). Likewise, ACh affected SSA
430 mainly through the activation of the muscarinic rather than the nicotinic receptors (Fig. 4G-
431 H). Muscarinic receptors are expressed both pre- and postsynaptically so they can alter the
432 excitability of the neurons as well as the release probability of other neurotransmitters
433 (Zhang et al., 2002; Thiele, 2013). In the IC, at least two types of muscarinic receptors
434 (M1- and M2-types) can functionally modify neural firing (Habbicht and Vater, 1996).
435 Since we used a general antagonist for muscarinic receptors, we cannot discriminate

436 between the effects of the two muscarinic subtypes, but it is likely that most of the
437 excitatory effect exerted by ACh was mediated by the activation of the M1-type since
438 selective blockade of the M1 receptor mostly leads to inhibition whereas the opposite effect
439 occurs with selective blockade of the M2-type (Habbicht and Vater, 1996).

440 The excitatory effects elicited by ACh might be mediated through the regulation of
441 K^+ channels (McCormick and Prince, 1986; Krnjevic, 2004). The activation of the M1-type
442 receptor induces a reduction in hyperpolarizing potassium currents through the closure of
443 K^+ channels such as the slow after-hyperpolarization K^+ (K_{sAHP}) or the inward rectifying K^+
444 of type 2 (KIR2) which, in turn, reduces spike frequency adaptation and increases driven
445 and spontaneous activity (Cole and Nicoll, 1984; Krause and Pedarzani, 2000; Thiele,
446 2013). Changes in potassium conductance can act as an activity-dependent adaptation
447 mechanism (Sanchez-Vives et al., 2000a,b) that contributes to a significant fraction of
448 cortical auditory adaptation (Abolafia et al., 2011). For those reasons, K^+-mediated
449 adaptation has been proposed as a potential mechanism underlying SSA (Abolafia et al.,
450 2011; reviewed in Malmierca et al., 2014). ACh might also increase the tone-evoked
451 responsivity in IC by modulating the release of other neurotransmitters as reported in the
452 AC (Metherate, 2011) where the activation of cholinergic receptors decreases the release of
453 GABA from interneurons (Salgado et al., 2007) or elicits the activation of NMDA receptor-
454 mediated glutamatergic neurotransmission (Metherate and Hsieh, 2003; Metherate, 2004;
455 Liang et al., 2008).

456 Our finding that ACh exerts a very delicate modulation by selectively increasing
457 the evoked response to the standard sound contrasts with the gain control exerted by
458 $GABA_A$-mediated inhibition in IC (Perez-Gonzalez et al., 2012) and MGB neurons (Duque

459 et al., 2014), where the blockade of the $GABA_A$ receptors exerts a dramatic, overall
460 increase in the neural responsiveness to both deviant and standard tones (Fig. 6A,B).
461 Likewise, our finding showing that cholinergic manipulation (Fig. 3E, 4H,I) affected only
462 the steady state of the time course of adaptation, markedly contrasts with the substantial
463 changes affecting the fast- and slow decays of adaptation when the $GABA_A$ receptors were
464 blocked or activated. In agreement with our observations on the evoked response (Fig. 3A-
465 E) and FSL, a change in strength but not in latency was found to be elicited by ACh in
466 somatosensory cortical neurons (Martin-Cortecero and Nuñez, 2014). From these results,
467 we can conclude that ACh in the IC contributes to maintain the encoding of repetitive
468 acoustical input by decreasing adaptation. This occurs mainly through the activation of
469 muscarinic receptors and acts at a different time course than that of GABAergic inhibition.

470 A second difference between cholinergic and inhibitory modulation of SSA is that
471 the strength of the cholinergic effect depends on the baseline level of SSA exhibited by the
472 IC neurons (Fig 2B, 4A,B, 5B) whereas $GABA_A$-mediated inhibition affects the firing of all
473 IC neurons, regardless of the neural type, *i.e.*, adapting and non-adapting neurons (Perez-
474 Gonzalez et al., 2012). Differences in the membrane potential of the neuron and/or
475 expression of cholinergic receptors might explain the lack, modest or profound effects of
476 ACh. Thus, we suggest that neurons with partial levels of SSA filter sensory information
477 according to different cognitive states, such as attention in which ACh levels increase
478 (Passetti et al., 2000; Hasselmo and McGaughy, 2004), while neurons exhibiting extreme
479 SSA are likely to play a role as specialized filters for redundant information, *i.e.*, repetitive
480 sounds.

481 Although cortical SSA (Ulanovsky et al., 2003) and subcortical SSA (Malmierca
482 et al., 2009) show many similarities, they are not the same and may play different roles
483 (Nelken, 2014). Moreover, due to their different sources of cholinergic projections, we
484 cannot generalize our results to ACh effects on cortical SSA. The main source of ACh to
485 the AC is the basal forebrain (Edeline et al., 1994; Zaborszky et al., 2012; Bajo et al., 2014)
486 while cholinergic input to the IC originates in the pontomesencephalic tegmentum (PMT,
487 Motts and Schofield, 2009; Schofield, 2010). These different ACh sources may constitute
488 two parallel pathways for modulating change detection in AC and IC. However it is likely
489 that changes in cortical excitability may affect subcortical SSA by trigering the release of
490 ACh since AC neurons inervate the PMT cholinergic neurons that project to the IC
491 (Schofield and Motts, 2009; Schofield, 2010). Deactivation of the AC exerts a
492 heterogeneous control on SSA in the IC (Anderson and Malmierca, 2013) that could be
493 indirectly mediated by ACh through a disynaptic AC → PMT → IC projection. Thus,
494 different states of cortical activation might exert a top-down control on the sensory signals
495 being processed at IC by gating the PMT cholinergic input.

496 The presence of sensitive and insensitive neurons to ACh within the same IC
497 subdivision (Fig. 5A) together with track-tracing data (Schofield, 2010; Schofield et al.,
498 2011) and radiolabelling studies of cholinergic receptors (Rotter et al., 1979; Clarke et al.,
499 1984; Clarke et al., 1985; Cortes and Palacios, 1986) suggest that the cholinergic projection
500 is diffuse throughout the IC and targets specific synaptic domains populated by neurons
501 with intermediate SSA. Alternatively, ACh may modulate specific features such as the
502 spectral sensitivity of one type of neuron and SSA of others. Future studies are needed to
503 address these possibilities. Here, we found that the microiontophoretic application of ACh

504 in the IC of the anesthetized rat reduces SSA which agrees with the low SSA indices
505 observed in awake animals (von der Behrens et al., 2009; Duque and Malmierca, 2014)
506 where ACh levels are higher (Kametani and Kawamura, 1990; Marrosu et al., 1995). Since
507 attention is known to increase ACh levels and neural activity (Ranganath and Rainer, 2003;
508 Deco and Thiele, 2009, 2011), our study provides a starting point to understand how
509 attention-demanding states (Passetti et al., 2000; Himmerlheber et al., 2000) might
510 modulate subcortical SSA.

511 Our finding that local augmentation of ACh increases the neural excitability (Fig.
512 3A) and attenuates adaptation to the repetitive sound (Fig. 3E) agrees with a general model
513 of how ACh affects sensory processing (reviewed in Thiele, 2013). According to this
514 model, ACh enhances the influence of feedforward afferent input relative to feedback so an
515 augmentation in ACh increase feedforward synaptic efficacy favoring information relayed
516 through the thalamus over ongoing intracortical activity. Studies in the AC (Metherate and
517 Ashe, 1993; Hsieh et al., 2000) and in other brain areas (Hasselmo and Bower, 1992;
518 Kimura, 2000; Hasselmo and McGaughy, 2004; Deco and Thiele, 2011) also support this
519 notion. Likewise, our findings support a key formulation of the predictive coding
520 framework (Friston, 2005, 2008); namely that the reduction in the neural signals evoked by
521 a repeated or predicted stimulus is attenuated by top-down processes such as attention (Kok
522 et al., 2012) or augmented by prior expectation (Todorovic et al., 2011). Recently, using
523 blocks of tone repetitions in an electroencephalographic study in humans, Moran et al.
524 (2013) found that the decreased responses to consecutive presentation of the same tone (*i.e.,*
525 repetition suppression) were markedly attenuated by systemic application of galantamine,

an acetylcholinesterase inhibitor. Thus, the increased availability of ACh enhances the sensory representation of predicted stimuli by boosting bottom-up sensory processing.

In conclusion, we showed that ACh alters the sensitivity of partially-adapting IC neurons by switching neural discriminability to a more linear transmission of sounds (encoding most of the stimulus occurrences). This effect potentially contributes to propagation of ascending sensory-evoked afferent signals through the thalamus *en route* to the cortex. Our results provide empirical support for the notion that high ACh levels may enhance attention to the environment, making neural circuits more responsive to external sensory stimuli.

536 **LEGENDS**

537 **Figure 1. Examples of neurons recorded in this study. A.** Dot rasters of the response to
538 the oddball paradigm of an on-sustained neuron lacking SSA (CSI = 0.076) under baseline,
539 ACh and recovery conditions. **B.** Time course of the Common SSA index (CSI) before,
540 during and after the microiontophoretic injection of ACh. Neither the firing response nor
541 the CSI were changed by the ACh application (Bootstrapping, 95% C.I.). **C.** Response of a
542 neuron showing strong SSA (CSI = 0.974) with a distinct onset firing pattern that was
543 unaffected by ACh (Bootstrapping, 95% C.I.). **D.** As, in B, the CSI of the strongly
544 adapting neuron remained unchanged. **E.** Dot raster of the response of a neuron with
545 moderate level of SSA (CSI = 0.732) that was profoundly affected by ACh showing an
546 increase of firing rate. **F.** The CSI of this partially adapting neuron decreased during ACh
547 injection (Bootstrapping, 95% C.I.). The tone duration (75 ms) is represented by the black
548 bar in **A,C,E**. The duration of the ACh injection is represented by the shaded area in **B,D,F**.
549 The small arrows in **B,D,F** indicate the times of the dot rasters displayed for each neuron.

550

551 **Figure 2. ACh effect on SSA in IC neurons. A.** The recorded IC neurons (n = 105)
552 showed different levels of CSI in the baseline condition (○) from –0.063 to 0.994. The low
553 and high 95% confidence interval (C.I.) of each baseline CSI is displayed (−). The CSI of a
554 subset of IC neurons changed during the application of ACh, being higher or lower than the
555 C.Is. of the baseline CSI value (orange symbols) while another subset of IC neurons was
556 insensitive to ACh application (green symbols). Most of the neurons insensitive to ACh
557 lacked SSA (CSI < 0.1) or exhibited extremely high values (CSI ≥ 0.9) in the baseline

558 condition (vertical histogram, left inset). Twelve neurons did not have a measurement in the
559 recovery condition (orange and green crosses) as they were lost before full recovery. **B.** The
560 strength of the effect of ACh depended on the baseline CSI. The baseline CSI values (o)
561 were fitted by a Sigmoid curve ($r^2 = 0.99$, $p < 0.0001$, gray line) while the absolute
562 difference (●, expressed in positive values) between the baseline and ACh condition
563 followed a Gaussian curve ($r^2 = 0.44$, $p < 0.0001$, black line). **C.** Scatter plot of the
564 difference in the frequency-specific index for f1 (SI1) and f2 (SI2) between the ACh and
565 baseline condition ($CSI_{ACh} - CSI_{baseline}$) for neurons with low (o: CSI < 0.1), intermediate
566 (○: $0.1 \leq CSI < 0.9$) and high CSI values (○ $CSI \geq 0.9$). Each dot represents one neuron. **D.**
567 The absolute change (positive values) in the CSI correlated similarly with the absolute
568 changes elicited by ACh in the SI1 (Spearman´s coefficient = 0.63, $p < 0.001$) and SI2
569 (0.59, $p < 0.001$) indicating that changes in the response to both frequencies contributed
570 similarly to the CSI change. Symbols with the same format as C. **E.** Box plots of the CSI
571 (left panel) and SI1,2 (right panel) under the baseline, ACh and recovery conditions. ACh
572 decreased the SSA indices in the population of neurons (Friedman test, *$p < 0.05$). The
573 decrement in the SSA persisted after the spontaneous activity (SA) was subtracted to the
574 driving response for each neuron. The dashed lines within each box represent the median
575 values, the edges of the box delimit the 25th and 75th percentiles, the whisker bars extent to
576 the 10th and 90th percentiles, and the circles represent the 95th and 5th percentiles.

577 **Figure 3. Effect of ACh on the driving response to deviant and standard sounds. A.**
578 Box plot of the response to the deviant (red) and standard tone (blue) of the whole
579 population of IC neurons (n = 105) before, during and after ACh injection, indicating that
580 ACh increased responses to both tones (Friedman test, * $p < 0.05$). **B.** Population PSTHs

581 (mean ± STD, shaded) for deviant (red) and standard (blue) tones in the baseline and ACh
582 (orange) conditions. Bin size = 1 ms; sps: spikes per second. **C.** Box plot of the firing
583 response for those neurons with $0.1 \leq CSI < 0.9$ whose CSI was significantly affected by
584 ACh (Bootstrapping, 95% C.I., n = 43). ACh increased only the response to the standard
585 tone (Friedman test and Dunn's method as post hoc test, $p < 0.05$, $*p < 0.05$). Same format
586 as A. **D.** Population PSTHs. Same format as B. **E.** Time course of adaptation for the mean
587 response to the standard tone for each position (trial) in the oddball sequence of neurons
588 with $0.1 < CSI < 0.9$ significantly affected by ACh (n = 43). The baseline (●) and ACh data
589 (●) had fast and slow decay components and a steady-state component that were fitted by a
590 double exponential function (blue lines). ACh increased only the steady-state component.
591 **F.** Normalized change (ACh – baseline) in the driving response (mean spikes per trial) to
592 deviant (•) and standard tone (•) for those neurons whose CSI was changed (CSI_{ACh} –
593 $CSI_{baseline}$) by ACh application (Bootstrapping, 95% C.I., n = 54). **G.** Normalized change in
594 the driving response as in F but for those neurons whose CSI was not affected by ACh
595 (Bootstrapping, 95% C.I., n = 51).

596 **Figure 4. Effect of scopolamine and mecamylamine on SSA. A.** The blockade of the
597 muscarinic receptors by the application of scopolamine increased the CSI (○) in most of the
598 recorded IC neurons. The baseline CSI values (○) were fitted by a Sigmoidal curve (r^2 =
599 0.993, $p < 0.001$, gray line). The low and high 95% bootstrapped C.I. values (–) are
600 displayed for each baseline CSI. Similarly, the absolute differences (expressed in positive
601 values) between the CSI in the baseline and scopolamine condition (•) were fitted by a
602 Gaussian curve ($r^2 = 0.52$, $p = 0.003$, black line). **B.** Effect of nicotinic receptor blockade
603 with mecamylamine. (•) Absolute differences between the CSI in the baseline and

604 mecamylamine condition. Same format as in A. Sigmoidal curve, $r^2 = 0.994$, $p < 0.001$;
605 Gaussian curve, $r^2 = 0.756$, $p < 0.0001$. **C.** Box plot of the population CSI showing that
606 scopolamine (Scop) increased the SSA as measured by the CSI (Friedman test, $*p < 0.05$, n
607 = 19). **D.** Box plot of the population CSI indicating that the mecamylamine application did
608 not affect the SSA (Friedman test, $*p > 0.05$, n = 28). **E.** Scatterplot of the change in the
609 frequency-specific index ($SI_{ACh} - SI_{baseline}$) for f1 (SI1) and f2 (SI2) elicited by scopolamine
610 (○) and mecamylamine (○). No difference between the change elicited in SI1 and SI2 by
611 scopolamine ($p = 0.502$) and mecamylamine was found ($p = 0.33$, Mann-Whitney Rank
612 Sum Test). **F.** Box plot of the frequency-specific index for both frequencies (SI1,2) under
613 the baseline, scopolamine and recovery condition. Scopolamine increased the SI (Friedman,
614 test, $*p < 0.05$, n = 38). **G.** Box plot of the SI1,2 indicating the lack of effect of
615 mecamylamine (Friedman test, $p > 0.05$, n = 56). **H.** Mean driven response to the standard
616 tone for each position (trial) in the oddball sequence in the baseline (•) and scopolamine
617 conditions (•). The responses were adjusted by a double exponential function (black lines)
618 with a fast and slow decay component and a steady-state part. Scopolamine decreased only
619 the steady-state component. **I.** Time course of the response under the baseline (•) and
620 scopolamine condition (•). Scopolamine did not affected the dynamics of adaptation. Same
621 format as H.

622 **Figure 5. Anatomical location and physiological properties of the recorded IC**
623 **neurons. A.** Box plot of the baseline CSI values in our sample of IC neurons with
624 recording sites localized in the central nucleus (CNIC), rostral (RCIC) and lateral cortex
625 (LCIC) of the IC. Population CSI in the RCIC and LCIC were significantly larger than CSI
626 from the CNIC (Kruskal-Wallis test, $*p < 0.05$). CSI values affected (–) and non-affected

627 (−) by ACh are displayed separately. **B,C.** Effect of the ACh on the CSI of neurons from
628 the RCIC and LCIC (B) and CNIC (C). (o) Baseline CSI with its low and high 95%
629 bootstrapped C.I. values (−). (○) CSI value under the ACh application. (•) Absolute
630 difference (expressed in positive values) between the CSI under the baseline and ACh
631 condition. The change exerted by ACh on the CSI of neurons from the RCIC was fitted by
632 a Gaussian curve (r^2 = 0.462, $p < 0.0001$, black line). **D.** The mean characteristic
633 frequencies (CF) of neurons with different CSI (sorted into groups of CSI intervals of 0.1
634 from 0.1 to 1) were fitted by a linear function (r^2 = 0.533, p = 0.016, black line) indicating
635 that neurons with low CSI are tuned to lower frequencies than those neurons with higher
636 CSI. **E.** The duration of the driving response of IC neurons with different CSI (sorted into
637 groups of CSI intervals of 0.1 from 0.1 to 1) were fitted by a linear function (r^2 = 0.526, p =
638 0.017, black line) indicating that neurons with higher CSI exhibited shorter responses than
639 those neurons with higher CSI.

640 **Figure 6. Schematic diagram of the acetylcholine effect (and gabazine for comparison**
641 **purposes) on the response (firing rate) and dynamics of adaptation (time course of**
642 **adaptation). A.** The microiontophoretic application of acetylcholine decreased the CSI by
643 selectively increasing the responses to the standard tone (blue) alone. Note that the response
644 to the deviant tone is virtually unaffected (red). **B**. The blockade of the $GABA_A$ receptors
645 using the microiontophoretic application of gabazine decreased the CSI by increasing *both*,
646 the response to the standard (blue) and deviant sound (red) as demonstrated by Perez-
647 Gonzalez et al., 2012. **C.** The time course of adaptation of the response to the standard tone
648 is affected differently by gabazine and acetylcholine. Gabazine increased the three

649 components of adaptation, *i.e.*, the fast and slow decay as well as the sustained component

650 of adaptation while the acetylcholine increased the sustained component only.

651

REFERENCES

Abolafia JM, Vergara R, Arnold MM, Reig R, Sanchez-Vives MV (2011) Cortical auditory adaptation in the awake rat and the role of potassium currents. Cereb Cortex 21:977-990.

Anderson LA, Malmierca MS (2012) The effect of auditory cortex deactivation on stimulus-specific adaptation in the inferior colliculus of the rat. Eur J Neurosci 37:52-62.

Antunes FM, Nelken I, Covey E, Malmierca MS (2010) Stimulus-specific adaptation in the auditory thalamus of the anesthetized rat. PLoS One 5:e14071.

Ashe, J. H., McKenna, T. M., & Weinberger, N. M. (1989). Cholinergic modulation of frequency receptive fields in auditory cortex: II. Frequency-specific effects of anticholinesterases provide evidence for a modulatory action of endogenous ACh. Synapse, 4(1), 44–54.

Ayala YA, Malmierca MS (2013) Stimulus-specific adaptation and deviance detection in the inferior colliculus. Front Neural Circuits 6:89.

Ayala YA, Malmierca MS (2014) Cholinergic modulation of stimulus-specific adaptation in the inferior colliculus. FENS-0809. 9th FENS Forum of Neuroscience. Milan. Italy.

Ayala YA, Malmierca MS (2015) Modulation of auditory deviant saliency in the inferior collisulus. PS-430. ARO MidWinter Meeting. Baltimore. USA.

Ayala YA, Udeh A, Dutta K, Bishop D, Malmierca MS, Oliver DL (2015) Differences in the strength of cortical and brainstem inputs to SSA and non-SSA neurons in the inferior colliculus. Scientific Rep. *In press.*

676 Ayala YA, Perez-Gonzalez D, Duque D, Nelken I, Malmierca MS (2013) Frequency
677 discrimination and stimulus deviance in the inferior colliculus and cochlear nucleus.
678 Front Neural Circuits 6:119.
679 Bajo VM, Leach ND, Cordery PM, Nodal FR, King AJ (2014) The cholinergic basal
680 forebrain in the ferret and its inputs to the auditory cortex. Eur J Neurosci 40:2922-
681 2940.
682 Barkai E, Hasselmo ME (1994) Modulation of the input/output function of rat piriform
683 cortex pyramidal cells. J Neurophysiol 72:644-658.
684 Boucetta S, Jones BE (2009) Activity profiles of cholinergic and intermingled GABAergic
685 and putative glutamatergic neurons in the pontomesencephalic tegmentum of
686 urethane-anesthetized rats. J Neurosci 29:4664-4674.
687 Clarke PB, Pert CB, Pert A (1984) Autoradiographic distribution of nicotine receptors in rat
688 brain. Brain Res 323:390-395.
689 Clarke PB, Schwartz RD, Paul SM, Pert CB, Pert A (1985) Nicotinic binding in rat brain:
690 autoradiographic comparison of [3H]acetylcholine, [3H]nicotine, and [125I]-alpha-
691 bungarotoxin. J Neurosci 5:1307-1315.
692 Cole AE, Nicoll RA (1984) The pharmacology of cholinergic excitatory responses in
693 hippocampal pyramidal cells. Brain Res 305:283-290.
694 Cortes R, Palacios JM (1986) Muscarinic cholinergic receptor subtypes in the rat brain. I.
695 Quantitative autoradiographic studies. Brain Res 362:227-238.
696 Deco G, Thiele A (2009) Attention: oscillations and neuropharmacology. Eur J Neurosci
697 30:347-354.

698 Deco G, Thiele A (2011) Cholinergic control of cortical network interactions enables
699 feedback-mediated attentional modulation. Eur J Neurosci 34:146-157.
700 Disney AA, Aoki C, Hawken MJ (2007) Gain modulation by nicotine in macaque v1.
701 Neuron 56:701-713.
702 Disney AA, Aoki C, Hawken MJ (2012) Cholinergic suppression of visual responses in
703 primate V1 is mediated by GABAergic inhibition. J Neurophysiol 108:1907-1923.
704 Duque D, Malmierca MS (2014) Stimulus-specific adaptation in the inferior colliculus of
705 the mouse: anesthesia and spontaneous activity effects. Brain Struct Funct.
706 Edeline JM, Hars B, Maho C, Hennevin E (1994) Transient and prolonged facilitation of
707 tone-evoked responses induced by basal forebrain stimulations in the rat auditory
708 cortex. Exp Brain Res 97:373-386.
709 Escera C, Malmierca MS (2014) The auditory novelty system: an attempt to integrate
710 human and animal research. Psychophysiology 51:111-123
711 Farley BJ, Quirk MC, Doherty JJ, Christian EP (2010) Stimulus-specific adaptation in
712 auditory cortex is an NMDA-independent process distinct from the sensory novelty
713 encoded by the mismatch negativity. J Neurosci 30:16475-16484.
714 Farley GR, Morley BJ, Javel E, Gorga MP (1983) Single-unit responses to cholinergic
715 agents in the rat inferior colliculus. Hear Res 11:73-91.
716 Faure PA, Fremouw T, Casseday JH, Covey E (2003) Temporal masking reveals properties
717 of sound-evoked inhibition in duration-tuned neurons of the inferior colliculus. J
718 Neurosci 23:3052-3065.

719 Flores-Hernandez J, Salgado H, De La Rosa V, Avila-Ruiz T, Torres-Ramirez O, Lopez-
720 Lopez G, Atzori M (2009) Cholinergic direct inhibition of N-methyl-D aspartate
721 receptor-mediated currents in the rat neocortex. Synapse 63:308-318.
722 Friston K (2005) A theory of cortical responses. Philos Trans R Soc Lond B Biol Sci
723 360:815-836.
724 Friston K (2008) Hierarchical models in the brain. PLoS Comput Biol 4:e1000211.
725 Froemke RC, Merzenich MM, Schreiner CE (2007) A synaptic memory trace for cortical
726 receptive field plasticity. Nature 450:425-429.
727 Garcia-Rill E (1991) The pedunculopontine nucleus. Prog Neurobiol 36:363-389.
728 Goldstein-Daruech N, Pedemonte M, Inderkum A, Velluti RA (2002) Effects of excitatory
729 amino acid antagonists on the activity of inferior colliculus neurons during sleep
730 and wakefulness. Hear Res 168:174-180.
731 Grimm S, Escera C (2012) Auditory deviance detection revisited: evidence for a
732 hierarchical novelty system. Int J Psychophysiol 85:88-92
733 Grupe M, Grunnet M, Laursen B, Bastlund, JF (2013) Neuropharmacol ogical modulation
734 of the P3-like event-related potential in a rat two-tone auditory discrimin ation task
735 with modafinil and NS9283, a positive allosteric modulator of a4b2 nAChRs J
736 Neuropharm 79: 444-455.
737 Habbicht H, Vater M (1996) A microiontophoretic study of acetylcholine effects in the
738 inferior colliculus of horseshoe bats: implications for a modulatory role. Brain Res
739 724:169-179.
740 Hasselmo ME, Bower JM (1992) Cholinergic suppression specific to intrinsic not afferent
741 fiber synapses in rat piriform (olfactory) cortex. J Neurophysiol 67:1222-1229.

742 Hasselmo ME, McGaughy J (2004) High acetylcholine levels set circuit dynamics for
743 attention and encoding and low acetylcholine levels set dynamics for consolidation.
744 Prog Brain Res 145:207-231.
745 Havey DC, Caspary DM (1980) A simple technique for constructing 'piggy-back'
746 multibarrel microelectrodes. Electroencephalogr Clin Neurophysiol 48: 249-251
747 Hernandez O, Espinosa N, Perez-Gonzalez D, Malmierca MS (2005) The inferior colliculus
748 of the rat: a quantitative analysis of monaural frequency response areas.
749 Neuroscience 132:203-217.
750 Himmelheber, A., Sarter, M. and Bruno, J. (2000) Increases in cortical acetylcholine
751 release during sustained attention performance in rats. Cognitive Brain Research, 9:
752 313–325.
753 Hsieh CY, Cruikshank SJ, Metherate R (2000) Differential modulation of auditory
754 thalamocortical and intracortical synaptic transmission by cholinergic agonist. Brain
755 Res 880:51-64.
756 Ji W, Gao E, Suga N (2001) Effects of acetylcholine and atropine on plasticity of central
757 auditory neurons caused by conditioning in bats. J Neurophysiol 86:211-225.
758 Jones BE (2008) Modulation of cortical activation and behavioral arousal by cholinergic
759 and orexinergic systems. Ann N Y Acad Sci 1129:26-34.
760 Kametani, H. and Kawamura, H. (1990) Alterations in
761 acetylcholine release in the rat hippocampus during sleep wakefulness detected by
762 intracerebral dialysis. Life Sci., 47: 421–426.
763 Kelly JB, Caspary DM (2005) Pharmacology of the inferior colliculus. In: The Inferior
764 Colliculus (Winer JA, Schreiner CE, eds), pp 248-281. New York: Springer.

765 Kiebel SJ, Daunizeau J, Friston KJ (2009) Perception and hierarchical dynamics. Front
766 Neuroinform 3:20.
767 Kimura F (2000) Cholinergic modulation of cortical function: a hypothetical role in shifting
768 the dynamics in cortical network. Neurosci Res 38:19-26.
769 Knott V, Impey D, Philippe T, Smith D, Choueiry J, de la Salle S, Dort H (2014)
770 Modulation of auditory deviance detection by acute nicotine is baseline and deviant
771 dependent in healthy nonsmokers: a mismatch negativity study. Hum
772 Psychopharmacol 29:446-458.
773 Kok P, Rahnev D, Jehee JF, Lau HC, de Lange FP (2012). Attention reverses the effect of
774 prediction in silencing sensory signals. Cereb Cortex 22:2197-2206.
775 Krause M, Pedarzani P (2000) A protein phosphatase is involved in the cholinergic
776 suppression of the Ca(2+)-activated K(+) current sI(AHP) in hippocampal
777 pyramidal neurons. Neuropharmacology 39:1274-1283.
778 Krnjevic K (2004) Synaptic mechanisms modulated by acetylcholine in cerebral cortex.
779 Prog Brain Res 145:81-93.
780 Kruglikov I, Rudy B (2008) Perisomatic GABA release and thalamocortical integration
781 onto neocortical excitatory cells are regulated by neuromodulators. Neuron 58:911-
782 924.
783 LeBeau FE, Malmierca MS, Rees A (2001) Iontophoresis in vivo demonstrates a key role
784 for GABA(A) and glycinergic inhibition in shaping frequency response areas in the
785 inferior colliculus of guinea pig. J Neurosci 21:7303-7312.

786 Levy RB, Aoki C (2002) Alpha7 nicotinic acetylcholine receptors occur at postsynaptic
787 densities of AMPA receptor-positive and -negative excitatory synapses in rat
788 sensory cortex. J Neurosci 22:5001-5015.
789 Liang K, Poytress BS, Weinberger NM, Metherate R (2008) Nicotinic modulation of tone-
790 evoked responses in auditory cortex reflects the strength of prior auditory learning.
791 Neurobiol Learn Mem 90:138-146.
792 Loftus WC, Malmierca MS, Bishop DC, Oliver DL (2008) The cytoarchitecture of the
793 inferior colliculus revisited: a common organization of the lateral cortex in rat and
794 cat. Neuroscience 12:196-205.
795 Lumani A, Zhang H (2010) Responses of neurons in the rat's dorsal cortex of the inferior
796 colliculus to monaural tone bursts. Brain Res 1351:115-129.
797 Malmierca MS, Cristaudo S, Perez-Gonzalez D, Covey E (2009) Stimulus-specific
798 adaptation in the inferior colliculus of the anesthetized rat. J Neurosci 29:5483-
799 5493.
800 Malmierca MS, Sanchez-Vives MV, Escera C, Bendixen A (2014) Neuronal adaptation,
801 novelty detection and regularity encoding in audition. Front Syst Neurosci 8:111.
802 Martin-Cortecero J, Nunez A (2014) Tactile response adaptation to whisker stimulation in
803 the lemniscal somatosensory pathway of rats. Brain Res 1591C:27-37.
804 Marrosu, F., Portas, C., Mascia, M.S., Casu, M.A., Fa, M., Giagheddu, M., Imperato, A.
805 and Gessa, G.L. (1995) Microdialysis measurement of cortical and hippocampal
806 acetylcholine release during sleep-wake cycle in freely moving cats. Brain Res.,
807 671: 329–332

808 McCormick DA (1993) Actions of acetylcholine in the cerebral cortex and thalamus and
809 implications for function. Prog Brain Res 98:303-308.
810 McCormick DA, Prince DA (1986) Acetylcholine induces burst firing in thalamic reticular
811 neurones by activating a potassium conductance. Nature 319:402-405.
812 Ma, X., & Suga, N. (2005). Long-term cortical plasticity evoked by electric stimulation and
813 acetylcholine applied to the auditory cortex. Proceedings of the National Academy of
814 Sciences of the United States of America, 102(26), 9335–9340.

815 Malmierca MS, Hernandez O, Falconi A, Lopez-Poveda EA, Merchan M, Rees A (2003)
816 The commissure of the inferior colliculus shapes frequency response areas in rat: an
817 in vivo study using reversible blockade with microinjection of kynurenic acid. Exp
818 Brain Res 153:522-529.

819 Malmierca MS, Izquierdo MA, Cristaudo S, Hernandez O, Perez-Gonzalez D, Covey E,
820 Oliver DL (2008) A discontinuous tonotopic organization in the inferior colliculus
821 of the rat. J Neurosci 28:4767-4776.
822 Malmierca MS, Sanchez-Vives MV, Escera C, Bendixen A (2014) Neuronal adaptation,
823 novelty detection and regularity encoding in audition. Front Syst Neurosci, 8:111.
824 doi:10.3389/fnsys.2014.00111

825 Merrill EG, Ainsworth A (1972) Glass-coated platinum coated tungsten microelectrodes.
826 Med Biol Eng 10:662– 672.

827 Metherate R (2004) Nicotinic acetylcholine receptors in sensory cortex. Learn Mem 11:50-
828 59.

829 Metherate R (2011) Functional connectivity and cholinergic modulation in auditory cortex.
830 Neurosci Biobehav Rev 35:2058-2063.
831 Metherate R, Ashe JH (1993) Nucleus basalis stimulation facilitates thalamocortical
832 synaptic transmission in the rat auditory cortex. Synapse 14:132-143.
833 Metherate R, Hsieh CY (2003) Regulation of glutamate synapses by nicotinic acetylcholine
834 receptors in auditory cortex. Neurobiol Learn Mem 80:285-290.
835 Metherate R, Weinberger NM (1989) Acetylcholine produces stimulus-specific receptive
836 field alterations in cat auditory cortex. Brain Res 480:372-377.
837 Metherate, R. and Weinberger, N.M. (1990) Cholinergic modulation of responses to single
838 tones produces tone-specific receptive-field alterations in cat auditory-cortex.
839 Synapse 6: 133–145.
840 Metherate, R., Ashe, J.H. and Weinberger, N.M. (1990) Acetylcholine modifies neuronal
841 acoustic rate level functions in guinea pig auditory cortex by an action at muscarinic
842 receptors. Synapse 6: 364–368.
843 Metherate R, Cox CL, Ashe JH (1992) Cellular bases of neocortical activation: modulation
844 of neural oscillations by the nucleus basalis and endogenous acetylcholine. J
845 Neurosci 12:4701-4711.
846 Moran RJ, Campo P, Symmonds M, Stephan KE, Dolan RJ, Friston KJ (2013) Free energy,
847 precision and learning: the role of cholinergic neuromodulation. J Neurosci
848 33:8227-8236.
849 Morley BJ, Kemp GE (1981) Characterization of a putative nicotinic acetylcholine receptor
850 in mammalian brain. Brain Res 228:81-104.

851 Motts SD, Schofield BR (2009) Sources of cholinergic input to the inferior colliculus.
852 Neuroscience 160:103-114.
853 Näätänen R (1992) Attention and brain function. Hillsdale, NJ: Lawrence Erlbaum.
854 Nelken I, Ulanovsky N (2007) Mismatch negativity and simulus-specific adaptation in
855 animal models. J Psychophysiol 21:214 –223.
856 Nelken I (2014) Stimulus-specific adaptation and deviance detection in the auditory
857 system: experiments and models. Biol Cybern doi:10.1007/s00422-014-0585-7
858 Passetti F, Dalley JW, O'Connell MT, Everitt BJ, Robbins TW (2000) Increased
859 acetylcholine release in the rat medial prefrontal cortex during performance of a
860 visual attentional task. Eur J Neurosci 12:3051-3058.
861 Paxinos G, Watson C (2005) The rat brain in stereotaxic coordinates. Burlington, VT:
862 Elsevier-Academic.
863 Pérez-González D, Malmierca MS, Covey E (2005) Novelty detector neurons in the
864 mammalian auditory midbrain. Eur J Neurosci 22:2879-2885.
865 Perez-Gonzalez D, Hernandez O, Covey E, Malmierca MS (2012) GABA(A)-Mediated
866 Inhibition Modulates Stimulus-Specific Adaptation in the Inferior Colliculus. PLoS
867 One 7:e34297.
868 Picciotto MR, Higley MJ, Mineur YS (2012). Acetylcholine as a neuromodulator:
869 cholinergic signaling shapes nervous system function and behavior. Neuron 76:116-
870 129.
871 Poorthuis RB, Goriounova NA, Couey JJ, Mansvelder HD (2009) Nicotinic actions on
872 neuronal networks for cognition: general principles and long-term consequences.
873 Biochem Pharmacol 78:668-676.

874 Ranganath C, Rainer G (2003) Neural mechanisms for detecting and remembering novel
875 events. Nat Rev Neurosci 4:193-202.
876 Rees A (1990) A close-field sound system for auditory neurophysiology. J of Physiol
877 430:2.
878 Rees A, Sarbaz A, Malmierca MS, Le Beau FE (1997) Regularity of firing of neurons in
879 the inferior colliculus. J Neurophysiol 77:2945-2965.
880 Richardson BD, Hancock KE, Caspary DM (2013) Stimulus-specific adaptation in auditory
881 thalamus of young and aged awake rats. J Neurophysiol 110:1892-1902.
882 Rotter A, Birdsall NJ, Field PM, Raisman G (1979) Muscarinic receptors in the central
883 nervous system of the rat. II. Distribution of binding of [3H]propylbenzilylcholine
884 mustard in the midbrain and hindbrain. Brain Res 180:167-183.
885 Salgado H, Bellay T, Nichols JA, Bose M, Martinolich L, Perrotti L, Atzori M (2007)
886 Muscarinic M2 and M1 receptors reduce GABA release by Ca2+ channel
887 modulation through activation of PI3K/Ca2+ -independent and PLC/Ca2+ -
888 dependent PKC. J Neurophysiol 98:952-965.
889 Sanchez-Vives, M. V., Nowak, L. G., and McCormick, D. A. (2000a). Cellular
890 mechanisms of long-lasting adaptation in visual cortical neurons in vitro.
891 J. Neurosci. 20, 4286–4299.
892 Sanchez-Vives, M. V., Nowak, L. G., and McCormick, D. A. (2000b). Membrane
893 mechanisms underlying contrast adaptation in cat area 17 in vivo. J. Neurosci.
894 20, 4267–4285.

895 Sarter M, Hasselmo ME, Bruno JP, Givens B (2005) Unraveling the attentional functions
896 of cortical cholinergic inputs: interactions between signal-driven and cognitive
897 modulation of signal detection. Brain Res Rev 48:98–111. CrossRef Medline
898 Schofield BR (2010) Projections from auditory cortex to midbrain cholinergic neurons that
899 project to the inferior colliculus. Neuroscience 166:231-240.
900 Schofield BR, Motts SD (2009) Projections from auditory cortex to cholinergic cells in the
901 midbrain tegmentum of guinea pigs. Brain Res Bull 80:163-170.
902 Schofield BR, Motts SD, Mellott JG (2011) Cholinergic cells of the pontomesencephalic
903 tegmentum: connections with auditory structures from cochlear nucleus to cortex.
904 Hear Res 279:85-95.
905 Steriade M, Pare D, Parent A, Smith Y (1988) Projections of cholinergic and non-
906 cholinergic neurons of the brainstem core to relay and associational thalamic nuclei
907 in the cat and macaque monkey. Neuroscience 25:47-67.
908 Thiele A (2013) Muscarinic signaling in the brain. Annu Rev Neurosci 36:271-294.
909 Thiel CM, Fink GR (2008) Effects of the cholinergic agonist nicotine on reorienting of
910 visual spatial attention and top-down attentional control. Neuroscience 152:381–
911 390.
912 Todorovic A, van Ede F, Maris E, de Lange FP (2011) Prior expectation mediates neural
913 adaptation to repeated sound in the auditory cortex: an MEG study. J Neurosc 31:
914 9118-9123.
915 von der Behrens W, Bauerle P, Kossl M, Gaese BH (2009) Correlating stimulus-specific
916 adaptation of cortical neurons and local field potentials in the awake rat. J Neurosci
917 29:13837-13849.

918 Watanabe T, Simada Z (1973) Pharmacological properties of cat's collicular auditory
919 neurons. Jpn J Physiol 23:291-308.
920 Watkins PV, Barbour DL (2011) Level-tuned neurons in primary auditory cortex adapt
921 differently to loud versus soft sounds. Cereb Cortex 21:178-190.
922 Zaborszky L, Van den A, Gyengesi E (2012) The basal forebrain cholinergic projection
923 system in mice. In: Watson C, Paxinos G, Puelles L, editors. The mouse nervous
924 system. 1st ed. Amsterdam: Elsevier. p. 684-718.
925 Zhang W, Yamada M, Gomeza J, Basile AS, Wess J (2002) Multiple muscarinic
926 acetylcholine receptor subtypes modulate striatal dopamine release, as studied with
927 M1-M5 muscarinic receptor knock-out mice. J Neurosci 22:6347-6352.

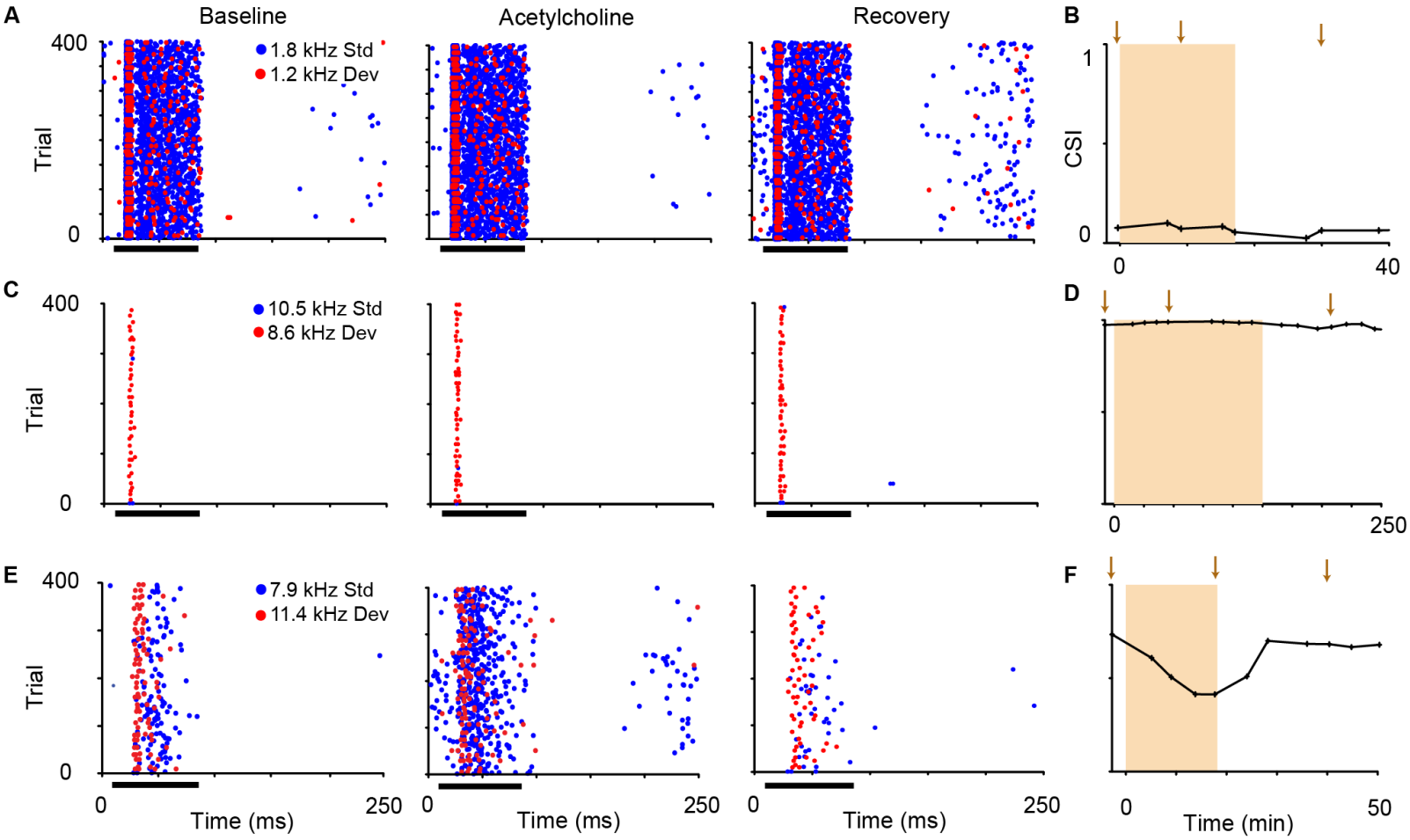
A
Baseline
Acetylcholine
Recovery
400
0
Trial
1.8 kHz Std
1.2 kHz Dev
B
1
0
CSI
0
40
C
400
0
Trial
10.5 kHz Std
8.6 kHz Dev
D
0
250
E
400
0
Trial
7.9 kHz Std
11.4 kHz Dev
0
250
Time (ms)
F
0
50
Time (min)

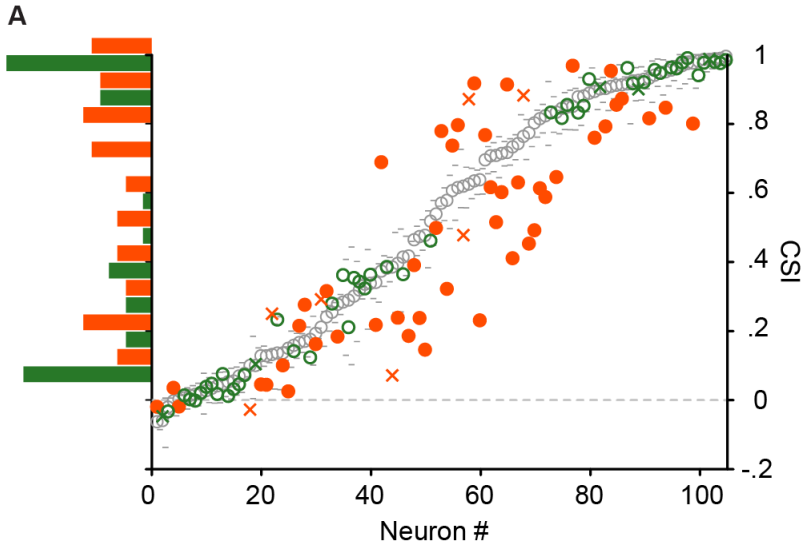
A
CSI
Neuron #

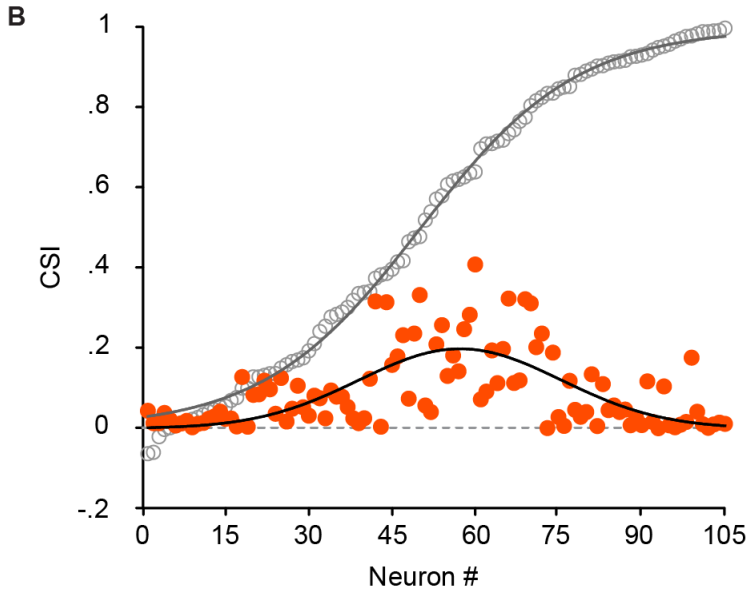
B
CSI
Neuron #

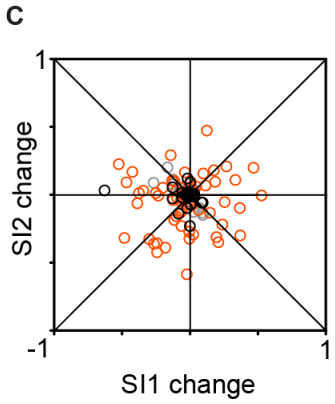
C
SI2 change
SI1 change

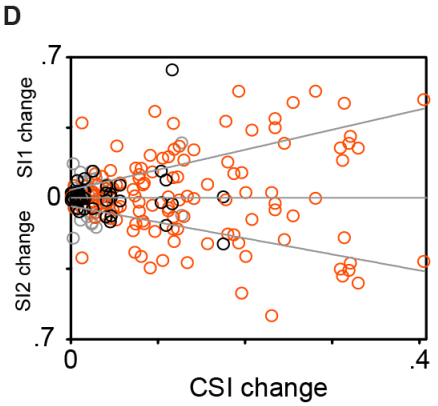
D
SI1 change
SI2 change
CSI change

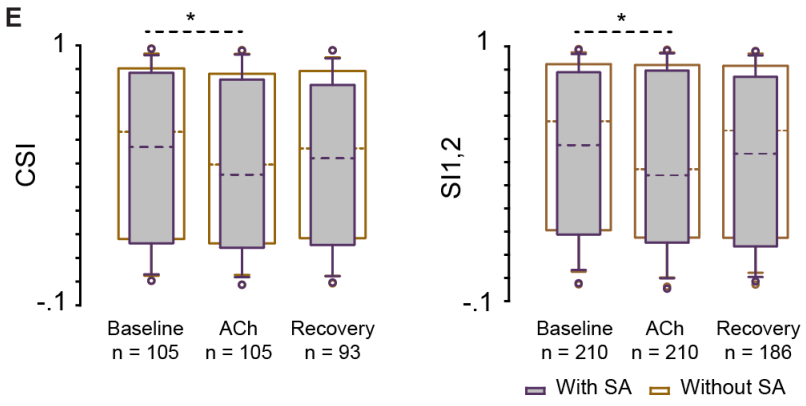
E
CSI
SI1,2
Baseline
n = 105
ACh
n = 105
Recovery
n = 93
Baseline
n = 210
ACh
n = 210
Recovery
n = 186
With SA
Without SA

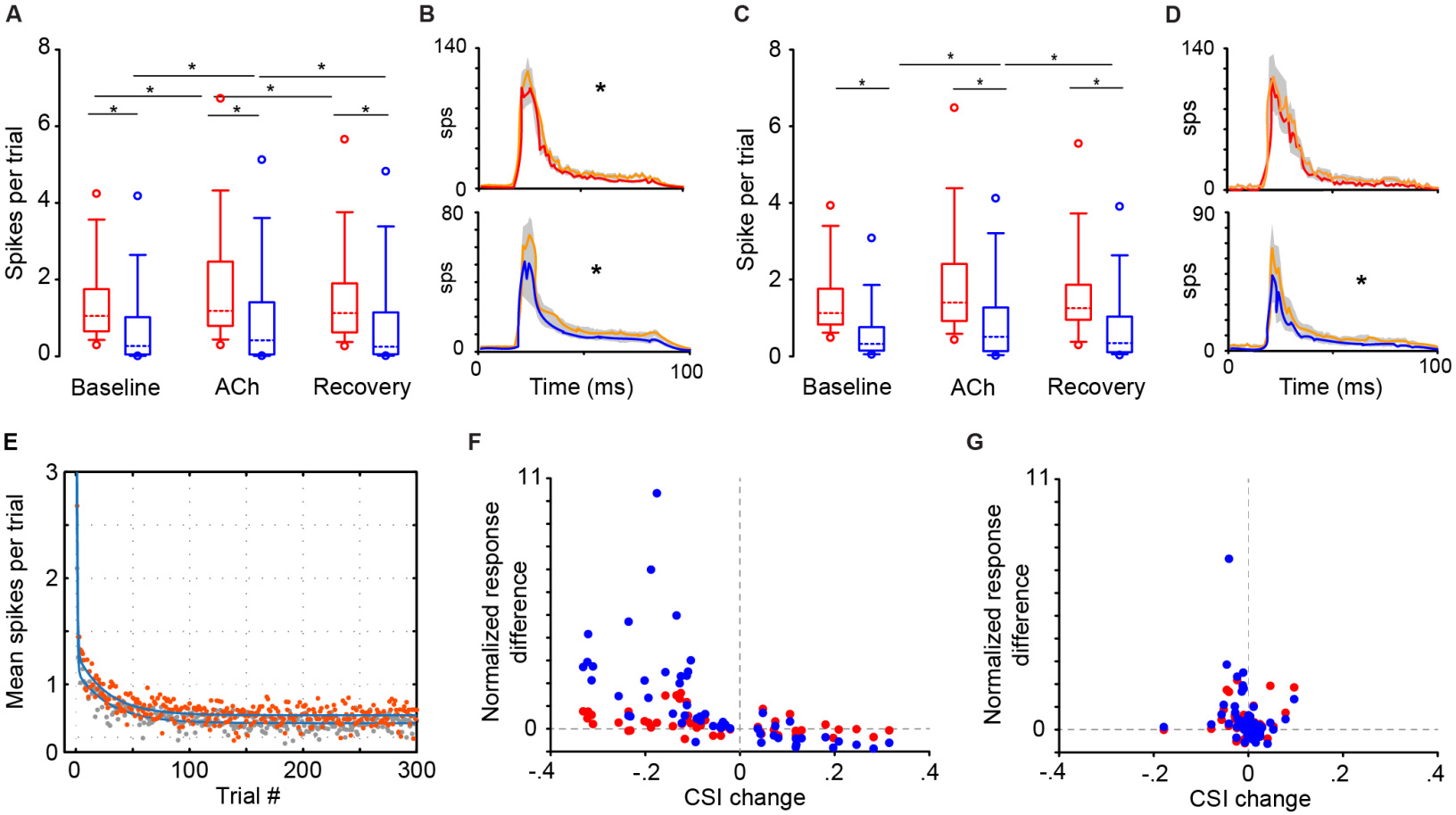
A
Spikes per trial
Baseline
ACh
Recovery
B
sps
Time (ms)
C
Spike per trial
Baseline
ACh
Recovery
D
sps
Time (ms)
E
Mean spikes per trial
Trial #
F
Normalized response difference
CSI change
G
Normalized response difference
CSI change

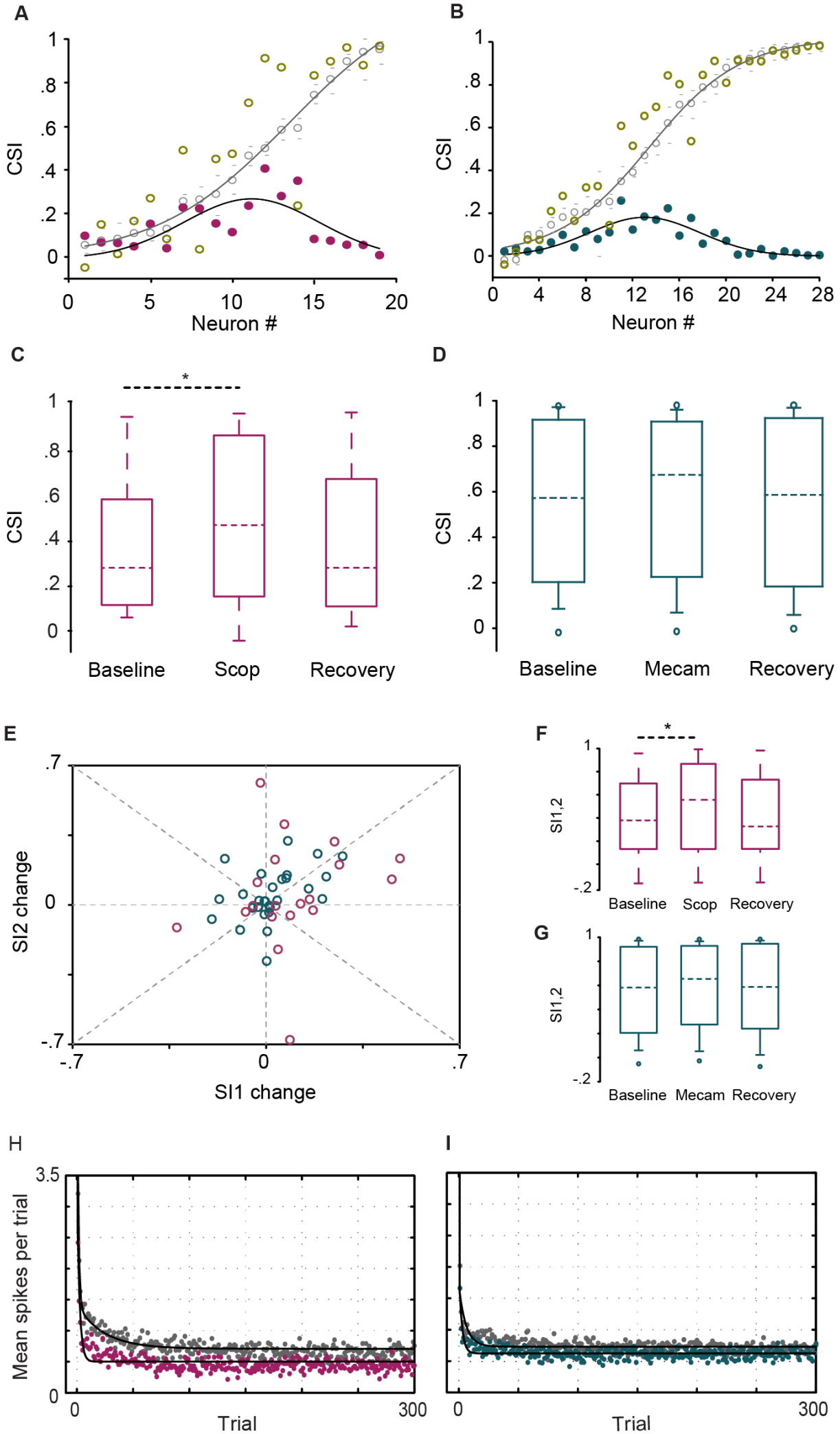
A
CSI
Neuron #
B
CSI
Neuron #
C
*
CSI
Baseline
Scop
Recovery
D
CSI
Baseline
Mecam
Recovery
E
SI2 change
SI1 change
F
*
SI1,2
Baseline
Scop
Recovery
G
SI1,2
Baseline
Mecam
Recovery
H
Mean spikes per trial
Trial
I
Trial

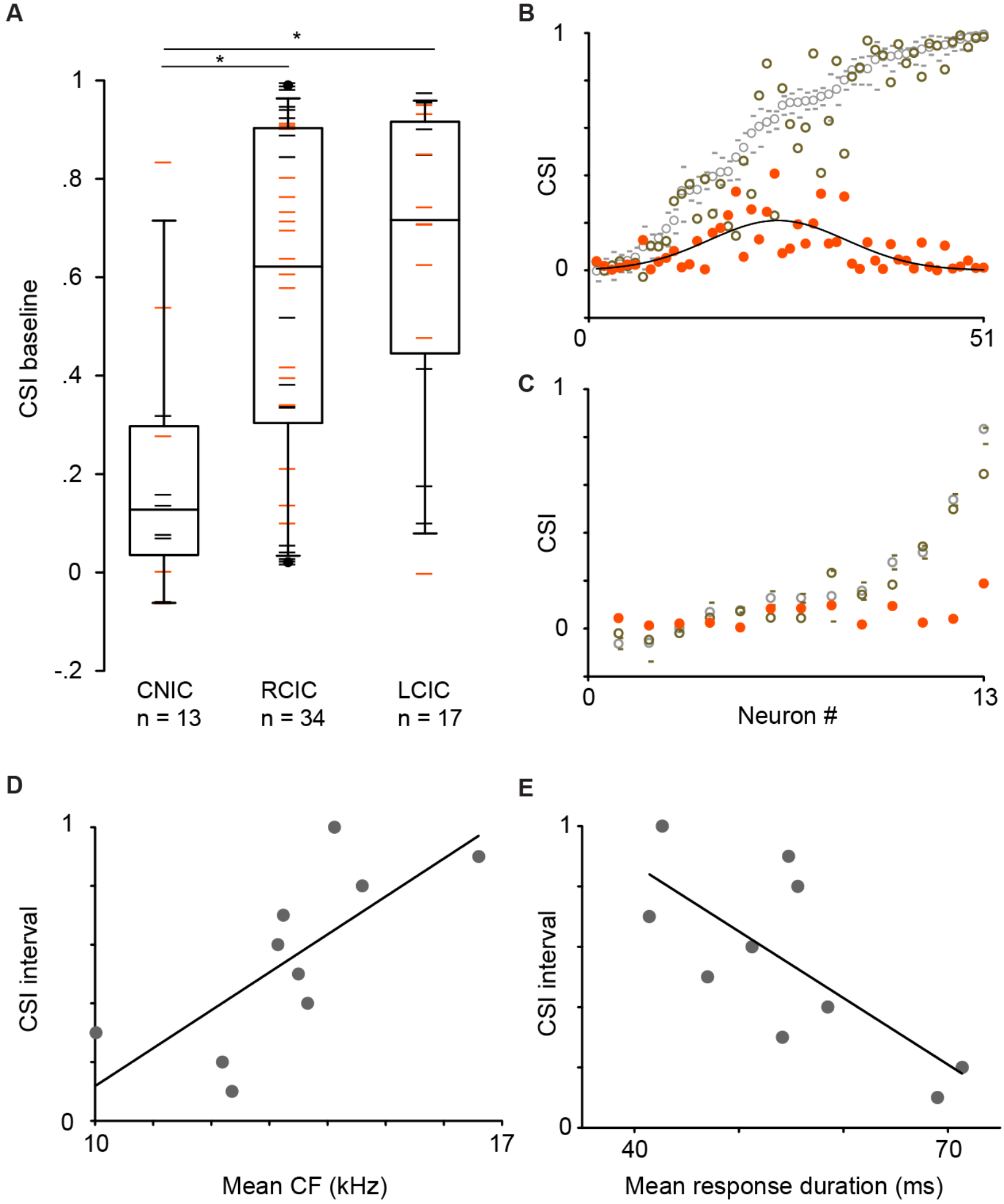
A
*
*
1
.8
.6
.4
.2
0
-.2
CSI baseline
CNIC
n = 13
RCIC
n = 34
LCIC
n = 17
B
1
CSI
0
0
51
C
1
CSI
0
0
13
Neuron #
D
1
CSI interval
0
10
17
Mean CF (kHz)
E
1
CSI interval
0
40
70
Mean response duration (ms)

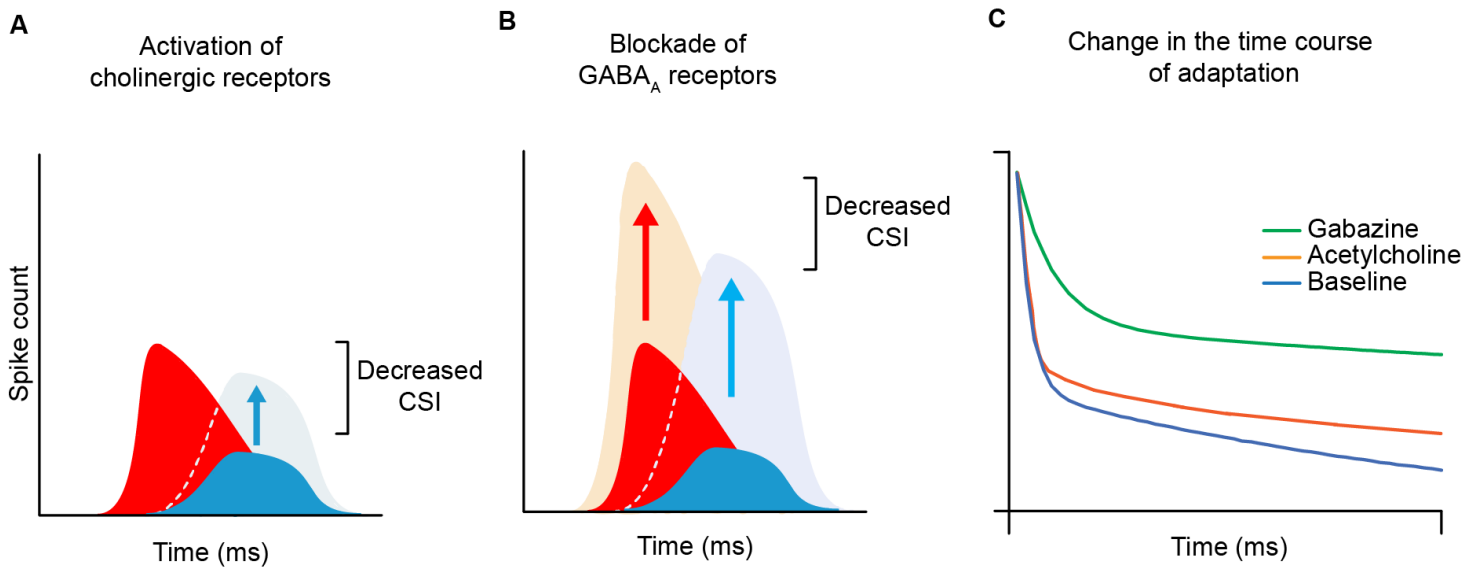
A
Activation of
cholinergic receptors
Spike count
Decreased
CSI
Time (ms)
B
Blockade of
GABA$_A$ receptors
Decreased
CSI
Time (ms)
C
Change in the time course
of adaptation
Gabazine
Acetylcholine
Baseline
Time (ms)

Cell Tissue Res
DOI 10.1007/s00441-015-2134-7

REVIEW

Deviance detection in auditory subcortical structures: what can we learn from neurochemistry and neural connectivity?

Daniel Duque · Yaneri A. Ayala · Manuel S. Malmierca

Received: 11 November 2014 / Accepted: 22 January 2015

Abstract A remarkable ability of animals that is critical for survival is to detect and respond to to unexpected stimuli in an ever-changing world. Auditory neurons that show stimulus-specific adaptation (SSA), i.e., a decrease in their response to frequently occurring stimuli while maintaining responsiveness when different stimuli are presented, might participate in the coding of deviance occurrence. Traditionally, deviance detection is measured by the mismatch negativity (MMN) potential in studies of evoked local field potentials. We present a review of the state-of-the-art of SSA in auditory subcortical nuclei, i.e., the inferior colliculus and medial geniculate body of the thalamus, and link the differential receptor distribution and neural connectivity of those regions in which extreme SSA has been found. Furthermore, we review both SSA and MMN-like responses in auditory and non-auditory areas that exhibit multimodal sensitivities that we suggest conform to a distributed network encoding for deviance detection. The understanding of the neurochemistry and response similarities across these different regions will contribute to a better understanding of the neural mechanism underlying deviance detection.

Keywords Auditory · Stimulus-specific adaptation · Mismatch negativity · Non-lemniscal · Inhibition · Deviance detection

Daniel Duque and Yaneri A. Ayala contributed equally to this work.

Financial support was provided by the Spanish MINECO (BFU2013-43608-P) and JCYL (SA343U14) to M.S.M.; D.D. held a fellowship from the Spanish MINECO (BES-2010-035649); Y.A.A. held fellowships from the Mexican CONACyT (216106) and SEP.

The funders had no role in the study design, data collection and analysis, decision to publish, or preparation of the manuscript.

D. Duque · Y. A. Ayala · M. S. Malmierca (✉)
Auditory Neuroscience Laboratory, Institute of Neuroscience of Castilla y León (INCyL), University of Salamanca, C/ Pintor Fernando Gallego, 1, Salamanca 37007, Spain
e-mail: msm@usal.es

M. S. Malmierca
Department of Cell Biology and Pathology, Faculty of Medicine, University of Salamanca, Campus Miguel de Unamuno, 37007 Salamanca, Spain

Introduction

In everyday life, animals are immersed in a continuous flow of sounds arriving from multiple sources, and the auditory system has the challenge of selecting those acoustic elements relevant for the creation of perceptual constructs (Fishman and Steinschneider 2010). One way of organizing the acoustic scene is as follows: (1) retaining it in a form of sound objects (Winkler et al. 2009), (2) storing the regularity of the objects in a sensory memory trace, (3) generating predictions about forthcoming events, and (4) comparing the subsequent incoming sounds with these predictions (Friston 2005; Bendixen et al. 2012). This is the current theoretical processing that occurs in deviance detection (Näätänen et al. 1978, 2001) in which biological systems identify new or deviant contextual events in an otherwise monotonous auditory scene.

The occurrence of auditory deviance detection has been classically associated with the human mismatch negativity (MMN) potential of the event-related potentials (Näätänen et al. 1978). MMN is classically measured by using an oddball paradigm in which a low probability of appearance (deviant) sound is randomly embedded within sequences of common (standard) sounds. MMN is defined as the difference between the event-related potentials evoked by the deviant (larger) and the standard (smaller) sounds. Human MMN peaks between the N1 (100 ms) and the P2 (180 ms) waves and can be

Published online: 08 March 2015

interpreted as an enhancement of the N1 wave or as an independent phenomenon. This differentiation is not trivial, because the N1 wave is attributed to basic auditory processing occurring in the auditory cortex (AC; Hari et al. 1984; Maess et al. 2007), and one of the current interpretations of MMN is that adaptation is related to MMN generation (Fishman and Steinschneider 2012; Fishman 2013). Two conceptually different hypotheses have been proposed to explain the neuronal mechanisms that generate MMN. The first hypothesis is based on the "predictive coding" theory (Friston 2005) that postulates that the brain performs Bayes-optimal sensory learning under uncertainty (Friston 2009, 2012; Moran et al. 2013), whereby the brain creates a prediction concerning the identity of the next sound within an ongoing acoustic sequence based on a memory trace generated by previous stimulation. The violation of the memory-based regularity by a deviant sound would allow the generation of error signals and, therefore, MMN. On the other hand, some other authors (Jaaskelainen et al. 2004; May and Tiitinen 2010) defend a second explanation, namely the so-called "neural adaptation" hypothesis, whereby MMN reflects the release from adaptation elicited by the standard stimulus by the occurrence of a deviant sound. As neurons activated by deviant sounds are stimulated much less than neurons activated by standard sounds, such neurons are consequently less adapted and would elicit a stronger response. Thus, deviant sounds are going to elicit larger responses because adaptation for the standard sound would reduce the N1 wave. To establish the occurrence of "deviance detection", i.e., the degree of enhancement in neuronal activity evoked by the occurrence of a deviant sound that is adaptation-independent, Schröger and colleagues (Schröger and Wolff 1996; Jacobsen and Schröger 2003) have designed a paradigm to control for the probability of occurrence and therefore for the adaptation elicited by the standard tone. Control paradigms have been implemented in subsequent human (Opitz et al. 2005; Maess et al. 2007; Cacciaglia et al. 2015) and animal (rat: Taaseh et al. 2011; Harms et al. 2014) studies. This approach has allowed researchers to separate the signals contributing to MMN attributable to neuronal refractoriness from those evoked by deviance occurrence.

MMN-like phenomena are well known to occur in several different animals, including cats (Csepe et al. 1987a, 1987b; Pincze et al. 2001, 2002), monkeys (Javitt et al. 1992, 1994; Fishman and Steinschneider 2012), guinea pigs (Kraus et al. 1994a, 1994b; Christianson et al. 2014), rabbits (Ruusuvirta et al. 1995a, 2010), rats (Ruusuvirta et al. 1998, 2013; Astikainen et al. 2006, 2011; Nakamura et al. 2011; Jung et al. 2013; Shiramatsu et al. 2013; Harms et al. 2014), and mice (Siegel et al. 2003; Umbricht et al. 2005). Recently, it has been reported that the rat brain is capable of generating human-MMN-like responses, and moreover, that part of the MMN signal is independent of adaptation driven by memory-like processing (Astikainen et al. 2006; Harms et al. 2014). In agreement with this study, true-deviance detection is also reflected at the single neuron level in the rat AC (Taaseh et al. 2011). Although deviance encoding has been largely thought to involve pure cortical processing, an elegant and recent study by Cacciaglia and colleagues (2015) has demonstrated that the human inferior colliculus (IC) and medial geniculate body (MGB) of the thalamus exhibit genuine deviance detection. This study confirms previous data indicating deviance detection at very short latency responses (~30–40 ms) in auditory-evoked potentials (Slabu et al. 2010, 2012).

Here, in an attempt to gain a better understanding of deviance detection, we review the anatomy and immunocytochemistry of the IC and MGB, since they might reveal the general organizational principles of the subcortical network for deviance detection. Likewise, we present data concerning auditory mismatch responses in non-auditory subcortical structures that might be part of the same network.

Stimulus-specific adaptation

Using the same oddball paradigm as in human MMN studies, Ulanovsky et al. (2003) have found that AC neurons of the cat reduce their response to frequently occurring stimuli (standard) but resume their firing when different rare stimuli are presented (deviant). This neuronal response has been referred to as stimulus-specific adaptation (SSA; Movshon and Lennie 1979). Later studies have demonstrated that SSA also occurs in the IC (rat: Perez-Gonzalez et al. 2005; Malmierca et al. 2009; Duque et al. 2012; Ayala et al. 2013) and the MGB (mouse: Anderson et al. 2009; rat: Antunes et al. 2010). By contrast, neurons in the cochlear nucleus lack SSA (rat: Ayala et al. 2013), suggesting that the IC is the first auditory relay station in which SSA occurs.

Throughout the auditory collicular, thalamic, and cortical areas, SSA has several common characteristics that are similar to the human MMN. SSA is a rapid phenomenon, with a time scale of a few seconds (Ulanovsky et al. 2004; Malmierca et al. 2009; Ayala and Malmierca 2013), and is highly sensitive to stimulus statistics: the smaller the probability of occurrence for the deviant, the larger the SSA (Ulanovsky et al. 2003; Malmierca et al. 2009; Antunes et al. 2010; Zhao et al. 2011; Ayala et al. 2013). These same studies have also revealed that increasing the frequency contrast (the physical separation between the two tones) or the presentation rate (the speed to which the tones are repeated) evokes stronger SSA responses, although SSA can be observed at interstimulus intervals as long as 2000 ms (Ulanovsky et al. 2003; Antunes et al. 2010; Ayala and Malmierca 2013, Fig. 1). As SSA in the AC was first observed in the core region of the AC (Ulanovsky et al. 2003), some authors proposed SSA emerged in the AC as a high order feature that can be "inherited" by the

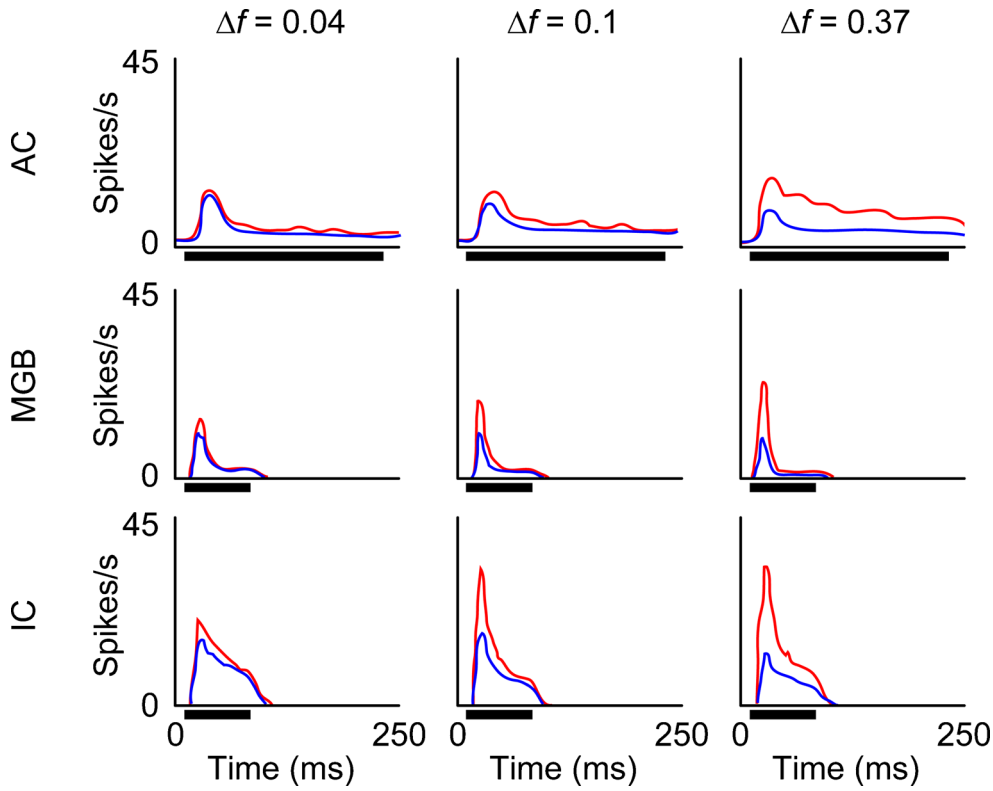

Fig. 1 Grand-average responses of neurons in the inferior colliculus (*IC*), the medial geniculate body (*MGB*), and the auditory cortex (*AC*). Averaged peristimulus time histograms (PSTH) for the entire population of neurons recorded at various frequency contrasts (Δ*f*) for a standard/deviant ratio of 90/10 %. The mean firing rate elicited by both stimuli (*blue lines* standard, *red lines* deviant) increased at the different Δ*f* (Δ*f*=0.04, 0.1, and 0.37; from *left to right*, respectively). *Black horizontal lines* under the PSTHs indicate the duration of the stimulus: 230 ms for the AC study and 75 ms for the IC and MGB studies (modified from Ulanovsky et al. 2003; Malmierca et al. 2009; Antunes et al. 2010)

IC and the MGB via the corticofugal pathway (Nelken and Ulanovsky 2007; Bäuerle et al. 2011). However, recent studies with the powerful technique of cortical cooling (Antunes and Malmierca 2011; Anderson and Malmierca 2013) have demonstrated that the corticofugal projections arising from the core AC regions modulate, but do not generate, subcortical SSA. Currently, SSA is thought to be created de novo at each auditory station or to be transmitted in a cascade process from low to higher order nuclei. In this review, we will describe possible mechanisms involved in SSA, with special emphasis on the anatomical substrate that might underlie the connectivity of SSA neurons and on the receptor distributions in the subcortical nuclei of the IC and the MGB.

Throughout the following, SSA will be used to describe a specific reduction of the responses at a neuronal level, whereas MMN (or MMN-like) will be used for differential responses observed at local field potentials. Conceptually, this is different from deviance detection, which refers to an enhancement in the neuronal response evoked by the occurrence of a rare sound and which is independent of adaptation.

SSA is not homogenously distributed in IC and MGB; connectivity of lemniscal and non-lemniscal subdivisions

Auditory processing between the midbrain and the cortex is carried by two parallel streams: the lemniscal (or primary) and non-lemiscal (or secondary) pathways (Fig. 2; Andersen et al. 1980; Lee and Sherman 2010, 2011). The non-lemniscal system comprises the lateral (LCIC), the rostral (RCIC), and the dorsal cortex (DCIC; Loftus et al. 2008, 2010) of the IC and the dorsal (MGBd) and medial subdivisions (MGBm) of the MGB in the thalamus. On the other hand, the lemniscal system comprises the central nucleus of the IC (CNIC) and the ventral division of the MGB (MGBv). Across these subcortical nuclei, SSA responses are not homogenously distributed. Neurons in the cortices of the IC (rat: Malmierca et al. 2009; Duque et al. 2012; Ayala et al. 2013) and in the MGBd and MGBm (mouse: Anderson et al. 2009; rat: Antunes et al. 2010) exhibit the strongest SSA responses. In agreement with SSA data, a pioneering study by Kraus et al. (1994b) has shown that auditory stimuli containing different frequencies or intensities consistently produce a mismatched field potential in the non-lemniscal divisions of the thalamus but not in the MGBv of the guinea pig (Fig. 3). Although such correlation has not been confirmed in the rat AC (Fig. 3, Nakamura et al. 2011; Jung et al. 2013; Shiramatsu et al. 2013), all these data suggest that subcortical acoustic deviance detection is primarily computed by neurons of the non-lemniscal pathway.

Lemniscal and non-lemniscal neurons differ in (1) their response properties (cat: Aitkin et al. 1975; Calford 1983; Calford and Aitkin 1983; Aitkin and Prain 1974; mouse: Anderson and Linden 2011; rat: Lumani and Zhang 2010), (2) their fine morphology, i.e., terminal size and arborization pattern (Oliver 2005; rat: Malmierca et al. 1995; 2011; Stebbings et al. 2014), and in (3) their set of afferent and

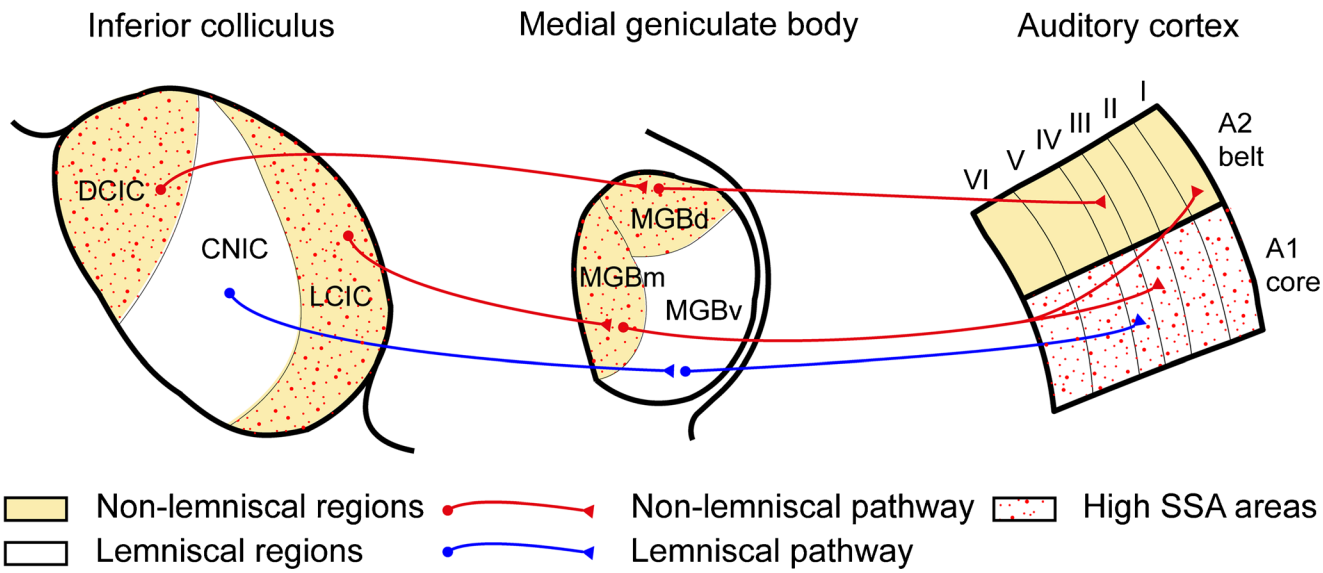

Fig. 2 Topographic segregation of the lemniscal and non-lemniscal projections between the inferior colliculus (IC), medial geniculate body (MGB) and auditory cortex (AC). The strongest SSA responses are distributed in the non-lemniscal subdivisions (*shaded areas*) of the IC (*DCIC* dorsal cortex, *LCIC* lateral cortex, *RCIC* rostral cortex) and MGB (*MGBd* dorsal subdivision, *MGBm* medial subdivision). On the contrary, poor SSA responses are found in the lemniscal areas of the IC (*CNIC* central nucleus) and MGB (*MGBv* ventral subdivision). At the cortical level, the primary auditory cortex (*A1*) exhibits SSA responses that remain to be addressed in areas beyond A1. The major bottom-up projections between non-lemniscal (*red*) and lemniscal (*blue*) collicular, thalamic, and cortical areas are illustrated by *lines* (modified from Escera and Malmierca 2014)

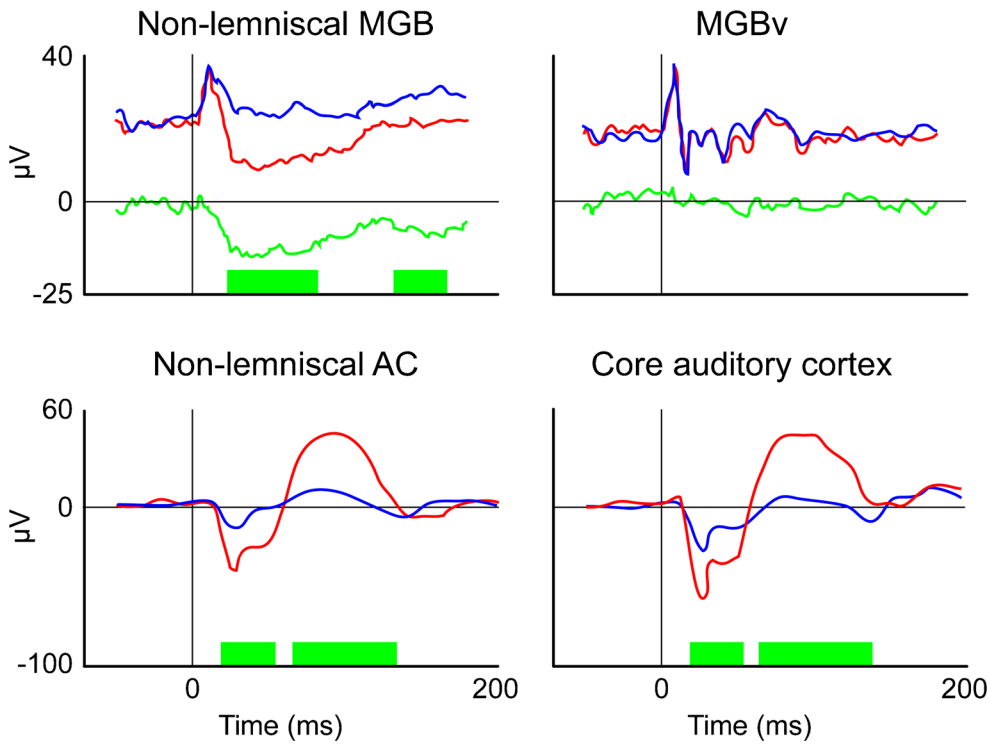

Fig. 3 Comparison of MMN-like responses through the lemniscal and non-lemniscal regions of the medial geniculate body (*MGB*) and the auditory cortex (*AC*). *Top* Grand average responses to standard (*blue lines*) and deviant (*red lines*) stimuli recorded from the non-lemniscal MGB (*left* caudomedial portion of the guinea pig equivalent to the cat MGBm and MGBd) and the MGBv (*right*). Significant differences between the responses to standard and deviant stimuli are indicated by the *green boxes* that appear *under* the various waves (*green lines*). *Bottom* Auditory evoked potentials to deviant (*red lines*) and standard stimuli (*blue lines*) elicited in a non-lemniscal region of the AC (*left* posterior auditory field) and in the core region of the AC of the rat (*right*). Significant differences between the responses to standard and deviant stimuli are indicated by the *green boxes*. Unlike the MGB, MMN-like waves in the AC have not been shown to be spatially distributed (modified from Kraus et al. 1994a; Jung et al. 2013)

efferent projections (rat: Coleman and Clerici 1987; Malmierca and Hackett 2010; for reviews, see Hu 2003; Lee and Sherman 2011). Lemniscal neurons are tonotopically organized exhibiting fast and high-fidelity responses (cat: Miller et al. 2001; rat: Malmierca et al. 2008), whereas non-lemniscal neurons are not tonotopically organized and show longer latencies and habituating responses to unvarying stimuli (cat: Calford 1983; Calford and Aitkin 1983; rat: Bordi and LeDoux 1994a, 1994b; Malmierca et al. 2009; guinea pig: He and Hu 2002). Furthermore, non-lemniscal neurons show broader frequency response areas, i.e., the combination of frequencies and intensities capable of evoking a response (Lennartz and Weinberger 1992; Perez-Gonzalez et al. 2005; Malmierca et al. 2009; Duque et al. 2012; Ayala et al. 2013) and respond preferentially to complex acoustic stimuli (cat: Aitkin et al. 1975). Moreover, the basal discharge and response strength are lower in the non-lemniscal than lemniscal neurons of the IC (rat: Duque et al. 2012) and MGB (cat: Aitkin and Prain 1974; Calford and Aitkin 1983). Interestingly, both the bandwidth of the frequency responses areas (rat: Duque et al. 2012; Ayala et al. 2013) and the onset firing pattern (rat: Duque et al. 2012) correlates with the strength of the SSA responses of IC neurons. Regarding their connectivity, the CNIC primarily sends excitatory and inhibitory projections to the MGBv (for reviews, see Oliver and Huerta 1992; Wenstrup 2005) with a high degree of topographic convergence (Lee and Sherman 2011), whereas the cortices of the IC innervate primarily the MGBd and MGBm (mouse: Romand and Ehret 1990; for reviews, see Hu 2003; Wenstrup 2005). At the level of the MGB, two major afferent streams arise en route to the auditory cortices (cat: Huang and Winer 2000; for a review, see Hu 2003). Generally speaking, secondary auditory cortices are targeted principally by non-tonotopic subcortical areas that mainly terminate in layer 1, whereas primary auditory cortices principally receive inputs from tonotopic lemniscal areas that target mainly the middle layers (cat: Kudo and Niimi 1980; Huang and Winer 2000; Lee and Winer 2011; for a review, see Winer 1992).

Traditionally, the early sensory processing neuronal stages are assumed to be unimodal and to operate independently of each other. However, a growing body of evidence has changed this classical view of the sensory hierarchical processing by demonstrating the convergence of multimodal inputs in subcortical nuclei (Stein and Meredith 1993; Stein and Stanford 2008) and early primary sensory cortices (Ghazanfar et al. 2005; Kayser and Logothetis 2007; Lakatos et al. 2007; King and Walker 2012; for a review, see Kayser et al. 2012). In agreement with the above-mentioned, another feature of the non-lemniscal tectal and thalamic areas includes their dense innervation by non-auditory afferents. For instance, the shell area of the IC receives visual (rat and monkey: Itaya and Van Hoesen 1982; rat: Yamauchi and Yamadori 1982; cat: Mascetti and Strozzi 1988) and somatosensory (cat: Aitkin et al. 1978, 1981; Coleman and Clerici 1987; for a review, see Wu et al. 2014) inputs and projections from the substantia nigra pars compacta lateralis (cat: Coleman and Clerici 1987), globus pallidus (rat: Yasui et al. 1991; cat: Shinonaga et al. 1992), and the ventral tegmental area (rat: Herbert et al. 1997). Likewise, the MGBd and MGBm are innervated by afferents from the tegmental nuclei, spinothalamic tract, and superior colliculus (cat: Graybiel 1972; rat: Ledoux et al. 1987; Iwata et al. 1992). The efferent connections of the non-lemniscal areas of the IC (cat: Aitkin et al. 1978; ferret: King et al. 1998) and MGB (cat: Shinonaga et al. 1994; rat: Doron and Ledoux 1999; 2000) also display divergent projections to non-auditory nuclei.

Together, these structural differences are associated with the different functions exerted by the lemniscal and non-lemniscal systems. The lemniscal pathway is associated primarily with the relay of purely auditory information, whereas the non-lemniscal pathway is part of an integrative system primarily involved in multisensory integration, temporal pattern recognition (cat: Kelly 1973; Layton et al. 1979), change detection (guinea pig: Kraus et al. 1994a; rat: Malmierca et al. 2009), and certain forms of learning (guinea pig: Edeline and Weinberger 1991; rat: Komura et al. 2001). Furthermore, the multimodal afferent and efferent projections characterizing the non-lemniscal pathway are potentially important for sound localization, attending to salient stimuli, and mediating the audio-visual integration of speech stimuli (human: Champoux et al. 2006; for reviews, see Gruters and Groh 2012; Wu et al. 2014).

Major excitatory and inhibitory neurotransmitter receptors

The distribution and expression of receptor subtypes for neurotransmitters and neuromodulators show subtle differences in the IC and MGB subdivisions (summarized in Table 1).

Excitatory neurotransmission is mediated by glutamate in both the IC (cat: Adams and Wenthold 1979) and the MGB (rat: Hu et al. 1994). Both ionotropic AMPA (α-amino-3-hydroxy-5-methylisoxazole-4-propionic acid) and NMDA (N-methyl-D-aspartate) receptors intervene in the synaptic transmission of the IC (rat: Ma et al. 2002; for a review, see Kelly and Zhang 2002) and the MGB (rat: Hu et al. 1994), but recordings from the non-lemniscal regions of the IC do not provide evidence for pharmacological differences from the CNIC (rat: Li et al. 1998, 1999). Immunostaining for AMPA receptors is homogeneous throughout the IC (rat: Petralia and Wenthold 1992; Gaza and Ribak 1997), although the presence of the GluR2-3 AMPA subunit is more common in the non-lemniscal regions of the IC (rat: Caicedo and Eybalin 1999). Additionally, NMDA receptors are more common in the LCIC and the DCIC (rat: Petralia et al. 1994). In accordance with the

Table 1 Main receptor distribution in the human inferior colliculus (*IC*) and medial geniculate body (*MGB*) shown with density (− absent, + to +++ increasing density levels, *SSA* stimulus-specific adaptation, *CNIC* central nucleus of IC, *LCIC* lateral cortex, *RCIC* rostral cortex, *DCIC* dorsal cortex, *MGBv* ventral division of MGB, *MGBd* dorsal subdivision of MGB, *MGBm* medial subdivision of MGB, *AMPA* α-amino-3-hydroxy-5-methylisoxazole-4-propionic acid, *NMDA* N-methyl-D-aspartate, *GABA* Gamma aminobutryic acid, *nNOS* Neural nitric oxide synthase)

Transmitter type receptor		IC				MGB			SSA implication
		Lemniscal	Non-lemniscal			Lemniscal	Non-lemniscal		
		CNIC	DCIC	LCIC	RCIC	MGBv	MGBd	MGBm	
Glutamate	AMPA	Homogeneous				Homogeneous			Unlikely
	NMDA	+	+++			+	+++		Likely
	mGluR	−	+++			−	+++		Likely
GABA	A	Dorsal	Clusters			Homogeneous			Gain control
	B	+++	+	+++	+	+++	+++	−	Low
Glycine		Ventral	+			−	−	−	Unlikely, IC only
Acetylcholine	Muscarinic	−	+	+	−	Homogeneous			Attention?
	Nicotinic	−	+++	+++	−	Homogeneous			Attention?
Serotonin		+	+++	+++	+++	+	+++	Unknown	Attention?
Norepinephrine		+	+++	+++	+++	Unknown			Learning?
Dopamine		+	+++	+++	+++	Very low			Learning? IC only
Endocannabinoids		Unknown	Unknown	Present		Unknown			Speculative
nNOS		+	+++	+++	+++	Unknown			Speculative
Dynorphin		+	+	+++	+++	Unknown			Unknown
Enkephalin		Homogeneous				Unknown			Unlikely
Substance P		+	+++	+++	+++	Unknown			Speculative

IC data, the presence of AMPA receptors in the MGB has been proved to be homogeneous and moderate in quantity (rat: Sato et al. 1993; Caicedo et al. 1998; for a review, see Parks 2000), whereas the presence of NMDA receptors seems more prominent in the non-lemniscal regions of the MGB (rat: Monaghan and Cotman 1985; Hu et al. 1994). Immunohistochemical studies have also demonstrated the presence of the metabotropic glutamate receptor $mGluR_5$ in the cortical regions of the IC (rat: Abe et al. 1992; Shigemoto et al. 1993). Group I mGluRs, including $mGluR_1$ and $mGluR_5$, are located mostly on postsynaptic parts of cells and act by increasing NMDA activity. Projections from the DCIC and LCIC to the non-lemniscal regions of the MGB recruit mGluR (rat: Bartlett and Smith 2002; mice: Lee and Sherman 2010), as opposed to the mainly ionotropic component of the postsynaptic receptors of the MGBv (for a review, see Lee and Sherman 2011). As NMDA receptors are classically linked to synaptic plasticity, learning, and memory (Morris 2013), the testing of the role, if any, that the NMDA receptors play on shaping SSA would be of great interest in future studies.

Inhibitory neurotransmission in the IC is mediated by both gamma-aminobutyric acid (GABA) and glycine (for a review, see Cant and Benson 2003). $GABA_A$ receptors are located in more dorsal regions of the IC (gerbil: Sanes et al. 1987; bat: Fubara et al. 1996; Lu and Jen 2001), whereas glycine puncta are more prominent in the ventral region of the IC (cat: Adams and Wenthold 1979; Saint Marie et al. 1989; rat: Merchan et al. 2005). Nevertheless, this is not the only pattern of distribution that emerges with inhibition in the IC, as GABAergic neurons are also organized in cluster modules in the DCIC and the LCIC (rat: Chernock et al. 2004), with an unknown function. Additionally, metabotropic $GABA_B$ receptors are present to a greater extent in the CNIC and the LCIC (rat: Bowery et al. 1983; bat: Fubara et al. 1996; rat: Jamal et al. 2011, 2012). In the thalamus, inhibition in the MGB is primarily mediated by GABA acting at both $GABA_A$ and $GABA_B$ receptors (rat: Bartlett and Smith 1999; Richardson et al. 2011), because MGB lacks glycinergic receptors (rat: Aoki et al. 1988; Friauf et al. 1997). GABAergic interneurons are virtually absent in the rat MGB (only ~1 %: Winer and Larue 1996; Bartlett and Smith 1999), but in this case, the nucleus receives significant GABAergic projections from the IC (bat, rat, cat, and monkey: Winer et al. 1996; rat: Peruzzi et al. 1997; mice and rat: Ito et al. 2011) and the thalamic reticular nucleus (cat: Rouiller et al. 1985).

Recent studies have addressed the effect of neuronal inhibition on SSA by local manipulation of GABA neurotransmission (Fig. 4). The blockade of the $GABA_A$ receptor by using the specific antagonist gabazine elicits an overall increase in the evoked and spontaneous activity in IC (rat: Perez-Gonzalez et al. 2012) and MGB (rat: Duque et al.

2014) neurons. This increase in neuronal discharge is independent of the SSA sensitivity and their discharge pattern. Together, these studies demonstrate that the blockade of $GABA_A$ receptors of IC and MGB neurons with high SSA sensitivity (typically located in non-lemniscal regions) does not abolish SSA (rat: Perez-Gonzalez et al. 2012; Duque et al. 2014), suggesting that the GABAergic system exerts a gain control function on the neuronal responses. Furthermore, the experiments performed in the MGB by Duque et al. (2014) suggest that the ability of GABA to modulate SSA in the MGB is likely to be mediated by the $GABA_A$ rather than by the $GABA_B$ receptors. The effects of gaboxadol, a $GABA_A$-selective agonist that does not bind to $GABA_B$ receptors (rat: Bowery et al. 1983), are no different from the effects elicited by GABA on SSA in MGB. Moreover, as the highest levels of SSA are found in the MGBm (rat: Antunes et al. 2010), an area that lacks $GABA_B$ receptors (rat: Smith et al. 2007), these metabotropic receptors do not seem to be involved in SSA generation. However, any possible synergic effect as a result of the co-application of antagonist or agonists of other subunit or subtype receptors cannot be excluded.

Indeed, as metabotropic receptors (mainly $GABA_B$) are linked to calcium (Ca^{2+}) signaling, Ca^{2+}-binding proteins (namely parvalbumin, calbindin, and calretinin) largely define the lemniscal and non-lemniscal pathways (monkey: Jones 2003; human: Tardif et al. 2003; bats and birds: Covey and Carr 2005; rat: Ouda and Syka 2012). In the IC, parvalbumin is distributed throughout the subdivisions but with a larger presence in the CNIC (bat: Vater and Braun 1994; rat: Lohmann and Friauf 1996; Ouda and Syka 2012). On the other hand, calretinin- and calbindin-positive neurons are usually located in the non-lemniscal regions of the IC (bat: Zettel et al. 1991; rat: Ouda and Syka 2012). In the MGB, parvalbumin is also associated with the lemniscal regions, whereas calbindin is associated with the non-lemniscal regions (rabbit: de Venecia et al. 1995; monkey: Molinari et al. 1995; mice: Cruikshank et al. 2001). The parvalbumin (lemniscal) and calbindin/calretinin (non-lemniscal) distributions are also maintained in the AC (Banks and Smith 2011). The presence of these Ca^{2+}-related proteins might play a critical role in second messenger systems (see: Neuronal mechanisms that might underlie SSA: synaptic depression and retrograde signaling).

Finally, although the presence of glycine in the non-lemniscal regions of the IC is small (Adams and Wenthold 1979; Merchan et al. 2005), the effect of glycinergic receptors in IC neurons on SSA remains unknown. This is an important point, because IC neurons show higher SSA sensitivity at high frequencies (Duque et al. 2012), and glycine is more abundant in the ventral region of the IC (Malmierca and Hackett 2010), a region whose neurons are high-frequency tuned (Malmierca et al. 2008). Thus, in order to have a global picture of the mechanisms that might operate at subcortical SSA, several open questions remain to be answered. Among others, these include: what is the effect on SSA mediated by the combined activation of the $GABA_A$- and $GABA_B$-receptors and glycinergic receptors, and what is the role, if any, of the NMDA-mediated excitation. Lastly, as will be explained in the following sections, the interactions of any of these systems with specific retrograde messengers could also be crucial to an understanding of the mechanisms that generate SSA.

Neuromodulators in IC and MGB

Recent studies have envisaged a pivotal role of neuromodulators on orienting attention and enhancing the memory for novel stimuli (for reviews, see Ranganath and Rainer 2003; Edeline 2012). Indeed, the four neuromodulatory systems, namely cholinergic (Metherate et al. 2012), serotoninergic (Hurley and Sullivan 2012), dopaminergic (Gittelman et al. 2013), and noradrenergic (Manunta and Edeline 2004), have been implicated in short-term plastic auditory phenomena suggesting that they might also mediate SSA.

Acetylcholine has been implicated in predictive coding and learning under uncertainty in humans (Moran et al. 2013). Moreover, acetylcholine is known to exert frequency-specific plasticity in both cortical (cat: Metherate and Weinberger 1989) and subcortical (bat: Ji et al. 2001) neurons. Cholinergic terminals are abundant in the DCIC and the LCIC (guinea pig: Jain and Shore 2006; for a review, see Shore 2008), and the receptors in these regions are mainly nicotinic. In the MGB, almost all the neurons present either muscarinic and/or nicotinic receptors and are excited by acetylcholine (cat: Tebecis 1970, 1972). Acetylcholine depolarizes most of the neurons in the lemniscal MGBv through the muscarinic receptors, whereas a large amount of the neurons in the MGBd remain unaffected (rat: Varela and Sherman 2007; for a review, see Varela 2014).

Serotoninergic projections to all the regions of the IC arise from the raphe nuclei (bat: Hurley and Pollak 2005), although fibers are denser in non-lemniscal regions such as the DCIC and the LCIC (for reviews, see Hurley et al. 2002; Hurley and Sullivan 2012). Raphe nuclei also present projections to the MGB (monkey: Lavoie and Parent 1991; rat: Vertes et al. 2010), modulating the responses of many of the neurons in the lemniscal MGBv and most of the neurons in the non-lemniscal MGBd (guinea pig: Pape and McCormick 1989; cat: McCormick and Pape 1990; ferret: Monckton and McCormick 2002; rat: Varela and Sherman 2009; Varela 2014).

Attention during task engagement is known to modulate neuronal responses (ferrets: Fritz et al. 2003, 2007), and thus, attention mediated by either acetylcholine or serotonin might produce this modulation, hence affecting the levels of SSA. Indeed, recent work concerning SSA in the IC of the awake mouse (Duque and Malmierca 2014) has demonstrated that

the lower the spontaneous firing rates, the higher the SSA sensitivity. As spontaneous activity can be modulated during attention and can enhance signal detection (gerbils: Buran et al. 2014), both neuromodulators might be involved in SSA sensitivity. In view of the involvement acetylcholine (Jones 2005) and serotonin (Kelly and Caspary 2005) in arousal and attention, the effect of such neurotransmitters on SSA might be more important than previously estimated, and we need further studies in this field.

The response of the neurons of the IC and the MGB are also affected by catecholamines, mainly through noradrenergic- (rat: Swanson and Hartman 1975; Foote et al. 1983; Klepper and Herbert 1991) and dopaminergic (rat, cat and bat: Olazabal and Moore 1989; cat: Paloff and Usunoff 2000) fibers. The locus coeruleus is the main source of noradrenaline for both the IC and the MGB (Aston-Jones 2004). The dopaminergic innervation for the IC arises from neurons in the substantia nigra (Moore and Bloom 1979; Olazabal and Moore 1989), whereas the dopamine sources for the MGB are highly diverse (macaque: Sanchez-Gonzalez et al. 2005). Recent findings suggest that the noradrenergic direct projection from the locus coeruleus to the IC is mainly ipsilateral and just reaches the non-lemniscal regions of the IC (rat: Klepper and Herbert 1991; Hormigo et al. 2012). The dopaminergic neurons identified in the IC also have a distinct distribution, the largest number of dopaminergic neurons being located in the LCIC and the DCIC (rat: Tong et al. 2005).

In summary, considering that (1) noradrenaline and dopamine act as learning signals, and both neuromodulators are released at times of novelty and uncertainty (Harley 2004), and that (2) acetylcholine and serotonin mediate attention, their involvement in SSA sensitivity might be critical. Since SSA is a pre-attentive feature observed under anesthesia (rat: Malmierca et al. 2009), in awake (mouse: Duque and Malmierca 2014), and sleep-like states (rat: Nir et al. 2013), SSA is probably affected by the variations in the levels of neuromodulators occurring during these states. Thus, future studies of the various modulatory substances will undoubtedly shed light on the way that the brain learns to discriminate potentially relevant sounds (Edeline 2012).

Neuronal mechanisms that might underlie SSA: synaptic depression and retrograde signaling

Since GABAergic inhibition plays a key role in modulating SSA rather than in its generation (Perez-Gonzalez et al. 2012; Duque et al. 2014), a synaptic depression model (Grill-Spector et al. 2006; Briley and Krumbholz 2013) might be a more likely explanation for SSA. In this model, the continuous activation of the same set of neurons will eventually produce a specific decrease of the neurotransmitter release at the presynaptic level, and consequently, the postsynaptic neuron will not generate a response. The frequency-specific adaptation channel theory supports this model (Eytan et al. 2003; Mill et al. 2011a, 2011b; Taaseh et al. 2011; Nelken 2014) in which all the frequencies that are within the same frequency channel will not evoke SSA, because they are encoded by the same neurons. Although recent data from the rat AC (Hershenhoren et al. 2014) suggest other, as yet unknown, more complex mechanisms to explain SSA at the cortical level, in the IC, SSA is not constant within the neuronal receptive field of the neuron, and SSA sensitivity is stronger on the high-frequency edge of the receptive field (Duque et al. 2012). This phenomenon presents interesting correlates in the auditory nerve fibers (Westerman and Smith 1985) and the IC (Dean et al. 2008) in which adaptation is also more prominent at high frequencies. Together, these studies suggest that synaptic depression (Chung et al. 2002; Rothman et al. 2009) might explain subcortical SSA, as it is an input-specific mechanism, and neural responses depend upon the previous history of afferent firing (Abbott et al. 1997; Rothman et al. 2009).

Moreover, as various retrograde signaling pathways can act at the synaptic level (Regehr et al. 2009), synaptic depression does not necessarily have to be a passive phenomenon (i.e., fatigue). Retrograde signaling mediates short-term synaptic plasticity (Regehr 2012), a likely explanation for synaptic depression (Abbott and Regehr 2004): lipids (endocannabinoids), gases (nitric oxide), peptides (i.e., met-enkephalin and/or dynorphin), and conventional amino acid transmitters (i.e., glutamate and/or GABA) can be released in an activation-dependent manner by postsynaptic neurons and then act on the axon terminals of presynaptic neurons (Regehr et al. 2009). The production and release of these messengers is regulated by the activation of postsynaptic glutamatergic metabotropic receptors (Regehr et al. 2009) and/or by postsynaptic Ca^{2+} (de Jong and Verhage 2009), two components mainly located in the non-lemniscal regions of the IC and the MGB (see above). In the mammalian brain, the endocannabinoid signaling system is the best-characterized retrograde signaling pathway and enables neurons specifically to regulate the strength of their inputs in a retrograde manner (Wilson and Nicoll 2002; Freund and Hajos 2003; Kano et al. 2009). Endocannabinoid type-1 (CB1) receptors are thought to be one of the most widely expressed G-protein-coupled receptors in the brain (Herkenham et al. 1990). The presynaptic localization of CB1 receptors and their inhibitory effect on neurotransmitter release has been shown to be a general feature of most axon terminals in the central nervous system (Kano et al. 2009), suppressing synaptic strength for tens of seconds (Wilson et al. 2001). The firing evoked by the standard stimuli in an oddball paradigm can activate group I mGluR, thus inducing endocannabinoid release (Chevaleyre et al. 2006) and contributing to short-term synaptic plasticity (Castillo et al. 2012), as in the fast adaptation occurring in the neuronal firing to the standard tone. Endocannabinoid signaling has been demonstrated to act in the auditory pathway at the level of the cochlear nucleus (Zhao et al. 2009; Zhao and Tzounopoulos 2011),

the superior olivary complex (Trattner et al. 2013), and the external cortex of the IC of the barn owl (Penzo and Pena 2009), but its affect on auditory SSA remains unknown.

Much less is known about other retrograde neurotransmitters. For example, the highest levels of nNOS (the neuronal enzyme that synthesizes nitric oxide) are evident in the DCIC and the LCIC, with much lower levels in the CNIC (Druga and Syka 1993; Paloff and Hinova-Palova 1998; Coote and Rees 2008). Few data are available for understanding the involvement of nNOS in the MGB. As another example, immunostaining for kappa (κ) opioid receptors (dynorphin) is significantly higher in the LCIC, but delta (δ) opioid receptors (met-enkephalins) are similarly distributed within the IC (Aguilar et al. 2004; Tongjaroenbuangam et al. 2006). Thus, the distribution of the opioid receptors cannot be correlated with specific regions of the IC. The data regarding opioid receptor distribution in the MGB are also sparse and difficult to interpret. Lastly, we should mention the existence of extensive labeling for fibers with both somatostatin and substance-P in the DCIC and the LCIC, with somatostatin showing the most extensive encircling of the CNIC (Wynne and Robertson 1997). Interestingly, no significant fibers labeling for either peptide have been observed within the CNIC (Wynne and Robertson 1997). Unfortunately, the involvement of retrograde signaling in SSA remains unknown, and much work is needed to gain an understanding of the functions of these systems in sound discrimination.

Detection of acoustic deviance in non-auditory nuclei

Beyond the auditory pathway, stronger neuronal responses to deviant sounds have also been found in some non-auditory

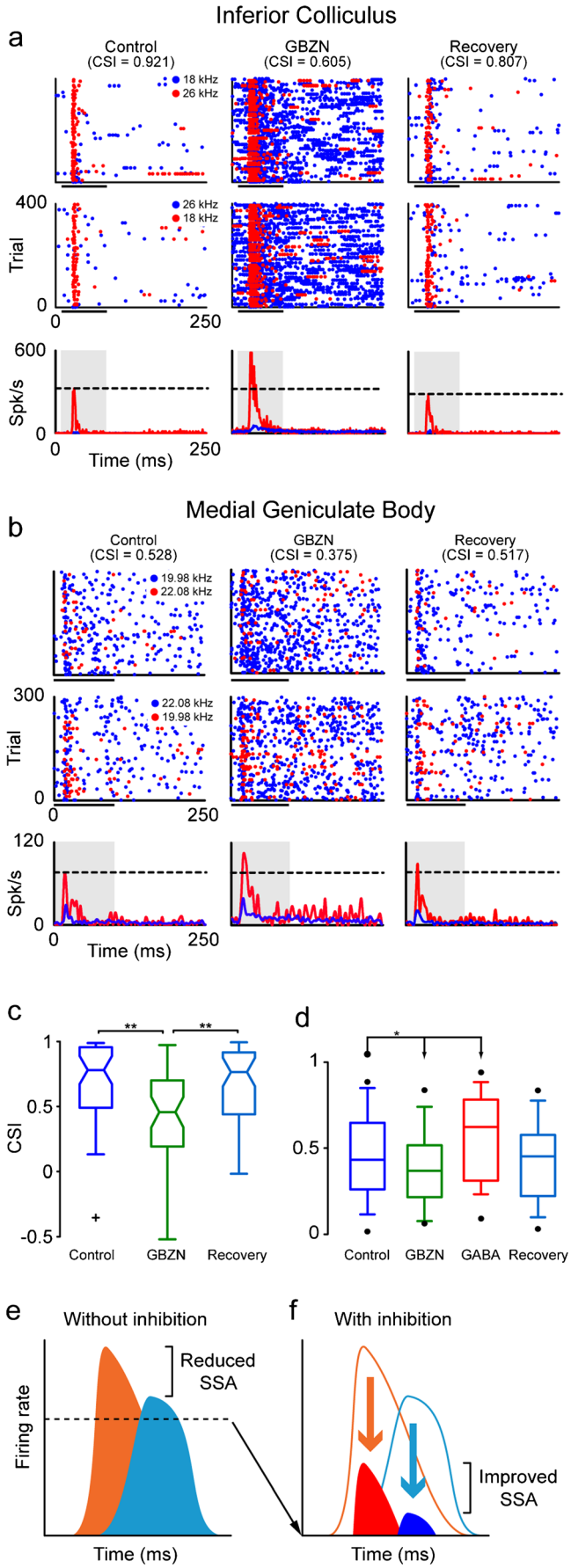

Fig. 4 Effect of neuronal inhibition on the SSA responses in IC and MGB neurons. **a** *Dot raster plots* obtained after an oddball paradigm for a pair of frequencies in an IC neuron. The *dot rasters* refer to the control (*left*), gabazine (*GBZN*, *middle*), and recovery (*right*) conditions. Frequencies are shown as *insets over* the control condition. The *first row* shows *f*1/*f*2 as a standard/deviant, whereas the *second row* shows the reverse condition (*f*2/*f*1 as standard/deviant). The *black line* lying *under* the *dot rasters* represents the stimulus duration. Common SSA index (*CSI*) values are shown over each condition. The mean peristimulus time histograms from both *dot rasters* are shown in the *third row* (*Spk* spike). **b** *Dot raster plots* obtained after an oddball paradigm for a pair of frequencies in an MGB neuron. Same format as in **a**. **c** *Box plot* of the CSI values for the population of neurons of the IC before, during, and after the application of GBZN. **d** *Box plot* of the CSI values for the population of neurons of the MGB before, during, and after the application of GBZN and GABA. In both cases, *asterisks* indicate significant differences (Friedman test, $P<0.01$). **e** In the absence of inhibition, neurons respond to deviants (*orange*) and standards (*light blue*) with high firing rates, and thus the deviant to standard ratio is small. **f** Inhibition reduces the responses to both deviants (*red*) and standards (*dark blue*) increasing the deviant to standard ratio and thus enhancing SSA. **a**, **c**, **e**, **f**: modified from Perez-Gonzalez et al. (2012). **b**, **d**: modified from Duque et al. (2014)

nuclei, including the substantia nigra (Minks et al. 2014), hippocampus (Ruusuvirta et al. 1995b, 1995c), basal ganglia (Mikell et al. 2014), optic tectum (Reches and Gutfreund 2008), and thalamic reticular nucleus (Yu et al. 2009). As mentioned in the previous section, some of these nuclei have anatomical connections with the non-lemniscal auditory subdivisions.

The substantia nigra is typically involved in sensorimotor coordination. However, recently, a study in humans by Mikell et al. (2014) has demonstrated that novel sounds evoke a greater firing rate compared with the activity following standard tones in substantia nigra neurons. The response following the deviant presentations displays a biphasic temporal pattern with peaks at approximately 300 and 500 ms (Fig. 5a). Interestingly, an inverse correlation occurs between the firing rate and the strength of the novelty response across all recorded neurons, i.e., neurons sensitive to deviant stimulus exhibit slow firing, whereas neurons with the highest firing rates are suppressed by the novel stimuli. Mikell and colleagues (2014) speculate that the substantia nigra neurons that discriminate deviant and standard tones correspond to dopaminergic neurons, since previous studies indicate dopaminergic neurons are sensitive to novelty (Bunzeck and Düzel 2006). Moreover, the former authors further suggest that the other group of substantia nigra neurons with high and tonic firing rates suppressed by the deviant tone correspond to GABAergic interneurons that are known to inhibit the local dopaminergic neurons (Tepper et al. 1995). Interestingly, the response in the substantia nigra, i.e., the first peak of the increased activity following novel sounds (250–350 ms after stimulus onset), occurs concurrently with the onset of the hippocampally-dependent potential P300, a scalp-recorded potential linked to novelty detection. Notably, MMN-like responses to pitch (Ruusuvirta et al. 1995b, 1995c; 1996), duration (Rosburg et al. 2007; Ruusuvirta et al. 2013), and frequency deviants (Ruusuvirta et al. 2010) have been recorded across the hippocampus in animal studies. The hippocampus is associated with involuntary attention switches toward auditory changes of high magnitude. Ruusuvirta et al. (2013) have found that MMN responses to duration deviants are elicited across the three hippocampal areas, i.e., CA1, dentate gyrus, and subiculum in anesthetized rats. In a previous report from the same group (Ruusuvirta et al. 2010), higher amplitude local field potentials in response to frequency deviants have been recorded in the CA1 of awake animals. The MMN response to frequency and duration deviants occurs within a similar time window, at 36–80 and 51.5–89 ms post-stimulus, respectively.

Recently, other non-auditory nuclei have been implicated in acoustic deviance detection. The subthalamic nucleus is integrated into the basal ganglia system, and traditionally, it is considered to play a role in cortical motor control regulation

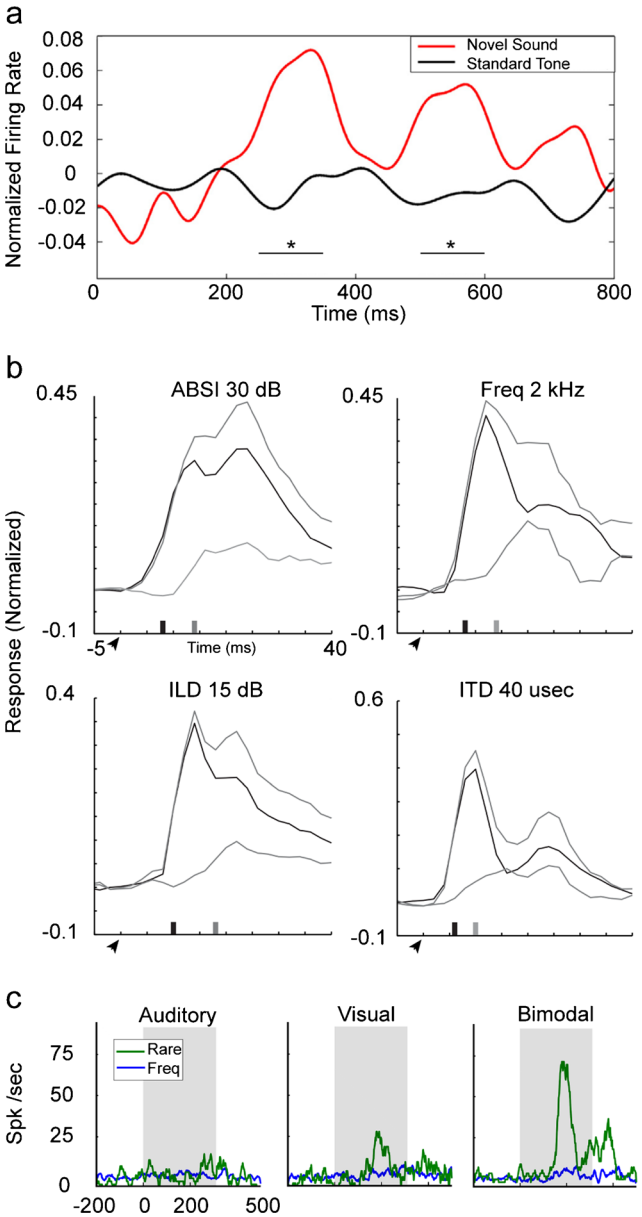

Fig. 5 Response to acoustic deviants in non-auditory subcortical nuclei. **a** Normalized firing response of neurons of the substantia nigra. Novel sound evoked a greater response (*red line*) compared with standard tones (*blue line*) over the 250–350 ms interval and over 500–600 ms (*black lines* regions of $*P<0.05$; modified from Mikell et al. 2014). **b** Optic tectum neuronal SSA responses to average binaural sound intensity (*ABSI*, 30 dB gap), frequency (*Freq*, 2 kHz gap), interaural level difference (*ILD*, 15 dB gap), and interaural time difference (*ITD*, 40 μs gap). *Top gray line* is the response to a rarely presented stimulus, *black line* the response to a frequently presented stimulus, *bottom gray line* the difference between the two, *arrowheads* stimulus onset, *black ticks* latency of the population response to the frequent stimulus, *gray ticks* latency of the difference signal (taken from Reches and Gutfreund 2008). **c** Entopallium neuronal responses to deviant occurrences (*green lines*) together with the corresponding responses to frequent occurrences (*blue lines*) of auditory, visual, and bimodal stimulus (modified from Reches et al. 2010)

(Rektor et al. 2001). Minks et al. (2014) have demonstrated that deviant pure tones elicit MMN-like responses in the

subthalamic nuclei by using intracranial electroencephalograph recordings in humans. The responses are evident in the far-field potentials (intracerebral electrodes referenced to the extracranial electrode) and near-field potentials (intracerebral contacts referenced to one another within the subthalamic nuclei) with a similar average time-to-peak, i.e., 202 and 214 ms, respectively.

SSA responses have been also found in the optic tectum, which is the avian homolog of the superior colliculus of mammals. The optic tectum is involved in orienting gaze toward salient stimuli and receives auditory inputs primarily from the cortices of the IC (Gutfreund 2012). In an elegant study performed by Reches and Gutfreund (2008), SSA responses to more than one acoustic feature, i.e., sound frequencies, amplitudes, and interaural and interlevel time difference, were found in the single- and multi-unit activity of the optic tectum neurons (Fig. 5b). All acoustic features elicited a similar pattern of adaptation developed several milliseconds after the onset of the response. Interestingly, neurons of the IC exhibited SSA only to sound frequency but showed a higher neuronal hyperacuity. These results led the authors to suggest that neurons in higher-level centers of the ascending gaze control system, such as the optic tectum where the IC neurons project to, encompass SSA to multiple acoustic features and not only to one single acoustic dimension as occurs in the IC of the barn own.

The studies highlighted above clearly demonstrate that deviance detection is a widely distributed neuronal network that goes beyond the auditory pathway (Ranganath and Rainer 2003). At the same time, these studies lead to questions regarding the possibility of whether these neuronal structures play an active role in the genesis of deviance detection or simply reflect adaptive neuronal processes taking place at their projecting sources. To gain information in order to permit a direct comparison with the SSA studies, an interesting project would be to record the responses of a single neuron to various acoustic stimuli in the hippocampus, subthalamic nuclei, or superior colliculus under the same paradigms as those used in the auditory SSA studies (Ulanovsky et al. 2003; Malmierca et al. 2009; Yaron et al. 2012).

Multisensory responses and deviance detection

Neurons showing SSA also participate in multisensory processing since information integrated across various sensory modalities can greatly enhance our ability to detect, discriminate, or respond to relevant sensory events (for reviews, see Stein and Meredith 1993; Gleiss and Kayser 2012). As described previously, the non-lemniscal subdivisions of the IC and MGB in which the strongest SSA responses are found receive afferent projections not only from auditory nuclei, but also from visual and somatosensory nuclei (Wu et al. 2014). Indeed, several studies indicate that other subcortical nuclei involved in deviance detection also engage multimodal sensitivities. Neurons with multimodal sensitivity exhibit suprathreshold responses to stimuli from more than one sensory modality, and often the response of these neurons is stronger to combined stimuli than to the most effective single-modality stimulus (Meredith et al. 2012). Examples of auditory neurons whose sensitivity differs significantly when they are stimulated by bimodal (e.g., audiovisual) stimuli are summarized below. Yu et al. (2009) have found SSA responses in the thalamic reticular nucleus, a multimodal area mainly conformed by GABAergic neurons and have shown that MGB acoustic responses are modulated in a cross-modal manner by a preceding light stimulus. This modulation of the auditory responses is abolished by the inactivation of the thalamic reticular nucleus. Moreover, eye position has been demonstrated to modulate auditory responses as early as in the shell area of the IC of primates (Groh et al. 2001; for reviews, see Gruters and Groh 2012; Wu et al. 2014).

Likewise, other subcortical non-auditory structures that are particularly sensitive to deviant sound also exhibit multimodal sensitivities. Neurons in the substantia nigra are responsive to visual, auditory, and somatosensory stimulation (Nagy et al. 2005; Chudler et al. 1995) exhibiting multisensory response enhancements (Nagy et al. 2006). In the barn owl, optic tectum neurons show multisensory enhancement (Zahar et al. 2009) and SSA for visual stimuli, in addition to SSA for sound frequency deviants (Reches and Gutfreund 2008). Moreover, Reches et al. (2010) have performed a pioneering study demonstrating that a bimodal stimulus enhances the SSA responses of entopallium neurons, a forebrain structure of the barn owl (Fig. 5c). This enhancement occurs only when the auditory and visual stimuli are congruent in space and time (Reches et al. 2010). Whether the same multimodal enhancement of the auditory SSA responses occurs at early subcortical processing stages remains to be determined in future studies.

The superior colliculus is also of special interest for the exploration of SSA, because (1) the optic tectum (which is its avian homolog) encompasses SSA for multiple acoustic parameters and for visual stimulus (Reches and Gutfreund 2008) and (2) the basic principles of multisensory integration have been revealed in single-cell studies in the superior colliculus (Stein and Wallace 1996; Stein and Stanford 2008; Meredith et al. 2012). Interestingly, neurons of the superior colliculus of the anesthetized cat with little or no spontaneous activity and weak sensory responses have the ability to exhibit large multisensory response enhancements in comparison with the poor response enhancements exhibited by superior colliculus neurons with modest spontaneous activity and robust sensory responses (Perrault et al. 2003). The response features of the ongoing multisensory enhancement of the superior colliculus resemble the poor response of the IC neurons showing strong SSA (Duque et al. 2012) and those of substantia nigra neurons sensitive to deviant stimulation

(Mikell et al. 2014). Finally, the tegmental nucleus is another multisensory structure (Koyama et al. 1994; Reese et al. 1995) in which acoustic SSA is likely to occur (Schofield et al. 2011), since its neurons attenuate or even abolish their response to repetitive auditory stimulation (Koyama et al. 1994). Furthermore, tegmental nucleus neurons project to the IC and receive projections from the AC (Schofield 2010).

All the above-mentioned studies support the notion that the subcortical nuclei engaged in auditory deviance detection constitute a neuronal microcircuitry based on the convergence of inputs from various sensory modalities that might act as early integration centers to enhance deviance detection. This wealth of data sets forth a promising field in which to explore and determine whether subcortical neurons allow better deviance coding under multisensory compared with unimodal conditions.

Final remarks

We have reviewed evidence of MMN-like and SSA responses occurring in the shell area of the IC and MGB and in non-auditory nuclei and suggest that they conform to a distributed subcortical network for deviance detection. Likewise, the topographic distribution of SSA in the shell areas of the IC and MGB suggests that the microcircuitry and neurochemistry of the non-lemniscal areas exert a critical role in the generation and modulation of SSA in these nuclei. Further studies combining physiological, anatomical, and molecular approaches will broaden our understanding of the microcircuits of SSA in the auditory and non-auditory nuclei. Moreover, these studies will contribute to the determination of the similar or different contribution of each nucleus to the processing of deviant sounds and to the triggering of the cascade of neuronal processes that allow animals to adapt rapidly to environmental changes.

References

Abbott LF, Regehr WG (2004) Synaptic computation. Nature 431:796–803

Abbott LF, Varela JA, Sen K, Nelson SB (1997) Synaptic depression and cortical gain control. Science 275:220–224

Abe T, Sugihara H, Nawa H, Shigemoto R, Mizuno N, Nakanishi S (1992) Molecular characterization of a novel metabotropic glutamate receptor mGluR5 coupled to inositol phosphate/Ca^{2+} signal transduction. J Biol Chem 267:13361–13368

Adams JC, Wenthold RJ (1979) Distribution of putative amino acid transmitters, choline acetyltransferase and glutamate decarboxylase in the inferior colliculus. Neuroscience 4:1947–1951

Aguilar LA, Malmierca MS, Covenas R, Lopez-Poveda EA, Tramu G, Merchan M (2004) Immunocytochemical distribution of Met-enkephalin-Arg6-Gly7-Leu8 (Met-8) in the auditory system of the rat. Hear Res 187:111–121

Aitkin LM, Prain SM (1974) Medial geniculate body: unit responses in the awake cat. J Neurophysiol 37:512–521

Aitkin LM, Webster WR, Veale JL, Crosby DC (1975) Inferior colliculus. I. Comparison of response properties of neurons in central, pericentral, and external nuclei of adult cat. J Neurophysiol 38: 1196–1207

Aitkin LM, Dickhaus H, Schult W, Zimmermann M (1978) External nucleus of inferior colliculus: auditory and spinal somatosensory afferents and their interactions. J Neurophysiol 41:837–847

Aitkin LM, Kenyon CE, Philpott P (1981) The representation of the auditory and somatosensory systems in the external nucleus of the cat inferior colliculus. J Comp Neurol 196:25–40

Andersen RA, Knight PL, Merzenich MM (1980) The thalamocortical and corticothalamic connections of AI, AII, and the anterior auditory field (AAF) in the cat: evidence for two largely segregated systems of connections. J Comp Neurol 194:663–701

Anderson LA, Linden JF (2011) Physiological differences between histologically defined subdivisions in the mouse auditory thalamus. Hear Res 274:48–60

Anderson LA, Malmierca MS (2013) The effect of auditory cortex deactivation on stimulus-specific adaptation in the inferior colliculus of the rat. Eur J Neurosci 37:52–62

Anderson LA, Christianson GB, Linden JF (2009) Stimulus-specific adaptation occurs in the auditory thalamus. J Neurosci 29:7359–7363

Antunes FM, Malmierca MS (2011) Effect of auditory cortex deactivation on stimulus-specific adaptation in the medial geniculate body. J Neurosci 31:17306–17316

Antunes FM, Nelken I, Covey E, Malmierca MS (2010) Stimulus-specific adaptation in the auditory thalamus of the anesthetized rat. PLoS One 5:e14071. doi:10.1371/journal.pone.0014071

Aoki E, Semba R, Keino H, Kato K, Kashiwamata S (1988) Glycine-like immunoreactivity in the rat auditory pathway. Brain Res 442:63–71

Astikainen P, Ruusuvirta T, Wikgren J, Penttonen M (2006) Memory-based detection of rare sound feature combinations in anesthetized rats. Neuroreport 17:1561–1564

Astikainen P, Stefanics G, Nokia M, Lipponen A, Cong F, Penttonen M, Ruusuvirta T (2011) Memory-based mismatch response to frequency changes in rats. PLoS One 6:e24208. doi:10.1371/journal.pone.0024208

Aston-Jones G (2004) Locus coeruleus, A5 and A7 noradrenergic cell groups. In: Paxinos G (ed) The rat nervous system, 3rd edn. Elsevier/Academic Press, San Diego, pp 259–294

Ayala YA, Malmierca MS (2013) Stimulus-specific adaptation and deviance detection in the inferior colliculus. Front Neural Circuits 6:89. doi:10.3389/fncir.2012.00089

Ayala YA, Perez-Gonzalez D, Duque D, Nelken I, Malmierca MS (2013) Frequency discrimination and stimulus deviance in the inferior colliculus and cochlear nucleus. Front Neural Circuits 6:119. doi: 10.3389/fncir.2012.00119

Banks MI, Smith PH (2011) Thalamocortical relations. In: Winer JA, Schreiner C (eds) The auditory cortex. Springer, New York, pp 75–97

Bartlett EL, Smith PH (1999) Anatomic, intrinsic, and synaptic properties of dorsal and ventral division neurons in rat medial geniculate body. J Neurophysiol 81:1999–2016

Bartlett EL, Smith PH (2002) Effects of paired-pulse and repetitive stimulation on neurons in the rat medial geniculate body. Neuroscience 113:957–974

Bäuerle P, Behrens W von der, Kossl M, Gaese BH (2011) Stimulus-specific adaptation in the gerbil primary auditory thalamus is the result of a fast frequency-specific habituation and is regulated by the corticofugal system. J Neurosci 31:9708–9722

Bendixen A, SanMiguel I, Schroger E (2012) Early electrophysiological indicators for predictive processing in audition: a review. Int J Psychophysiol 83:120–131

Bordi F, LeDoux JE (1994a) Response properties of single units in areas of rat auditory thalamus that project to the amygdala. I. Acoustic discharge patterns and frequency receptive fields. Exp Brain Res 98: 261–274

Bordi F, LeDoux JE (1994b) Response properties of single units in areas of rat auditory thalamus that project to the amygdala. II. Cells receiving convergent auditory and somatosensory inputs and cells antidromically activated by amygdala stimulation. Exp Brain Res 98:275–286

Bowery NG, Hill DR, Hudson AL (1983) Characteristics of GABAB receptor binding sites on rat whole brain synaptic membranes. Br J Pharmacol 78:191–206

Briley PM, Krumbholz K (2013) The specificity of stimulus-specific adaptation in human auditory cortex increases with repeated exposure to the adapting stimulus. J Neurophysiol 110:2679–2688

Bunzeck N, Düzel E (2006) Absolute coding of stimulus novelty in the human substantia nigra/VTA. Neuron 51:369–79

Buran BN, Trapp G von, Sanes DH (2014) Behaviorally gated reduction of spontaneous discharge can improve detection thresholds in auditory cortex. J Neurosci 34:4076–4081

Cacciaglia R, Escera C, Slabu L, Grimm S, Sanjuán A, Ventura-Campos N, Ávila C (2015)Involvement of the human midbrain and thalamus in auditory deviance detection.Neuropsychologia 68C:51–58

Caicedo A, Eybalin M (1999) Glutamate receptor phenotypes in the auditory brainstem and mid-brain of the developing rat. Eur J Neurosci 11:51–74

Caicedo A, Kungel M, Pujol R, Friauf E (1998) Glutamate-induced Co^{2+} uptake in rat auditory brainstem neurons reveals developmental changes in Ca^{2+} permeability of glutamate receptors. Eur J Neurosci 10:941–954

Calford MB (1983) The parcellation of the medial geniculate body of the cat defined by the auditory response properties of single units. J Neurosci 3:2350–2364

Calford MB, Aitkin LM (1983) Ascending projections to the medial geniculate body of the cat: evidence for multiple, parallel auditory pathways through thalamus. J Neurosci 3:2365–2380

Cant NB, Benson CG (2003) Parallel auditory pathways: projection patterns of the different neuronal populations in the dorsal and ventral cochlear nuclei. Brain Res Bull 60:457–474

Castillo PE, Younts TJ, Chavez AE, Hashimotodani Y (2012) Endocannabinoid signaling and synaptic function. Neuron 76:70–81

Champoux F, Tremblay C, Mercier C, Lassonde M, Lepore F, Gagné JP, Théoret H (2006) A role for the inferior colliculus in multisensory speech integration. Neuroreport 17:1607–1610

Chernock ML, Larue DT, Winer JA (2004) A periodic network of neurochemical modules in the inferior colliculus. Hear Res 188:12–20

Chevaleyre V, Takahashi KA, Castillo PE (2006) Endocannabinoid-mediated synaptic plasticity in the CNS. Annu Rev Neurosci 29: 37–76

Christianson GB, Chait M, Cheveigne A de, Linden JF (2014) Auditory evoked fields measured non-invasively with small-animal MEG reveal rapid repetition suppression in the guinea pig. J Neurophysiol 112:3053–3065. doi:10.1152/jn.00189.2014

Chudler EH, Sugiyama K, Dong WK (1995) Multisensory convergence and integration in the neostriatum and globus pallidus of the rat. Brain Res 674:33–45

Chung S, Li X, Nelson SB (2002) Short-term depression at thalamocortical synapses contributes to rapid adaptation of cortical sensory responses in vivo. Neuron 34:437–446

Coleman JR, Clerici WJ (1987) Sources of projections to subdivisions of the inferior colliculus in the rat. J Comp Neurol 262:215–226

Coote EJ, Rees A (2008) The distribution of nitric oxide synthase in the inferior colliculus of guinea pig. Neuroscience 154:218–225

Covey E, Carr CE (2005) The auditory midbrain in bats and birds. In: Winer JA, Schreiner CE (eds) The inferior colliculus. Springer, New York, pp 493–536

Cruikshank SJ, Killackey HP, Metherate R (2001) Parvalbumin and calbindin are differentially distributed within primary and secondary subregions of the mouse auditory forebrain. Neuroscience 105:553–569

Csepe V, Karmos G, Molnar M (1987a) Effects of signal probability on sensory evoked potentials in cats. Int J Neurosci 33:61–71

Csepe V, Karmos G, Molnar M (1987b) Evoked potential correlates of stimulus deviance during wakefulness and sleep in cat–animal model of mismatch negativity. Electroencephalogr Clin Neurophysiol 66:571–578

Dean I, Robinson BL, Harper NS, McAlpine D (2008) Rapid neural adaptation to sound level statistics. J Neurosci 28:6430–6438

Doron NN, Ledoux JE (1999) Organization of projections to the lateral amygdala from auditory and visual areas of the thalamus in the rat. J Comp Neurol 412:383–409

Doron NN, Ledoux JE (2000) Cells in theposterior thalamus project to both amygdala and temporal cortex: a quantitative retrograde double-labeling study in the rat. J Comp Neurol 425:257–274

Druga R, Syka J (1993) NADPH-diaphorase activity in the central auditory structures of the rat. Neuroreport 4:999–1002

Duque D, Malmierca MS (2014) Stimulus-specific adaptation in the inferior colliculus of the mouse: anesthesia and spontaneous activity effects. Brain Struct Funct. doi:10.1007/s00429-014-0862-1

Duque D, Perez-Gonzalez D, Ayala YA, Palmer AR, Malmierca MS (2012) Topographic distribution, frequency, and intensity dependence of stimulus-specific adaptation in the inferior colliculus of the rat. J Neurosci 32:17762–17774

Duque D, Malmierca MS, Caspary DM (2014) Modulation of stimulus-specific adaptation by GABAA receptor activation or blockade in the medial geniculate body of the anaesthetized rat. J Physiol (Lond) 592:729–743

Edeline JM (2012) Beyond traditional approaches to understanding the functional role of neuromodulators in sensory cortices. Front Behav Neurosci 30:6–45. doi:10.3389/fnbeh.2012.00045

Edeline JM, Weinberger NM (1991) Subcortical adaptive filtering in the auditory system: associative receptive field plasticity in the dorsal medial geniculate body. Behav Neurosci 105:154–175

Escera C, Malmierca MS (2014) The auditory novelty system: an attempt to integrate human and animal research. Psychophysiology 51:111–123

Eytan D, Brenner N, Marom S (2003) Selective adaptation in networks of cortical neurons. J Neurosci 23:9349–9356

Fishman YI (2013) The mechanisms and meaning of the mismatch negativity. Brain Topogr 27:500–526

Fishman YI, Steinschneider M (2010) Formation of auditory streams. In: Rees A, Palmer AR (eds) The Oxford handbook of auditory science: auditory brain. Oxford University Press, New York, pp 215–245

Fishman YI, Steinschneider M (2012) Searching for the mismatch negativity in primary auditory cortex of the awake monkey: deviance detection or stimulus specific adaptation? J Neurosci 32: 15747–15758

Foote SL, Bloom FE, Aston-Jones G (1983) Nucleus locus ceruleus: new evidence of anatomical and physiological specificity. Physiol Rev 63:844–914

Freund TF, Hajos N (2003) Excitement reduces inhibition via endocannabinoids. Neuron 38:362–365

Friauf E, Hammerschmidt B, Kirsch J (1997) Development of adult-type inhibitory glycine receptors in the central auditory system of rats. J Comp Neurol 385:117–134

Friston K (2005) A theory of cortical responses. Philos Trans R Soc Lond B Biol Sci 360:815–36

Friston K (2009) The free-energy principle: a rough guide to the brain. Trends Cogn Sci 13:293–301

Friston K (2012) Prediction, perception and agency. Int J Psychophysiol 83:248–252

Fritz J, Shamma S, Elhilali M, Klein D (2003) Rapid task-related plasticity of spectrotemporal receptive fields in primary auditory cortex. Nat Neurosci 6:1216–1223

Fritz JB, Elhilali M, David SV, Shamma SA (2007) Auditory attention–focusing the searchlight on sound. Curr Opin Neurobiol 17:437–455

Fubara BM, Casseday JH, Covey E, Schwartz-Bloom RD (1996) Distribution of GABAA, GABAB, and glycine receptors in the central auditory system of the big brown bat, *Eptesicus fuscus*. J Comp Neurol 369:83–92

Gaza WC, Ribak CE (1997) Immunocytochemical localization of AMPA receptors in the rat inferior colliculus. Brain Res 774:175–183

Ghazanfar AA, Maier JX, Hoffman KL, Logothetis NK (2005) Multisensory integration of dynamic faces and voices in rhesus monkey auditory cortex. J Neurosci 25:5004–5012

Gittelman JX, Perkel DJ, Portfors CV (2013) Dopamine modulates auditory responses in the inferior colliculus in a heterogeneous manner. J Assoc Res Otolaryngol 14:719–729

Gleiss S, Kayser C (2012) Audio-visual detection benefits in the rat. PLoS One 7:e45677. doi:10.1371/journal.pone.0045677

Graybiel AM (1972) Some ascending connections of the pulvinar and nucleus lateralis posterior of the thalamus in the cat. Brain Res 44: 99–125

Grill-Spector K, Henson R, Martin A (2006) Repetition and the brain: neural models of stimulus-specific effects. Trends Cogn Sci 10:14–23

Groh JM, Trause AS, Underhill AM, Clark KR, Inati S (2001) Eye position influences auditory responses in primate inferior colliculus. Neuron 29:509–518

Gruters KG, Groh JM (2012) Sounds and beyond: multisensory and other non-auditory signals in the inferior colliculus. Front Neural Circuits 6:96. doi:10.3389/fncir.2012.00096

Gutfreund Y (2012) Stimulus-specific adaptation, habituation and change detection in the gaze control system. Biol Cybern 106:657–668

Hari R, Hamalainen M, Ilmoniemi R, Kaukoranta E, Reinikainen K, Salminen J, Alho K, Naatanen R, Sams M (1984) Responses of the primary auditory cortex to pitch changes in a sequence of tone pips: neuromagnetic recordings in man. Neurosci Lett 50:127–132

Harley CW (2004) Norepinephrine and dopamine as learning signals. Neural Plast 11:191–204

Harms L, Fulham WR, Todd J, Budd TW, Hunter M, Meehan C, Penttonen M, Schall U, Zavitsanou K, Hodgson DM, Michie PT (2014) Mismatch negativity (MMN) in freely-moving rats with several experimental controls. PLoS One 9:e110892. doi:10.1371/journal.pone.0110892

He J, Hu B (2002) Differential distribution of burst and single-spike responses in auditory thalamus. J Neurophysiol 88:2152–2156

Herbert H, Klepper A, Ostwald J (1997) Afferent and efferent connections of the ventrolateral tegmental area in the rat. Anat Embryol (Berl) 196:235–259

Herkenham M, Lynn AB, Little MD, Johnson MR, Melvin LS, Costa BR de, Rice KC (1990) Cannabinoid receptor localization in brain. Proc Natl Acad Sci U S A 87:1932–1936

Hershenhoren I, Taaseh N, Antunes FM, Nelken I (2014) Intracellular correlates of stimulus-specific adaptation. J Neurosci 34:3303–3319

Hormigo S, Horta Junior Jde A, Gomez-Nieto R, Lopez DE (2012) The selective neurotoxin DSP-4 impairs the noradrenergic projections from the locus coeruleus to the inferior colliculus in rats. Front Neural Circuits 6:41. doi:10.3389/fncir.2012.00041

Hu B (2003) Functional organization of lemniscal and nonlemniscal auditory thalamus. Exp Brain Res 153:543–549

Hu B, Senatorov V, Mooney D (1994) Lemniscal and non-lemniscal synaptic transmission in rat auditory thalamus. J Physiol (Lond) 479:217–231

Huang CL, Winer JA (2000) Auditory thalamocortical projections in the cat: laminar and areal patterns of input. J Comp Neurol 427:302e331

Hurley LM, Pollak GD (2005) Serotonin shifts first-spike latencies of inferior colliculus neurons. J Neurosci 25:7876–7886

Hurley LM, Sullivan MR (2012) From behavioral context to receptors: serotonergic modulatory pathways in the IC. Front Neural Circuits 6:58. doi:10.3389/fncir.2012.00058

Hurley LM, Thompson AM, Pollak GD (2002) Serotonin in the inferior colliculus. Hear Res 168:1–11

Itaya SK, Van Hoesen GW (1982) Retinal innervation of the inferior colliculus in rat and monkey. Brain Res 233:45–52

Ito T, Bishop DC, Oliver DL (2011) Expression of glutamate and inhibitory amino acid vesicular transporters in the rodent auditory brainstem. J Comp Neurol 519:316–340

Iwata K, Kenshalo DR Jr, Dubner R, Nahin RL (1992) Diencephalic projections from the superficial and deep laminae of the medullary dorsal horn in the rat. J Comp Neurol 321:404–420

Jaaskelainen IP, Ahveninen J, Bonmassar G, Dale AM, Ilmoniemi RJ, Levanen S, Lin FH, May P, Melcher J, Stufflebeam S, Tiitinen H, Belliveau JW (2004) Human posterior auditory cortex gates novel sounds to consciousness. Proc Natl Acad Sci U S A 101:6809–6814

Jacobsen T, Schröger E (2003) Measuring duration mismatch negativity. Clin Neurophysiol 114:1133–1143

Jain R, Shore S (2006) External inferior colliculus integrates trigeminal and acoustic information: unit responses to trigeminal nucleus and acoustic stimulation in the guinea pig. Neurosci Lett 395:71–75

Jamal L, Zhang H, Finlayson PG, Porter LA, Zhang H (2011) The level and distribution of the GABA(B)R2 receptor subunit in the rat's central auditory system. Neuroscience 181:243–256

Jamal L, Khan AN, Butt S, Patel CR, Zhang H (2012) The level and distribution of the GABA(B)R1 and GABA(B)R2 receptor subunits in the rat's inferior colliculus. Front Neural Circuits 6:92. doi:10.3389/fncir.2012.00092

Javitt DC, Schroeder CE, Steinschneider M, Arezzo JC, Vaughan HG Jr (1992) Demonstration of mismatch negativity in the monkey. Electroencephalogr Clin Neurophysiol 83:87–90

Javitt DC, Steinschneider M, Schroeder CE, Vaughan HG Jr, Arezzo JC (1994) Detection of stimulus deviance within primate primary auditory cortex: intracortical mechanisms of mismatch negativity (MMN) generation. Brain Res 667:192–200

Ji W, Gao E, Suga N (2001) Effects of acetylcholine and atropine on plasticity of central auditory neurons caused by conditioning in bats. J Neurophysiol 86:211–225

Jones BE (2005) From waking to sleeping: neuronal and chemical substrates. Trends Pharmacol Sci 26:578–586

Jones EG (2003) Chemically defined parallel pathways in the monkey auditory system. Ann N Y Acad Sci 999:218–233

Jong AP de, Verhage M (2009) Presynaptic signal transduction pathways that modulate synaptic transmission. Curr Opin Neurobiol 19: 245–253

Jung F, Stephan KE, Backes H, Moran R, Gramer M, Kumagai T, Graf R, Endepols H, Tittgemeyer M (2013) Mismatch responses in the awake rat: evidence from epidural recordings of auditory cortical fields. PLoS One 8:e63203. doi:10.1371/journal.pone.0063203

Kano M, Ohno-Shosaku T, Hashimotodani Y, Uchigashima M, Watanabe M (2009) Endocannabinoid-mediated control of synaptic transmission. Physiol Rev 89:309–380

Kayser C, Logothetis NK (2007) Do early sensory cortices integrate cross-modal information? Brain Struct Funct 212:121–132

Kayser C, Petkov CI, Remedios R, Logothetis NK (2012) Multisensory influences on auditory processing: perspectives from fMRI and electrophysiology. In: Murray MM, Wallace MT (eds) The neural bases of multisensory processes. CRC Press, Boca Raton, pp 99-114

Kelly JB (1973) The effects of insular and temporal lesions in cats on two types of auditory pattern discrimination. Brain Res 62:71–87

Kelly J, Caspary D (2005) Pharmacology of the inferior colliculus. In: Winer J, Schreiner CE (eds) The inferior colliculus. Springer, New York, pp 248–281

Kelly JB, Zhang H (2002) Contribution of AMPA and NMDA receptors to excitatory responses in the inferior colliculus. Hear Res 168:35–42

King AJ, Walker KM (2012) Integrating information from different senses in the auditory cortex. Biol Cybern 106:617–25

King AJ, Jiang ZD, Moore DR (1998) Auditory brainstem projections to the ferret superior colliculus: anatomical contribution to the neural coding of sound azimuth. J Comp Neurol 390:342–365

Klepper A, Herbert H (1991) Distribution and origin of noradrenergic and serotonergic fibers in the cochlear nucleus and inferior colliculus of the rat. Brain Res 557:190–201

Komura Y, Tamura R, Uwano T, Nishijo H, Kaga K, Ono T (2001) Retrospective and prospective coding for predicted reward in the sensory thalamus. Nature 412:546–549

Koyama Y, Jodo E, Kayama Y (1994) Sensory responsiveness of "broad-spike" neurons in the laterodorsal tegmental nucleus, locus coeruleus and dorsal raphe of awake rats: implications for cholinergic and monoaminergic neuron-specific responses. Neuroscience 63:1021–1031

Kraus N, McGee T, Carrell T, King C, Littman T, Nicol T (1994a) Discrimination of speech-like contrasts in the auditory thalamus and cortex. J Acoust Soc Am 96:2758–2768

Kraus N, McGee T, Littman T, Nicol T, King C (1994b) Nonprimary auditory thalamic representation of acoustic change. J Neurophysiol 72:1270–1277

Kudo M, Niimi K (1980) Ascending projections of the inferior colliculus in the cat: an autoradiographic study. J Comp Neurol 191:545–556

Lakatos P, Chen CM, O'Connell MN, Mills A, Schroeder CE (2007) Neuronal oscillations and multisensory interaction in primary auditory cortex. Neuron 53:279–292

Lavoie B, Parent A (1991) Serotoninergic innervation of the thalamus in the primate: an immunohistochemical study. J Comp Neurol 312:1–18. doi:10.1002/cne.903120102

Layton BS, Toga AW, Horenstein S, Davenport DG (1979) Temporal pattern discrimination survives simultaneous bilateral ablation of suprasylvian cortex but not sequential bilateral ablation of insular-temporal cortex in the cat. Brain Res 173:337–340

LeDoux JE, Ruggiero DA, Forest R, Stornetta R, Reis DJ (1987) Topographic organization of convergent projections to the thalamus from the inferior colliculus and spinal cord in the rat. J Comp Neurol 264:123–146

Lee CC, Sherman SM (2010) Topography and physiology of ascending streams in the auditory tectothalamic pathway. Proc Natl Acad Sci U S A 107:372–377

Lee CC, Sherman SM (2011) On the classification of pathways in the auditory midbrain, thalamus, and cortex. Hear Res 276:79–87

Lee CC, Winer JA (2011) Convergence of thalamic and cortical pathways in cat auditory cortex. Hear Res 274:85–94

Lennartz RC, Weinberger NM (1992) Frequency selectivity is related to temporal processing in parallel thalamocortical auditory pathways. Brain Res 583:81–92

Li Y, Evans MS, Faingold CL (1998) In vitro electrophysiology of neurons in subnuclei of rat inferior colliculus. Hear Res 121:1–10

Li Y, Evans MS, Faingold CL (1999) Synaptic response patterns of neurons in the cortex of rat inferior colliculus. Hear Res 137:15–28

Loftus WC, Malmierca MS, Bishop DC, Oliver DL (2008) The cytoarchitecture of the inferior colliculus revisited: a common organization of the lateral cortex in rat and cat. Neuroscience 154:196–205

Loftus WC, Bishop DC, Oliver DL (2010) Differential patterns of inputs create functional zones in central nucleus of inferior colliculus. J Neurosci 30:13396–13408

Lohmann C, Friauf E (1996) Distribution of the calcium-binding proteins parvalbumin and calretinin in the auditory brainstem of adult and developing rats. J Comp Neurol 367:90–109

Lu Y, Jen PH (2001) GABAergic and glycinergic neural inhibition in excitatory frequency tuning of bat inferior collicular neurons. Exp Brain Res 141:331–339

Lumani A, Zhang H (2010) Responses of neurons in the rat's dorsal cortex of the inferior colliculus to monaural tone bursts. Brain Res 1351:115–129

Ma CL, Kelly JB, Wu SH (2002) AMPA and NMDA receptors mediate synaptic excitation in the rat's inferior colliculus. Hear Res 168:25–34

Maess B, Jacobsen T, Schroger E, Friederici AD (2007) Localizing pre-attentive auditory memory-based comparison: magnetic mismatch negativity to pitch change. Neuroimage 37:561–571

Malmierca MS, Hackett TA (2010) Structural organization of the ascending auditory pathway. In: Rees A, Palmer AR (eds) The Oxford handbook of auditory science: auditory brain. Oxford University Press, New York, pp 9–41

Malmierca MS, Seip KL, Osen KK (1995) Morphological classification and identification of neurons in the inferior colliculus: a multivariate analysis. Anat Embryol (Berl) 191:343–350

Malmierca MS, Izquierdo MA, Cristaudo S, Hernandez O, Perez-Gonzalez D, Covey E, Oliver DL (2008) A discontinuous tonotopic organization in the inferior colliculus of the rat. J Neurosci 28:4767–4776

Malmierca MS, Cristaudo S, Perez-Gonzalez D, Covey E (2009) Stimulus-specific adaptation in the inferior colliculus of the anesthetized rat. J Neurosci 29:5483–5493

Malmierca MS, Blackstad TW, Osen KK (2011) Computer-assisted 3-D reconstructions of Golgi-impregnated neurons in the cortical regions of the inferior colliculus of rat. Hear Res 274:13–26

Manunta Y, Edeline JM (2004) Noradrenergic induction of selective plasticity in the frequency tuning of auditory cortex neurons. J Neurophysiol 92:1445–1463

Mascetti GG, Strozzi L (1988) Visual cells in the inferior colliculus of the cat. Brain Res 442:387–390

May PJ, Tiitinen H (2010) Mismatch negativity (MMN), the deviance-elicited auditory deflection, explained. Psychophysiology 47:66–122

McCormick DA, Pape HC (1990) Noradrenergic and serotonergic modulation of a hyperpolarization-activated cation current in thalamic relay neurones. J Physiol (Lond) 431:319–342

Merchan M, Aguilar LA, Lopez-Poveda EA, Malmierca MS (2005) The inferior colliculus of the rat: quantitative immunocytochemical study of GABA and glycine. Neuroscience 136:907–925

Meredith MA, Allman BL, Keniston LP, Clemo HR (2012) Are bimodal neurons the same throughout the brain? In: Murray MM, Wallace MT (eds) The neural bases of multisensory processes. CRC Press, Boca Raton, http://www.ncbi.nlm.nih.gov/books/NBK92874/

Metherate R, Weinberger NM (1989) Acetylcholine produces stimulus-specific receptive field alterations in cat auditory cortex. Brain Res 480:372–377

Metherate R, Intskirveli I, Kawai HD (2012) Nicotinic filtering of sensory processing in auditory cortex. Front Behav Neurosci 6:44. doi:10.3389/fnbeh.2012.00044

Mikell CB, Sheehy JP, Youngerman BE, McGovern RA, Wojtasiewicz TJ, Chan AK, Pullman SL, Yu Q, Goodman RR, Schevon CA, McKhann GM 2nd (2014) Features and timing of the response of single neurons to novelty in the substantia nigra. Brain Res 1542:79–84

Mill R, Coath M, Wennekers T, Denham SL (2011a) Abstract stimulus-specific adaptation models. Neural Comput 23:435–476

Mill R, Coath M, Wennekers T, Denham SL (2011b) A neurocomputational model of stimulus-specific adaptation to oddball and Markov sequences. PLoS Comput Biol 7:e1002117

Miller LM, Escabi MA, Read HL, Schreiner CE (2001) Functional convergence of response properties in the auditory thalamocortical system. Neuron 32:151–160

Minks E, Jurák P, Chládek J, Chrastina J, Halámek J, Shaw DJ, Bareš M (2014) Mismatch negativity-like potential (MMN-like) in the subthalamic nuclei in Parkinson's disease patients. J Neural Transm 121:1507–1522. doi:10.1007/s00702-014-1221-3

Molinari M, Dell'Anna ME, Rausell E, Leggio MG, Hashikawa T, Jones EG (1995) Auditory thalamocortical pathways defined in monkeys by calcium-binding protein immunoreactivity. J Comp Neurol 362: 171–194

Monaghan DT, Cotman CW (1985) Distribution of N-methyl-D-aspartate-sensitive L-[3H]glutamate-binding sites in rat brain. J Neurosci 5:2909–2919

Monckton JE, McCormick DA (2002) Neuromodulatory role of serotonin in the ferret thalamus. J Neurophysiol 87:2124–2136

Moore RY, Bloom FE (1979) Central catecholamine neuron systems: anatomy and physiology of the norepinephrine and epinephrine systems. Annu Rev Neurosci 2:113–168

Moran RJ, Campo P, Symmonds M, Stephan KE, Dolan RJ, Friston KJ (2013) Free energy, precision and learning: the role of cholinergic neuromodulation. J Neurosci 33:8227–8236

Morris RG (2013) NMDA receptors and memory encoding. Neuropharmacology 74:32–40

Movshon JA, Lennie P (1979) Pattern-selective adaptation in visual cortical neurons. Nature 278:850–852

Näätänen R, Gaillard AW, Mantysalo S (1978) Early selective-attention effect on evoked potential reinterpreted. Acta Psychol (Amst) 42: 313–329

Näätänen R, Tervaniemi M, Sussman E, Paavilainen P, Winkler I (2001) "Primitive intelligence" in the auditory cortex. Trends Neurosci 24: 283–288

Nagy A, Paróczy Z, Norita M, Benedek G (2005) Multisensory responses and receptive field properties of neurons in the substantia nigra and in the caudate nucleus. Eur J Neurosci 22:419–424

Nagy A, Eördegh G, Paróczy Z, Márkus Z, Benedek G (2006) Multisensory integration in the basal ganglia. Eur J Neurosci 24: 917–924

Nakamura T, Michie PT, Fulham WR, Todd J, Budd TW, Schall U, Hunter M, Hodgson DM (2011) Epidural auditory event-related potentials in the rat to frequency and duration deviants: evidence of mismatch negativity? Front Psychol 2:367. doi:10.3389/fpsyg.2011.00367

Nelken I (2014) Stimulus-specific adaptation and deviance detection in the auditory system: experiments and models. Biol Cybern 108: 655–663. doi:10.1007/s00422-014-0585-7

Nelken I, Ulanovsky N (2007) Mismatch negativity and stimulus-specific adaptation in animal models. J Psychophysiol 21:214–223

Nir Y, Vyazovskiy VV, Cirelli C, Banks MI, Tononi G (2013) Auditory responses and stimulus-specific adaptation in rat auditory cortex are preserved across NREM and REM sleep. Cereb Cortex. doi:10.1093/cercor/bht328

Olazabal UE, Moore JK (1989) Nigrotectal projection to the inferior colliculus: horseradish peroxidase transport and tyrosine hydroxylase immunohistochemical studies in rats, cats, and bats. J Comp Neurol 282:98–118

Oliver DL (2005) Neuronal organization in the inferior colliculus. In: Schreiner CE, Winer JA (eds) The inferior colliculus. New York, Springer, pp 69–131

Oliver DL, Huerta MF (1992) Inferior and superior colliculi. In: Webster DB, Popper AN, Fay RR (eds) Springer handbook of auditory research, vol 1. The mammalian auditory pathway: neuroanatomy. Springer, New York, pp 168–221

Opitz B, Schröger E, Cramon DY von (2005) Sensory and cognitive mechanismsfor preattentive change detection in auditory cortex. Eur J Neurosci 21:531–535

Ouda L, Syka J (2012) Immunocytochemical profiles of inferior colliculus neurons in the rat and their changes with aging. Front Neural Circuits 6:68. doi:10.3389/fncir.2012.00068

Paloff AM, Hinova-Palova DV (1998) Topographical distribution of NADPH-diaphorase positive neurons in the cat's inferior colliculus. J Hirnforsch 39:231–243

Paloff AM, Usunoff KG (2000) Tyrosine hydroxylase-like immunoreactive synaptic boutons in the inferior colliculus of the cat. Ann Anat 182:423–426

Pape HC, McCormick DA (1989) Noradrenaline and serotonin selectively modulate thalamic burst firing by enhancing a hyperpolarization-activated cation current. Nature 340:715–718

Parks TN (2000) The AMPA receptors of auditory neurons. Hear Res 147:77–91

Penzo MA, Pena JL (2009) Endocannabinoid-mediated long-term depression in the avian midbrain expressed presynaptically and postsynaptically. J Neurosci 29:4131–4139

Perez-Gonzalez D, Malmierca MS, Covey E (2005) Novelty detector neurons in the mammalian auditory midbrain. Eur J Neurosci 22: 2879–2885

Perez-Gonzalez D, Hernandez O, Covey E, Malmierca MS (2012) GABA(A)-mediated inhibition modulates stimulus-specific adaptation in the inferior colliculus. PLoS One 7:e34297. doi:10.1371/journal.pone.0034297

Perrault TJ Jr, Vaughan JW, Stein BE, Wallace MT (2003) Neuron-specific response characteristics predict the magnitude of multisensory integration. J Neurophysiol 90:4022–4026

Peruzzi D, Bartlett E, Smith PH, Oliver DL (1997) A monosynaptic GABAergic input from the inferior colliculus to the medial geniculate body in rat. J Neurosci 17:3766–3777

Petralia RS, Wenthold RJ (1992) Light and electron immunocytochemical localization of AMPA-selective glutamate receptors in the rat brain. J Comp Neurol 318:329–354

Petralia RS, Yokotani N, Wenthold RJ (1994) Light and electron microscope distribution of the NMDA receptor subunit NMDAR1 in the rat nervous system using a selective anti-peptide antibody. J Neurosci 14:667–696

Pincze Z, Lakatos P, Rajkai C, Ulbert I, Karmos G (2001) Separation of mismatch negativity and the N1 wave in the auditory cortex of the cat: a topographic study. Clin Neurophysiol 112:778–784

Pincze Z, Lakatos P, Rajkai C, Ulbert I, Karmos G (2002) Effect of deviant probability and interstimulus/interdeviant interval on the auditory N1 and mismatch negativity in the cat auditory cortex. Brain Res Cogn Brain Res 13:249–253

Ranganath C, Rainer G (2003) Neural mechanisms for detecting and remembering novel events. Nat Rev Neurosci 4:193–202

Reches A, Gutfreund Y (2008) Stimulus-specific adaptation in the gaze control system of the barn owl. J Neurosci 28:1523–1533

Reches A, Netser S, Gutfreund Y (2010) Interactions between stimulus-specific adaptation and visual auditory integration in the forebrain of the barn owl. J Neurosci 30:6991–6998

Reese NB, Garcia-Rill E, Skinner RD (1995) Auditory input to the pedunculopontine nucleus. II. Unit responses. Brain Res Bull 37: 265–273

Regehr WG (2012) Short-term presynaptic plasticity. Cold Spring Harb Perspect Biol 4:a005702. doi:10.1101/cshperspect.a005702

Regehr WG, Carey MR, Best AR (2009) Activity-dependent regulation of synapses by retrograde messengers. Neuron 63:154–170

Rektor I, Bares M, Kubová D (2001) Movement-related potentials in the basal ganglia: a SEEG readiness potential study. Clin Neurophysiol 112:2146–2153

Richardson BD, Ling LL, Uteshev VV, Caspary DM (2011) Extrasynaptic GABA(A) receptors and tonic inhibition in rat auditory thalamus. PLoS One 6:e16508. doi:10.1371/journal.pone.0016508

Romand R, Ehret G (1990) Development of tonotopy in the inferior colliculus. I. Electrophysiological mapping in house mice. Brain Res Dev Brain Res 54:221–234

Rosburg T, Trautner P, Ludowig E, Schaller C, Kurthen M, Elger CE, Boutros NN (2007) Hippocampal event-related potentials to tone duration deviance in a passive oddball paradigm in humans. Neuroimage 37:274–281

Rothman JS, Cathala L, Steuber V, Silver RA (2009) Synaptic depression enables neuronal gain control. Nature 457:1015–1018

Rouiller EM, Colomb E, Capt M, De Ribaupierre F (1985) Projections of the reticular complex of the thalamus onto physiologically characterized regions of the medial geniculate body. Neurosci Lett 53:227–232

Ruusuvirta T, Korhonen T, Penttonen M, Arikoski J (1995a) Hippocampal evoked potentials to pitch deviances in an auditory oddball situation in the rabbit: no human mismatch-like dependence on standard stimuli. Neurosci Lett 185:123–126

Ruusuvirta T, Korhonen T, Penttonen M, Arikoski J, Kivirikko K (1995b) Behavioral and hippocampal evoked responses in an auditory oddball situation when an unconditioned stimulus is paired with deviant tones in the cat: experiment II. Int J Psychophysiol 20:41–47

Ruusuvirta T, Korhonen T, Penttonen M, Arikoski J, Kivirikko K (1995c) Hippocampal event-related potentials to pitch deviances in an auditory oddball situation in the cat: experiment I. Int J Psychophysiol 20:33–39

Ruusuvirta T, Korhonen T, Arikoski J, Kivirikko K (1996) ERPs to pitch changes: a result of reduced responses to standard tones in rabbits. Neuroreport 7:413–416

Ruusuvirta T, Penttonen M, Korhonen T (1998) Auditory cortical event-related potentials to pitch deviances in rats. Neurosci Lett 248:45–48

Ruusuvirta T, Astikainen P, Wikgren J, Nokia M (2010) Hippocampus responds to auditory change in rabbits. Neuroscience 170:232–237

Ruusuvirta T, Lipponen A, Pellinen E, Penttonen M, Astikainen P (2013) Auditory cortical and hippocampal-system mismatch responses to duration deviants in urethane-anesthetized rats. PLoS One 8: e54624. doi:10.1371/journal.pone.0054624

Saint Marie RL, Ostapoff EM, Morest DK, Wenthold RJ (1989) Glycine-immunoreactive projection of the cat lateral superior olive: possible role in midbrain ear dominance. J Comp Neurol 279:382–396

Sanchez-Gonzalez MA, Garcia-Cabezas MA, Rico B, Cavada C (2005) The primate thalamus is a key target for brain dopamine. J Neurosci 25:6076–6083

Sanes DH, Geary WA, Wooten GF, Rubel EW (1987) Quantitative distribution of the glycine receptor in the auditory brain stem of the gerbil. J Neurosci 7:3793–3802

Sato K, Kiyama H, Park HT, Tohyama M (1993) AMPA, KA and NMDA receptors are expressed in the rat DRG neurones. Neuroreport 4: 1263–1265

Schofield BR (2010) Projections from auditory cortex to midbrain cholinergic neurons that project to the inferior colliculus. Neuroscience 166:231–240

Schofield BR, Motts SD, Mellott JG (2011) Cholinergic cells of the pontomesencephalic tegmentum: connections with auditory structures from cochlear nucleus to cortex. Hear Res 279:85–95

Schröger E, Wolff C (1996) Mismatch response of the human brain to changes in sound localization. Neuroreport 7:3005–3008

Shigemoto R, Nomura S, Ohishi H, Sugihara H, Nakanishi S, Mizuno N (1993) Immunohistochemical localization of a metabotropic glutamate receptor, mGluR5, in the rat brain. Neurosci Lett 163:53–57

Shinonaga Y, Takada M, OgawaMeguro R, Ikai Y, Mizuno N (1992) Direct projections from the globus pallidus to the midbrain and pons in the cat. Neurosci Lett 135:179–183

Shinonaga Y, Takada M, Mizuno N (1994) Direct projections from the non-laminated divisions of the medial geniculate nucleus to the temporal polar cortex and amygdala in the cat. J Comp Neurol 340:405–426

Shiramatsu TI, Kanzaki R, Takahashi H (2013) Cortical mapping of mismatch negativity with deviance detection property in rat. PLoS One 8:e82663. doi:10.1371/journal.pone.0082663

Shore SE (2008) Auditory/somatosensory interactions. In: Adelman G, Smith BH (eds) The new encyclopedia of neurosciences. Elsevier Science, Amsterdam

Siegel SJ, Connolly P, Liang Y, Lenox RH, Gur RE, Bilker WB, Kanes SJ, Turetsky BI (2003) Effects of strain, novelty, and NMDA blockade on auditory-evoked potentials in mice. Neuropsychopharmacology 28:675–682

Slabu L, Escera C, Grimm S, Costa-Faidella J (2010) Early change detection in humans as revealed by auditory brainstem and middle-latency evoked potentials. Eur J Neurosci 32:859–865

Slabu L, Grimm S, Escera C (2012) Novelty detection in the human auditory brainstem. J Neurosc 32:1447–452

Smith PH, Bartlett EL, Kowalkowski A (2007) Cortical and collicular inputs to cells in the rat paralaminar thalamic nuclei adjacent to the medial geniculate body. J Neurophysiol 98:681–695

Stebbings KA, Lesicko AM, Llano DA (2014) The auditory corticocollicular system: molecular and circuit-level considerations. Hear Res 314:51–59

Stein BE, Meredith MA (1993) The merging of the senses. MIT Press, Cambridge

Stein BE, Stanford TR (2008) Multisensory integration: current issues from the perspective of the single neuron. Nat Rev Neurosci 9: 255–266

Stein BE, Wallace MT (1996) Comparisons of cross-modality integration in midbrain and cortex. Prog Brain Res 112:289–299

Swanson LW, Hartman BK (1975) The central adrenergic system. An immunofluorescence study of the location of cell bodies and their efferent connections in the rat utilizing dopamine-beta-hydroxylase as a marker. J Comp Neurol 163:467–505

Taaseh N, Yaron A, Nelken I (2011) Stimulus-specific adaptation and deviance detection in the rat auditory cortex. PLoS One 6:e23369. doi:10.1371/journal.pone.0023369

Tardif E, Chiry O, Probst A, Magistretti PJ, Clarke S (2003) Patterns of calcium-binding proteins in human inferior colliculus: identification of subdivisions and evidence for putative parallel systems.Neuroscience 116:1111–1121

Tebecis AK (1970) Effects of monoamines and amino acids on medial geniculate neurones of the cat. Neuropharmacology 9:381–390

Tebecis AK (1972) Cholinergic and non-cholinergic transmission in the medial geniculate nucleus of the cat. J Physiol 226:153–172

Tepper JM, Martin LP, Anderson DR (1995) GABAA receptor mediated inhibition of rat substantia nigra dopaminergic neurons by pars reticulata projection neurons. J Neurosci 15:3092–3103

Tong L, Altschuler RA, Holt AG (2005) Tyrosine hydroxylase in rat auditory midbrain: distribution and changes following deafness. Hear Res 206:28–41

Tongjaroenbuangam W, Jongkamonwiwat N, Phansuwan-Pujito P, Casalotti SO, Forge A, Dodson H, Govitrapong P (2006) Relationship of opioid receptors with GABAergic neurons in the rat inferior colliculus. Eur J Neurosci 24:1987–1994

Trattner B, Berner S, Grothe B, Kunz L (2013) Depolarization-induced suppression of a glycinergic synapse in the superior olivary complex by endocannabinoids. J Neurochem 127:78–90

Ulanovsky N, Las L, Nelken I (2003) Processing of low-probability sounds by cortical neurons. Nat Neurosci 6:391–398

Ulanovsky N, Las L, Farkas D, Nelken I (2004) Multiple time scales of adaptation in auditory cortex neurons. J Neurosci 24:10440–10453

Umbricht D, Vyssotki D, Latanov A, Nitsch R, Lipp HP (2005) Deviance-related electrophysiological activity in mice: is there mismatch negativity in mice? Clin Neurophysiol 116:353–363

Varela C (2014) Thalamic neuromodulation and its implications for executive networks. Front Neural Circuits 8:69. doi:10.3389/fncir.2014.00069

Varela C, Sherman SM (2007) Differences in response to muscarinic activation between first and higher order thalamic relays. J Neurophysiol 98:3538–3547

Varela C, Sherman SM (2009) Differences in response to serotonergic activation between first and higher order thalamic nuclei. Cereb Cortex 19:1776–1786

Vater M, Braun K (1994) Parvalbumin, calbindin D-28 k, and calretinin immunoreactivity in the ascending auditory pathway of horseshoe bats. J Comp Neurol 341:534–558

Venecia RK de, Smelser CB, Lossman SD, McMullen NT (1995) Complementary expression of parvalbumin and calbindin D-28 k delineates subdivisions of the rabbit medial geniculate body. J Comp Neurol 359:595–612

Vertes RP, Linley SB, Hoover WB (2010) Pattern of distribution of serotonergic fibers to the thalamus of the rat. Brain Struct Funct 215:1–28

Wenstrup JJ (2005) The tectothalamic system. In: Winer JA, Schreiner CE (eds) The inferior colliculus. Springer, New York, pp 69–131

Westerman LA, Smith RL (1985) Rapid adaptation depends on the characteristic frequency of auditory nerve fibers. Hear Res 17:197–198

Wilson RI, Nicoll RA (2002) Endocannabinoid signaling in the brain. Science 296:678–682

Wilson RI, Kunos G, Nicoll RA (2001) Presynaptic specificity of endocannabinoid signaling in the hippocampus. Neuron 31:453–462

Winer JA (1992) The functional architecture of the medial geniculate body and the primary auditory cortex. In: Webster DB, Popper AN, Fay RR (eds) Springer handbook of auditory research, vol 1. The mammalian auditory pathway: neuroanatomy. Springer, New York, pp 222–409

Winer JA, Larue DT (1996) Evolution of GABAergic circuitry in the mammalian medial geniculate body. Proc Natl Acad Sci U S A 93: 3083–3087

Winer JA, Saint Marie RL, Larue DT, Oliver DL (1996) GABAergic feedforward projections from the inferior colliculus to the medial geniculate body. Proc Natl Acad Sci U S A 93:8005–8010

Winkler I, Denham SL, Nelken I (2009) Modeling the auditory scene: predictive regularity representations and perceptual objects. Trends Cogn Sci 13:532–540

Wu C, Stefanescu RA, Martel DT, Shore SE (2014) Listening to another sense: somatosensory integration in the auditory system. Cell Tissue Res. doi:10.1007/s00441-014-2074-7

Wynne B, Robertson D (1997) Somatostatin and substance P-like immunoreactivity in the auditory brainstem of the adult rat. J Chem Neuroanat 12:259–266

Yamauchi K, Yamadori T (1982) Retinal projection to the inferior colliculus in the rat. Acta Anat (Basel) 114:355–360

Yaron A, Hershenhoren I, Nelken I (2012) Sensitivity to complex statistical regularities in rat auditory cortex. Neuron 76:603–615

Yasui Y, Nakano K, Kayahara T, Mizuno N (1991) Nondopaminergic projections from the substantia nigra pars lateralis to the inferior colliculus in the rat. Brain Res 559:139–144

Yu XJ, Xu XX, He S, He J (2009) Change detection by thalamic reticular neurons. Nat Neurosci 12:1165–1170

Zahar Y, Reches A, Gutfreund Y (2009) Multisensory enhancement in the optic tectum of the barn owl: spike count and spike timing. J Neurophysiol 101:2380–2394

Zettel ML, Carr CE, O'Neill WE (1991) Calbindin-like immunoreactivity in the central auditory system of the mustached bat, *Pteronotus parnelli*. J Comp Neurol 313:1–16

Zhao L, Liu Y, Shen L, Feng L, Hong B (2011) Stimulus-specific adaptation and its dynamics in the inferior colliculus of rat. Neuroscience 181:163–174

Zhao Y, Tzounopoulos T (2011) Physiological activation of cholinergic inputs controls associative synaptic plasticity via modulation of endocannabinoid signaling. J Neurosci 31:3158–3168

Zhao Y, Rubio ME, Tzounopoulos T (2009) Distinct functional and anatomical architecture of the endocannabinoid system in the auditory brainstem. J Neurophysiol 101:2434–2446

Stimulus-specific adaptation in the inferior colliculus: The role of excitatory, inhibitory and modulatory inputs

Yaneri A. Ayala[1*], D. Pérez-González[1*] and M.S. Malmierca[1,2]

*These authors contributed equally

Affiliations:
[1] Auditory Neurophysiology Unit, Institute of Neuroscience of Castilla y León, University of Salamanca, 37007 Salamanca, Spain
[2] Department of Cell Biology and Pathology, Faculty of Medicine, University of Salamanca, 37007 Salamanca, Spain

Corresponding author:
Manuel S. Malmierca
Auditory Neurophysiology Laboratory (Lab 1)
Institute of Neuroscience of Castilla y León
University of Salamanca
C/ Pintor Fernando Gallego, 1
37007 Salamanca, Spain

Figures**: 11**
Tables**: 1**
Abstract**: 241 words**
Main text**: 3900 words**

Keywords: **MMN, GABA, glutamate, acetylcholine, auditory**
Running title: **Neuropharmachology of auditory change detection**

Abstract

Patients suffering from pathologies such as schizophrenia, depression or dementia exhibit cognitive impairments, some of which can be reflected in event-related potential (ERP) measurements as the mismatch negativity (MMN). The MMN is one of the most commonly used ERPs and provides an electrophysiological index of auditory change or deviance detection. Moreover, MMN has been positioned as a potentially promising biomarker candidate for the diagnosis and prediction of the outcome of schizophrenia. Dysfunction of neural receptors has been linked to the etiopathology of schizophrenia or the induction of psychophysiological anomalies similar to those observed in schizophrenia.Stimulus-specific adaptation (SSA) is a neural mechanism that contributes to the upstream processing of auditory change detection. Auditory neurons that exhibit SSA specifically adapt their response to repetitive sounds but maintain their excitability to respond to rare ones. Thus, by studying the role of neuronal receptors on SSA, we can contribute to detangle the cellular bases of the impairments in deviance processing occurring in mental pathologies. Here, we review the current knowledge on the effect of $GABA_A$-mediated inhibition and the modulation of acetylcholine on SSA in the inferior colliculus, and we add unpublished original data obtained blocking glutamate receptors. We found that the blockade of $GABA_A$ and glutamate receptors mediates an overall increase or decrease of the neural response, respectively, while acetylcholine affects only the response to the repetitive sounds. These results demonstrate that GABAergic, glutamatergic and cholinergic receptors play different and complementary roles on shaping SSA.

Overview

Event-related potentials such as the mismatch negativity response (MMN) have been extensively used as a neurophysiological index of preattentive auditory sensory memory as it occurs in response to a sensory stimulus that violates previously established patterns of regularity (1). The MMN is measured as the difference between the auditory-evoked potential elicited by a repetitive sound compared with the potential elicited by a rare, unexpected sound (larger amplitude) in electroencephalographic studies. MMN has been positioned as a potentially promising biomarker candidate for the diagnosis of pathologies such as schizophrenia (2, 3) among others. Patients with schizophrenia exhibited a reduced ability to detect acoustic changes reflected in reduced MMN (4-6). Schizophrenia has been associated with alterations in neurotransmission as the one mediated by the NMDA receptor (7). Moreover, diverse studies have showed that acoustic MMN is sensitive to cholinergic modulation (8-11) or to nitrous oxide e.g. (N_2O) (12). Thus, a starting point for elucidating how alterations in neurotransmission contribute to deficits in deviance detection is to employ animal models to pharmacologically isolate the role of specific modulatory substances on event-related potentials or on correlated neuronal activity. Recent studies have demonstrated that MMN-like responses occur in animal models like the rat (3, 13). Likewise, neurons that exhibit a specific decrement in their response to repetitive but not to rare sounds have been characterized in animals. This specialized neural response is referred as 'stimulus-specific adaptation' (SSA). SSA is a particular type of neuronal adaptation (14) that occurs in the non-lemniscal subdivisions of the inferior colliculus (IC) (15), auditory thalamus (16) and primary auditory cortex (17). SSA is thought to contribute to the upstream processing of deviant and repetitive signals reflected in event-related potentials (18, 19). Cellular mechanisms underlying SSA are likely to act at the sites of

synaptic input on IC neurons and those might include synaptic depression and/or facilitation or inhibition. Moreover, several studies have demonstrated that different neuromodulators disinhibit neural circuits representing a mechanism for gating excitatory and inhibitory synaptic plasticity (revised in (20)). For example, acetylcholine transiently disrupts excitatory-inhibitory balance underlying neural receptive fields (21, 22). Thus, recent work in our laboratory has focused on the effect of blocking or activating putative excitatory, inhibitory and neuromodulatory inputs on IC neurons exhibiting SSA. In the following, we will first describe hitherto unpublished original data obtained blocking glutamate receptors and then we review our previous work on the effect of $GABA_A$ mediated inhibition (23, 24) and the modulation of acetylcholine (ACh) on SSA (25).

Excitatory, inhibitory, and cholinergic inputs to the IC

The IC is the main auditory midbrain center (26) and is characterized by the convergence of ascending and descending auditory projections. Hence, multiple excitatory, inhibitory and modulatory inputs converge onto single IC neurons (26-30) that also receive neuromodulatory inputs from multiple sources (for a review see (31)).

Excitatory inputs to the IC are made of glutamatergic projections and arise from the ventral and dorsal cochlear nuclei, lateral and medial superior olive and ventral nucleus of the lateral lemniscus (26, 32, 33) (Fig. 1). The excitatory neurotransmission in the auditory midbrain is mostly mediated through glutamatergic receptors. Ionotropic glutamate receptors mediate excitatory input at most nuclei in the ascending auditory pathway including the IC. For example, recordings in brain slices of the IC after electrical stimulation of the lateral lemniscus fibers demonstrated that there were two distinct components of the excitatory responses (34): a rapid, short latency component

that was mediated by AMPA receptors, and a component with longer latency and duration that was mediated by NMDA receptors. NMDA receptors have been associated with the generation of MMN (35-39). Interestingly, Umbricht *et al.* (40) applied NMDA antagonists to human volunteers and found a reduced MMN, similar to that previously found in schizophrenia (41-44). In a recent study, Kompus *et al.* (45) found that healthy individuals with increased indicators of glutamatergic neurotransmission presented shorter latencies to MMN for changes in sound duration. But animal studies are controversial. While Farley *et al.* (46) found that SSA in auditory cortical neurons of rats was insensitive to the systemic application of NMDA antagonists, Featherstone *et al.* (47), using a probably more sensitive murine model with a heterozygous alteration of the NMDA receptor NR1 subunit gene, reported a significant reduction in the expression of NMDA receptors that caused a distinct decrement of MMN. Thus NMDA receptors may be linked to the generation, shaping and/or modulation of SSA.

Inhibitory inputs to the IC are mediated by GABA and glycine (48-51). Glycinergic inhibition arises from the ipsilateral lateral superior olive and the ventral nucleus of the lateral lemniscus (50, 52) while GABAergic inputs arise from several extrinsic and intrinsic sources (Fig. 1). Extrinsic GABAergic sources includes the lateral superior olive and the superior paraolivary nucleus (53), ventral nucleus of the lateral lemniscus ipsilaterally, and the dorsal nucleus of the lateral lemniscus bilaterally (54-57). In addition local IC GABAergic neurons (51, 58, 59) affect neural responsiveness through intrinsic or commissural projections (60, 61). The GABAergic-mediated inhibition acts on $GABA_A$ and $GABA_B$ receptors expressed across IC neurons. The pharmacological manipulation of the $GABA_A$ receptors significantly affects sound-evoked responses (62, 63), modifying different response properties including frequency tuning (62, 64-66),

response to sound intensity (67), coding of interaural time and level differences (68-70) as well as IC responsiveness to binaural motion cues (71).

Neuromodulatory influences to the IC include those mediated by noradrenergic (72, 73), serotoninergic (29, 74-76), dopaminergic (77, 78) and cholinergic projections (30). The cholinergic inputs originate in the pontomesencephalic tegmentum that includes the pedunculopontine and laterodorsal tegmental nucleus. Those cholinergic neurons are innervated by auditory cortical neurons from layer V (30, 79) (Fig. 1). Very little is known about the type and distribution of the cholinergic receptors on IC neurons and their functional impact on neural firing. Overall, both cholinergic receptors (muscarinic and nicotinic) are expressed in the IC (80, 81) and they are likely to be pre- as well as postsynaptic receptors (reviewed in (82)). Earlier studies revealed diverse effects of ACh on IC neural responses (potentiated and suppressed sound-evoked activity) suggesting ACh exerts a complex and dynamic modulation (83-85).

Experimental Approach

In vivo iontophoresis is a powerful technique that allows the pharmacological manipulation of neuronal responses at the synaptic level. Therefore, it is an excellent choice to determine the role of synaptic inputs on sensory processing, since it allows maintaining intact the whole neural circuitry. This technique consists in the minute release of different and selective compounds (agonists, antagonists, e.g.) very close (usually around 20-40 µm) to the recorded neuron to reversibly block or activate specific receptors. Recordings are performed using so-called piggy-back electrodes, which are made of a recording electrode (usually a glass or tungsten electrode) attached to a multibarrel glass micropipette (Fig. 2A). The glass barrels contain the neuroactive substances that are retained and ejected by the application of current injections (in the

range of nA) (86, 87). Then, different neuroactive compounds can be co-released to simulate the natural heather of neurotransmitters and neuromodulators that occurs in natural conditions.

To study auditory SSA, one pair of frequencies usually surrounding the characteristic frequency of each neuron (frequency of a sound capable of evoking a response at the lowest sound intensity) is chosen from its frequency response area (FRA; spectrum of frequencies and intensities that evoke a suprathreshold response, Fig. 2B). Those frequencies are presented under the 'oddball paradigm' widely used in human studies (88) and more recently in animal studies (17). The oddball paradigm consists in the presentation of one frequency at high probability of occurrence (standard tone) while the second frequency is presented rarely (deviant tone). Afterwards, the relative probabilities of the pair of frequencies are switched to validate that the neuron adapts to the repetitive stimulus and the decrease in response is due the frequency response (Fig. 2C). The amount of SSA to both frequencies is estimated by the Common-SSA index (CSI) which reflects the normalized difference in the evoked response between deviant and standard tones with values between −1 and 1. Positive CSI values indicate a stronger response to deviant tones while negative CSIs indicate a stronger response to standard tones. A CSI value of zero reflects an equal response to deviant and standard tones (Fig. 2D). By repeating this paradigm before, during and after the iontophoretic application of specific drugs we can dissect the contribution and specificity of different receptors on the neural response to deviant and to standard tones and its effect on CSI, i.e., we can determine what role, if any, they play on SSA.

Effect of glutamatergic excitation on SSA

In order to study the effect glutamate on SSA, we recorded from 37 neurons in the IC using an oddball stimulation paradigm, as described above, before, during and after the microiontophoresis application of either CPP or NBQX. These drugs are selective antagonists of the NMDA or AMPA/kainate glutamate receptors, respectively. Here we report for the first time a total of 53 applications of drugs, consisting of 28 applications of CPP and 25 applications of NBQX. In 15 cases both drugs were tested sequentially on the same neuron, so the second drug was applied after the effects of the first one had disappeared. At the beginning of each experiment we isolated a single unit, and then we played trains of stimuli in an oddball paradigm, in order to obtain the baseline response of the neuron. We continued recording the responses to this stimulation protocol during the local application and afterwards until the neuronal responses returned to their baseline levels.

Effect on spike counts

The application of both CPP and NBQX produced a significant decrement on the neuronal response, measured as spike counts. Since we measured two sound frequencies for each drug application, we took 56 measurements of the effect of CPP (Fig. 3A), and most of those (47 for standards, 43 for deviants) showed a significant decrease in the number of spikes evoked per trial (Bootstrapping, 95% confidence interval). The application of CPP caused an average decrement of ~60% on the responses to both standard and deviant stimuli (Fig. 3A). The measurements for the application of glutamate antagonists are summarized in Table 1.

The application of NBQX also resulted in a decrement of the spike counts (Fig. 3B). In this case, we obtained 50 measurements during the application of NBQX, where 40 standard cases and 33 deviant cases showed a significant decrease in the number of spikes evoked per trial. The application of NBQX caused an average decrement of ~70% on the responses to the standard stimuli (Fig. 3B). In contrast, (Fig. 3B), the application of NBQX caused an average decrement of ~54% on the responses to deviant stimuli.

As previously reported (15), the responses before the application of drugs were stronger for deviant stimuli than for standard stimuli (Fig. 3C,D). The reduction of the spike rates due to the effect of both drugs was significant (2-way ANOVA) for the standard stimuli as well as for the deviant stimuli, as shown in Figure 3C,D.

Effect on first spike latency

We found that the first spike latency (FLS) of the responses to standard stimuli was larger than in response to deviant stimuli, which is consistent with previous studies (15). The application of CPP produced a significant increment of the FSL (Bootstrapping, 95% confidence interval) in 20/56 cases in response to the standard stimuli (Fig. 4A) and 26/56 cases in response to the deviant stimuli (Fig. 4A). The effect of the FSL was larger during the application of NBQX, which caused a significant increment in 24/50 standard cases (Fig. 4B) and 30/50 deviant cases (Fig. 4B). Moreover, NBQX not only increased the latency of more neurons, but also the increment was larger. While some neurons experienced a significant increment of latency during the application of CPP, it did not cause a significant change at the population level (2-way ANOVA) in response to standard nor deviant stimuli (Fig. 4C). In contrast, the effect of NBQX (Fig. 4D) was

large enough to be significant at the population level, for both standard and deviant stimuli.

Effect on SSA index

The effect of the drugs on the common SSA index (CSI) was very variable. We recorded from units with a very large range of baseline CSI, from -0.06 up to 0.93 (Fig. 5A,B). Out of the 28 units tested with CPP, 20 showed an increment of the CSI during the application, while 8 showed a decrement. In the case of NBQX, in 13 out of 25 units the CSI increased during the application of the drug, while in 12 units it decreased. For both drugs the average effect was an overall increment of the CSI, ~0.1 in the case of CPP (Fig. 5A) and ~0.05 in the case of NBQX (Fig. 5B). Nevertheless, due to the high individual variability, the effects of the drugs on the CSI at the population level were not significant (2-way ANOVA, Fig. 5C), probably because the effects on individual neurons were averaged out. The values found for the frequency-specific SSA index (SI_f) were very similar to those obtained for the CSI (Table 1).

Effect on the time course of adaptation

We analyzed separately the temporal dynamics of adaptation to the standard and deviant stimuli across the population, during the oddball paradigm (Fig. 6). As in previous studies (24), the time course of adaptation for the standard stimuli was fitted by a double exponential function $f(t) = A_{ss} + A_r \times e^{-t/\tau(r)} + A_s \times e^{-t/\tau(s)}$. This function contains rapid and slow decay components, before reaching a steady-state.

The goodness of fit of the double exponential function to the responses to standard stimuli was good, with $r^2 > 0.65$ in all cases. As expected from the spike count results, the overall response was smaller during the application of the drugs (Fig. 6A,B), due

mainly to a smaller steady-state component (A_{ss}) (Fig. 6A,B). The application of both drugs made the fast time constant (τ_r) faster, especially in the case of NBQX. The application of the drugs made the slow time constant (τ_s) slower in the case of the CPP application, but not for NBQX.

The adaptation to the deviant stimuli was very low under the control (Fig. 6C,D; red dots) and effect (Fig. 6C,D; yellow dots) conditions, for both drugs. The time course of adaptation for deviant stimuli was best fitted to a linear function f(t) = a + bt, and in none of the cases the slope coefficient (b) was significantly different to zero. The main effect of the drugs was to reduce the constant component (a), from to roughly the half.

Effect of GABAergic-mediated inhibition on SSA

The first attempt to disentangle how the synaptic inhibitory inputs shape SSA was carried out by (24). This study manipulated the GABAergic inhibition that adapting neurons in the IC receive to address whether the adaptation to the standard tone was generated by the activation of the $GABA_A$ receptors. The blockade of the $GABA_A$ receptors using the specific antagonist (gabazine) exerted a profound effect on the magnitude and dynamics of SSA by increasing the neural firing rate and by altering the temporal response pattern. An example of the typical effect exerted by gabazine on the firing of adapting IC neurons is illustrated in Figure 7. This neuron exhibited significant SSA during the control condition, i.e. previous to the gabazine application (Fig. 7A), and responded to the deviant sound presentations but quickly adapted its response to the standard tone after a few presentations. Neurons like this one exhibit shorter response latency to the deviant than to the standard tone. The overall effect of blocking $GABA_A$ receptors is an augmentation in the response strength to both, deviant and standard stimulus (Fig. 7B). As clearly shown for this neuron, the number of spikes per trial

increased but the response strength remained larger for the deviant tone (Fig. 7C). Gabazine also decreases the response latency to deviant and standard stimuli but does not abolish the difference between them. These results demonstrate that the firing pattern and response latency of these neurons depends mainly on the probability of the stimulus even during gabazine application. Another interesting finding of the study by Pérez-González and colleagues was that the effect of gabazine was faster on the response to the standard tone than to the deviant in some neurons (34%) but the contrary did not occur in any IC neuron. This variability of the gabazine effect was reflected in the time course of the difference signal (difference in the neural PSTH) between the response to deviant and to standard tone (23). Consistent with the effect of GABA in other sensory systems (89, 90), the blockade of GABAergic-mediated inhibition elicits a generalized augmentation in the neural excitability of IC neurons by increasing their evoked response to both tones regardless of their probability of occurrence (Fig. 7C,D). This enhanced responsiveness decreases the ratio between the deviant/standard responses. This is known as iceberg-effect (89) and in the particular case of the application of gabazine, the simultaneous increment of the firing rate to both stimuli results in a drop of the CSI (Fig. 8), reflecting the decrease in the deviant to standard response ratio. Hence, synaptic inhibition acting on $GABA_A$ receptors regulates the strength of the response to deviant and standard tones but does not generate the SSA. These results point to the possibility that other neurotransmitters may be also participating in the generation or modulation of SSA in the IC.

Effect of cholinergic modulation on SSA

The control of attention engages different modulatory substances such as ACh (91, 92). In humans, cholinergic manipulation affects auditory novelty detection (9, 10, 93).

Likewise, diverse studies in animals support the notion that ACh release is necessary for the induction of auditory plasticity (94-97). Moreover, it is likely that the mechanism of attentional modulation on sensory processing operates at multiple stages, including cortical and subcortical nuclei. To understand the relation between large scale signals as the MMN and neuronal processing at different stages along the auditory pathway, a first approach was to study the influences of ACh on single-neuron SSA responses (25).

The local application of ACh and antagonists of the muscarinic and nicotinic receptors elicited a heterogeneous and baseline-dependent effect on SSA. An example of single neuron response is displayed in Figure 9. This neuron showed an intermediate SSA index (CSI = 0.73, Fig. 9A) that significantly decreased during the ACh application (CSI = 0.41, Fig. 9B). The firing pattern of the response became more robust to the deviant and standard stimuli as shown by the temporal course of the neural firing (Fig. 9C). Interestingly, the strength of the cholinergic effect was stronger on the driving response to the standard tone than to the deviant one (Fig. 9D). In general, ACh exerts a drop in the SSA index (Fig. 10) mainly due to an augmentation of the response to the standard tone, i.e, ACh decreases response adaptation. The diminished adaptation agrees with the role of ACh in exerting a neural circuit disinhibition by transiently altering the excitatory-inhibitory balance (revised in (20)). Our original study (Ayala and Malmierca, 2015) also revealed that not all IC neurons undergo cholinergic modulation. A subset of IC neurons (partially adapting) were significantly affected by ACh and a second group of neurons (extremely and not adapting) exhibited responses insensitive to ACh (Fig. 10B). Interestingly, the non-affected neurons are the ones that lack of or exhibit extreme levels of SSA. This baseline-dependent effect contrasts with the generalized drop of SSA exerted by the $GABA_A$-receptor blockade across neuron with different SSA levels (Fig. 8B). The same selective effect on partially adapting neurons

was elicited when the muscarinic and nicotinic receptors were blocked. The blockade of the muscarinic receptors elicited a stronger effect indicating these receptors are mainly mediating the cholinergic modulation on SSA. In conclusion, the study by Ayala and Malmierca (25) showed that ACh decreases the CSI of IC neurons with intermediate SSA levels by selectively decreasing the adaptation to the standard tone.

The functional significance of the cholinergic modulation on subcortical SSA can be though under the framework that indicates ACh affects the balance between feedback and feedforward neural processing (82, 92). ACh increases the efficacy of feedforward/thalamocortical input connections onto excitatory neurons in layer IV (98-102). Increased ACh levels switch sensory processing from a predominant influence of internal, corticocortical inputs to a predominant influence of external, thalamocortical inputs (92, 103). Thus, the cholinergic modulation occurring on SSA responses in IC neurons might contribute to enhance the ascending processing converging in the auditory thalamus *en route* to the auditory cortex. Finally, it is worth to mention the similarity in the baseline-dependent effects of cholinergic modulation exerted on population coding of more complex acoustic regularities. In this regard, a MMN study performed in non-smoker individuals found that nicotine enhances and diminishes change detection according to their baseline change detection processing (9). Also, nicotine has been shown to alleviate the MMN amplitude attenuation induced by NMDA blockade (104). Complementary studies at different neural stages of processing recording single-neuron and population activity under pharmacological manipulation or under behavioral tasks known to modify the animal's attentional demands will contribute to bridge the gap between cellular and large-scale effects of neuromodulators on change detection.

General discussion and final remarks

The iontophoretic manipulation of GABAergic, glutamatergic and cholinergic receptors on SSA suggests those receptors play different roles on shaping SSA in the IC. At the population level, the blockade of $GABA_A$-mediated inhibition increases the overall spike count and decreases the response latency to deviant and standard stimuli (Fig. 11A), while the blockade of glutamatergic excitation has an opposite effect (Fig. 11B). On the other hand, the activation of cholinergic receptors exerts a delicate modulation only on the response to the standard stimuli without affecting the timing of the response (Fig. 11C). Moreover, the different effect produced by Ach, excitation and inhibition is reflected on the time course of the response to the standard tone. The adaptation in the response to the standard tone fits a double exponential function which includes rapid and slow decays as well as a steady-state component in the response (24). While the magnitude and timing of all these three components are drastically affected by gabazine, only the magnitude of the sustained component is augmented by ACh application (Fig. 11D). The delicate modulation of ACh that selectively increases the evoked response to the standard sound without affecting the timing of the neural response contrasts with the gain control exerted by $GABA_A$-mediated inhibition in IC (24) and MGB neurons (105), as well as by glutamatergic excitation. From these results, we can conclude that glutamatergic excitation, ACh and $GABA_A$-mediated inhibition produce different effects on the adaptation dynamics. While GABA and glutamate may work together to preserve an exquisite excitatory/inhibitory balance to act together as a balanced gain control system, maintaining the responses within a range that optimizes the deviant to standard ratio, ACh contributes to maintain the encoding of repetitive sounds more selectively.

Taken together, these studies highlight the differential and complementary role of putative receptors on the modulation of SSA. Moreover, these experiments contribute to reveal how glutamatergic- or other neurotransmitter-related dysfunctions linked to the etiopathology of mental illness might be affecting the upstream neural processing supporting MMN-like responses observed along the auditory pathway. Likewise, our data might indicate how such a basic auditory response as the SSA will be affected by pharmacological interventions using agonist or antagonist compounds for the clinical treatment of mental disorders like schizophrenia.

Acknowledgements

This project was funded by the MINECO grant BFU201343608-P and the JCYL grant SA343U14 to MSM, YAA held a CONACyT (216106) and a SEP fellowship.

Author contribution:

YAA, DPG and MSM wrote the manuscript. DPG performed the experiments of glutamate iontophoresis, analyzed the data and wrote the results.

Financial Disclosures

The authors declare no competing financial interests.

References

1. Näätänen R, Paavilainen P, Rinne T, Alho K (2007): The mismatch negativity (MMN) in basic research of central auditory processing: a review. *Clin Neurophysiol* 118:2544-2590.
2. Nagai T, Tada M, Kirihara K, Yahata N, Hashimoto R, Araki T, *et al.* (2013): Auditory mismatch negativity and P3a in response to duration and frequency changes in the early stages of psychosis. *Schizophr Res* 150:547-554.
3. Harms L, Fulham WR, Todd J, Budd TW, Hunter M, Meehan C, *et al.* (2014): Mismatch negativity (MMN) in freely-moving rats with several experimental controls. *PLoS ONE* 9:e110892.
4. Michie PT (2001): What has MMN revealed about the auditory system in schizophrenia? *Int J Psychophysiol* 42:177-194.
5. Fisher DJ, Grant B, Smith DM, Borracci G, Labelle A, Knott VJ (2012): Nicotine and the hallucinating brain: effects on mismatch negativity (MMN) in schizophrenia. *Psychiatry Res* 196:181-187.
6. Hong LE, Moran LV, Du X, O'Donnell P, Summerfelt A (2012): Mismatch negativity and low frequency oscillations in schizophrenia families. *Clin Neurophysiol* 123:1980-1988.
7. Matsuno H, Ohi K, Hashimoto R, Yamamori H, Yasuda Y, Fujimoto M, *et al.* (2015): A Naturally Occurring Null Variant of the NMDA Type Glutamate Receptor NR3B Subunit Is a Risk Factor of Schizophrenia. *PLoS One* 10:e0116319.
8. Dunbar G, Boeijinga PH, Demazieres A, Cisterni C, Kuchibhatla R, Wesnes K, *et al.* (2007): Effects of TC-1734 (AZD3480), a selective neuronal nicotinic receptor agonist, on cognitive performance and the EEG of young healthy male volunteers. *Psychopharmacology (Berl)* 191:919-929.
9. Knott V, Impey D, Philippe T, Smith D, Choueiry J, de la Salle S, *et al.* (2014): Modulation of auditory deviance detection by acute nicotine is baseline and deviant dependent in healthy nonsmokers: a mismatch negativity study. *Hum Psychopharmacol* 29:446-458.
10. Moran RJ, Campo P, Symmonds M, Stephan KE, Dolan RJ, Friston KJ (2013): Free energy, precision and learning: the role of cholinergic neuromodulation. *J Neurosci* 33:8227-8236.
11. Mathalon DH, Ahn KH, Perry EB, Jr., Cho HS, Roach BJ, Blais RK, *et al.* (2014): Effects of nicotine on the neurophysiological and behavioral effects of ketamine in humans. *Front Psychiatry* 5:3.
12. Pang EW, Fowler B (1999): Dissociation of the mismatch negativity and processing negativity attentional waveforms with nitrous oxide. *Psychophysiology* 36:552-558.
13. Jung F, Stephan KE, Backes H, Moran R, Gramer M, Kumagai T, *et al.* (2013): Mismatch responses in the awake rat: evidence from epidural recordings of auditory cortical fields. *PLoS One* 8:e63203.
14. Pérez-González D, Malmierca MS (2014): Adaptation in the auditory system: an overview. *Front Integr Neurosci* 8:19.
15. Malmierca MS, Cristaudo S, Perez-Gonzalez D, Covey E (2009): Stimulus-specific adaptation in the inferior colliculus of the anesthetized rat. *J Neurosci* 29:5483-5493.

16. Antunes FM, Nelken I, Covey E, Malmierca MS (2010): Stimulus-specific adaptation in the auditory thalamus of the anesthetized rat. *PLoS ONE* 5:e14071.
17. Ulanovsky N, Las L, Nelken I (2003): Processing of low-probability sounds by cortical neurons. *Nat Neurosci* 6:391-398.
18. Escera C, Malmierca MS (2014): The auditory novelty system: An attempt to integrate human and animal research. *Psychophysiology* 51:111-123.
19. Malmierca MS, Sanchez-Vives MV, Escera C, Bendixen A (2014): Neuronal adaptation, novelty detection and regularity encoding in audition. *Front Syst Neurosci* 8:111.
20. Froemke RC (2015): Plasticity of Cortical Excitatory-Inhibitory Balance. *Annual review of neuroscience*.
21. Froemke RC, Carcea I, Barker AJ, Yuan K, Seybold BA, Martins AR, *et al.* (2013): Long-term modification of cortical synapses improves sensory perception. *Nat Neurosci* 16:79-88.
22. Froemke RC, Merzenich MM, Schreiner CE (2007): A synaptic memory trace for cortical receptive field plasticity. *Nature* 450:425-429.
23. Pérez-González D, Malmierca MS (2012): Variability of the time course of stimulus-specific adaptation in the inferior colliculus. *Front Neural Circuits* 6:107.
24. Pérez-González D, Hernandez O, Covey E, Malmierca MS (2012): GABA(A)-Mediated Inhibition Modulates Stimulus-Specific Adaptation in the Inferior Colliculus. *PLoS One* 7:e34297.
25. Ayala YA, Malmierca MS (2015): Modulation of auditory deviant saliency in the inferior colliculus (IC). *ARO MidWinter Meeting*, Vol Abstract PS-430. Baltimore, USA.
26. Malmierca MS (2004): The Inferior Colliculus: A Center for Convergence of Ascending and Descending Auditory Information. *Neuroembryol Aging* 3:215-229.
27. Ito T, Oliver DL (2012): The basic circuit of the IC: tectothalamic neurons with different patterns of synaptic organization send different messages to the thalamus. *Front Neural Circuits* 6:48.
28. Ito T, Oliver DL (2010): Origins of Glutamatergic Terminals in the Inferior Colliculus Identified by Retrograde Transport and Expression of VGLUT1 and VGLUT2 Genes. *Front Neuroanat* 4:135.
29. Hurley LM, Sullivan MR (2012): From behavioral context to receptors: serotonergic modulatory pathways in the IC. *Front Neural Circuits* 6:58.
30. Schofield BR (2010): Projections from auditory cortex to midbrain cholinergic neurons that project to the inferior colliculus. *Neuroscience* 166:231-240.
31. Duque D, Ayala YA, Malmierca MS (2015): Deviance detection in auditory subcortical structures: what can we learn from neurochemistry and neural connectivity? *Cell Tissue Res*.
32. Kelly JB, Caspary DM (2005): Pharmacology of the inferior colliculus. In: Winer JA, Schreiner CE editors. *The Inferior Colliculus*. New York: Springer, pp 248-281.
33. Malmierca MS (2015): Auditory system. In: Paxinos G editor. *The rat nervous system*, 4th ed. Amsterdam: Academic Press.
34. Ma CL, Kelly JB, Wu SH (2002): AMPA and NMDA receptors mediate synaptic excitation in the rat's inferior colliculus. *Hear Res* 168:25-34.

35. Korostenskaja M, Nikulin VV, Kicic D, Nikulina AV, Kahkonen S (2007): Effects of NMDA receptor antagonist memantine on mismatch negativity. *Brain Res Bull* 72:275-283.
36. Tikhonravov D, Neuvonen T, Pertovaara A, Savioja K, Ruusuvirta T, Naatanen R, *et al.* (2010): Dose-related effects of memantine on a mismatch negativity-like response in anesthetized rats. *Neuroscience* 167:1175-1182.
37. Tikhonravov D, Neuvonen T, Pertovaara A, Savioja K, Ruusuvirta T, Näätänen R, *et al.* (2008): Effects of an NMDA-receptor antagonist MK-801 on an MMN-like response recorded in anesthetized rats. *Brain Res* 1203:97-102.
38. Wacongne C, Changeux JP, Dehaene S (2012): A neuronal model of predictive coding accounting for the mismatch negativity. *The Journal of neuroscience : the official journal of the Society for Neuroscience* 32:3665-3678.
39. Schmidt A, Diaconescu AO, Kometer M, Friston KJ, Stephan KE, Vollenweider FX (2013): Modeling ketamine effects on synaptic plasticity during the mismatch negativity. *Cereb Cortex* 23:2394-2406.
40. Umbricht D, Schmid L, Koller R, Vollenweider FX, Hell D, Javitt DC (2000): Ketamine-induced deficits in auditory and visual context-dependent processing in healthy volunteers: implications for models of cognitive deficits in schizophrenia. *Archives of general psychiatry* 57:1139-1147.
41. Naatanen R, Michie PT (1979): Early selective-attention effects on the evoked potential: a critical review and reinterpretation. *Biol Psychol* 8:81-136.
42. Javitt DC, Steinschneider M, Schroeder CE, Arezzo JC (1996): Role of cortical N-methyl-D-aspartate receptors in auditory sensory memory and mismatch negativity generation: implications for schizophrenia. *Proc Natl Acad Sci USA* 93:11962-11967.
43. Todd J, Michie PT, Schall U, Karayanidis F, Yabe H, Naatanen R (2008): Deviant matters: duration, frequency, and intensity deviants reveal different patterns of mismatch negativity reduction in early and late schizophrenia. *Biol Psychiatry* 63:58-64.
44. Catts SV, Shelley AM, Ward PB, Liebert B, McConaghy N, Andrews S, *et al.* (1995): Brain potential evidence for an auditory sensory memory deficit in schizophrenia. *The American journal of psychiatry* 152:213-219.
45. Kompus K, Westerhausen R, Craven AR, Kreegipuu K, Poldver N, Passow S, *et al.* (2015): Resting-state glutamatergic neurotransmission is related to the peak latency of the auditory mismatch negativity (MMN) for duration deviants: An H-MRS-EEG study. *Psychophysiology*.
46. Farley BJ, Quirk MC, Doherty JJ, Christian EP (2010): Stimulus-specific adaptation in auditory cortex is an NMDA-independent process distinct from the sensory novelty encoded by the mismatch negativity. *J Neurosci* 30:16475-16484.
47. Featherstone RE, Shin R, Kogan JH, Liang Y, Matsumoto M, Siegel SJ (2014): Mice with subtle reduction of NMDA NR1 receptor subunit expression have a selective decrease in mismatch negativity: Implications for schizophrenia prodromal population. *Neurobiology of disease* 73C:289-295.
48. Oliver DL (1984): Dorsal cochlear nucleus projections to the inferior colliculus in the cat: a light and electron microscopic study. *J Comp Neurol* 224:155-172.
49. Saint Marie RL, Baker RA (1990): Neurotransmitter-specific uptake and retrograde transport of [3H]glycine from the inferior colliculus by ipsilateral projections of the superior olivary complex and nuclei of the lateral lemniscus. *Brain Res* 524:244-253.

50. Riquelme R, Saldaña E, Osen KK, Ottersen OP, Merchán MA (2001): Colocalization of GABA and glycine in the ventral nucleus of the lateral lemniscus in rat: an in situ hybridization and semiquantitative immunocytochemical study. *J Comp Neurol* 432:409-424.
51. Merchán M, Aguilar LA, Lopez-Poveda EA, Malmierca MS (2005): The inferior colliculus of the rat: quantitative immunocytochemical study of GABA and glycine. *Neuroscience* 136:907-925.
52. Vater M, Covey E, Casseday JH (1997): The columnar region of the ventral nucleus of the lateral lemniscus in the big brown bat (*Eptesicus fuscus*): synaptic arrangements and structural correlates of feedforward inhibitory function. *Cell Tissue Res* 289:223-233.
53. Kulesza RJ, Jr., Spirou GA, Berrebi AS (2003): Physiological response properties of neurons in the superior paraolivary nucleus of the rat. *J Neurophysiol* 89:2299-2312.
54. Adams JC, Mugnaini E (1984): Dorsal nucleus of the lateral lemniscus: a nucleus of GABAergic projection neurons. *Brain Res Bull* 13:585-590.
55. Li L, Kelly JB (1992): Inhibitory influence of the dorsal nucleus of the lateral lemniscus on binaural responses in the rat's inferior colliculus. *J Neurosci* 12:4530-4539.
56. Saldaña E, Merchán MA (1992): Intrinsic and commissural connections of the rat inferior colliculus. *J Comp Neurol* 319:417-437.
57. Zhang DX, Li L, Kelly JB, Wu SH (1998): GABAergic projections from the lateral lemniscus to the inferior colliculus of the rat. *Hear Res* 117:1-12.
58. Hernández O, Espinosa N, Pérez-González D, Malmierca MS (2005): The inferior colliculus of the rat: A quantitative analysis of monaural frequency response areas. *Neuroscience* 132:203-217.
59. Gonzalez-Hernandez T, Mantolan-Sarmiento B, Gonzalez-Gonzalez B, Perez-Gonzalez H (1996): Sources of GABAergic input to the inferior colliculus of the rat. *J Comp Neurol* 372:309-326.
60. Malmierca MS, Hernández O, Falconi A, Lopez-Poveda EA, Merchán M, Rees A (2003): The commissure of the inferior colliculus shapes frequency response areas in rat: an in vivo study using reversible blockade with microinjection of kynurenic acid. *Exp Brain Res* 153:522-529.
61. Malmierca MS, Hernández O, Rees A (2005): Intercollicular commissural projections modulate neuronal responses in the inferior colliculus. *Eur J Neurosci* 21:2701-2710.
62. Yang L, Pollak GD, Resler C (1992): GABAergic circuits sharpen tuning curves and modify response properties in the mustache bat inferior colliculus. *J Neurophysiol* 68:1760-1774.
63. Faingold CL, Boersma Anderson CA, Caspary DM (1991): Involvement of GABA in acoustically-evoked inhibition in inferior colliculus neurons. *Hear Res* 52:201-216.
64. Palombi PS, Caspary DM (1996): GABA inputs control discharge rate primarily within frequency receptive fields of inferior colliculus neurons. *J Neurophysiol* 75:2211-2219.
65. Le Beau FE, Rees A, Malmierca MS (1996): Contribution of GABA- and glycine-mediated inhibition to the monaural temporal response properties of neurons in the inferior colliculus. *J Neurophysiol* 75:902-919.

66. LeBeau FE, Malmierca MS, Rees A (2001): Iontophoresis in vivo demonstrates a key role for GABA(A) and glycinergic inhibition in shaping frequency response areas in the inferior colliculus of guinea pig. *J Neurosci* 21:7303-7312.
67. Sivaramakrishnan S, Sterbing-D'Angelo SJ, Filipovic B, D'Angelo WR, Oliver DL, Kuwada S (2004): GABA(A) synapses shape neuronal responses to sound intensity in the inferior colliculus. *J Neurosci* 24:5031-5043.
68. Fujita I, Konishi M (1991): The role of GABAergic inhibition in processing of interaural time difference in the owl's auditory system. *J Neurosci* 11:722-739.
69. Vater M, Habbicht H, Kossl M, Grothe B (1992): The functional role of GABA and glycine in monaural and binaural processing in the inferior colliculus of horseshoe bats. *J Comp Physiol A* 171:541-553.
70. D'Angelo WR, Sterbing SJ, Ostapoff EM, Kuwada S (2005): Role of GABAergic inhibition in the coding of interaural time differences of low-frequency sounds in the inferior colliculus. *J Neurophysiol* 93:3390-3400.
71. McAlpine D, Palmer AR (2002): Blocking GABAergic inhibition increases sensitivity to sound motion cues in the inferior colliculus. *J Neurosci* 22:1443-1453.
72. Hormigo S, Horta Junior Jde A, Gomez-Nieto R, Lopez DE (2012): The selective neurotoxin DSP-4 impairs the noradrenergic projections from the locus coeruleus to the inferior colliculus in rats. *Front Neural Circuits* 6:41.
73. Klepper A, Herbert H (1991): Distribution and origin of noradrenergic and serotonergic fibers in the cochlear nucleus and inferior colliculus of the rat. *Brain Res* 557:190-201.
74. Thompson AM, Thompson GC (2009): Serotonin-immunoreactive neurons in the postnatal MAO-A KO mouse lateral superior olive project to the inferior colliculus. *Neurosci Lett* 460:47-51.
75. Obara N, Kamiya H, Fukuda S (2014): Serotonergic modulation of inhibitory synaptic transmission in mouse inferior colliculus. *Biomed Res* 35:81-84.
76. Ramsey LC, Sinha SR, Hurley LM (2010): 5-HT1A and 5-HT1B receptors differentially modulate rate and timing of auditory responses in the mouse inferior colliculus. *Eur J Neurosci* 32:368-379.
77. Olazabal UE, Moore JK (1989): Nigrotectal projection to the inferior colliculus: horseradish peroxidase transport and tyrosine hydroxylase immunohistochemical studies in rats, cats, and bats. *J Comp Neurol* 282:98-118.
78. Gittelman JX, Perkel DJ, Portfors CV (2013): Dopamine modulates auditory responses in the inferior colliculus in a heterogeneous manner. *J Assoc Res Otolaryngol* 14:719-729.
79. Schofield BR, Motts SD (2009): Projections from auditory cortex to cholinergic cells in the midbrain tegmentum of guinea pigs. *Brain Res Bull* 80:163-170.
80. Cortes R, Palacios JM (1986): Muscarinic cholinergic receptor subtypes in the rat brain. I. Quantitative autoradiographic studies. *Brain Res* 362:227-238.
81. Morley BJ, Kemp GE (1981): Characterization of a putative nicotinic acetylcholine receptor in mammalian brain. *Brain Res* 228:81-104.
82. Thiele A (2013): Muscarinic signaling in the brain. *Annual review of neuroscience* 36:271-294.
83. Watanabe T, Simada Z (1971): Picrotoxin: effect on collicular auditory neurons. *Brain Res* 28:582-585.
84. Farley GR, Morley BJ, Javel E, Gorga MP (1983): Single-unit responses to cholinergic agents in the rat inferior colliculus. *Hear Res* 11:73-91.

85. Habbicht H, Vater M (1996): A microiontophoretic study of acetylcholine effects in the inferior colliculus of horseshoe bats: implications for a modulatory role. *Brain Res* 724:169-179.
86. Windhorst U, Johansson Hk, Lalley P (1999): Microiontophoresis and Pressure Ejection. *Modern Techniques in Neuroscience Research*: Springer Berlin Heidelberg, pp 193-212.
87. Perkins MN, Stone TW (1983): In vivo release of [3H]-purines by quinolinic acid and related compounds. *Br J Pharmacol* 80:263-267.
88. Näätänen R (1992): *Attention and brain function*. Hillsdale, NJ: Erlbaum.
89. Isaacson JS, Scanziani M (2011): How inhibition shapes cortical activity. *Neuron* 72:231-243.
90. Katzner S, Busse L, Carandini M (2011): GABAA inhibition controls response gain in visual cortex. *The Journal of neuroscience : the official journal of the Society for Neuroscience* 31:5931-5941.
91. Passetti F, Dalley JW, O'Connell MT, Everitt BJ, Robbins TW (2000): Increased acetylcholine release in the rat medial prefrontal cortex during performance of a visual attentional task. *Eur J Neurosci* 12:3051-3058.
92. Hasselmo ME, McGaughy J (2004): High acetylcholine levels set circuit dynamics for attention and encoding and low acetylcholine levels set dynamics for consolidation. *Prog Brain Res* 145:207-231.
93. Klinkenberg I, Blokland A, Riedel WJ, Sambeth A (2013): Cholinergic modulation of auditory processing, sensory gating and novelty detection in human participants. *Psychopharmacology (Berl)* 225:903-921.
94. Bjordahl TS, Dimyan MA, Weinberger NM (1998): Induction of long-term receptive field plasticity in the auditory cortex of the waking guinea pig by stimulation of the nucleus basalis. *Behav Neurosci* 112:467-479.
95. Leach ND, Nodal FR, Cordery PM, King AJ, Bajo VM (2013): Cortical cholinergic input is required for normal auditory perception and experience-dependent plasticity in adult ferrets. *J Neurosci* 33:6659-6671.
96. Metherate R, Weinberger NM (1989): Acetylcholine produces stimulus-specific receptive field alterations in cat auditory cortex. *Brain Res* 480:372-377.
97. Edeline JM (2012): Beyond traditional approaches to understanding the functional role of neuromodulators in sensory cortices. *Front Behav Neurosci* 6:45.
98. Barkai E, Hasselmo ME (1994): Modulation of the input/output function of rat piriform cortex pyramidal cells. *J Neurophysiol* 72:644-658.
99. Disney AA, Aoki C, Hawken MJ (2007): Gain modulation by nicotine in macaque v1. *Neuron* 56:701-713.
100. Gil Z, Connors BW, Amitai Y (1997): Differential regulation of neocortical synapses by neuromodulators and activity. *Neuron* 19:679-686.
101. Hsieh CY, Cruikshank SJ, Metherate R (2000): Differential modulation of auditory thalamocortical and intracortical synaptic transmission by cholinergic agonist. *Brain Res* 880:51-64.
102. Kimura F (2000): Cholinergic modulation of cortical function: a hypothetical role in shifting the dynamics in cortical network. *Neurosci Res* 38:19-26.
103. Giocomo LM, Hasselmo ME (2007): Neuromodulation by glutamate and acetylcholine can change circuit dynamics by regulating the relative influence of afferent input and excitatory feedback. *Mol Neurobiol* 36:184-200.
104. Knott V, McIntosh J, Millar A, Fisher D, Villeneuve C, Ilivitsky V, *et al.* (2006): Nicotine and smoker status moderate brain electric and mood activation induced

by ketamine, an N-methyl-D-aspartate (NMDA) receptor antagonist. *Pharmacol Biochem Behav* 85:228-242.
105. Duque D, Malmierca MS, Caspary DM (2014): Modulation of stimulus-specific adaptation by GABA(A) receptor activation or blockade in the medial geniculate body of the anaesthetized rat. *J Physiol* 592:729-743.

Legends

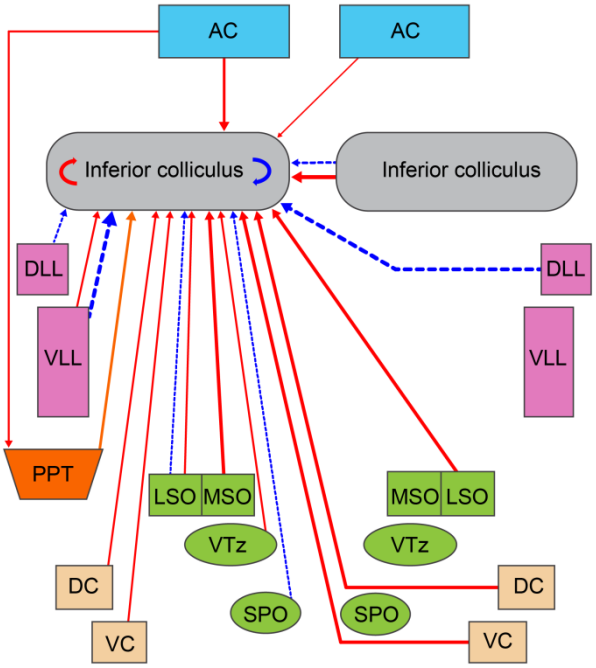

Figure 1. Schematic diagram of the excitatory (red), inhibitory (blue) and cholinergic (orange) projections to the inferior colliculus. The strength of the inhibitory and excitatory projections are depicted by the thickness of the lines. AC: auditory cortex, DLL, VLL: dorsal and ventral nucleus of the lateral lemniscus, respectively, PPT: pedunculopontine tegmental nucleus, LSO, MSO: lateral and medial superior olive, respectively, VTz, ventral nucleus of the trapezoid body, SPO: superior periolivary complex, DC, VC: dorsal and ventral subdivisions of the cochlear nucleus. Modified from (26).

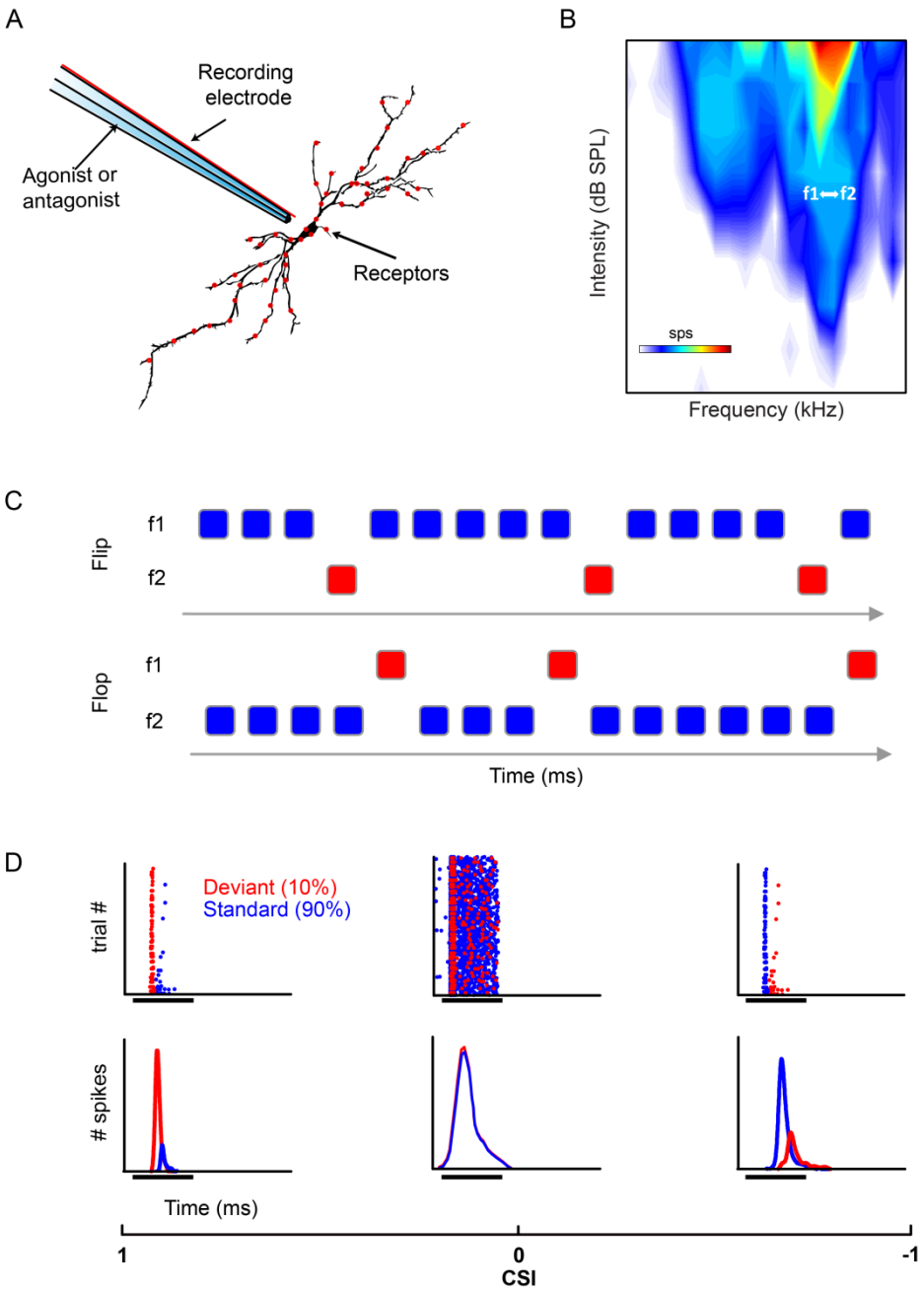

Figure2. Iontophoresis and oddball paradigm. A. A 'piggy-back' electrode is used to record single-neuron activity and to release neuroactive substance in the vicinity of the recorded neuron in order to block or activate specific receptors. The piggy-back electrode consists in a tungsten recording electrode attached to a glass multibarrel pipette which contains the neuroactive substances. B. Representation of a frequency response area, i.e., frequencies and intensities that evoke a suprathreshold respond, of an

IC neuron. Two frequencies (f1, f2) at the same intensity and evoking similar firing response are selected by the experimenter to be presented under the oddball paradigm. C. The oddball paradigm consists in the presentation of one frequency (f1) as a common or repetitive sound (blue: standard, high probability of occurrence) while the second frequency (f2) is presented as a rare sound (red: deviant, high probability of occurrence). This first sequence is often referred as flip, while a second flop sequence consists in the inversion of the relative probabilities of f1 and f2. D. Examples of dot rasters and peri-stimulus time histograms of the response to the deviant (red) or standard (blue) tone of IC neurons with different levels of SSA. The amount of SSA is quantified by the Common SSA index (CSI) whose positive values indicate adaptation in the response to the standard tone, zero value represents an equal and not adapted response to both tones, and negative index values indicate an adapted and smaller response to the deviant sound.

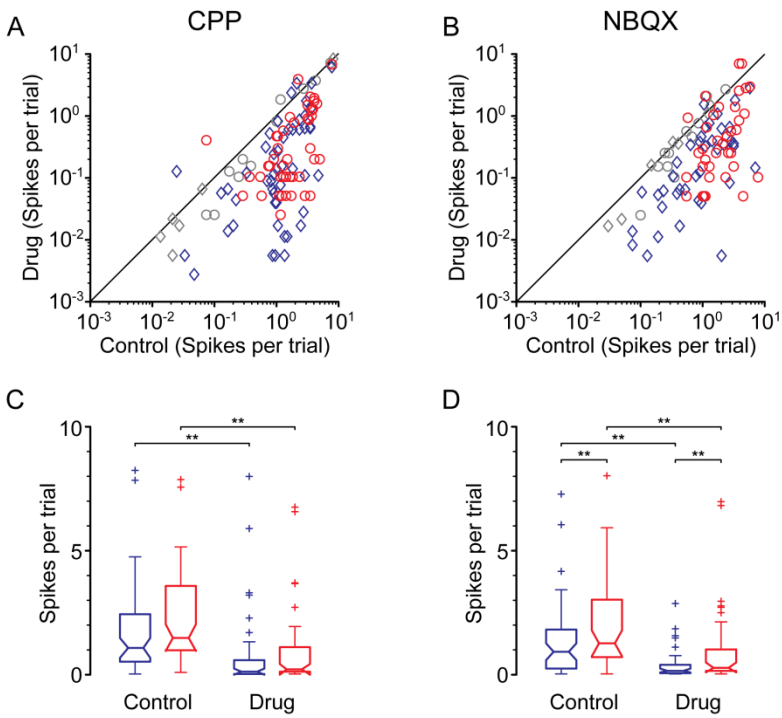

Figure 3: Effect of glutamate receptor antagonists on the responses of neurons during an oddball paradigm. The majority of neurons showed a decreased response (expressed as spikes per trial) during the application of either CPP (A) or NBQX (B), independently of whether the tone was presented as a standard (diamonds) or a deviant (circles). The colored markers indicate a significant change in the response relative to the control condition. At the population level, both drugs (C, CPP; D, NBQX) caused a significant decrement on the neuronal responses, for the standard (blue) and the deviant (red) stimuli alike.

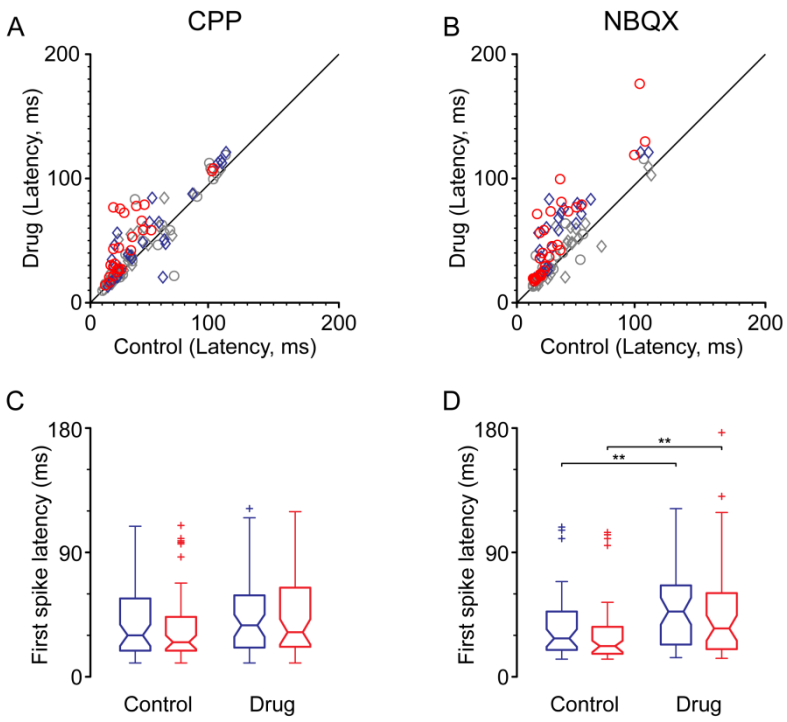

Figure 4: Effect of glutamate receptor antagonists on the first spike latency of during an oddball paradigm. The application of CPP (A) and NBQX (B) caused a significant increment of the first spike latency in most of the neurons recorded, regardless of whether the stimuli were presented as standard (diamonds) or deviants (circles). The colored markers indicate a significant change in the response relative to the control condition. At the population level, while the change due to the drug application was not significant in the case of CPP (C), the application of NBQX caused a significant increment of the first spike latency for both the standard (blue) and the deviant (red) stimuli.

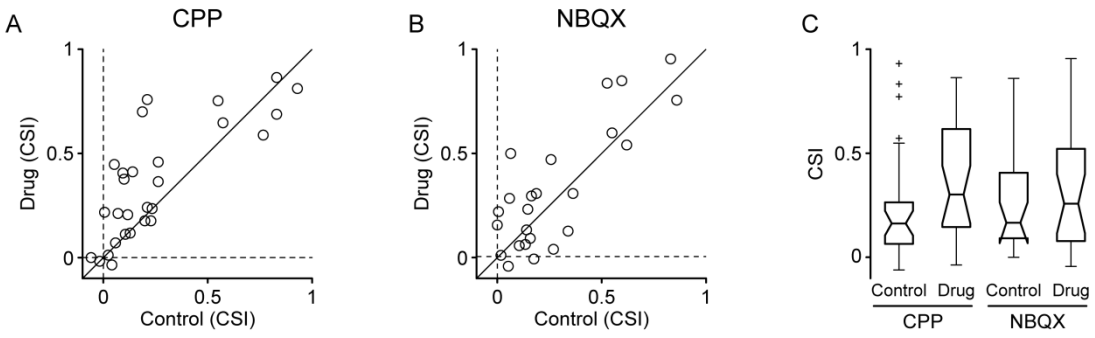

Figure 5: Effect of glutamate receptor antagonists on the common SSA index (CSI). While the overall effect was an increment of the CSI during the application of both drugs (A, CPP; B, NBQX), at the population level (C) the amount of increment was not statistically significant.

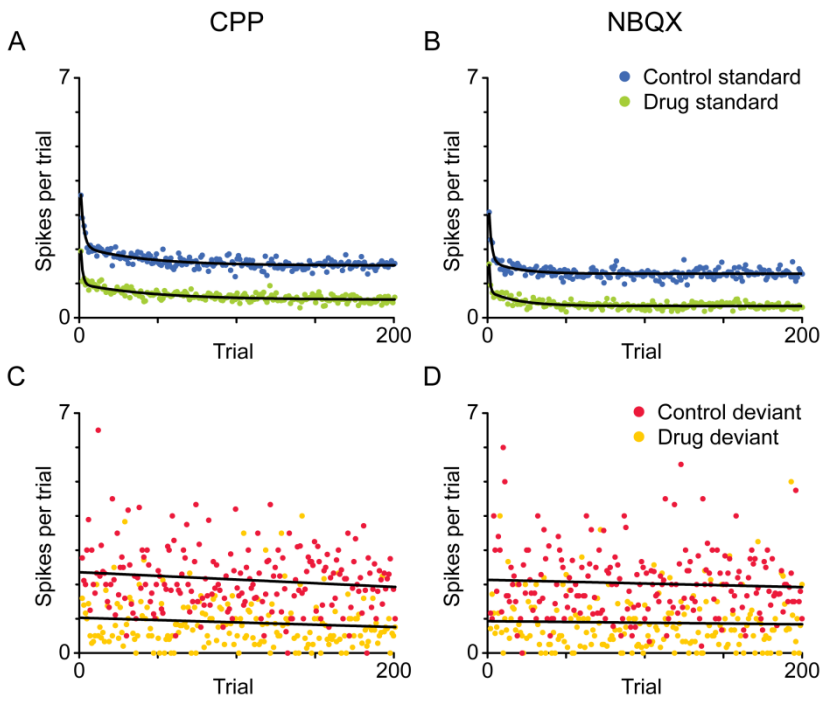

Figure 6: Time course of adaptation during the oddball paradigm and glutamatergic receptor antagonists. The application of CPP and NBQX (green dots in A and B, respectively) reduced the responses to the standard stimuli, compared to the control condition (blue dots), and also made the adaptation faster. In contrast, there was very little adaptation for the deviant stimuli (C, D) where the effect of both drugs (yellow dots) was essentially a linear decrement of the responses compared to the control condition (red dots). One trial equals 250 ms.

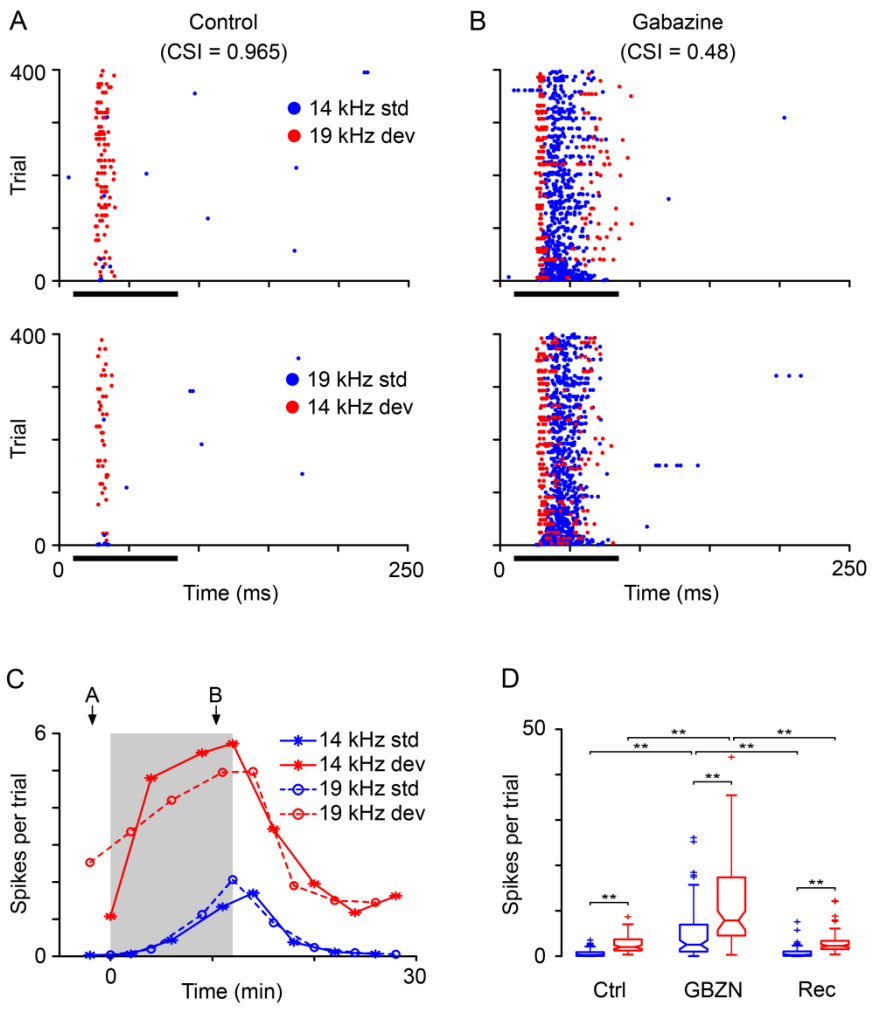

Figure 7. Typical effect of the blockade of the $GABA_A$-mediated inhibition on neural firing. A. Dot raster of the response of an adapting IC neuron to deviant and standard tones previous to the gabazine application. Black bars: tone duration. B. Dot raster of the neural response to the oddball paradigm during the blockade of the $GABA_A$ receptors with gabazine. C. Time course of the spike count in response to f1 and f2 presented as deviant and standard tones before, during and after the application of gabazine. Gray shaded area: duration of the gabazine injection which starts at T = 0. The A and B arrows correspond to the times of the response displayed in panels A and B. D. Population box plot of the spike count to the deviant and standard tone in the control (Ctrl), gabazine application (GBZN) and recovery condition (Rec). The asterisks

indicate significant differences (Friedman test, $p < 0.01$). Deviant, red; standard, blue in all panels. Modified from (24).

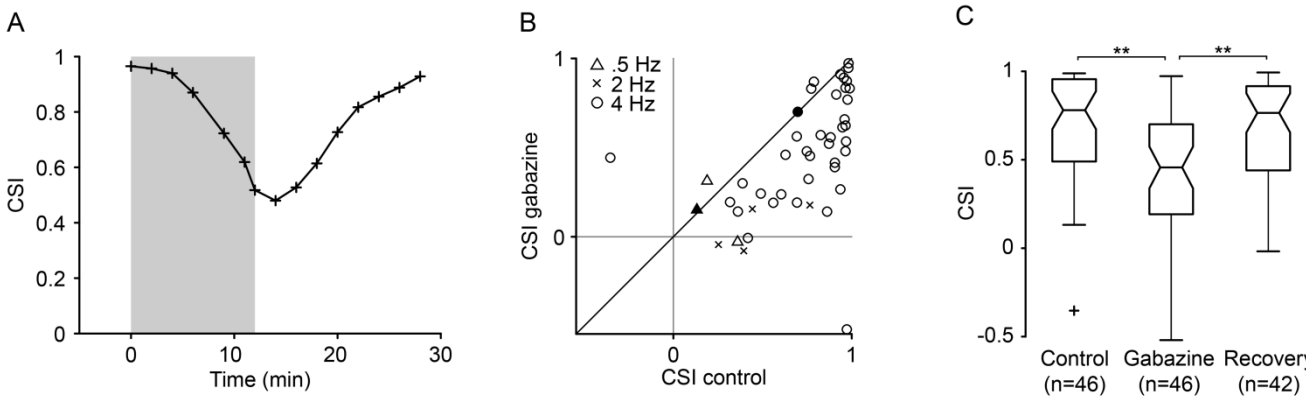

Figure 8. Effect of the blockade of the $GABA_A$-mediated inhibition on SSA index. A. Time course of the CSI of the example neuron displayed in Fig. Gaba1A-C before, during and after the injection of gabazine. Gray shaded area: duration of the gabazine injection which starts at T = 0. B. Change in the CSI of a population of IC neurons (n = 46). Gabazine significantly decreased most of the CSI (open symbols) obtained at different repetition rates of stimulation (symbols). C. Population box plot of the CSI values during the control, gabazine injection and recovery condition. The asterisks indicate significant differences (Friedman test, $p < 0.01$). Modified from (24).

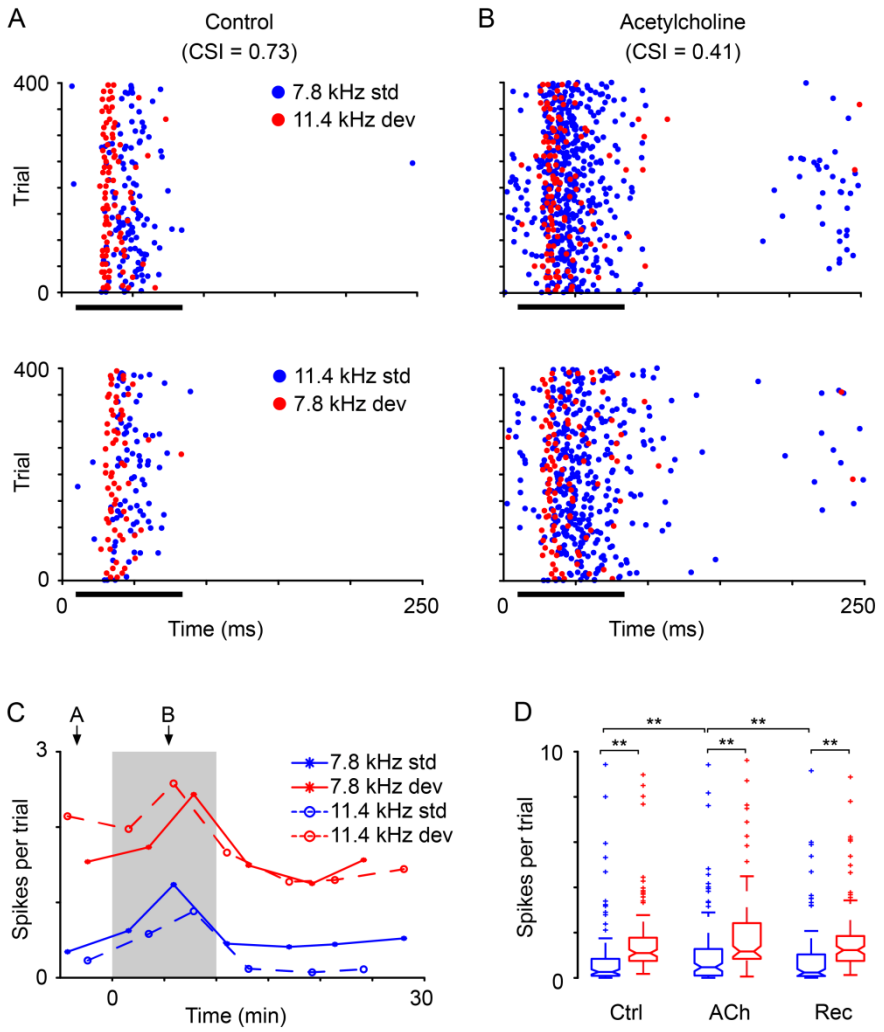

Figure 9. Typical effect of the activation of the cholinergic receptors on neural firing. A. Dot raster of the response of a partially adapting IC neuron to deviant and standard tones previous to the acetylcholine application. Black bars: tone duration. B. Change in the spiking response to deviant and standard tones during the acetylcholine injection. C. Time course of the spike count in response to f1 and f2 presented as deviant and standard tones before, during and after the application of acetylcholine. Gray shaded area: duration of the acetylcholine injection which starts at T = 0. The A and B arrows correspond to the times of the response displayed in panels A and B. D. Population box plot of the spike count to the deviant and standard tone in the control

(Ctrl), acetylcholine application (ACh) and recovery condition (Rec). The asterisks indicate significant differences (Friedman test, $p < 0.01$). Deviant, red; standard, blue in all panels.

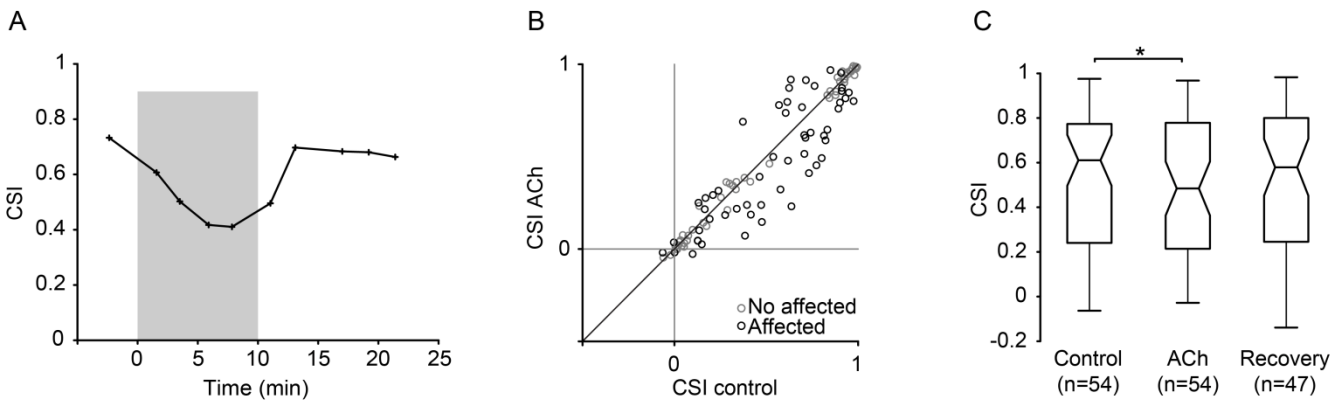

Figure 10. Effect of the activation of the cholinergic receptors on SSA index. A. Time course of the CSI of the example neuron displayed in Fig. 9A-C before, during and after the injection of acetylcholine. Gray shaded area: duration of the acetylcholine injection which starts at T = 0. B. Change in the CSI of a population of IC neurons (n = 105) elicited by acetylcholine. An augmentation of acetylcholine significantly modified the CSI of the majority of IC neurons with intermediate levels of SSA (open symbols) while those neurons that lack or exhibit extreme SSA remain unaffected by acetylcholine application. C. Population box plot of the CSI values during the control, acetylcholine injection and recovery condition. The asterisks indicate significant differences (Friedman test, $p < 0.05$).

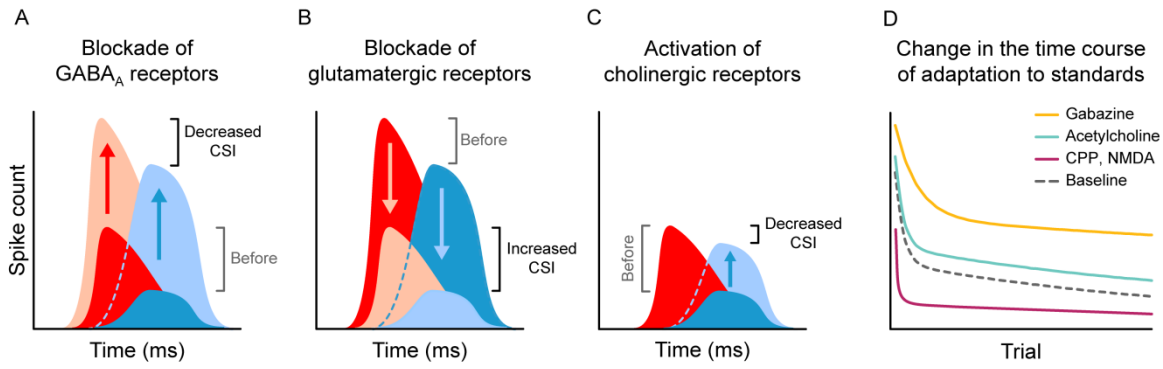

Figure 11. Schema of the effect of inhibition and acetylcholine on SSA. A. The blockade of the $GABA_A$ receptor by the iontophoretic injection of gabazine increased the overall response (shown here as PSTH) of IC neurons to both deviant (red) and standard (blue) stimuli, decreasing the CSI. B. On the other hand, the application of glutamatergic receptor antagonists reduced the responses to deviants and standards and increased the CSI. C. The activation of the cholinergic receptors by acetylcholine increases only the response to the standard tone of IC neurons with partial levels of SSA. D. Gabazine exerts a drastic change in the time course of adaptation in the response to the standard tone by increasing the fast and slow components of adaptation as well as the steady-state of adaptation. Acetylcholine affects only the sustained component of the time course of adaptation. CPP and NMDA make the time constants faster and reduce the steady-state. Modified from (24).

Table 1: Effect of glutamate receptor antagonists on neuronal responses. Mean and SD for the different measurements taken. The units are trials (equivalent to 250 ms) for τ_r and τ_s, and spikes per trial for A_{ss}, A_r and A_r. CSI: common SSA index, SI(f): frequency-specific SSA index, *: significant effect of the drug ($p < 0.05$, ANOVA; 95% confidence interval for the fittings).

	CPP (n = 28)		**NBQX (n = 25)**	
	Control	**Effect**	**Control**	**Effect**
Spikes per trial				
Standard	1.628 ± 1.707	0.634 ± 1.426 *	1.321 ± 1.529	0.384 ± 0.564 *
Deviant	2.187 ± 1.791	0.866 ± 1.416 *	2.002 ± 1.747	0.917 ± 1.487 *
First spike latency (ms)				
Standard	40.257 ± 28.656	45.478 ± 30.933	36.926 ± 24.200	49.429 ± 28.787 *
Deviant	36.279 ± 26.990	44.628 ± 30.700	31.166 ± 23.261	45.733 ± 37.461 *
CSI	0.254 ± 0.284	0.359 ± 0.277	0.271 ± 0.253	0.324 ± 0.299
SIf	0.235 ± 0.292	0.339 ± 0.426	0.268 ± 0.308	0.338 ± 0.408
Time course fitting (standards)				
τ_r	1.883	1.199 *	1.563	0.678 *
τ_s	38.65	47.55	17.47	18.410
A_{ss}	1.526	0.525 *	1.283	0.342 *
A_r	2.574	2.234	2.665	3.533
A_s	0.560	0.460	0.394	0.442
Time course fitting (deviants)				
a	2.358	1.029 *	2.134	0.930 *
b	-0.002	-0.001	-0.001	0.000